

**Ph.D DISSERTATION**

**DEVELOPMENT OF A STORM EVENT BASED  
TWO-DIMENSIONAL UPLAND EROSION MODEL**

**Submitted By :**

**Billy E. Johnson**

**Department of Civil Engineering**

**In partial fulfillment of the requirements**

**for the Degree of Doctor of Philosophy**

**Colorado State University**

**Fort Collins, Colorado**

**Spring, 1997**

**UMI Number: 9735024**

---

**UMI Microform 9735024**  
**Copyright 1997, by UMI Company. All rights reserved.**

**This microform edition is protected against unauthorized  
copying under Title 17, United States Code.**

---

**UMI**  
**300 North Zeeb Road**  
**Ann Arbor, MI 48103**

**COLORADO STATE UNIVERSITY**

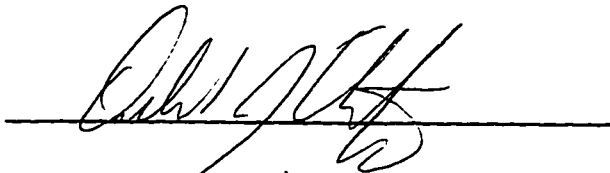
**March 27, 1997**

**WE HEREBY RECOMMEND THAT THE DISSERTATION PREPARED  
UNDER OUR SUPERVISION BY BILLY E. JOHNSON ENTITLED  
DEVELOPMENT OF A STORM EVENT BASED TWO-DIMENSIONAL  
UPLAND EROSION MODEL BE ACCEPTED AS FULFILLING IN PART  
REQUIREMENTS FOR THE DEGREE OF DOCTOR OF PHILOSOPHY.**

**Committee on Graduate Work**



---



---

*Pierre Julien*  

---

**Advisor**

*Chad C. Watts*  

---

**Co-Advisor**

*N. Smith*  

---

**Department Head**

**ABSTRACT OF DISSERTATION**  
**DEVELOPMENT OF A STORM EVENT BASED**  
**TWO-DIMENSIONAL UPLAND EROSION MODEL**

In the past, sediment yield analyses have been done primarily on an annual basis. In the cases where a single event sediment yield analysis has been performed, lumped parameter models were used to estimate the rainfall-runoff. With the recent development of the physically based two-dimensional hydrologic model, Cascade Two-Dimensions (CASC2D), more detailed computations of upland erosion can now be accomplished whereby not only can sediment yield at the outlet be computed, but sediment yield at interior points can also be computed.

CASC2D is an event-based model which divides the watershed into grid elements and can represent the spatial variability present in the watershed. The principal hydrologic processes of infiltration, overland flow, and channel flow are simulated and can be spatially and temporally analyzed. The objectives of this research were to: 1) formulate a time-varying physically based two-dimensional upland erosion/transport scheme; 2) incorporate the upland sediment scheme into CASC2D; 3) develop visualization capabilities to view the time and spatial varying erosion and sediment transport; and 4) test the upland sediment scheme with field measurements.

The Geographic Resources Analysis Support System (GRASS), a raster-based GIS, was used to manipulate the input grid data for CASC2D and to visualize the output grid data from CASC2D. The integration of the model within GRASS GIS provides the user with the means to easily input data into the model and to easily visualize the output data in

such a way as to expedite the calibration and verification of the model on actual storm events.

Field observations and computer simulations were performed on the test plot scale (Nelson Farm Test Plot) and on the watershed scale (Goodwin Creek Watershed) in North Mississippi in order to evaluate the proposed upland sediment scheme.

On the test plot scale, CASC2D was able to do a good job (-50% to 200%) computing surface runoff and sediment concentration when the land use was idle. There are cases where CASC2D may not be able to do as well on an event basis, however when computing annual sediment yield, CASC2D was within approximately 20% of the measured value.

On the watershed scale, the upland sediment scheme was able to compute erosion and deposition patterns consistent with field observations. In the upland drainage areas, the upland sediment scheme was able to compute sediment yield well within the acceptable range of -50% to 200%. At gage sites within the channel system, the contribution of upland sediments to the total sediment yield was computed to be in the range of 20% to 40%. From field observations and data collection activities carried out by the Agricultural Research Service (ARS), the upland contribution could be within this range when compared to the total sediment load. In those drainage areas where significant channel processes were not evident, model results were able to correlate better with the observed sediment yield, as well as, with the measured rate of sediment discharge than in drainage areas that displayed gully and channel erosion.

In conclusion, the upland sediment scheme was able to compute sediment yield in the upland drainage areas well within the accepted range of accuracy (-50% to 200%). In the

channel system, the model results did not compare as well to the observed total sediment yield due to gully erosion, bank failures, and channel bed erosion. As finer resolution data sets become available and the channel processes are incorporated into the model, the model results should compare better with the observed total sediment yield.

The linkage of CASC2D with the GRASS GIS made the development of spatial input data more efficient and the visualization of the spatial and temporal output data more efficient. As more work is done with the graphical interfaces for distributive models, the calibration and verification of these models will greatly improve.

Billy E. Johnson  
Department of Civil Engineering  
Colorado State University  
Fort Collins, CO. 80523  
Spring, 1997

## ACKNOWLEDGEMENTS

In performing this research, there are a number of individuals and organizations that have been instrumental in its successful completion. First and foremost, I would like to thank the U. S. Army Corps of Engineers Waterways Experiment Station (WES) for giving me the opportunity to attend Colorado State University (CSU) on the long term training program. Upon my return from CSU, WES allowed me the opportunity to continue my dissertation research, thus allowing me to finish in a timely fashion.

I would also like to thank Dr. Pierre Julien, Dr. Chester Watson, Dr. Steve Abt, and Dr. Deborah Anthony for serving on my PhD. committee. The guidance of my committee kept me on the fast track to completing this research and for that I will forever be grateful.

The National Sedimentation Laboratory (NSL), located in Oxford Mississippi, deserves a special thanks. The work of Dr. Carlos Alonso and Mr. William Blackmarr in the development of the Goodwin Creek database and report were very important in the calibration of the model on the watershed scale. Dr. Seth Dabney and his staff's efforts in providing the Nelson Farm Test Plot data, in a timely fashion, was greatly appreciated. Finally, conversations with Dr. Ron Bingner and Dr. Roger Kuhnle provided important insight into the sediment sources and distribution within the Goodwin Creek watershed.

I would like to take this opportunity to thank Dr. Bahram Saghafian and Dr. Fred Ogden. Their initial work on the development of the CASC2D model provided the starting point of this research. Without their ground breaking work and consultation, this research would not have been possible in the time frame that it was accomplished.

In pursuing my Masters Degree, from Memphis State University, I was first introduced to the CASC2D model. In performing that research, Dr. Roger Smith and I became colleagues as well as friends. His insight in calibrating and verifying distributive hydrologic models as well as discussions about performing sediment routings proved helpful in the completion of this work.

I am a firm believer that no one accomplishes very much by themselves. I have been very lucky to have excellent bosses where ever I have worked. Starting with my co-op days at the Lower Mississippi Valley Division, I would like to thank Mr. John Brooks, Mr. Jim Tuttle, and Mr. Max Lamb. These are the people who showed my what true professionalism is all about. From there, I went to the Memphis District and worked for Mr. Carl Seckt, Mr. James Pendergrass, and Mr. Dewey Jones. In Memphis, I was allowed the opportunity to further develop my hydraulic modeling skills as well as my programming skills. These were absolutely essential in completing this research. Finally, I went to work for WES under the direction of Mr. Tom Pokrefke, Mr. Michael Trawle, and Dr. Nolan Raphelt. Their guidance and support, in pursuing this degree as well as their friendship, are greatly appreciated.

Finally, I would like to thank all of my family and friends for their support and understanding. I was not able to see them very much during this period of time, but hopefully they know that they were always on my mind.



## **DEDICATION**

In life it is important to have role models, for without them we can never know what heights we can truly rise too. In my life, I was given a huge break right from the beginning. My father has shown me by example that it doesn't matter where you start in life, rather, how hard you work throughout your life will be the determining factor in the end. He started from very humble beginnings, but through hard work, encouragement by family and friends, and a strong belief in himself, he rose to not only finish his doctorate, but to also become a world wide expert in the field of hydraulics. While all of this was very important in my desire to pursue this degree and my belief that I could finish, the one thing that I admire the most, about my dad, is the fact that no matter how high he has risen, he has never forgotten where he came from nor the people who helped him get to his state in life. He has always reached down in hopes of helping others climb their own ladders of success. Hopefully, I will be able to carry on in his footsteps.

**With great pleasure,**

**I dedicate this to my dad, Dr. Billy Harvey Johnson,**

**and all of the ROLE MODELS working to make**

**a positive difference in a young persons life.**

## TABLE OF CONTENTS

<u>Topic</u>	<u>Page Number</u>
Abstract of Dissertation .....	iii
Chapter 1 : Introduction .....	1
1.1 Background .....	1
1.2 Research Objectives .....	3
Chapter 2 : Literature Review .....	5
2.1 Channel Flow .....	5
2.1.1 Kinematic Wave .....	6
2.1.2 Diffusive Wave .....	6
2.1.3 Dynamic Wave .....	7
2.2 Channel Sediment Transport .....	7
2.3 Overland Flow .....	10
2.4 Upland Erosion .....	14
2.4.1 AGNPS .....	18
2.4.2 SWAT .....	18
2.4.3 ANSWERS .....	18
2.4.4 WEPP .....	19
2.4.5 EUROSEM .....	22
2.4.6 Wang-Hjelmfelt .....	23

## TABLE OF CONTENTS

<u>Topic</u>	<u>Page Number</u>
<b>Chapter 3 : Approach and Methodology</b> .....	<b>25</b>
<b>3.1 Surface Hydrology</b> .....	<b>25</b>
<b>3.1.1 Spatial Rainfall Distribution</b> .....	<b>25</b>
<b>3.1.2 Infiltration</b> .....	<b>26</b>
<b>3.1.3 Overland Flow</b> .....	<b>26</b>
<b>3.1.4 Channel Flow</b> .....	<b>29</b>
<b>3.2 Upland Erosion</b> .....	<b>29</b>
<b>3.3 Numerical Formulation</b> .....	<b>31</b>
<b>3.4 GIS Integration</b> .....	<b>37</b>
<b>Chapter 4 : Observed Data</b> .....	<b>38</b>
<b>4.1 Nelson Farm Test Plot</b> .....	<b>38</b>
<b>4.2 Goodwin Creek Watershed</b> .....	<b>44</b>
<b>Chapter 5 : Model Applications and Results</b> .....	<b>58</b>
<b>5.1 Nelson Farm Test Plot</b> .....	<b>58</b>
<b>5.1.1 Single Event Sediment Yield Analysis</b> .....	<b>58</b>
<b>5.1.1.1 Storm Event 1</b> .....	<b>59</b>
<b>5.1.1.2 Storm Event 2</b> .....	<b>69</b>
<b>5.1.2 Annual Sediment Yield Analysis</b> .....	<b>70</b>
<b>5.2 Goodwin Creek Watershed</b> .....	<b>73</b>

## TABLE OF CONTENTS

<u>Topic</u>	<u>Page Number</u>
5.2.1 Sensitivity Analysis .....	75
5.2.2 Storm Event 1 .....	82
5.2.3 Storm Event 2 .....	89
5.2.4 Storm Event 3 .....	96
<b>Chapter 6 : Summary, Conclusions, and Recommendations .....</b>	<b>103</b>
6.1 Summary .....	103
6.2 Conclusions .....	104
6.3 Recommendations .....	105
<b>Bibliography .....</b>	<b>107</b>
<b>Appendix A - Tables and Gage Plots .....</b>	<b>120</b>
<b>Appendix B - Output Grids from CASC2D - .....</b> <b>Nelson Farm Test Plot #2 - February 17-19, 1991.</b>	<b>152</b>
<b>Appendix C - Output Grids from CASC2D - .....</b> <b>Goodwin Creek Watershed - October 17-18, 1981.</b>	<b>183</b>
<b>Appendix D - Computer Listing and ASCII Input Data for CASC2D.</b>	<b>209</b>

## LIST OF TABLES

<u>Table</u>	<u>Page Number</u>
<b>Table 2.1 - Upland Erosion Model Comparisons . . . . .</b>	<b>24</b>
<b>Table 4.1 - Crop Management histories and yields for three . . . . . Nelson Farm research watersheds from 1988 through 1996.</b>	<b>41</b>
<b>Table 4.2 - Annual Rainfall, Runoff, and Sediment Yield from . . . . . watershed #2 (Nelson Farm).</b>	<b>43</b>
<b>Table 5.1 - SCS Type II - 24 Hour Rainfall Distribution . . . . .</b>	<b>71</b>
<b>Table 5.2 - Crop Management Factors (C) . . . . . for Nelson Farm Test Plot #2.</b>	<b>72</b>
<b>Table 5.3 - Computed Sediment Yield for Various Return Periods . . . . . (Nelson Farm Test Plot #2).</b>	<b>72</b>
<b>Table 5.4 - Overland Roughness for Goodwin Creek . . . . .</b>	<b>73</b>
<b>Table 5.5 - Soil Erodibility Factors (K) for Goodwin Creek . . . . .</b>	<b>73</b>
<b>Table 5.6 - Crop Management Factors (C) for Goodwin Creek . . . . .</b>	<b>74</b>

## LIST OF FIGURES

<b>Figure</b>	<b>Page Number</b>
Figure 3.1 - Flow Chart for the Upland Erosion Scheme . . . . .	32
Figure 3.2 - Topological Representation in Overland Flow . . . . . Routing Scheme.	34
Figure 3.3 - Schematic of Upland Erosion Scheme . . . . .	36
Figure 4.1 - Nelson Farm Test Plots . . . . .	39
Figure 4.2 - Runoff, Sediment Concentration, and Rainfall versus . . . . Time for Watershed #2 (Nelson Farm).	42
Figure 4.3 - Goodwin Creek Watershed . . . . .	45
Figure 4.4 - Standard Climatological Station near the center of the . . Goodwin Creek Watershed.	46
Figure 4.5 - Goodwin Creek Watershed Elevation Grid . . . . .	47
Figure 4.6 - Goodwin Creek Watershed Land Use Grid . . . . .	47
Figure 4.7 - Goodwin Creek Watershed Soil Texture Grid . . . . .	48
Figure 4.8 - Rill and gully erosion (Goodwin Creek) . . . . .	49
Figure 4.9 - Upland sediment deposits (Goodwin Creek) . . . . .	50
Figure 4.10 - Rill and gully erosion (Goodwin Creek) . . . . .	50
Figure 4.11 - Gully erosion (Goodwin Creek) . . . . .	51
Figure 4.12 - Rill erosion in pasture lands (Goodwin Creek) . . . . .	51
Figure 4.13 - Gully erosion (Goodwin Creek) . . . . .	52
Figure 4.14 - Rill erosion (Goodwin Creek) . . . . .	52

## LIST OF FIGURES

<b>Figure</b>	<b>Page Number</b>
Figure 4.15 - Gully erosion (Goodwin Creek) . . . . .	53
Figure 4.16 - Steep bank angles (Goodwin Creek) . . . . .	54
Figure 4.17 - Block failures (Goodwin Creek) . . . . .	54
Figure 4.18 - Bank undermining (Goodwin Creek) . . . . .	55
Figure 4.19 - Bank undermining (Goodwin Creek) . . . . .	55
Figure 4.20 - Local scour at gaging structure (Goodwin Creek). . . . .	56
Figure 4.21 - Vegetative undermining (Goodwin Creek) . . . . .	56
Figure 5.1 - Nelson Farm Test Plot #2 - Flow Hydrographs . . . . .	60
Figure 5.2 - Nelson Farm Test Plot #2 - Sediment Concentrations . . . . .	61
Figure 5.3 - Schematic of CASC2D Output Grids . . . . .	63
Figure 5.4 - CASC2D Output Grid (Nelson Farm) . . . . . (February 17-19, 1991 at Time = 540.0 minutes)	64
Figure 5.5 - CASC2D Output Grid (Nelson Farm) . . . . . (February 17-19, 1991 at Time = 1140.0 minutes)	65
Figure 5.6 - CASC2D Output Grid (Nelson Farm) . . . . . (February 17-19, 1991 at Time = 1740.0 minutes)	66
Figure 5.7 - CASC2D Output Grid (Nelson Farm) . . . . . (February 17-19, 1991 at Time = 2340.0 minutes)	67
Figure 5.8 - CASC2D Output Grid (Nelson Farm) . . . . . (February 17-19, 1991 at Time = 3420.0 minutes)	68

## LIST OF FIGURES

<u>Figure</u>	<u>Page Number</u>
Figure 5.9 - Sensitivity Analysis .....	76
Figure 5.10 - Final Total Net Volume Grids for the Goodwin Creek Watershed Sensitivity Analysis. ....	81
Figure 5.11 - CASC2D Output Grid (Goodwin Creek) .....	84
(October 17-18, 1981 at Time = 80.0 minutes)	
Figure 5.12 - CASC2D Output Grid (Goodwin Creek) .....	85
(October 17-18, 1981 at Time = 180.0 minutes)	
Figure 5.13 - CASC2D Output Grid (Goodwin Creek) .....	86
(October 17-18, 1981 at Time = 280.0 minutes)	
Figure 5.14 - CASC2D Output Grid (Goodwin Creek) .....	87
(October 17-18, 1981 at Time = 380.0 minutes)	
Figure 5.15 - CASC2D Output Grid (Goodwin Creek) .....	88
(October 17-18, 1981 at Time = 480.0 minutes)	
Figure 5.16 - CASC2D Output Grid (Goodwin Creek) .....	91
(December 2-3, 1983 at Time = 840.0 minutes)	
Figure 5.17 - CASC2D Output Grid (Goodwin Creek) .....	92
(December 2-3, 1983 at Time = 1720.0 minutes)	
Figure 5.18 - CASC2D Output Grid (Goodwin Creek) .....	93
(December 2-3, 1983 at Time = 2600.0 minutes)	
Figure 5.19 - CASC2D Output Grid (Goodwin Creek) .....	94
(December 2-3, 1983 at Time = 3480.0 minutes)	
Figure 5.20 - CASC2D Output Grid (Goodwin Creek) .....	95
(December 2-3, 1983 at Time = 4320.0 minutes)	



## LIST OF FIGURES

<u>Figure</u>	<u>Page Number</u>
<b>Figure 5.21 - CASC2D Output Grid (Goodwin Creek) . . . . . (May 2-3, 1984 at Time = 840.0 minutes)</b>	<b>98</b>
<b>Figure 5.22 - CASC2D Output Grid (Goodwin Creek) . . . . . (May 2-3, 1984 at Time = 1720.0 minutes)</b>	<b>99</b>
<b>Figure 5.23 - CASC2D Output Grid (Goodwin Creek) . . . . . (May 2-3, 1984 at Time = 2600.0 minutes)</b>	<b>100</b>
<b>Figure 5.24 - CASC2D Output Grid (Goodwin Creek) . . . . . (May 2-3, 1984 at Time = 3480.0 minutes)</b>	<b>101</b>
<b>Figure 5.25 - CASC2D Output Grid (Goodwin Creek) . . . . . (May 2-3, 1984 at Time = 4320.0 minutes)</b>	<b>102</b>

## **CHAPTER 1**

### **Introduction**

Every sediment particle that passes a given stream cross section must satisfy the following two conditions (Einstein, 1964): 1) It must have been eroded somewhere in the watershed above the cross section; 2) It must be transported by the flow from the place of erosion to the cross section.

#### **1.1 Background**

The presence of sediment in streams and rivers has its origin in soil erosion. Erosion encompasses a series of complex and interrelated natural processes that have the effect of loosening and moving away soil and rock materials under the action of water, wind, and other geologic agents. In the long term, the effect of erosion is the denudation of the land surface, i.e., the removal of soil and rock particles from exposed surfaces, their transport to lower elevations, and eventual deposition. Sediment has a threefold effect on the environment : a) depleting the productive capacity of the land from which it is transported; b) impairing the quality of the water in which it is transported and the land on which it is deposited; and c) carrying chemical and biological pollutants.

That accelerated soil erosion is a serious global problem is widely recognized. What are difficult to assess reliably and precisely, however, are the dimensions (the extent, magnitude, and rate) of soil erosion and its economic and environmental consequences.

Modeling soil erosion is the process of mathematically describing soil particle detachment, transport, and deposition on land surfaces. There are at least three reasons for modeling erosion : a) erosion models can be used as predictive tools for assessing soil loss for conservation planning, project planning, soil erosion inventories, and for regulation; b) physically-based mathematical models can predict where and when erosion is occurring, thus helping the conservation planner to target efforts to reduce erosion; c) models can be used as tools for understanding erosion processes and their interactions and for setting research priorities.

In the United States, the prediction of upland erosion amounts (i.e., sheet and rill erosion) is commonly made by the Universal Soil Loss Equation, USLE, developed by the United States Department of Agricultural, USDA, Research Service in cooperation with the USDA Soil Conservation Service and certain other state experiment stations. The original USLE method is only able to compute annual soil loss due to sheet and rill erosion in tons per acre per year. The USLE has been the workhorse of the erosion prediction and conservation planning technology in the U.S. and even worldwide. In 1985, at a meeting of the USDA and other erosion researchers, it was decided that the USLE should be revised to incorporate additional research and technology developed after the 1978 USLE handbook. The results of this effort was the Revised Universal Soil Loss Equation (RUSLE). While the RUSLE is an improvement over the USLE, it still only computes annual soil loss. This shortcoming was actually recognized in 1972 by Williams and Berndt. As a result, the Modified Universal Soil Loss Equation (MUSLE) was developed which computes sediment yield in tons for a single storm event. However, from field tests,

the use of the USLE equation to predict sediment yield on an event or event-series basis, resulted in rather large errors from those measured in the field (Smith, 1976).

As a result of the limitations and errors discussed above, an increasing number of scientists and engineers are turning to distributed hydrologic models. Recent advances in hydrology, soil science, erosion mechanics, and computer technology have provided the technological basis for the development of physically-based erosion prediction technology. Physically based models are one class of formal models of real systems in which the governing physical laws are well known and can be described by the equations of mathematical physics. Watershed runoff can be generated by several mechanisms, all of which can be described by the theory of unsaturated or saturated porous media flow. The equations of continuity and momentum provide a physically based model for unsteady free surface flow, and the diffusive approximation is usually appropriate for overland flow. Therefore, the development of detailed physically based models of the erosion-sedimentation process, which incorporates the talents of diverse interests such as engineers, hydrologists, and agronomists, will lead to improved understanding of the mechanics of soil detachment, transport, and deposition (Renard and Foster, 1983).

### **1.2 Research Objectives**

The objectives of this research are : 1) formulate a time-varying physically based two-dimensional upland erosion/transport scheme; 2) incorporate the upland scheme into the two-dimensional hydrology model, Cascade Two-Dimensions (CASC2D); 3) develop visualization capabilities to view the time and spatial varying erosion and sediment transport; and 4) test the model with field measurements.

Most physically-based upland erosion models in the past have used lumped techniques for their hydrologic modeling components, USLE techniques for the overland erosion scheme or erosion schemes that only erode a single grain size ( $D_{50}$ ), and no sediment transport from one overland cell to the next. This model will take advantage of the two-dimensional diffusive wave overland flow routing scheme present in CASC2D, and will erode and transport three size fractions (i.e., sand, silt, and clay) from one grid cell to the next.

In the past, hydrologic and sediment modelers were limited in the graphical tools available with which to manipulate input and output data. However, with the increase in computer speed and storage, graphical manipulation of input data and visualization of output data is now feasible. This research will develop the model in such a way that it can take advantage of existing GIS tools to help in the development of input data and the visualization of spatial and time varying output data.

## CHAPTER 2

### Literature Review

The literature review will be divided into four parts. Part 2.1 will focus on channel flow, Part 2.2 will focus on sediment transport in channels, Part 2.3 will focus on overland flow, and Part 2.4 will focus on upland erosion.

#### 2.1 Channel Flow

The mathematical description of channel flow begins with the equation of mass conservation of fluid mechanics, also referred to as the continuity equation. In one-dimension, this equation states that the change in flow per unit length (in the flow direction) in a control volume is balanced by the change in flow area per unit time :

$$\frac{\partial Q}{\partial x} + \frac{\partial A}{\partial t} = q_L \quad (2.1)$$

where  $q_L$  is lateral inflow or outflow depending upon the direction of lateral flow.

There are four methods for routing flows : 1) storage concept; 2) kinematic wave; 3) diffusive wave; 4) dynamic wave. In principle, the kinematic wave is an improvement over the storage concept. In turn, the diffusive wave is an improvement over the kinematic wave, whereas the dynamic wave is an improvement over the diffusive wave. Invariably, the effort involved in obtaining a solution increases in direct relation to the complexity of the governing equations, including initial and boundary conditions. Since the storage

concept is a rarely used method, this discussion will focus on the kinematic wave, diffusive wave, and dynamic wave routing methods.

### **2.1.1 Kinematic Wave**

According to the kinematic wave theory, the unit flow rate can be approximated by a single value flow depth rating at any point:

$$q = bh^m \quad (2.2)$$

where  $b$  and  $m$  are constants. Unlike Horton's approach (storage concept), which bases the rating on the storage volume on the entire plane, the kinematic wave approach bases the rating on flow depths at individual cross sections. This difference has substantial implications for computer modeling because whereas the Horton approach is lumped in space, the kinematic approach is not, and therefore is better suited to distributed computation.

### **2.1.2 Diffusive Wave**

According to diffusion wave theory, the flow depth gradient in the equation of motion is largely responsible for the diffusion mechanism, which is naturally present in unsteady free surface flows. Therefore, its inclusion in the analysis should provide runoff concentration with diffusion. For very low values of  $S_o$ , channel diffusivity grows and the kinematic wave approximation is no longer valid. However, for realistic mild channel slopes (approximately 0.001 to 0.0001), the contribution of the diffusion term can be quite significant. The diffusive wave approximation applies to channels with milder slopes for which kinematic wave theory is not sufficient.

### 2.1.3 Dynamic Wave

Kinematic waves were formulated by simplifying the momentum conservation principle to a statement of steady uniform flow. Diffusion waves were formulated by simplifying the equation of motion to a statement of steady nonuniform flow. A third type of wave is the dynamic wave. The dynamic wave formulation, equation 2.3, takes into account the complete equation of motion, including its inertial components. As such, the dynamic wave contains more physical information than either the kinematic or diffusion waves. However, the dynamic wave solution is more complicated than the kinematic or diffusion wave solutions. Dynamic wave solutions are particularly applicable to flow over very flat slopes, flow into large reservoirs, strong backwater conditions, and flow reversals.

$$\frac{\partial V}{\partial t} + V \frac{\partial V}{\partial x} + g \frac{\partial h}{\partial x} - g(S_o - S_f) = 0 \quad (2.3)$$

## 2.2 Channel Sediment Transport

Stream erosion and sediment transport equations may be modified and used in land erosion, because the mechanics of stream channel erosion and land erosion are complementary. From the hydraulic standpoint, understanding the mechanism of stream channel erosion is both a necessity and a great aid in understanding land erosion.

Noncohesive bed particles enter motion as soon as the shear stress applied on the bed material exceeds the critical shear stress. Generally, silt and clay particles enter suspension, while sand and gravel particles roll and slide in a thin layer near the bed. Therefore, two types of transport equations have been developed to describe the movement of sediment in the channel : 1) bedload equations; and 2) suspended load equations.



Early sediment transport equations were developed by such investigators as DuBoys (1879), Schoklitsch (1935), MacDougall (1934), Kalinske (1942), Meyer-Peter, Muller, and Colby (1947), and Bagnold (1966). They generally related the sediment discharge (bedload) to tractive forces, stream power, slope, flow rate, roughness, and particle properties. Any bedload transport equation for alluvial channels using tractive force or stream power methods may be modified for overland flow and used as a transport equation for land erosion.

As hydraulic forces exerted on sediment particles exceed the threshold condition for beginning of motion, coarse sediment particles move in contact with the bed surface. However, finer particles are brought into suspension when turbulent velocity fluctuations are sufficiently large to maintain the particles within the mass of fluid without frequent bed contact. The unit suspended sediment discharge,  $q_s$ , in natural streams and canals is computed from the depth-integrated advective flux of sediment,  $Cv_x$ , above the bed layer (Julien, 1995a) :

$$q_s = \int_a^h Cv_x dz \quad (2.4)$$

where  $a$  is a reference elevation above the bed elevation and  $h$  is the flow depth.

The corresponding total suspended sediment discharge,  $Q_s$ , is obtained from integration of the unit suspended sediment discharge over the entire width of the channel :

$$Q_s = \int_{width} q_s dw \quad (2.5)$$

The suspended load,  $L_s$ , defines the amount of sediment in suspension passing a cross section over a certain period of time :

$$L_s = \int_{\text{time}} Q_s dt \quad (2.6)$$

The total sediment load in a stream can be divided in three ways : 1) by the type of movement; 2) by the method of measurement; and 3) by the source of sediment. It must be recognized that it is virtually impossible to determine the total sediment load from any one equation.

Some of the more popular sediment transport equations are (Thomas et al., 1993; and Julien, 1995a) : 1) Ackers-White  $D_{50}$ , is a single grain function for sand bed streams; 2) Ackers-White, is a modification of Ackers-White  $D_{50}$  which has been modified at the Waterways Experiment Station (WES), for multiple grain size calculations on sand and/or gravel bed streams; 3) Brownlie (1981), is a single grain size function for sand transport; 4) Colby (1964), is a single grain size function for sand transport in streams and small rivers; 5) Laursen (Copeland) (1958), is a modification to Laursen's function to extend its range to larger gravel sizes; 6) Laursen (Madden) (1985), is a multiple grain size function developed by E. M. Laursen and modified by E. B. Madden for sand bed transport; 7) Meyer-Peter and Muller (MPM) (1948), is a multiple grain size function for gravel bed rivers. It is not valid when appreciable suspended load is present; 8) Toffaleti (1966), is a multiple grain size function for sand bed rivers. It is not valid for gravel transport; 9) Toffaleti-MPM (1966), is a combined function for sand and gravel bed streams. The sand portion is calculated by the Toffaleti function which is combined with the gravel portion calculated by MPM 1948; 10) Toffaleti-Schoklitsch (1966), is a combined function for sand and gravel bed streams. The sand portion is calculated by the Toffaleti function which is then combined with the gravel portion calculated by Schoklitsch; 11) Simon, Li,

and Fullerton (1981), is based on easy to apply power relationships that estimate sediment transport based on the flow depth and velocity. These power relationships were developed from a computer solution of the MPM bedload transport equation and Einstein's integration of the suspended bed sediment discharge; 12) Bagnold (1966), developed a sediment transport formula based on the concepts of energy balance which combines bedload and suspended load. He stated that the available power of the flow supplies the energy for sediment transport; 13) Engelund and Hansen (1967), applied Bagnold's stream power concept and the similarity principle to obtain a total bedload equation to compute the sediment concentration by weight; 14) Yang (1973), suggested that the total sediment concentration is related to potential energy dissipation per unit weight of water (stream power), which he expressed as the product of the velocity and slope. He developed one equation for sand and one equation for gravel to compute sediment concentration by weight; 15) Shen and Hung (1972), recommended a regression formula for total bedload based on available data for engineering analysis of sediment transport. They selected the sediment concentration as the dependent variable and the fall velocity, median diameter of bed material, flow velocity, and energy slope as independent variables; and 16) Karim and Kennedy (1981), developed a total bedload equation from carrying out a regression analysis on sediment data from laboratory and natural streams.

### **2.3 Overland Flow**

Overland flow is surface runoff that occurs in the form of sheet and rill flow on the land surface without concentrating in clearly defined channels. This type of flow is the first manifestation of surface runoff, since the latter occurs first as overland flow before it has a chance to flow into channels and become stream flow.

Overland flow theory uses deterministic methods to describe surface runoff in overland flow planes. The theory is based on established principles of fluid mechanics such as laminar and turbulent flow, mass and momentum conservation, and unsteady free surface flow. The spatial and temporal description leads to differential equations and to their solution by analytical or numerical means.

In small-catchment hydrology, overland flow is assumed to take place on the overland flow plane. This is a plane of length  $L$  (in the flow direction), slope  $S_o$ , and theoretically infinite width. Therefore, a unit-width analysis is appropriate. For a unit width, the equation of continuity for 1-D converts to (Ponce, 1989):

$$\frac{\partial q}{\partial x} + \frac{\partial h}{\partial t} = i \quad (2.7)$$

where,  $q$  is the flow rate per unit width,  $h$  is the overland flow depth, and  $i$  is the rainfall excess.

Thus, flow over the plane can be described as follows: As excess rainfall begins, water accumulates on the plane surface and begins to flow out of the plane at its lower end. Flow at the outlet gradually increases from zero, while the total volume of water stored over the plane also increases gradually. Eventually, if rainfall excess continues, both outflow and total volume of water stored over the plane reaches a constant value. These constants are referred to as equilibrium outflow and equilibrium storage volume. Immediately after excess rainfall ceases, outflow begins to draw water from storage, gradually decreasing while depleting the storage volume. Eventually, outflow returns to zero as the storage volume is completely drained.

Woolhiser and Kibler (1970), investigated the use of kinematic cascades to perform hydrologic routings. The cascade solutions were compared with characteristic-analytic solutions and with experimental data for flow over a linearly converging section. In 1971, Smith and Woolhiser investigated overland flow over an infiltrating surface. A nonlinear Crank-Nicholson implicit finite difference scheme was used to develop an equation solution that predicts infiltration under realistic upper boundary and soil matrix conditions. The kinematic wave approximation to the equations of unsteady overland flow on a cascade of planes were solved by a second order explicit difference scheme. The equations of infiltration and overland flow were combined into a simple watershed model in which boundary conditions match at the soil surface. The model was tested by comparing data from a 40 foot laboratory flume fitted with a rainfall simulator to data from the USDA-ARS experimental watershed at Hastings, NB. The results indicated that a theoretically-based model can be used to describe simple watershed response when appropriate physical parameters can be obtained. Singh and Woolhiser (1976) investigated a nonlinear kinematic wave model for watershed runoff. The kinematic flow on a converging surface was considered as a simple nonlinear model to describe watershed surface runoff. The converging overland flow model has 3 parameters; 2 are geometric parameters and 1 is a kinematic wave friction relationship parameter. The geometric parameters were determined from watershed topography, and a simple procedure for transforming the complex geometry of a natural watershed into an equivalent converging section geometry was developed. The kinematic wave friction relationship parameter was obtained by an optimization procedure. The model's utility was appraised by considering its application to several natural agricultural watersheds located in two geographically distinct regions. In

1977, Rovey, Woolhiser, and Smith, incorporated a parametric infiltration model with a surface routing model based upon a kinematic cascade of planes and channels to constitute a watershed model. Relationships were developed to compute flows by kinematic approximation in channels of circular cross section for routing through storm drains. The infiltration model was tested on some infiltrometer experiments; model parameters were estimated from measured data and by comparison to characteristics of soils used in previous studies. Morris and Woolhiser (1980) presented a comparison of solutions of the shallow water (Saint Venant) equations for unsteady one-dimensional flow over a plane and solutions of the diffusion and kinematic wave equations, which are approximations of the Saint Venant equations.

All of the previously mentioned work involved kinematic routing over square grids of uniform size. In 1991, Goodrich, Woolhiser, and Keefer developed a model that performed kinematic routing using finite elements on a triangular irregular network. The results indicated that shock conditions were readily handled, computed depths match analytic results to within 3% and volume balances were typically within 1%. The final conclusion was that this model illustrates the viability of kinematic routing over a TIN DEM derived directly from digital mapping data.

In 1991, Julien and Saghafian, developed a two-dimensional rainfall-runoff watershed model (CASC2D). CASC2D is a physically based model that consists of infiltrating planes, two-dimensional diffusive overland routing, and one-dimensional diffusive channel routing. This model has been tested and has proven to be more accurate when modeling ungaged watersheds than the typically used lumped models (Johnson, 1993).

## 2.4 Upland Erosion

A quantitative analysis of the amount of sediment supplied to a stream from the watershed is usually difficult to perform because of the complexity of the physical processes involved and the spatial and temporal variability of all the parameters describing upland erosion, local rainstorms, and bank erosion processes.

The analysis of sediment sources aims at estimating the total amount of sediment eroded on the watershed on an annual basis, called “annual gross erosion”. The annual gross erosion,  $A_T$ , depends on the source of sediments in terms of upland erosion ( $A_U$ ), gully erosion ( $A_G$ ), and local bank erosion ( $A_B$ ); thus,  $A_T = A_U + A_G + A_B$ .

Erosion and sedimentation by water embody the processes of detachment, transportation, and deposition of soil particles by the erosive and transport agents of raindrop impact and runoff over the soil surface (ASCE 1975). The major factors affecting upland erosion processes are : Hydrology, Topography, Soil Erodibility, Soil Transportability, Cover, Incorporated Residue, Residual land use, Subsurface Effects, Tillage, Roughness, and Tillage Marks (Foster, 1982).

The main concept for modeling upland erosion is that sediment load is controlled by either the amount of sediment made available for transport by the detachment processes or by the transport capacity of the transport agents (Meyer and Wischmeier, 1969). The continuity equation normally used in dynamic upland erosion models is (Bennett, 1974) :

$$\frac{\partial q_s}{\partial x} + \rho_s \frac{\partial (cy)}{\partial t} = D_r + D_i \quad (2.8)$$

where,

$q_s$  = sediment load (mass per unit width per unit time)

$x$  = distance along the slope

$\rho_s$  = mass density of the sediment particles

$c$  = concentration of the sediment in the flow (volume of sediment per volume of flow)

$y$  = flow depth

$t$  = time

$D_r$  = rill erosion rate (mass per unit area per unit time)

$D_i$  = delivery rate of sediment from interrill areas (mass per unit area per unit time)

In some cases, quasi-steady sediment movement may be assumed; this reduces the continuity equation to (Curtis, 1976; Foster and Huggins, 1977; Thomas, 1976) :

$$\frac{dq_s}{dx} = D_r + D_i \quad (2.9)$$

Flow depth  $y$  in equation (2.8) is assumed to be available from other hydrologic computations, but  $q_s$ ,  $D_r$ , and  $D_i$  are not independent variables. Rill detachment (or deposition)  $D_r$  may be assumed to be directly proportional to the difference between the sediment transport capacity and sediment load or (Foster and Meyer, 1975; Simons et al., 1977) :

$$D_r = \alpha(T_c - q_s) \quad (2.10)$$

where  $\alpha$  is a first order reaction coefficient for deposition and  $T_c$  is the flow transport capacity. Foster and Meyer (1972a) developed the equation for erosion as :

$$\frac{D_r}{D_{rc}} + \frac{q_s}{T_c} = 1 \quad (2.11)$$

where  $D_{rc}$  is the rill erosion detachment capacity rate (mass per unit area per unit time). Maximum rill erosion rate is assumed to occur when there is no sediment load. The coefficient  $\alpha$  for erosion is given by  $D_{rc}/T_c$ .



Equations (2.10) and (2.11) introduce the concept that sediment load may be different from transport capacity. Deposition by flow occurs when sediment load exceeds transport capacity. Detachment by flow can occur when transport capacity exceeds sediment load. Detachment capacity can be defined based on the local conditions but the actual detachment rate depends on the degree to which the transport capacity is filled (Foster, 1982).

Equations (2.10) and (2.11) are most applicable to the deposition of suspended load. They have been reasonably well validated by Einstein (1968) for deposition of suspended silt and gravel beds in channel flow and by Foster and Huggins (1977) and Davis (1978) for deposition by overland flow. The equation is less well validated for erosion, although Apmann and Rumer (1970) did show a similar effect for erosion and suspension of noncohesive sediment. The equations are a simplification of the more complete continuity equation having terms for dispersion.

No general solution to equations (2.8) through (2.11) exists. Consequently, in the most general case, the equations are solved numerically. However, in some cases for both steady and unsteady conditions, analytical solutions are possible. Also, complex problems can sometimes be reduced to a form where analytical solutions apply (Foster, 1982).

The Universal Soil Loss Equation (USLE) is the most widely used empirical overland flow or sheet-rill erosion equation (Wischmeier and Smith, 1978). The equation was originally developed as a tool for soil conservationists to use in developing farm management plans to control erosion and maintain soil productivity. The USLE is given by:

$$A = RKLSCP \quad (2.12)$$

where A is the annual soil loss averaged over the soil length, R is the combined erosivity of rainfall and runoff, K is the soil erodibility factor, LS is the length-slope factor, C is the crop management factor, and P is the conservation practice factor.

Sediment yield is sometimes estimated by estimating gross erosion with the USLE and then multiplying by a delivery ratio to obtain sediment yield (ASCE, 1975). For small watersheds, especially fields, this method is often inadequate and can lead to totally false conclusions. As a result, fundamental models have several advantages over empirical equations (Foster, 1982) : 1) they are generally more physically based and consequently can be more accurately extrapolated; 2) they more accurately represent the processes, for example, rill and interrill erosion are considered separately rather than being lumped; 3) they are more accurate for single event storms; 4) they can consider more complex areas; 5) they consider deposition processes directly; and 6) they can consider channel erosion and deposition. Four models that are currently being developed by the USDA are the AGNPS, SWAT, ANSWERS, and WEPP.

The European Soil Erosion Model (EUROSEM) is a cooperative model-building project of the European Community with collaborating scientists in seven countries and purpose built runoff plots for validating the model in England and in Spain (Morgan et al 1992, Quinton and Morgan 1993).

Recently a Digital Elevation Map (DEM) based physically distributed model was developed for simulating event runoff and erosion on an agricultural watershed (Wang and Hjelmfelt, 1996). Runoff is described using the diffusion equation with flow links

determined from the DEM. Interrill soil loss was estimated using rainfall intensity raised to a power and transport by a transport capacity deficit relationship.

#### **2.4.1 AGNPS**

The Agricultural Non-Point Source Pollution Model (AGNPS) is a grid based computer model developed by the USDA. AGNPS is a single event model that estimates runoff, sediment yield, and nutrient runoff from watersheds up to several thousand acres in size. AGNPS uses the SCS curve number method (lumped method) to obtain runoff depth. AGNPS uses a modified version of the USLE (not MUSLE) to obtain erosion and uses five sediment classes in its computations (clay, silt, small and large aggregates, and sand). Since a modified USLE is used for overland erosion estimation, it is likely that transport between grid cells is not explicitly considered.

#### **2.4.2 SWAT**

Like AGNPS, the Soil and Water Assessment Tool (SWAT) is a grid erosion model developed by the USDA with a water quality emphasis. Unlike AGNPS, SWAT is a continuous model based on the Simulator for Water Resources in Rural Basins (SWRRB) lumped model. SWAT can accommodate hundreds of cells, operates on daily time steps, and can simulate a one hundred year span of time for watershed of thousands of square miles. Runoff volume is determined by the SCS curve number approach and the peak discharge is determined by the rational method. SWAT uses the MUSLE to determine erosion. Sediment is not divided into classes, but is represented by the  $D_{50}$  size.

#### **2.4.3 ANSWERS**

Areal Nonpoint Source Watershed Environment Response Simulation (ANSWERS) is quite different from other grid erosion models in that it makes a physical computation of

upland erosion, rather than using USLE or MUSLE. ANSWERS is a single event grid model that can be used on watersheds of several thousand acres. ANSWERS computes infiltration of precipitation physically, and from continuity obtains runoff. Peak discharge is obtained from an accounting of the runoff occurring within a time increment. Overland erosion is computed from detachment caused by raindrops and overland flow, as determined by the Meyer and Wischmeier equations while transport capacity is determined by the Yalin equation.

#### **2.4.4 WEPP**

The USDA - Water Erosion Prediction Project (WEPP) model represents a new erosion prediction technology based on fundamentals of stochastic weather generation, infiltration theory, hydrology, soil physics, plant science, hydraulics, and erosion mechanics. The hillslope or landscape profile application of the model provides major advantages over existing erosion prediction technology. The most notable advantages include capabilities for estimating spatial and temporal distributions of soil loss (net soil loss for an entire hillslope or for each point on a slope profile can be estimated on a daily, monthly, or average annual basis), and since the model is process-based it can be extrapolated to a broad range of conditions that may not be practical or economical to field test.

Processes considered in hillslope profile model applications include rill and interrill erosion, sediment transport and deposition, infiltration, soil consolidation, residue and canopy effects on soil detachment and infiltration, surface sealing, rill hydraulics, surface runoff, plant growth, residue decomposition, percolation, evaporation, transpiration, snow melt, frozen soil effects on infiltration and erodibility, climate, tillage effects on soil

properties, effects of soil random roughness, and contour effects including potential overtopping of contour ridges. The model accommodates the spatial and temporal variability in topography, surface roughness, soil properties, crops, and land use conditions on hillslopes.

In watershed applications, WEPP allows linkage of hillslope profiles in channels and impoundments. Water and sediment from one or more hillslopes can be routed through a small field scale watershed. Almost all of the parameter updating for hillslopes is duplicated for the channels. The model simulates channel detachment, sediment transport and deposition. Impoundments such as farm ponds, terraces, culverts, filter fences and check dams can be simulated to remove sediment from the flow.

The WEPP erosion model computes soil loss along a slope and sediment yield at the end of a hillslope. Interrill and rill erosion processes are considered. Interrill erosion is described as a process of soil detachment by raindrop impact, transport by shallow sheet flow, and sediment delivery to rill channels. Sediment delivery rate to rill flow areas is assumed to be proportional to the product of rainfall intensity and interrill runoff rate. Rill erosion is described as a function of the flow's ability to detach sediment, sediment transport capacity, and the existing sediment load in the flow.

Overland flow processes, within WEPP, are conceptualized as a mixture of broad sheet flow occurring in interrill areas and concentrated flow in rill areas. Broad sheet flow on an idealized surface is assumed for overland flow routing and hydrograph development. Overland flow routing procedures include both an analytical solution to the kinematic wave equations and regression equations derived from the kinematic approximation for a range of slope steepness and lengths, friction factors (surface

roughness coefficients), soil texture classes, and rainfall distributions. Because the solution to the kinematic wave equations are restricted to an upper boundary condition of zero depth, the routing process for strip cropping (cascading planes) uses the concept of the equivalent plane. Once the peak runoff rate and the duration of runoff have been determined from the overland flow routing, or by solving the regression equations to approximate the peak runoff and duration, steady-state conditions are assumed at the peak runoff rate for erosion calculations. Runoff duration is calculated so as to maintain conservation of mass for total runoff volume.

The erosion equations are normalized to the discharge of water and flow shear stress at the end of a uniform slope and are then used to calculate sediment detachment, transport, and deposition at all points along the hillslope profile. Net detachment in a rill segment is considered to occur when hydraulic shear stress of flow exceed the critical shear stress of the soil and when sediment load in the rill is less than sediment transport capacity. Net deposition in a rill segment occurs whenever the existing sediment load in the flow exceeds the sediment transport capacity.

In watershed applications, detachment of soil in a channel is predicted to occur if the channel flow shear stress exceeds a critical value and the sediment load in the flow is below the sediment transport capacity. Deposition is predicted to occur if channel sediment load is above the flow sediment transport capacity. Flow shear stress in channels is computed using regression equations that approximate the spatially varied flow equations. Channel erosion to a nonerodible layer and subsequent channel widening can also be simulated. Deposition within and sediment discharge from impoundments is modeled using conservation of mass and overflow rate concepts.

The appropriate scales for application, of the WEPP model, are tens of meters for hillslope profiles, and up to hundreds of meters for small watersheds. For scales greater than 100 meters, a watershed representation is necessary to prevent erosion predictions from becoming excessively large.

Expected users of the WEPP model include all current users of the USLE. Anticipated applications include conservation planning, project planning, and inventory assessment. WEPP model overland flow profile simulations are applicable to hillslopes without concentrated flow channels, while watershed simulations are applicable to field situations with multiple profiles, channels (such as ephemeral gullies, grassed waterways, terraces), and impoundments (Foster and Lane, 1987). The length of the representative profile to which the WEPP hillslope model components can be applied depends upon the topography and land use controlling stream channel density.

#### **2.4.5 EUROSEM**

The objective of EUROSEM are : 1) assess erosion on field and catchment scales; 2) assess pollution by sediment or solutes to water bodies; 3) operate on an event basis; 4) be useful as a design tool for selecting soil protection measures.

Within EUROSEM, rainfall is assessed by the amount of interception by vegetative cover and proportions of intercepted rainfall reaching the ground as stemflow or leaf drip. Soil surface condition is based on quantifying roughness to assess surface storage. Runoff generation is separated into two components : 1) surface depression; and 2) stream flow. The hydrologic model simulates runoff as both Hortonian and saturation flow expressed as a depth. Soil detachment by raindrop impact is assessed from the kinetic energy of the throughfall and separately the energy of leaf drip from the canopy. Soil detachment by

runoff is assessed from a comparison of the estimated velocity of runoff compared with critical velocity required to detach soil particles, modeled as a function of grain shear velocity. Transport capacity is modeled as a function of stream power defined as the product of flow velocity and slope. Finally, a comparison is made of the availability of detached soil for transport, and the transport capacity of flow, done separately for flow in depressions and for surface flow. In each case, there can be net erosion or deposition.

#### **2.4.6 Wang-Hjelmfelt**

Wang (1995) used the DEM to delineate drainage patterns for the Goodwater Creek watershed, located in Missouri, to create an attribute file as input for this model. The attribute file includes cell sequence order from upstream to downstream, land slope, flow direction, receiving cells, and cell type (channel cell or overland flow cell).

The mathematical equations governing the shallow flows are the St. Venant equations. The diffusion wave approximation to the equations is used in this model. Water caused erosion and sedimentation involve processes of detachment, transportation, and deposition of soil particle by raindrop impact and runoff from the soil surface. Soil erosion is modeled using rainfall intensity raised to a power for estimating interrill detachment and a transport capacity deficit relation for rill detachment. In this model, the two approaches are coupled with the diffusion wave runoff model to route sediment transport in a watershed.

From a study performed on the Goodwater Creek watershed, the DEM based hydrologic and sediment transport model was developed and its application demonstrated. Manning's roughness coefficient was calibrated using twenty six events, and the calibrated model was verified using six events. Simulated results indicated that the physically based diffusion model is acceptable for Goodwater Creek, a very flat watershed in central



Missouri. The model parameters for sediment transport were calibrated, and model predictions were investigated using six storm events during 1993. The model results showed good agreement between observed data and computed results (Wang and Hjelmfelt, 1996).

Table 2.1 - Upland Erosion Model Comparisons

Model	Grid/Tin	Hydrology	Erosion	Single/Annual
AGNPS	Grid	Lumped Method	USLE	Annual
SWAT	Grid	Lumped Method	MUSLE	Single
ANSWERS	Grid	One-Dimension Kinematic Wave	1D - Physical Processes	Single
WEPP	Grid	One-Dimension Kinematic Wave	1D - Physical Processes	Single
EUROSEM	Grid	One-Dimension Kinematic Wave	1D - Physical Processes	Single
WANG-HJELMFELT	Tin	One-Dimension Diffusive Wave	1D - Physical Processes	Single
CASC2D	Grid	Two-Dimension Diffusive Wave	2D - Physical Processes	Single

## CHAPTER 3

### Approach and Methodology

#### 3.1 Surface Hydrology

Surface hydrology consists of those processes that describe the distribution of rainfall, infiltration of the rainfall into the ground, and the routing of excess rainfall across the overland planes into the channels and ultimately to the watershed outlet.

##### 3.1.1 Spatial Rainfall Distribution

When analyzing rainfall data from rainfall gages, an interpolation scheme based on the inverse distance squared approximates the distribution of rainfall intensity over the watershed :

$$i'(j,k) = \frac{\sum_{m=1}^{NRG} \frac{i_m^t(jrg, krg)}{d_m^2}}{\sum_{m=1}^{NRG} \frac{1}{d_m^2}} \quad (3.1)$$

where,

$i'(j,k)$  = rainfall intensity in element (j,k) at time t.

$i_m^t(jrg, krg)$  = rainfall intensity recorded by the m-th rainfall gages located at (jrg, krg).

$d_m$  = distance from element (j,k) to m-th raingage located at (jrg, krg).

NRG = total number of rainfall gages

### 3.1.2 Infiltration

The Green-Ampt infiltration scheme has gained considerable attention in the past decade (Philip, 1983), partially due to the ever growing trend towards physically based hydrologic modeling. The parameters of the Green-Ampt equation are based on the physical characteristics of the soil and therefore can be determined by field measurements or experiments. The Green-Ampt equation may be written as (Philip, 1983):

$$f = K_s \left( 1 + \frac{H_f M_d}{F} \right) \quad (3.2)$$

where,

$f$  = infiltration rate

$K_s$  = hydraulic conductivity at normal saturation

$H_f$  = capillary pressure head at the wetting front

$M_d$  = soil moisture deficit equal to  $(\theta_e - \theta_i)$

$\theta_e$  = effective porosity equal to  $(\phi - \theta_r)$

$\phi$  = total soil porosity

$\theta_r$  = residual saturation

$\theta_i$  = initial soil moisture content

$F$  = total infiltration depth

The head due to surface depth has been neglected as  $H_f$  easily overpowers shallow overland depth.

### 3.1.3 Overland Flow

The Saint-Venant equations of continuity and momentum describe the mechanics of overland flow : The two-dimensional continuity equation in partial differential form reads

as :

$$\frac{\partial h}{\partial t} + \frac{\partial q_x}{\partial x} + \frac{\partial q_y}{\partial y} = i_e \quad (3.3)$$

where,

$h$  = surface flow depth

$q_x$  = unit flow rate in the x-direction

$q_y$  = unit flow rate in the y-direction

$i_e$  = excess rainfall equal to  $(i-f)$

$i$  = rainfall intensity

$f$  = infiltration rate

$x, y$  = cartesian spatial coordinates

$t$  = time

The momentum equation in the x and y direction may be derived by equating the net forces per unit mass in each direction to the acceleration of flow in the same direction. The two-dimensional form of the equations of motion are :

$$\frac{\partial u}{\partial t} + u \frac{\partial u}{\partial x} + v \frac{\partial u}{\partial y} = g(S_{ox} - S_{fx} - \frac{\partial h}{\partial x}) \quad (3.4)$$

$$\frac{\partial v}{\partial t} + u \frac{\partial v}{\partial x} + v \frac{\partial v}{\partial y} = g(S_{oy} - S_{fy} - \frac{\partial h}{\partial y}) \quad (3.5)$$

where,

$u, v$  = average velocities in the x and y directions

$S_{ox}, S_{oy}$  = bed slopes in the x and y directions

$S_{fx}, S_{fy}$  = friction slopes in the x and y directions

$g$  = acceleration due to gravity

The right hand side of the momentum equations describes the net forces along the x and y directions, while the left hand side represents the local and convective acceleration terms.

In simplifying the momentum equations, the kinematic wave approximation assumes that all terms, except the bed slope and the friction slope, are negligible. This assumption which is particularly valid for steep bed slopes, has been the basis for many rainfall-runoff models. Kinematic wave, however, can not predict backwater effects due to downstream disturbances that may be important when simulating floods (Beven, 1985). On the other

hand, diffusive wave can simulate backwater effects and is considered to be applicable for overland flow over rough surfaces and for channel flows. The momentum equation based on the diffusive wave approximation reduces to :

$$S_{fx} = S_{ax} - \frac{\partial h}{\partial x} \quad (3.6)$$

From the three equations of continuity and momentum, five hydraulic variables need to be determined. Therefore, a resistance law should be established to relate flow rate to depth and to other parameters. A general depth-discharge relationship may be written, in the x-direction as :

$$q_x = \alpha_x h^\beta \quad (3.7)$$

where  $\alpha_x$  and  $\beta$  are parameters which depend on flow regime; i.e. laminar or turbulent.

For laminar flow in the x-direction :

$$\alpha_x = \frac{8g}{K\nu} S_{fx} \quad (3.8)$$

$$\beta = 3 \quad (3.9)$$

where  $K$  = resistance coefficient, and  $\nu$  = kinematic viscosity. Similarly, for turbulent flow over a rough boundary, the Manning empirical resistance equation is used :

$$\alpha_x = \frac{S_{fx}^{1/2}}{n} \quad (3.10)$$

$$\beta = \frac{5}{3} \quad (3.11)$$

where  $n$  = Manning's roughness coefficient.

### 3.1.4 Channel Flow

The governing equations are similar to those of overland flow except for a finite width.

The one dimensional equation of continuity reads as follows :

$$\frac{\partial A}{\partial t} + \frac{\partial Q}{\partial x} = q_l \quad (3.12)$$

where,

A = channel flow cross section

Q = total discharge in the channel

$q_l$  = lateral inflow rate per unit length, into or out of the channel

Most cases of channel flow occur in the turbulent flow regime. The following equation represents the application of Manning's resistance equation to channel flow :

$$Q = \frac{1}{n} AR^{\frac{2}{3}} S_f^{\frac{1}{2}} \quad (3.13)$$

where,

R = hydraulic radius

$S_f$  = friction slope

### 3.2 Upland Erosion

Langhaar (1967) defined dimensional analysis as a treatment of general forms of equations that describe natural phenomena. It has been used in all fields of engineering, especially in fluid mechanics and hydraulics. The application of dimensional analysis to any particular phenomena is based on the assumption that certain variables, which are named, are the independent variables of the problem, and that all variables, other than these and the dependent variables, are redundant or irrelevant. The purpose of dimensional analysis is to reduce information about a phenomena from a single premise, which is that the phenomena can be described by a dimensionally correct equation among certain variables.

Sediment discharge by means of overland flow is a function of the hydraulic properties of flow, the physical properties of soil, and surface characteristics. Sediment transport as a result of erosion under simulated rainfall can be assumed to be related to a number of different variables. Elimination of some of the variables is possible since some are closely related to others, some are redundant, and some have relatively less effect than others on sediment discharge. Therefore, sediment transport is related to the following variables :

$$q_s = \phi(u, q_o, d, d_{50}, X, \nu, g, \rho, \rho_s, S_o, P) \quad (3.14)$$

where,

$q_s$  = unit sediment discharge

$u$  = longitudinal mean velocity

$q_o$  = unit discharge

$d$  = flow depth

$d_{50}$  = grain size at which 50 percent of the particles are finer than the indicated size

$X$  = longitudinal distance

$\nu$  = kinematic viscosity of water

$g$  = gravity

$\rho$  = mass density of water

$\rho_s$  = mass density of solid particles

$S_o$  = bed slope

$P$  = porosity

In 1972 (Kilinc and Richardson) the mechanics of soil erosion from overland flow generated by simulated rainfall were studied experimentally and analytically. The experiments were conducted in a 4' deep, 5' wide, and 16' long flume at the Colorado State University Engineering Research Center. The results of this investigation resulted in the following sediment transport equation for sheet and rill erosion for bare sandy soil :

$$q_s = 25500q_o^{2.035}S_o^{1.664} \quad (3.15)$$

where  $q_s$  is in the units of (tons/m x s).

Considering various soil types, vegetation, cropping factors, and conservation practices yields the following equation (Julien, 1995a) :

$$q_s = 25500q_o^{2.035} S_o^{1.664} \frac{K}{0.15} CP \quad (3.16)$$

where K, C, and P are USLE coefficients.

The approach that is being used in this research is to use the modified Kilinc and Richardson equation to determine the sediment transport, transport the sediment from one overland grid cell to the next by three grain sizes (i.e., sand, silt, and clay), and then determine how much sediment stays in suspension and how much deposits on the receiving cell. In this scheme, the sediment transported out of a grid cell will first be assumed to come from sediment already in suspension, second from previously deposited sediment, and lastly from the soil surface (Figure 3.1).

### 3.3 Numerical Formulation

As mentioned above, the upland erosion scheme will take advantage of the overland flow routing in CASC2D.

Application of a first order approximation to the continuity equation for element (j,k) results in (Julien et al., 1995b) :

$$h^{t+\Delta t}(j,k) = h^t(j,k) + i_s \Delta t - \left[ \frac{q'_x(k \rightarrow k+1) - q'_x(k-1 \rightarrow k)}{W} + \frac{q'_y(j \rightarrow j+1) - q'_y(j-1 \rightarrow j)}{W} \right] \Delta t \quad (3.17)$$



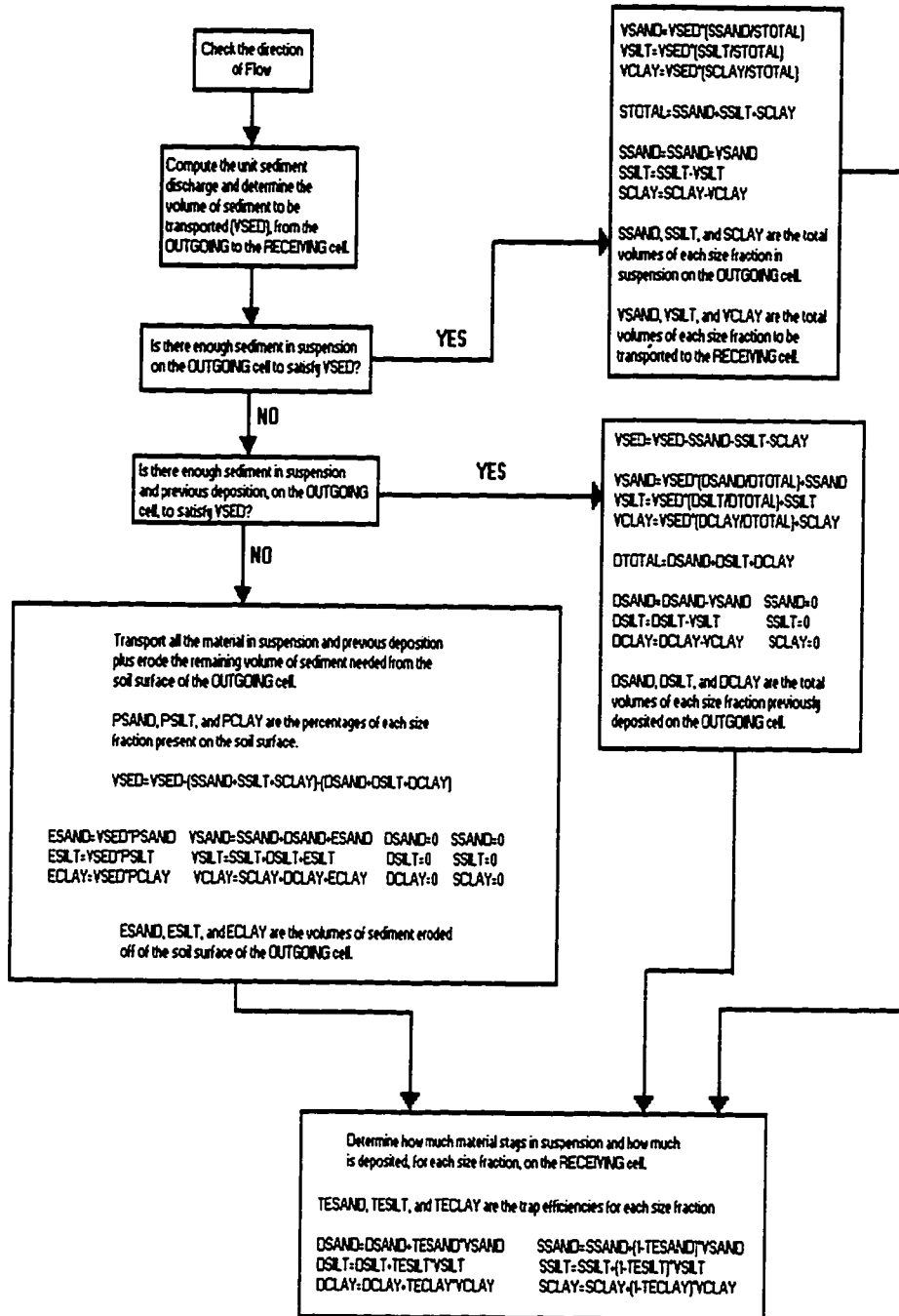


Figure 3.1 - Flow Chart for the Upland Erosion Scheme.

where  $h^{t+\Delta t}(j,k)$  and  $h^t(j,k)$  denote flow depths at the element  $(j,k)$  at  $t+\Delta t$  and  $t$ , respectively;  $i_e$  is the average excess rainfall rate over one time step beginning from time  $t$ ;  $q_x^t(k \rightarrow k+1)$  and  $q_x^t(k-1 \rightarrow k)$  describe unit flow rates in the x-direction at time  $t$ , from  $(j,k)$  to  $(j,k+1)$ , and from  $(j,k-1)$  to  $(j,k)$  consecutively; likewise  $q_y^t(j \rightarrow j+1)$ ,  $q_y^t(j-1 \rightarrow j)$  denotes unit flow rates in the y-direction at time  $t$ , from  $(j,k)$  to  $(j+1,k)$ , and from  $(j-1,k)$  to  $(j,k)$  respectively; and  $W$  = grid size.

The momentum equation in the x and y directions may be derived by relating the net forces per unit mass to flow acceleration. The diffusion wave approximation of the momentum equation in the x-direction is :

$$S_{fx} = S_{\alpha x} - \frac{\partial h}{\partial x} \quad (3.18)$$

where  $S_{fx}$  = friction slope in the x-direction; and  $S_{\alpha x}$  = land surface slope in the x-direction. With reference to Figure 3.2, the land surface slope in the x and y directions is calculated as the difference in the elevation between two adjacent cells divided by the grid size,  $W$ .

The unit discharge at any position and any time depends primarily upon the flow direction, which is determined by the sign of the friction slope. For example, in the x-direction, first the friction based upon the diffusive wave approximation is computed as :

$$S_{fx}^t(k-1 \rightarrow k) = S_{\alpha x}(k-1 \rightarrow k) - \frac{h^t(j,k) - h^t(j,k-1)}{W} \quad (3.19)$$

in which the bed slope is given by :

$$S_{\alpha x}(k-1 \rightarrow k) = \frac{E(j,k-1) - E(j,k)}{W} \quad (3.20)$$

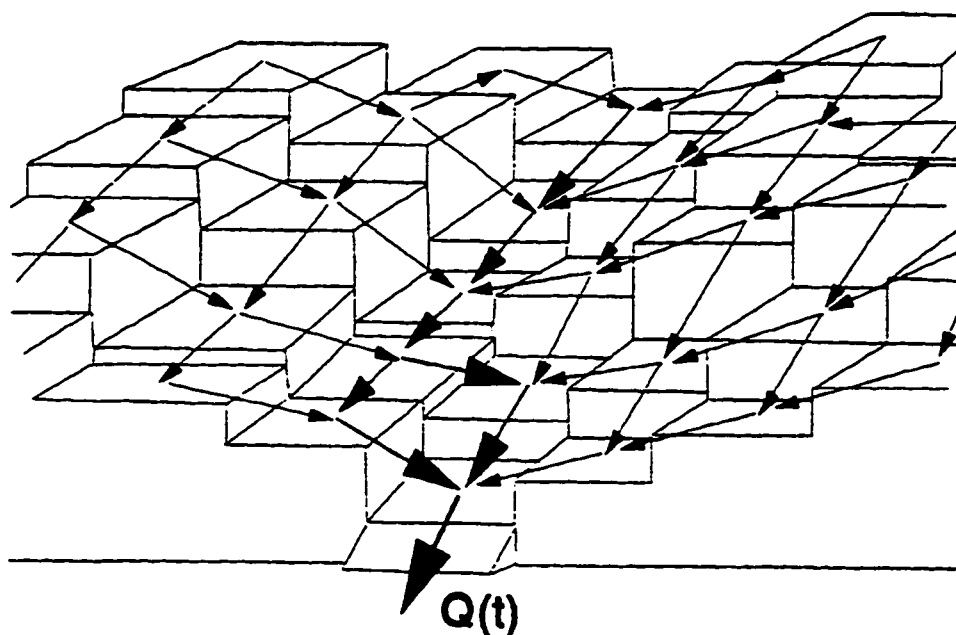


Figure 3.2 - Topographical Representation in Overland Flow Routing Scheme.

where  $E$  represents the ground surface elevation of the element, and the arrows imply the computational direction. From the three equations of continuity and momentum, five hydraulic variables must be determined. Therefore, a resistance law in terms of depth-discharge relationship is required (Equation 3.7). For turbulent flow over a rough boundary, the Manning resistance equation, in SI units, is used (Equations 3.10-3.11).

Therefore the calculated unit discharge and unit sediment discharge for turbulent flow is given by :

for  $S_{fx}(k-1 \rightarrow k) \geq 0$

$$q'_x(k-1 \rightarrow k) = \frac{1}{n(j, k-1)} [h'(j, k-1)]^{\frac{5}{3}} \quad (3.21)$$

$$q'_{sx}(k-1 \rightarrow k) = e^{11.727} q'_x(k-1 \rightarrow k)^{2.035} S_{ox}(k-1 \rightarrow k)^{1.664} \frac{K}{0.15} CP \quad (3.22)$$

where  $q_x$  implies unit discharge and  $q_{sx}$  implies unit sediment discharge in the x-direction at time t from (j,k-1) to (j,k).

For  $S_{ox}(k-1 \rightarrow k) < 0$

$$q'_x(k-1 \rightarrow k) = \frac{-1}{n(j,k)} [h'(j,k)]^{\frac{5}{3}} \quad (3.23)$$

$$q'_{sx}(k-1 \rightarrow k) = -e^{11.727} q'_x(k-1 \rightarrow k)^{2.035} S_{ox}(k-1 \rightarrow k)^{1.664} \frac{K}{0.15} CP \quad (3.24)$$

where equation (3.23) and equation (3.24) corresponds to a negative friction slope, negative unit discharge, and negative unit sediment discharge respectively, thus implying that the flow direction is actually from (j,k) to (j,k-1).

The unit discharge and unit sediment discharge in the y-direction are calculated based on the sign of the friction slope in the y-direction. Once the direction of flow and the unit sediment discharge have been computed, the upland erosion is broken down into three size fractions (sand, silt, and clay) and routed based upon how much sediment is in suspension, previous deposition, and how much sediment has been eroded from the soil surface (Figure 3.3). In determining how much sediment is transported from the outing cell, the model first gives priority to the volume of sediment in suspension, secondly to the volume of sediment in previous deposition, and lastly the remaining volume of sediment, is eroded from the soil surface. In order to determine how much sediment stays in suspension and how much is deposited on the receiving cell, the trap efficiency for each size fraction must be computed :

$$T_{E_i} = 1 - e^{-\frac{X\omega_i}{hV}} \quad (3.25)$$

where,

$T_{E_i}$  = trap efficiency for each size fraction

$X$  = longitudinal length

$\omega_i$  = fall velocity for each size fraction

$h$  = flow depth

$V$  = flow velocity

The trap efficiency indicates how much sediment drops out for each size fraction, thus the remaining volume of sediment is assumed to stay in suspension.

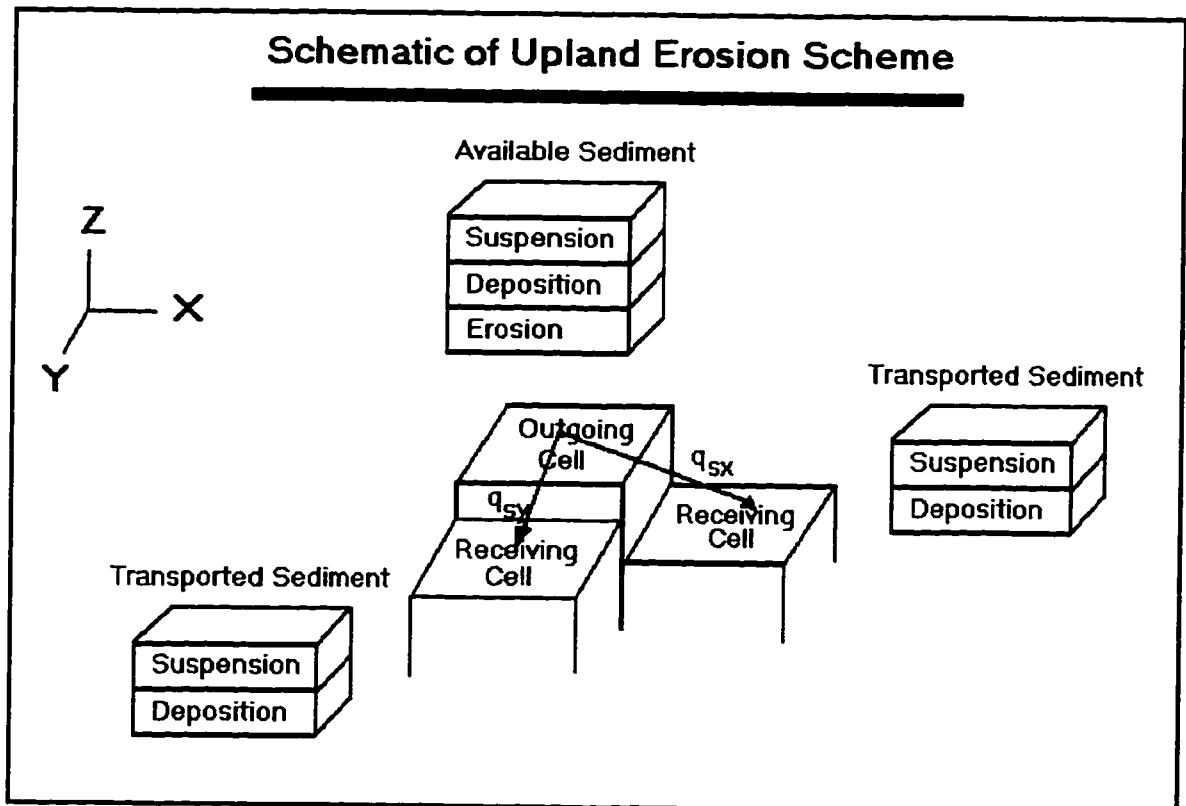


Figure 3.3 - Schematic of Upland Erosion Scheme

### 3.4 GIS Integration

The GIS that was used to develop input data for CASC2D and to visualize output data from CASC2D for the purpose of calibration and verification was the Geographical Resource Analysis Support System (GRASS) version 4.1.

GRASS4.1 was originally developed by the researchers at the U.S. Army Construction Engineering Research Laboratories (USACERL) located in Champaign, Illinois. The GRASS system is used by both military, non-military, public, and private agencies based in North America, Europe, and other parts of the world. The GRASS GIS system has the capability to handle both raster (grid) files and vector (line) files. GRASS has excellent data manipulation and visualization tools that greatly enhanced this research effort.

In recent times, the linkage of GIS to hydraulic and hydrologic models has become more popular due to faster computers, more storage space for large amounts of data, and more availability of geographic data such as elevation grids, land use grids, and soil texture grids. Some recent efforts in linking GIS to models are : 1) Chansheng (1993) integrated a GIS with a computer model to evaluate the impacts of agricultural runoff on water quality; 2) Tachikawa (1994) developed a basin geographic information system using a TIN structure; 3) Vieux (1991) has been working on adding a one-dimensional upland erosion model to the GRASS GIS; and 4) Nelson (1994) has been working on the development of a watershed modeling system that will import both raster and vector data for use in a number of different hydraulic and hydrologic models.

## **CHAPTER 4**

### **Observed Data**

#### **4.1 - Nelson Farm Test Plot**

In 1987, the USDA-ARS National Sedimentation Laboratory (NSL), in cooperation with Mississippi Agriculture and Forestry Experiment Station (MAFES), and Mississippi personnel of the USDA-NRCS, initiated interdisciplinary research to develop economically profitable and environmentally sustainable conservation production systems for silty upland soil resource areas.

Research was conducted at the A.E. Nelson Farm to determine the conservation and economic impacts of alternative soybean cropping systems on field-size areas within DEC watersheds. Runoff and sediment yield were monitored on three watersheds (WS), ranging from 5 to 8 acres in size with slopes averaging 4% and ranging from 1% to 8%, that were planted with soybean (Figure 4.1) (Dabney et al., 1997).

Runoff and sediment yield from natural rainfall were measured on three watersheds starting in 1989. Soils were primarily Grenada silt loam (fine silty, mixed, thermic Glossic Fragiudalf), with some areas of Memphis and Loring series. Runoff was gaged with 2-ft Parshall flumes equipped with a calibrated potentiometer attached to a stilling-well float. Discharge-weighted runoff samples were collected with peristaltic samplers programmed to pump an aliquot for every 0.02 inches of runoff. Six aliquots were accumulated in each

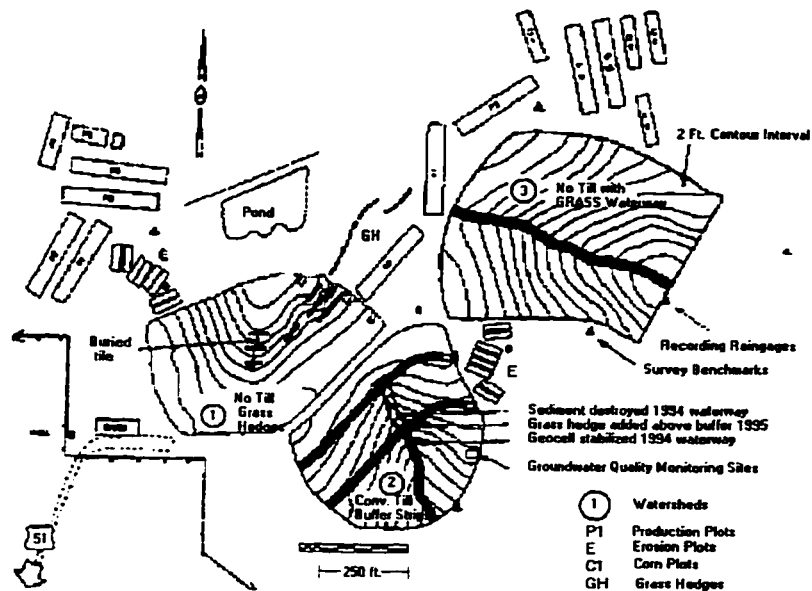


Figure 4.1 - Nelson Farm Test Plots.

of up to 24 bottles contained in each sampler's carousel (eight aliquots per bottle for larger WS#3 to permit an extension in sampling duration since it had larger and longer duration flows). Further information on measuring equipment was presented by Grissinger and Murphree (1991).

All watersheds were in sod for several years before being tilled in 1987. They were managed identically during 1988 and 1989 in a reduced tillage soybean production system consisting of a single pass of a mulch-finishing prior to planting, and two row cultivations. Beginning in 1990, WS#2 was farmed with conventional (chisel, disk twice, cultivate) tillage and the other two with no-tillage. One no-tillage watershed (#3) had a tall fescue (*Festuca arundinacea* Schreb.) grassed waterway seeded in the fall of 1990. Conventionally-tilled WS#2 had two 18-foot wide fescue buffer strips planted 150 feet apart in the fall of 1991 (Table 4.1).

To deal with serious headcut erosion where landforms concentrated runoff, conservation treatments in WS#1 and WS#2 were modified in 1994 and 1995. A 3 foot



deep headcut in WS#2 was filled during August 1994 after it had progressed to midway through the lower buffer strip. Soil borrowed from the footslope (upslope from the flume) was used. Four 16 foot wide by 20 foot long sections of a 6 inch high honeycomb like flexible plastic product was buried into the surface along 80 feet of the flow area through and below the lower buffer strip (Figure 4.1). By 1995, excessive sedimentation had buried

much of the fescue in the waterway between the two buffer strips. To protect the lower buffer strip from similar inundation with sediment, a row of switch grass (*Panicum virgatum* L.) was transplanted (with 6 inch spacing) to form a "grass hedge" (Dabney et al., 1997) along 40 feet of the upper edge of the buffer strip.

In 1994, several 3 foot wide switch grass hedges were transplanted across eroding swales on the east side of WS#1 to stop potential growth into gullies. That gullies could continue to develop even under no-till management was evident from the behavior of a 2 foot deep headcut in the main swale area of WS#1. This larger gully was filled during July 1995, but no plastic soil reinforcement was used. Instead, a 100 foot long, 4 inch diameter porous black plastic tile was placed in the bottom of the gully before it was filled with soil borrowed from the footslope and three 40 foot long switch grass hedges were established at 40 foot intervals across the former gully area. The tile was installed to avoid development of wet spots above the hedges. Its lower end was returned to the soil surface immediately downslope of the lowest hedge so that any drainage was gauged as surface runoff.

From discussions with NSL personnel, WS#2 had a significantly large sediment yield than did WS#1 or WS#3, therefore for the purpose of model application and results, only WS#2 was used.

Table 4.1 - Crop management histories and yields for three Nelson Farm research watersheds from 1988 through 1996. All yields are soybean except WS#3 in 1996.

Year	Watershed #1 (5.27 acres)	Watershed #2 (5.16 acres)	Watershed #3 (7.83 acres)
1988	Tilled, 36" Row 28.6 bu/a	Tilled, 36" Row 27.7 bu/a	Tilled, 36" Row 25.4 bu/a
1989	Tilled, 36" Row 14.6 bu/a	Tilled, 36" Row 13.8 bu/a	Tilled, 36" Row 12.8 bu/a
1990	No-till, 36" Row 17.1 bu/a	Tilled, 36" Row 15.3 bu/a	No-till, 36" Row 12.4 bu/a waterway seeded May & October
1991	No-till, 36" Row 30.0 bu/a	Tilled, 36" Row 26.6 bu/a buffer strips seeded October	No-till, 36" Row 23.8 bu/a
1992	No-till, 36" Row 40.6 bu/a	Tilled, 36" Row 42.1 bu/a	No-till, 36" Row 45.1 bu/a
1993	No-till, 7" drill 31.1 bu/a	Tilled, 36" Row 29.2 bu/a	No-till, 36" Row 27.0 bu/a
1994	No-till, 7" drill 40.0 bu/a grass hedges transplanted May	Tilled, 36" Row 31.8 bu/a gully filled/waterway seeded August	No-till, 36" Row 37.4 bu/a
1995	No-till, 7" drill 25.3 bu/a gully filled/three hedges July	Tilled, 36" Row 23.0 bu/a switchgrass added to buffer June	No-till, 36" Row 16.7 bu/a
1996	No-till, 7" drill 29.1 bu/a	Tilled, 36" Row 23.0 bu/a	Corn, No-till, 36" Row, 140 bu/a

Rainfall was much higher in the first three years of the study than in subsequent years (Table 4.2). Only in 1994 did rainfall approach the long term average value of 55.0 inches.

Sediment yield from WS#2 primarily reflected changes in sediment concentration throughout the year (Figure 4.2). Largest concentrations and sediment yields occurred in

June, although rainfall amounts were only average and runoff amounts were less than average. In contrast, high runoff between December and April was associated with low sediment concentrations and yields. During this period, rainfall intensities are commonly lower, the soil is covered with crop residue and winter weed growth, and the soil has not been recently loosened by tillage.

The differences in the patterns of sediment yield from WS#2 relative to that from the conventionally-tilled soybean erosion plots reported by Meyer et al. (1997) are noteworthy. On the plots, maximum monthly soil loss was only 1.8 t/a and occurred during May, while from the watershed maximum monthly sediment yield was 3.0 t/a and occurred during June. This difference is attributed to two factors. First, concentrated flow erosion, including both furrow and ephemeral gully erosion, contributed to sediment yield

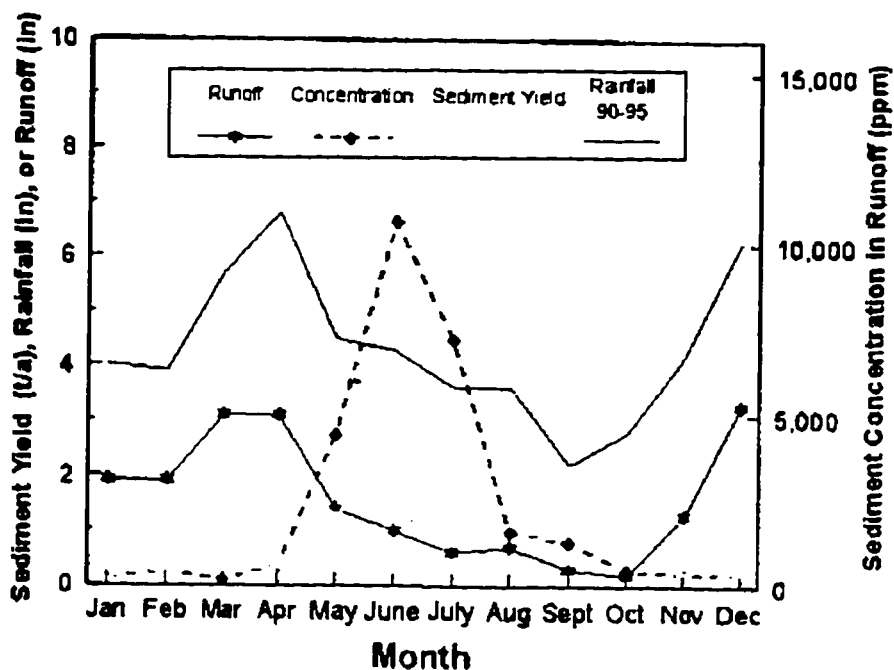


Figure 4.2 - Runoff, Sediment Concentration, and Rainfall versus Time for Watershed # 2 (Dabney et al., 1997).

on the watershed scale but not on the plot scale. Second, row cultivation loosened the soil and created tillage paths that facilitated the rapid delivery of runoff from the watershed. In contrast, on the erosion plots all cultivation was done by backing the tractor into the plots, dropping the cultivator onto the soil, and plowing up hill. This procedure removed soil from immediately upslope of the flume collection troughs and frequently created slight depressions that could trap sediment. Thus measured erosion on the conventionally tilled plots could be less than the amount of erosion that would occur on similar slope positions within a watershed.

Table 4.2 - Annual Rainfall, Runoff, and Sediment Yield from Watershed # 2.

Year	Runoff (Inches)	Sediment Yield (Tons/Acre)
1989	27.2	19.59
1990	27.2	4.52
1991	34.3	14.53
1992	11.2	8.46
1993	11.8	1.29
1994	17.2	34.51*
1995	14.3	2.85

\* : 25.3 t/a of this total was measured during August (1.9 inches of runoff averaging 118,000 ppm) after gully filling. Based on measured runoff and concentrations observed during August in other years, estimated August 1994 sediment yield without gully filling was 0.13 t/a, and the annual estimate was 9.37 t/a, (Dabney et al., 1997).

## 4.2 - Goodwin Creek Watershed

Goodwin Creek (Figure 4.3) is a tributary of Long Creek which flows into the Yocona River, one of the main rivers of the Yazoo River Basin. The Goodwin Creek watershed is located in North Mississippi, approximately 60 miles from Memphis, Tennessee and is extensively gaged by the Agricultural Research Service (ARS) as a research watershed in the areas of upland erosion, instream sediment transport, and watershed hydrology. The Vicksburg COE provided most of the construction funds when this watershed was originally established in 1977 (Blackmarr, 1995).

The Goodwin Creek watershed is divided into fourteen nested subcatchments with a flow measuring flume constructed at each of the drainage outlets. The drainage areas above these stream gaging sites range from 0.63 to 8.26 square miles. Twenty-nine standard recording rain gages are uniformly located within and just outside the watershed.

Instrumentation at each gaging site includes an electronic data acquisition system which consists of a VHF-radio telemetry system with a microcomputer. This system collects, temporarily stores, and transmits the data at the predetermined intervals to a central computer at the National Sedimentation Laboratory (NSL).

The Climate of the watershed is humid, hot in the summer and mild in the winter. The average annual rainfall during 1982 to 1992 from all storms was 56.7 inches, and the mean annual runoff measured at the watershed outlet was 5.7 inches per year. Data from a standard climatological station near the center of the watershed is also transmitted through the telemetry system (Figure 4.4). This information complements climatological data

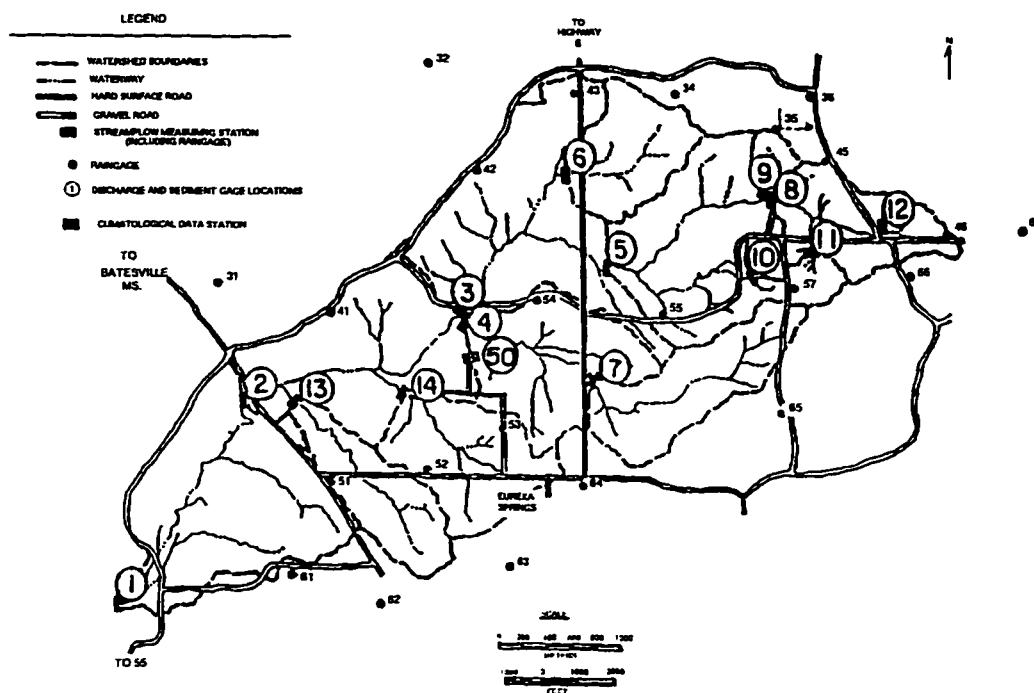


Figure 4.3 - Goodwin Creek Watershed

available from the U.S. Weather station at Batesville, Mississippi. The scope and quality of data being collected at the Goodwin Creek watershed has recently attracted the attention of scientists from NASA and NOAA working on large scale hydrometeorology.

The watershed flows approximately from northeast to southwest, it drains a total area of 8.26 square miles, with the outlet at latitude  $34^{\circ}13'55''$  and longitude  $89^{\circ}54'50''$ . Terrain elevation ranges from 72 meters to 123 meters above mean sea level (Figure 4.5) with an average channel slope of 0.004 in Goodwin Creek. Land use and management practices that influence the rate and amount of sediment delivered to streams from the uplands, range from timbered areas to row crops. The Goodwin Creek watershed is largely free of land management activities with 13 percent of it's area being under

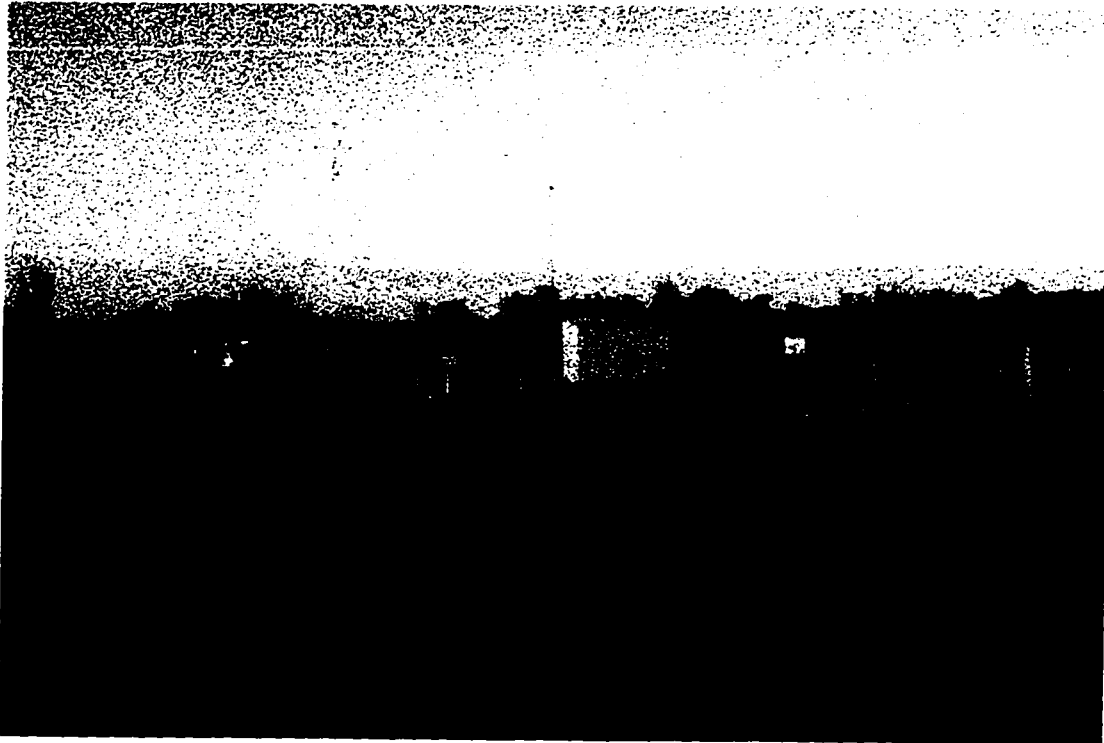


Figure 4.4 - Standard Climatological Station near the center of the Goodwin Creek Watershed

cultivation and the rest in idle pasture and forest land (Figure 4.6). Periodic acquisition of aerial photography and satellite data contribute to complete aerial coverage of land use and surface conditions. The predominant soil texture for Goodwin Creek watershed is silt loam with a small percent of sandy loam (Figure 4.7).

Measurements collected at each site and transmitted through the telemetry system includes water stage, accounting of automatically pumped sediment samples, air and water temperature, and precipitation. Manual sampling of total sediment loads is also carried out during storm events at stations 1 and 2 using bedload and depth-integrating suspended

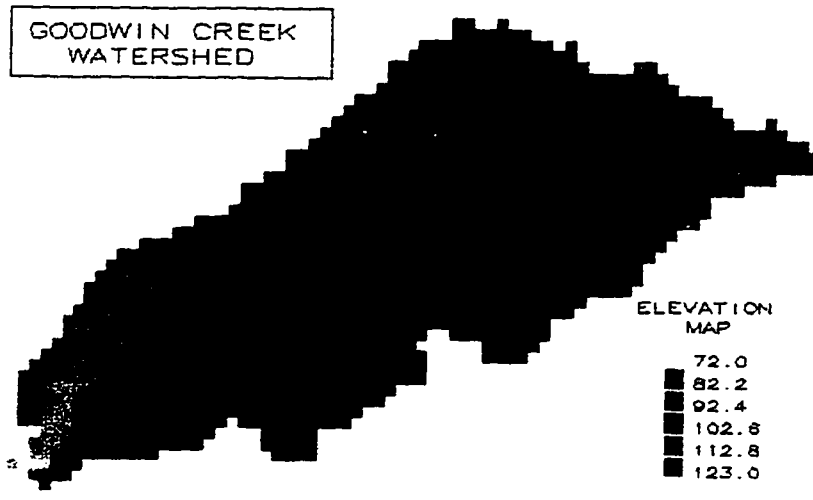


Figure 4.5 - Goodwin Creek Watershed Elevation Grid

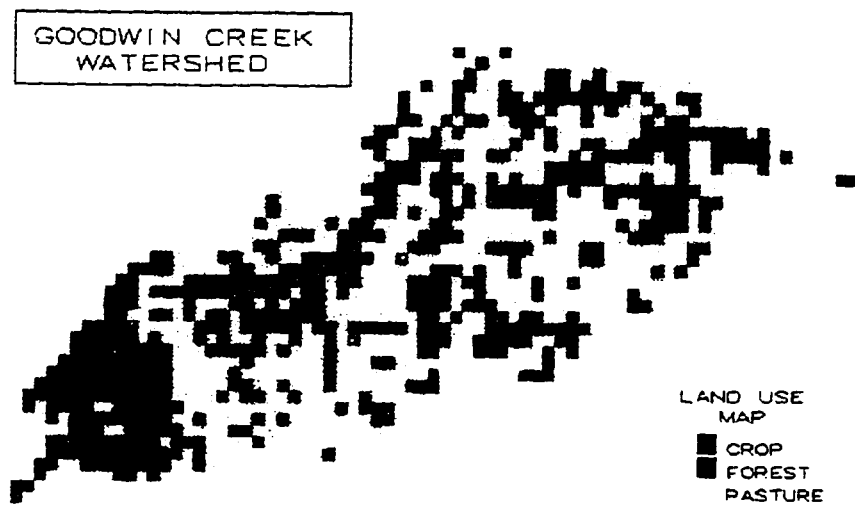


Figure 4.6 - Goodwin Creek Watershed Land Use Grid



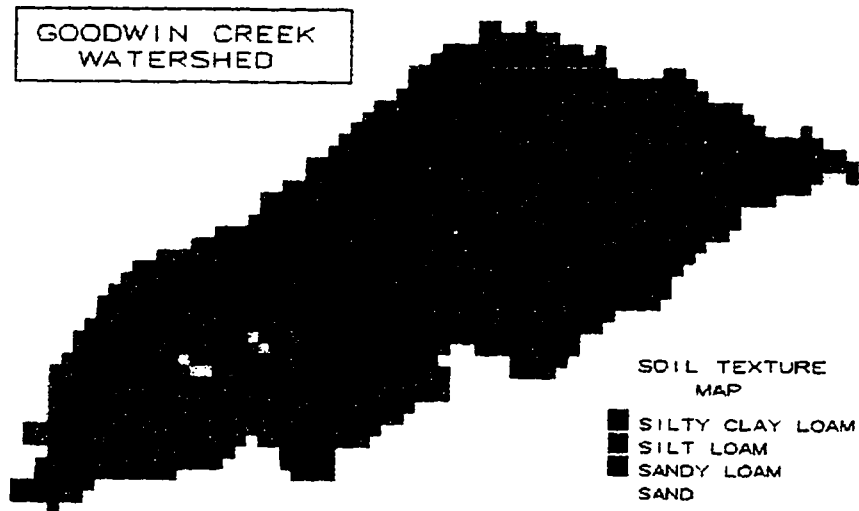


Figure 4.7 - Goodwin Creek Watershed Soil Texture Grid

samplers. Surveys of channel geometry, bed material, bank geotechnical properties, and channel migration were conducted at periodic intervals to keep track of channel morphological change.

On November 13, 1996, a field reconnaissance trip was performed by Dr. Chester Watson and Mr. Bill Johnson on the Goodwin Creek Watershed. In the lower portion of the Goodwin Creek Watershed, there was evidence of rill and gully erosion. From walking in the fields north of the main channel, between gages 2 and 3, one can see the formation of rills (Figure 4.8) as well as sediment deposits from the upland areas (Figure 4.9).

In the case of Figure 4.9, one can see sand material from the upland area depositing on the milder sloped fields. As the runoff from the fields neared the main channel, the rills turn into gullies (Figure 4.10) and (Figure 4.11). In the pasture lands located along the watershed boundary, there was evidence of rill and gully formations (Figure 4.12) and (Figure 4.13). In these areas, the ground cover made it somewhat difficult to determine

the extent to which rill erosion was taking place (Figure 4.14). However, gully erosion was very noticeable in most cases (Figure 4.15).

Along the main stem and tributary channels, there was evidence of bank and bed erosion. The bank angles were very steep, in the vicinity of gage 9 (Figure 4.16). There was evidence of block failures (Figure 4.17) and of bank undermining (Figure 4.18) and (Figure 4.19). Around some of the gaging structures, there was evidence of local scour taking place (Figure 4.20). Along the channel banks, of the tributary flowing into gage 9, there was evidence of vegetation being undermined (Figure 4.21) with trees and shrubs ultimately falling into the channel.

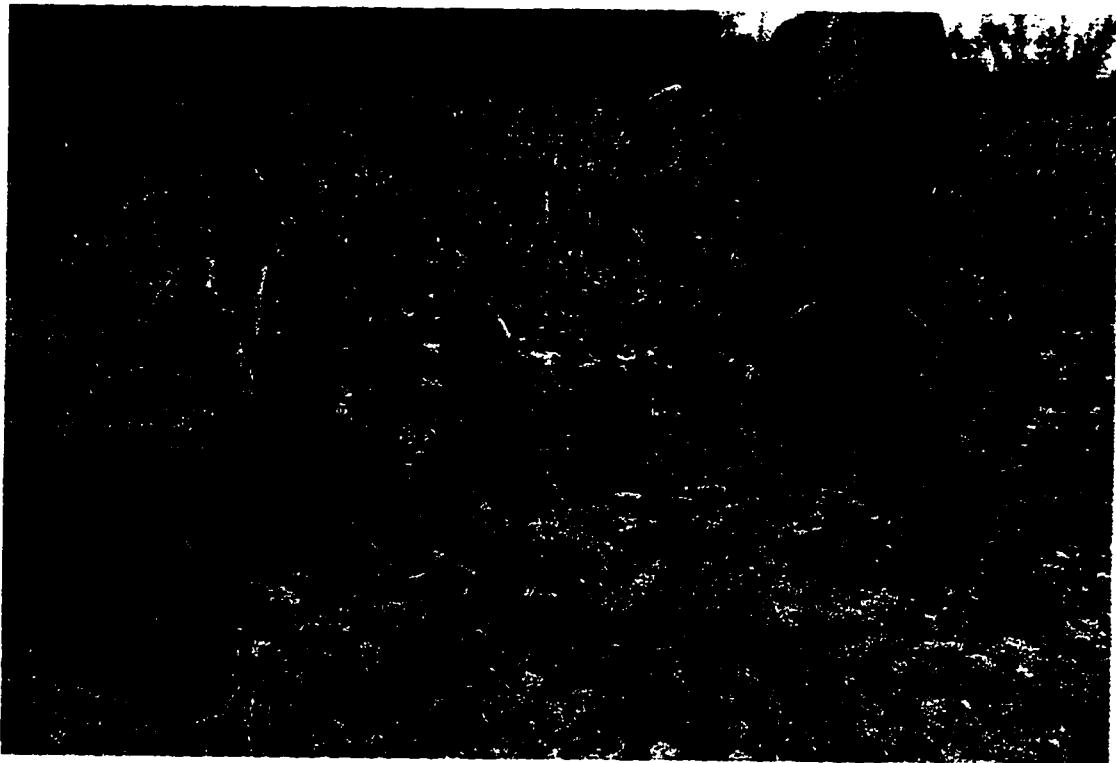


Figure 4.8 - rill and gully erosion



Figure 4.9 - upland sediment deposits



Figure 4.10 - rill and gully erosion



Figure 4.11 - gully erosion



Figure 4.12 - rill erosion in pasture lands.

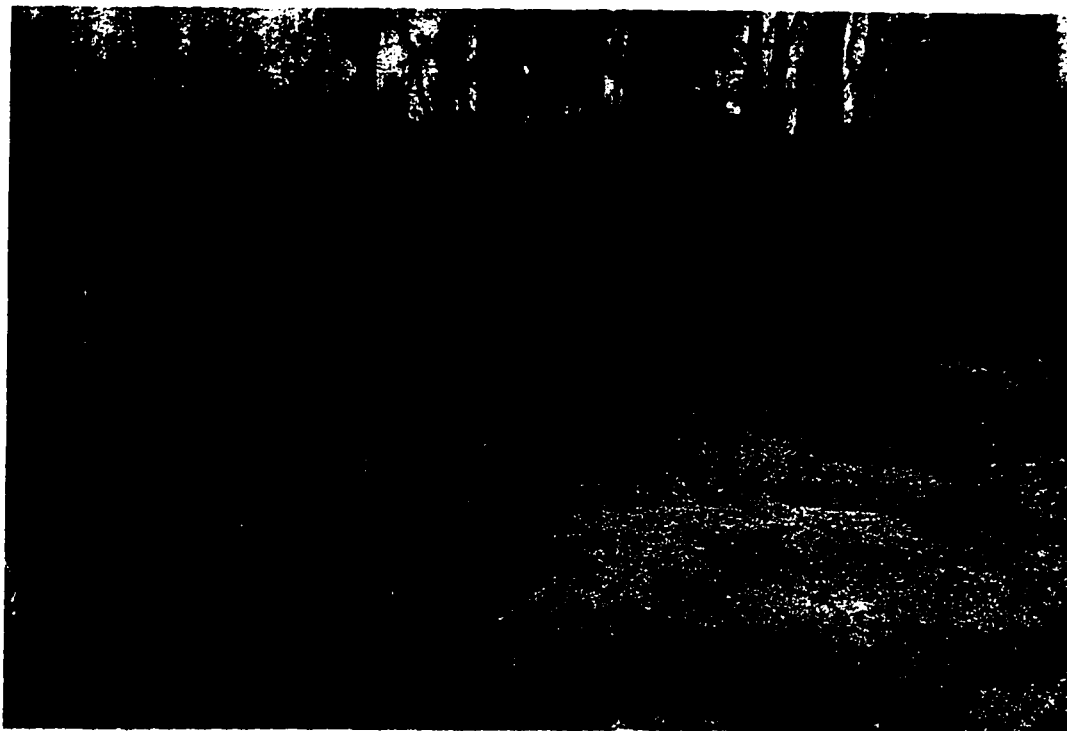


Figure 4.13 - gully erosion.



Figure 4.14 - rill erosion



Figure 4.15 - gully erosion

The primary land use above gage 9 is pasture, however the primary sediment supply is from the stream banks and bed (Figure 4.17 to Figure 4.21). From extensive field observations made by the ARS, this area is one of the most active, in terms of gully erosion, within the Goodwin Creek Watershed.

The drainage area above gage 10 consists primarily of forests. This sub-area was established to determine the sediment runoff due to a wooded land use. From field observations, dense vegetation was observed and there appeared to be very little rill and gully erosion taking place. A search of the Goodwin Creek Database revealed very little sediment runoff measured in the field. The drainage area above gage 11 consists



Figure 4.16 - steep bank angles

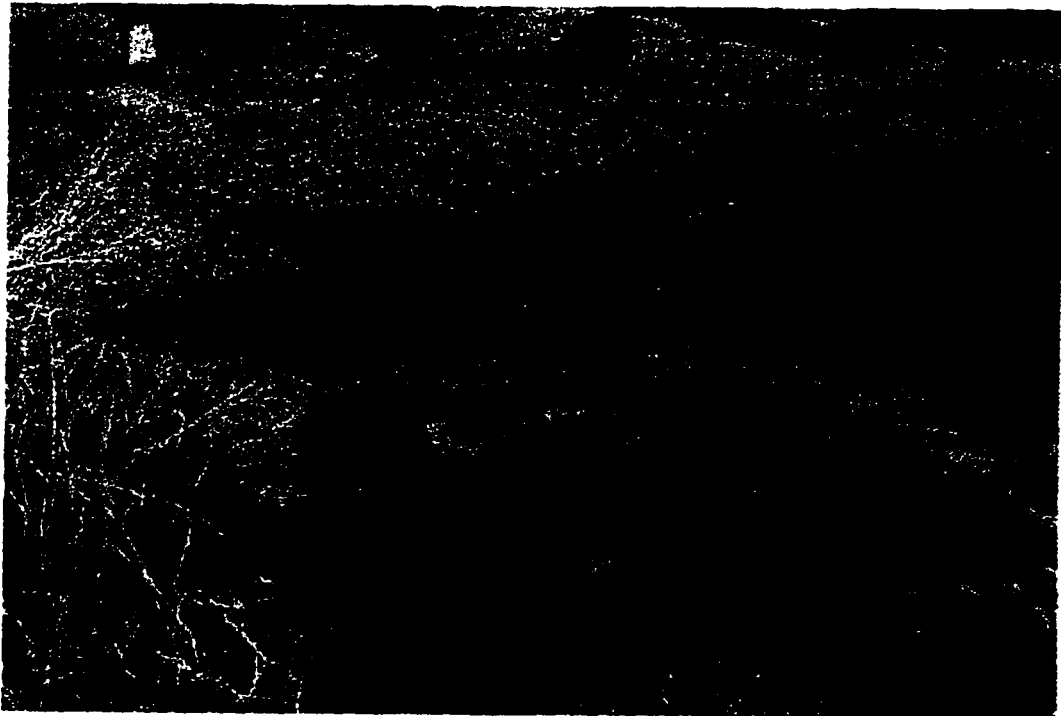


Figure 4.17 - block failures

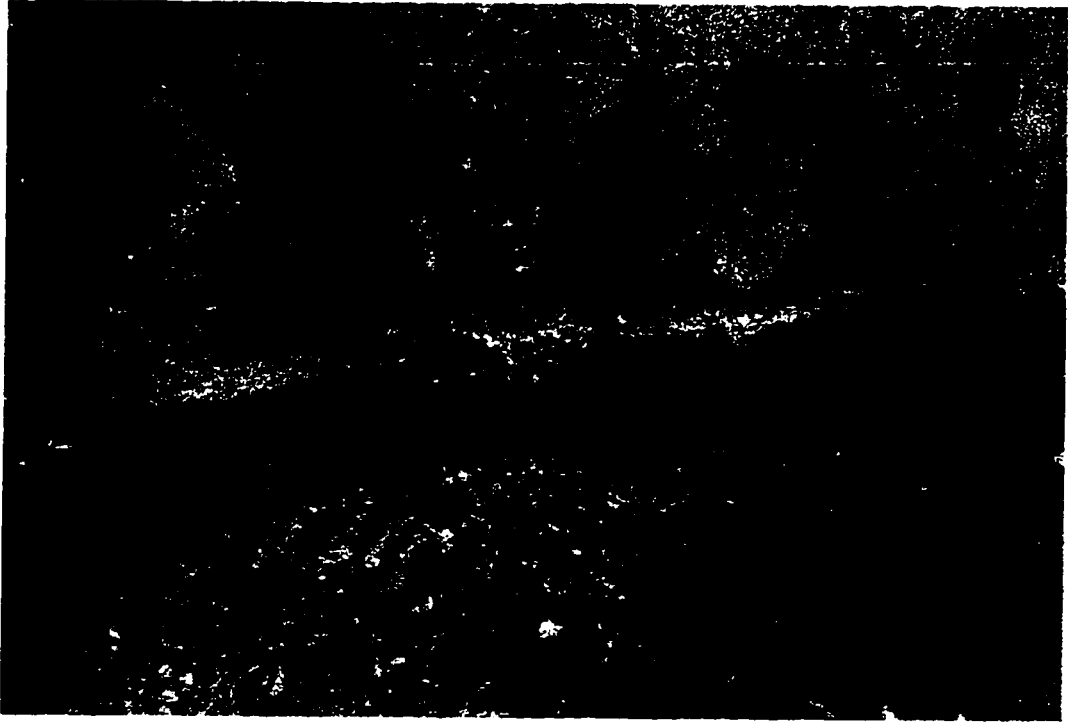


Figure 4.18 - bank undermining



Figure 4.19 - bank undermining





Figure 4.20 - local scour at gaging structure



Figure 4.21 - vegetation undermining

primarily of pasture or idle land. In this area, there was evidence of gully erosion, but not on the same scale as the drainage area above gage 9. The drainage area above gage 12 consists of essentially the same land use as gage 11, however the channel changes dramatically in size and depth. This would seem to indicate the base lowering of the channel network has not fully reached the upper portion of the watershed. The drainage area above gage 14 consists primarily of pasture and idle land. The primary interest in this sub-area is the character of the channel bed material above the gaging site, which consists primarily of gravel. As a result, the sediment load resulting from this sub-area is expected to be primarily wash load.

From discussions with NSL personnel and review of previous reports, the annual sediment yield consists approximately of 30% upland erosion and 70% bank failure and bed erosion as measured in the main channel of the Goodwin Creek Watershed. From field observations made along the main channel, there was strong evidence of gully erosion and bed lowering as well as bank undercutting and block failures taking place.

Field observations in the upland areas did not indicate wide spread extreme rill or gully formations. Gully erosion was extreme in some cases, but seemed to be in isolated upland areas. From the field observations, the general conclusion that the main sediment source is due to gully and channel erosion seems to be valid for the main channel. However, observed measurements made at the upland gages should reflect a higher percentage of upland erosion when compared to the total sediment load.

## **CHAPTER 5**

### **Model Application and Results**

#### **5.1 - Nelson Farm Test Plot**

##### **5.1.1 - Single Event Sediment Yield Analysis**

In evaluating the ability of CASC2D to accurately simulate upland erosion on the test plot scale, two storm events were modeled. The first storm event occurred on February 17-19, 1991 and had an intermittent rainfall occurring over a 56 hour period. The second storm event occurred on June 3, 1992 and had rainfall occurring over a 11.5 hour period. The first storm event was chosen during a period of idle land use management, while the second storm event was chosen during a period when the ground was tilled into rows and a crop was planted. This analysis was able to evaluate the model for two drastically different land use management practices.

Since there was only one rainfall gage for the Nelson Farm test plots, rainfall was applied uniformly in space and temporally in time. During the February time period the Crop Management factor (C) was estimated to be 0.07 while during the June time period the Crop Management factor (C) was estimated to be 0.65. In both cases, the Soil Erodibility factor (K) was estimated to be 0.48 since the primary soil type is silt loam and the Conservation Practice factor (P) was estimated to be 1.0.

For all of the input grids (ie., elevation, roughness, and soil texture) the grid cell resolution was set to be 20 feet in height and 20 feet in width. Also, all of the output grids were computed at this same grid cell resolution.

#### **5.1.1.1 - Storm Event 1**

The storm event of February 17-19, 1991 began at 12:02 am and had intermittent rainfall occurring for 56 hours with a moderate amount of rainfall preceding this event. The actual hyetograph for the rain gage is shown in Figure A-1. The total runoff for this event was 4.2 inches and the total amount of infiltration occurring over the test plot was 2.2 inches. Therefore the infiltration losses amounted to 33.8%.

Comparing the observed flow hydrograph versus the computed flow hydrograph (Figure 5.1), for this storm event, shows that CASC2D was able to accurately simulate the overall shape, rate of rise, the time to peak, and the peak flow rate.

A comparison of the observed sediment concentrations versus the computed sediment concentrations (Figure 5.2) shows that CASC2D did a reasonably good job of estimating the erosion of sediment off of the test plot. In the beginning of the storm event, the observed sediment concentration is higher than the observed. During this part of the storm event the flow rates are small and there is sediment being dislodged due to rain splash, which is not taken into account in CASC2D, which could cause the model to underestimate the sediment concentration. As the flow rate increases, CASC2D was able to do a better job of accurately estimating the sediment concentration since the majority of sediment movement is due to sediment eroded off of the overland plane.

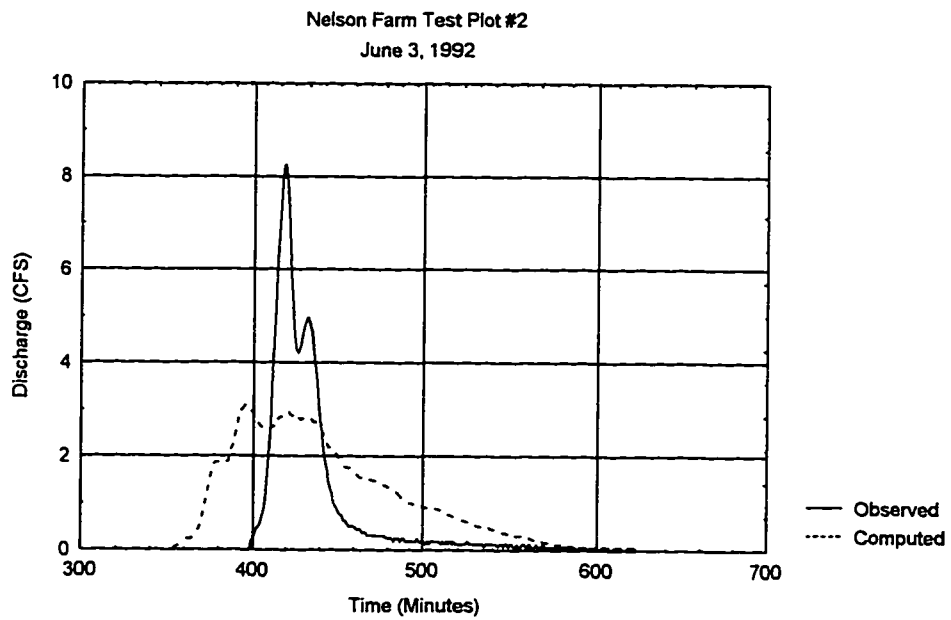
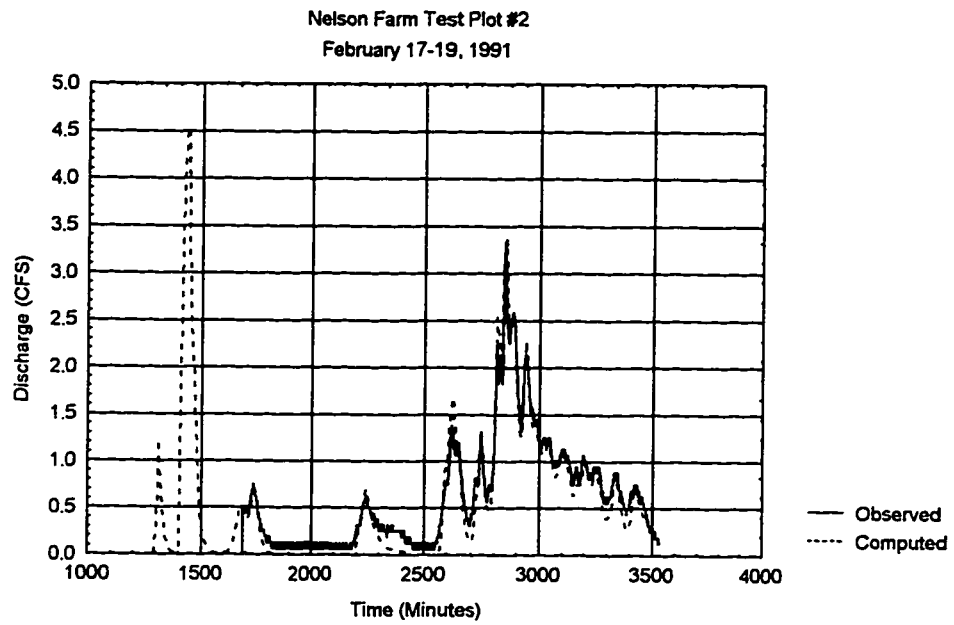


Figure 5.1 - Nelson Farm Test Plot #2 - Flow Hydrographs.

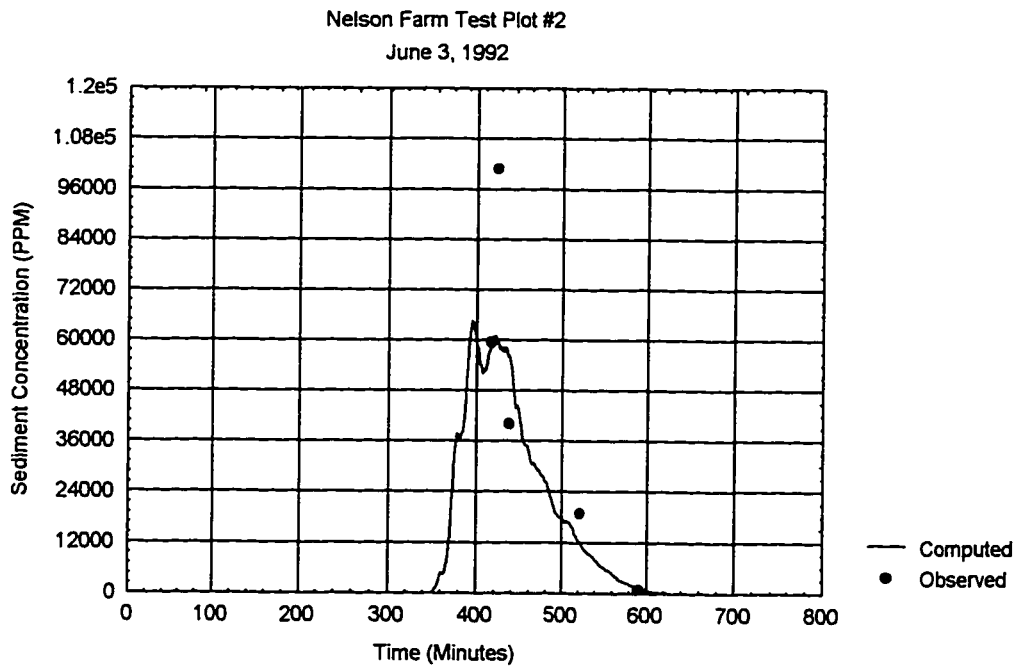
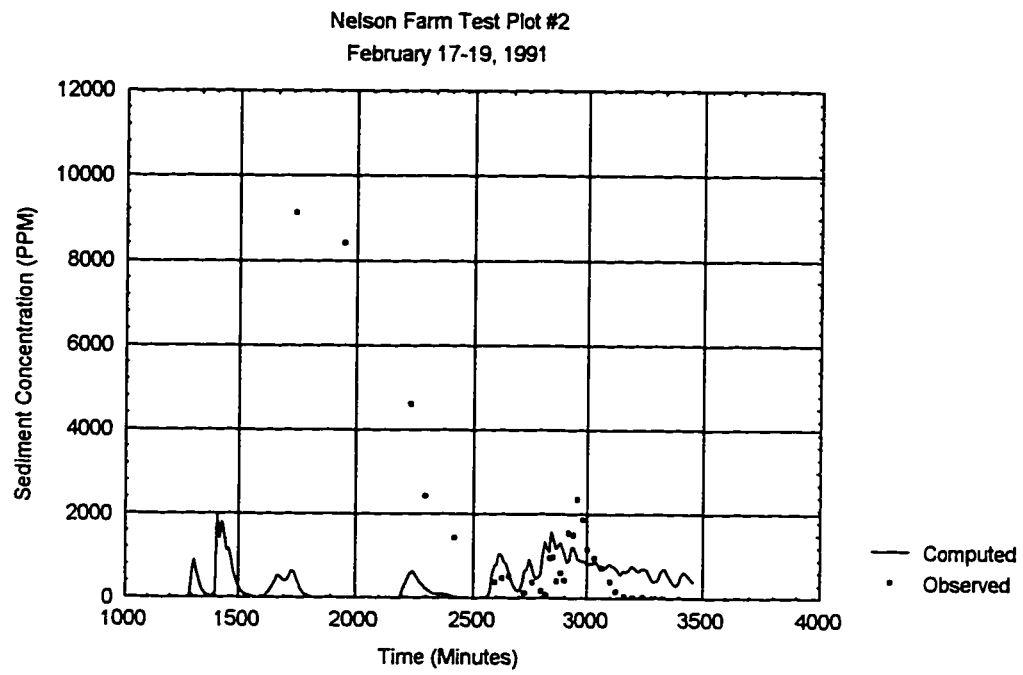


Figure 5.2 - Nelson Farm Test Plot #2 - Sediment Concentrations.

The CASC2D output grids (Appendix B) show the general pattern of erosion taking place in the upland areas and as the water and sediment get close to the concentrated flow area, some deposition takes place. A schematic of the various CASC2D output grids are shown in figure 5.3. The top row of grids are static windows, which means that they do not change with time and they show the spatial variability in the land use, soil texture, and topology. For the test plot, the land use and soil texture grids are uniform. However, for the Goodwin Creek Watershed, these grids do show spatial variability in land use and soil texture. The middle row contains the rainfall intensity grid, the infiltration depth grid, and the flow depth grid. All of the grids are dynamic grids, which is to say that they all change with time. The rainfall intensity grid is generated by CASC2D from the raingage data and then interpolated using the inverse distanced squared method. The infiltration depth grid displays the accumulated infiltration depth computed from the Green-Ampt equation. The flow depth grid is a composite of the overland flow depths and the channel flow depths. If the grid cell is an overland cell then the overland depth is displayed and if the grid cell is a channel cell, then the channel depth is displayed. CASC2D determines which cells are overland and channel by using the SHAP.DAT file. The bottom row of grids are dynamic and show the sediment computations being made by CASC2D. The first grid in this row shows the maximum sediment flux out of each grid cell. The second grid shows the volume of sediment in suspension at a particular time. CASC2D makes its computations based upon three size classes, however in displaying the volumes of sediment, the sum of the three size classes is used. The third grid in this row is the total

Land Use	Soil Texture	Elevation
Rainfall Intensity	Infiltration Depth	Flow Depth
Maximum Sediment Flux	Suspended Volume	Total Net Volume

Figure 5.3 - Schematic of CASC2D Output Grids.

net volume grid. This grid shows the total volume of sediment eroded or deposited on a grid cell at a particular time.

In 1994, the ARS placed hedgerows and switch grass in the concentrated flow areas to help reduce gully erosion. The model results (Figure 5.4 to Figure 5.8 ), when compared to field observations made by the ARS, did show expected patterns of erosion and deposition. CASC2D simulations show the maximum volume of sediment deposited on a grid cell was 10.1 cubic meters, which results in a deposition depth of 271.6 millimeters. The average depth of deposition, over the grid cells that showed deposition, was 12.1 millimeters. The maximum volume of sediment eroded off of a grid cell was 7.9 cubic meters, which results in an erosion depth of 212.5 millimeters. The average erosion depth, over the grid cells that showed erosion, was 4.0 millimeters.



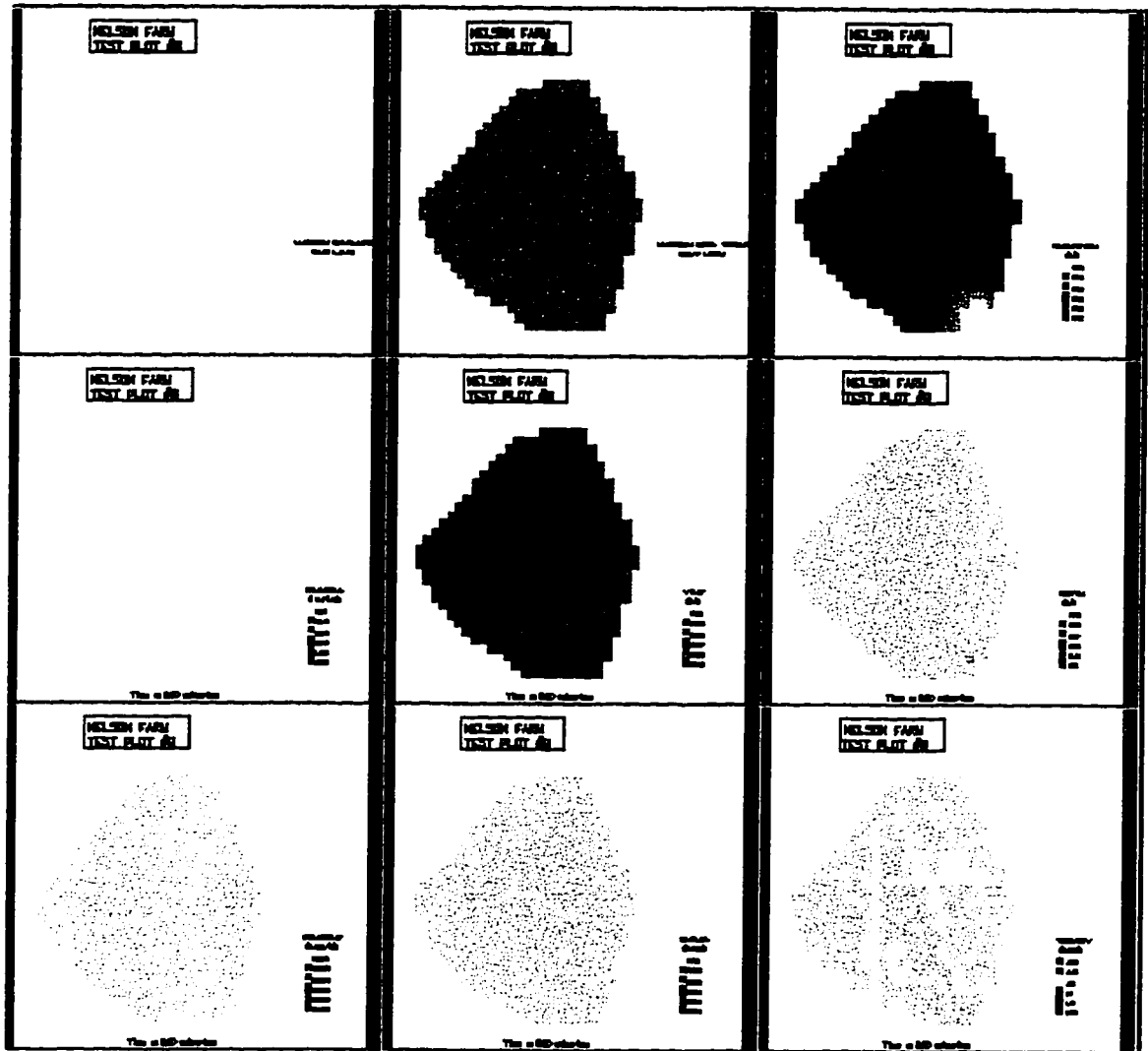


Figure 5.4 - February 17-19, 1991 at Time = 540.0 minutes.

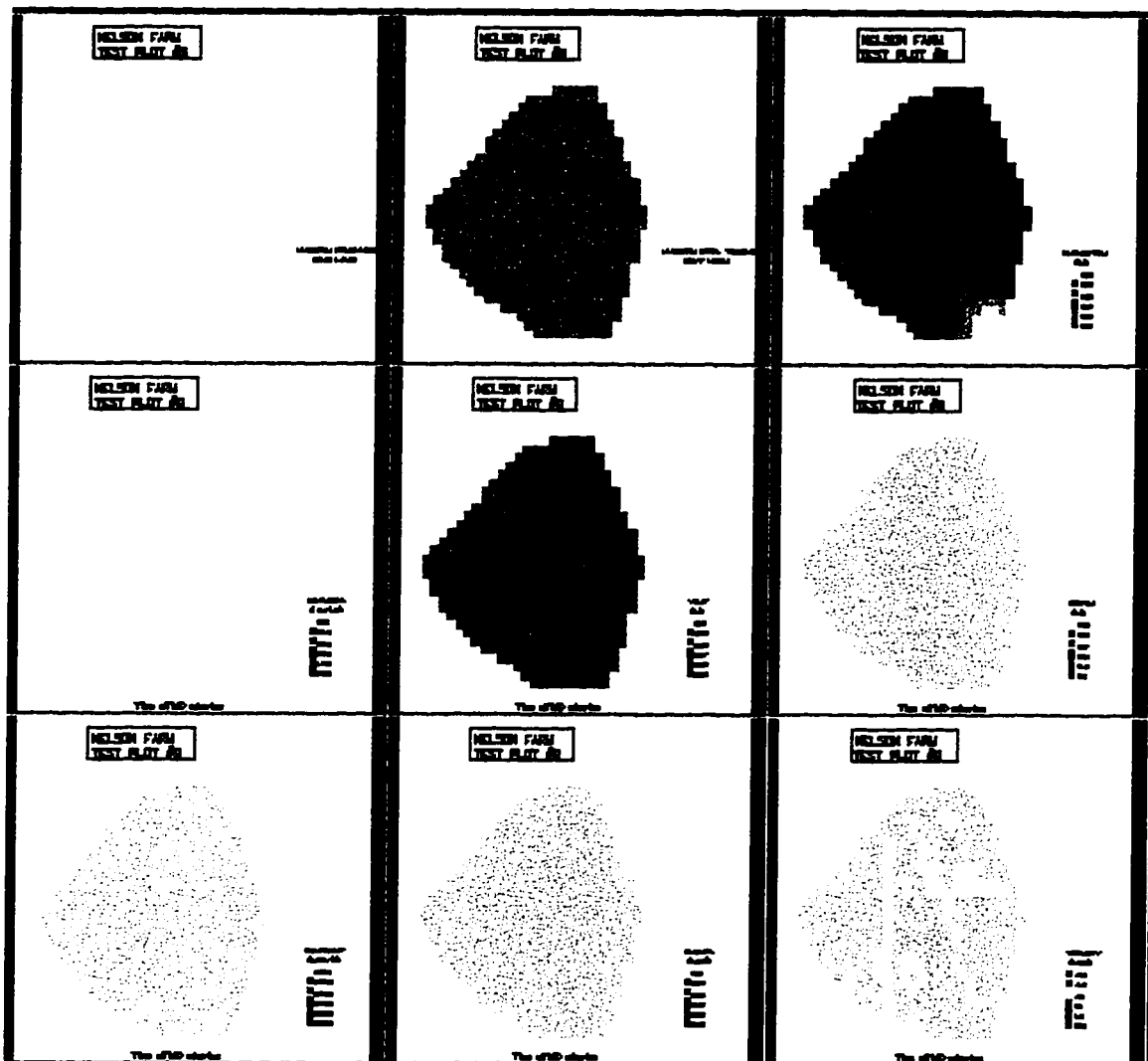


Figure 5.5 - February 17-19, 1991 at Time = 1140.0 minutes.

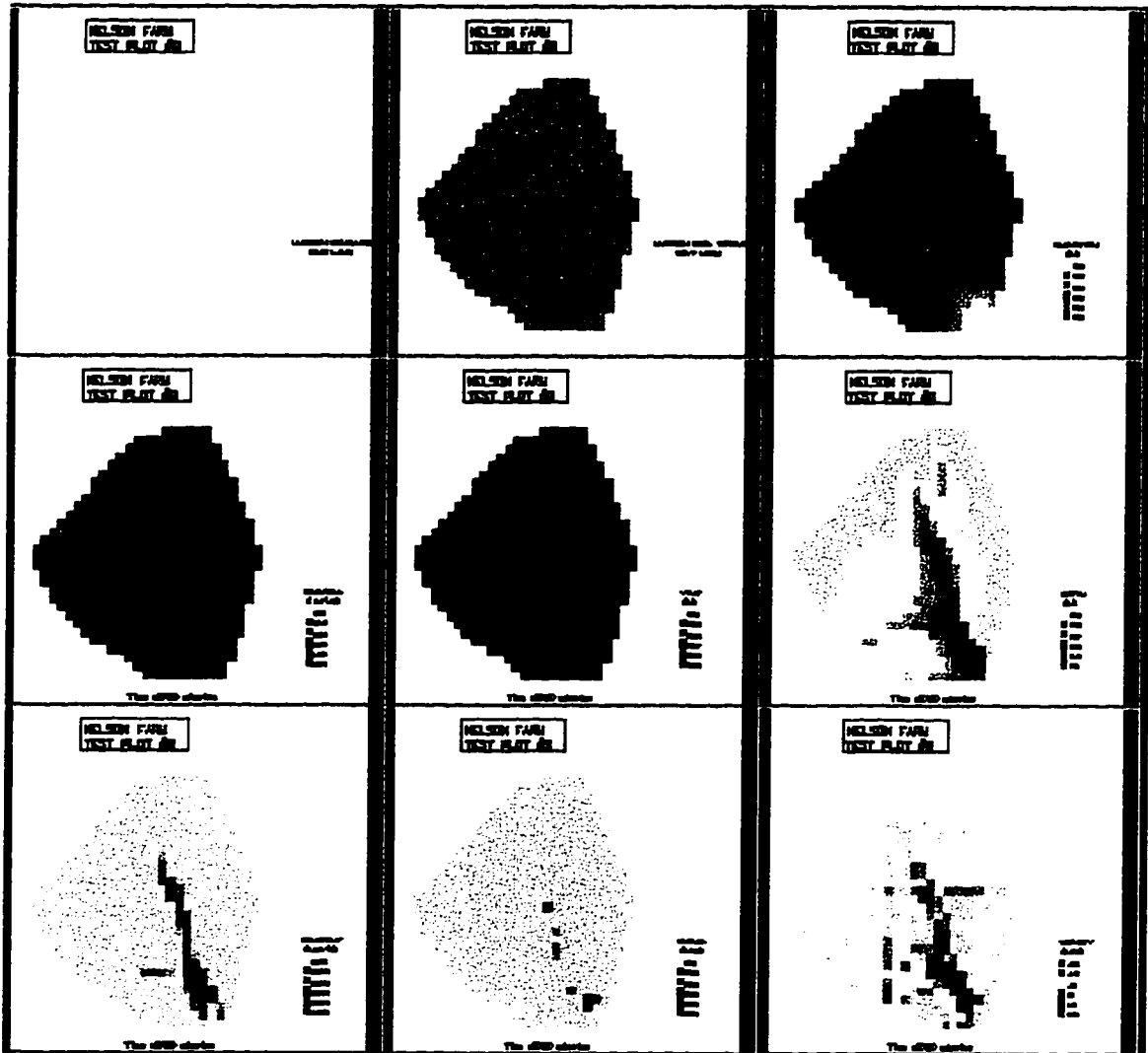


Figure 5.6 - February 17-19, 1991 at Time = 1740.0 minutes.

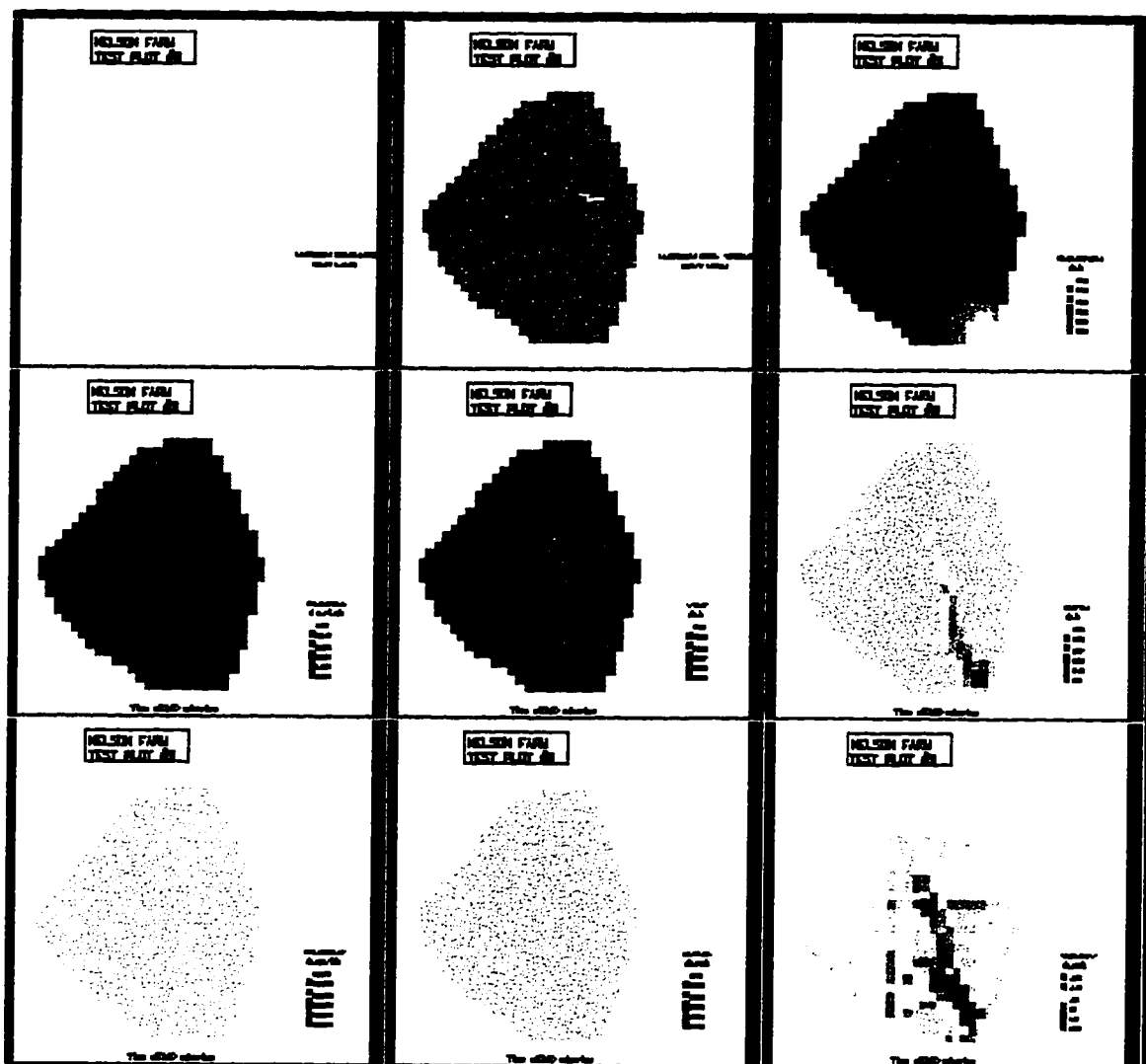


Figure 5.7 - February 17-19, 1991 at Time = 2340.0 minutes.

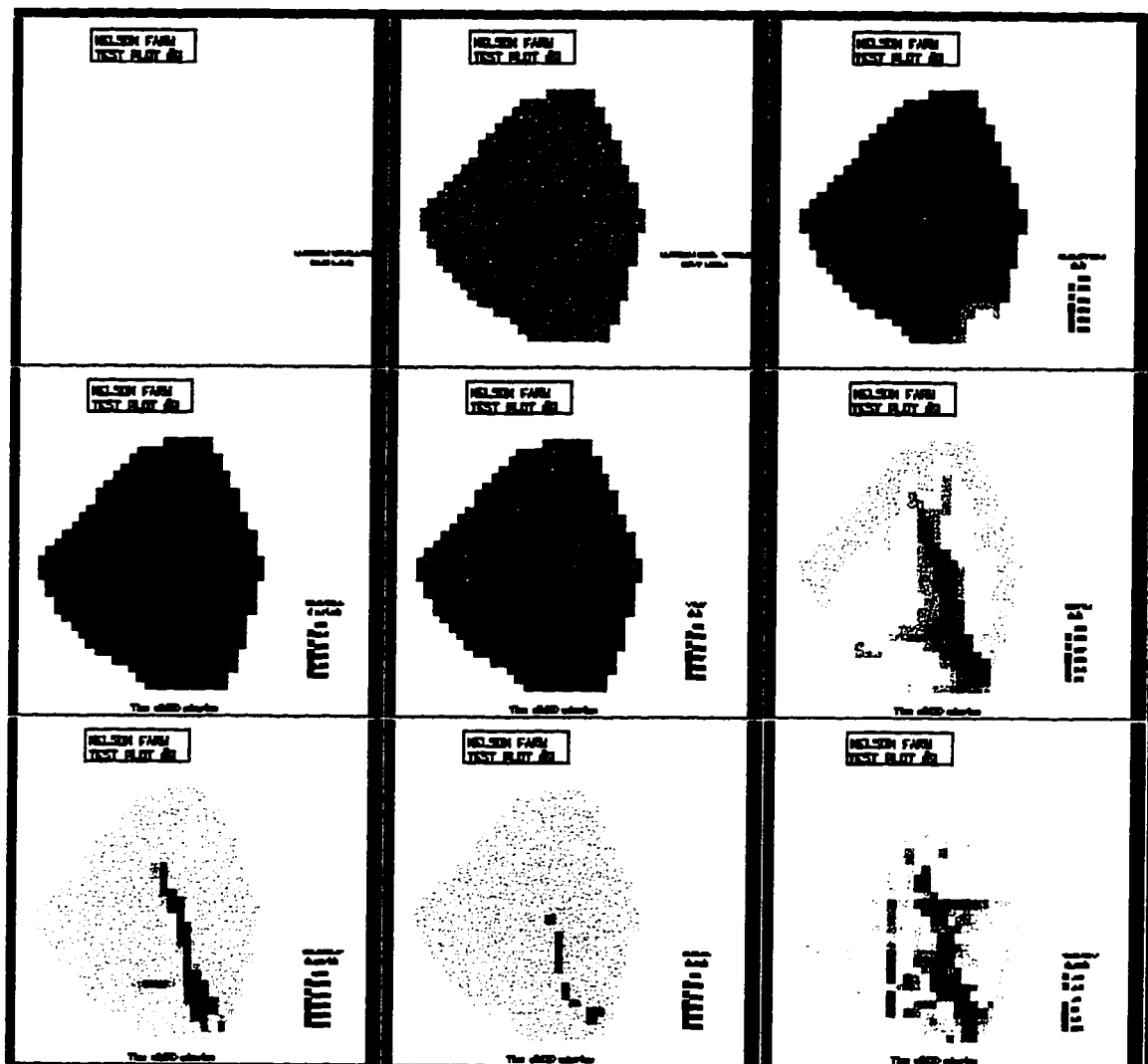


Figure 5.8 - February 17-19, 1991 at Time = 3420.0 minutes.

### 5.1.1.2 - Storm Event 2

The event of June 3, 1992 began at 10:50 pm on June 2, 1992 and had two main storm cells that lasted for approximately 11.5 hours with very little rainfall preceding this event. The actual rainfall hyetograph for the rain gage is shown in Figure A-1. The total runoff for this event was 0.99 inches and the total amount of infiltration occurring over the test plot was 1.65 inches. Therefore the infiltration losses amounted to 62.4%.

Comparing the observed flow hydrograph versus the computed flow hydrograph (Figure 5.1), shows that CASC2D was able to simulate the general shape and runoff volume. CASC2D computed a slower rising and falling flow hydrograph than was measured in the field. In preparation for planting the row crops, the test plot was tilled and rows were formed. The formation of rows significantly altered the hydrology of the area since flow would be concentrated in the furrows and act as channel flow rather than overland flow. The grid cell resolution for this test plot (20 feet) was too large to capture these furrows, so CASC2D was not able to accurately model the test plot under these land use conditions. Simulations were made whereby the roughness coefficients were lowered in an attempt to compute a faster rising and falling hydrograph, however, this only caused the model to compute pulses of flow rather than one continuous flow hydrograph.

A comparison of the observed sediment concentrations versus the computed sediment concentrations (Figure 5.2) show that CASC2D was able to simulate the general pattern, however since the computed flow rates were significantly reduced, the computed sediment concentrations were also lower than those measured in the field.

The maximum volume of sediment deposited on a grid cell was 28.5 cubic meters, which results in a deposition depth of 766.5 millimeters. The average depth of deposition,

over the grid cells that showed deposition, was 33.6 millimeters. The maximum volume of sediment eroded off a grid cell was 26.4 cubic meters, which results in an erosion depth of 710.1 millimeters. The average depth of erosion, over the grid cells that showed erosion, was 11.0 millimeters.

### **5.1.2 - Annual Sediment Yield Analysis**

If the sediment yield from the land surface on an annual basis rather than a single storm event is desired, then the results from the single event analysis can still be used. This application is accomplished by determining the soil loss for events of varying return periods. Recommended return periods are 2, 10, 25, 50, and 100 years. The sediment yields are then weighted according to their incremental probability, resulting in a weighted storm average.

In performing this analysis for the Nelson Farm Test Plot #2, the 24 hour rainfall for the 2, 10, 25, 50, and 100 year frequency storm events were uniformly applied over the test plot area. The rainfall amounts were taken from the Technical Paper No. 40, Weather Bureau Manual dated May 1961. The SCS Type II storm distribution (Table 5.1) was used to temporally distribute the rainfall over the test plot area. An average value of 0.35 was used for the Crop Management Factor (C) which corresponds to a land use of row crops and for a land use of hedgerows and switch grass, a C-Factor of 0.07 was used (Table 5.2). An average value of 0.48 for Soil Erodibility (K), which corresponds to a soil texture of silt loam, was uniformly applied over the test plot area. A Conservation Practice Factor (P) of 1.0 was uniformly applied over the test plot area.

To compute the annual sediment yield, the weighted storm yield is multiplied by the ratio of annual water yield to an incremental probability-weighted water yield. For the return periods recommended, the computation is :

$$A_s = Q_A \frac{0.4Y_{s_2} + 0.06Y_{s_{10}} + 0.02Y_{s_{25}} + 0.01Y_{s_{50}} + 0.01Y_{s_{100}}}{0.4Q_{v_2} + 0.06Q_{v_{10}} + 0.02Q_{v_{25}} + 0.01Q_{v_{50}} + 0.01Q_{v_{100}}} \quad (5.1)$$

where,

$A_s$  = Annual Sediment Yield (Tons)

$Q_A$  = Average Annual Runoff Volume (Acre-Feet)

$Y_s$  = Sediment Yield for various return periods (Tons)

$Q_v$  = Runoff Volume for various return periods (Acre-Feet)

Table 5.1 - SCS Type II - 24 Hour Rainfall Distribution

Time (Hours)	Incremental Multiplication Factor
0	0.0
1.5	0.015
3.0	0.015
4.5	0.02
6.0	0.025
7.5	0.025
9.0	0.045
10.5	0.055
12.0	0.40
13.5	0.20
15.0	0.05
16.5	0.05
18.0	0.02
19.5	0.03
21.0	0.01
22.5	0.02
24.0	0.02
Total	1.0

The long term average annual rainfall was estimated to be 55 inches per year and the average annual runoff was estimated to be 17.9 inches per year. The test plot area (Nelson



Farm Test Plot #2) was estimated to be 5.2 acres, thus the average annual runoff volume is 7.76 acre-feet. From the results of the various storm simulations, the average annual sediment yield without hedgerows and switch grass for the test plot was computed to be

Table 5.2 - Crop Management Factors (C) for Nelson Farm Test Plot #2.

Land Use	Crop Management Factor (C)
Hedgerows and Switchgrass	0.07
Row Crops	0.35

68.39 tons and 13.15 t/a. The annual sediment yield with hedgerows and switch grass was estimated to be 37.69 tons and 7.25 tons/acre.

Table 5.3 - Computed Sediment Yield for various return periods.

Return Period	24-Hour Rainfall (Inches)	Runoff Volume (Acre-Feet)	Sediment Yield with H&SG (Tons)	Sediment Yield without H&SG (Tons)
2	4.2	0.35	1.29	2.38
10	5.9	0.96	5.32	9.58
25	6.8	1.27	8.15	14.60
50	7.7	1.59	11.34	20.25
100	8.3	1.80	13.62	24.28

H&SG : Hedgerows and Switch Grass

The total rainfall for 1994 was closest to the long term average annual rainfall.

Comparing the observed sediment yield of 1994, 9.37 tons/acre, versus the computed annual sediment yield with hedgerows and switch grass, 7.25 tons/acre, results in a percent difference of -22.6%.

## 5.2 - Goodwin Creek Watershed

In order to evaluate the upland erosion scheme, on a watershed basis, a sensitivity analysis was conducted, whereby nine cases were simulated. In each case, uniform soil texture and uniform land use was assumed. The rainfall, October 17-18, 1981, was both spatially and temporally variable, while the topography was spatially variable.

In evaluating the ability of CASC2D to accurately simulate upland erosion on the watershed scale, three storm events were modeled. The first storm event occurred on October 17-18, 1981 and had a storm duration of eight hours. The second storm event occurred on December 2-3, 1983 and had a storm duration of thirty hours. The third storm event occurred on May 2-3, 1984 and had a storm duration of twenty eight hours. In choosing these three storm events, the goal was to select storms that occurred at different times of the year, but were grouped close enough together such that there would not be a significant change in the land use management practices other than due to agricultural practices.

Table 5.4 - Overland Roughness Coefficients for Goodwin Creek Watershed

Land Use	Manning's Roughness Coefficient
Pasture, Idle Land	0.070
Forest	0.110
Row Crop	0.050

Table 5.5 - Soil Erodibility Factors (K) for Goodwin Creek Watershed

Soil Texture	Soil Erodibility (K)
Sand	0.12
Sandy-Loam	0.27
Silt-Loam	0.40
Silty-Clay-Loam	0.38

Table 5.6 - Crop Management Factors (C) for Goodwin Creek Watershed

Land Use	Crop Management Factor (C)
Pasture, Idle Land	0.070
Forest	0.008
Row Crop	0.650

Simulated streamflow hydrographs were compared to observed hydrographs at five locations on the main stem channel and one major tributary. Simulated sediment discharge hydrographs were compared to observed hydrographs at eleven locations along the main stem, tributaries, and upland areas. A total of seventeen rainfall gages were used to calculate overland flow runoff in the watershed. Plots of the simulated streamflows versus the observed data, plots of the sediment discharge versus observed data, and plots of rainfall hyetographs for gage 54 are shown in Appendix A. Plots of simulated output grids, for the October 17-18, 1981 event, from CASC2D (i.e., land use, soil texture, elevation, rainfall, infiltration, depth, maximum sediment flux, suspended sediment, and total net volume grids) are shown in Appendix C. The land use grid is broken down into three categories; pasture, crop, and forest. The soil texture grid is broken down into four categories; silty clay loam, silt loam, clay loam, and sand.

Streamflow, rainfall, and sediment gage data for Goodwin Creek Watershed were available from 1981 to 1993. Total rainfall in inches for the three selected storms are shown in (Table A-1) for all seventeen rainfall gages. Streamflow hydrograph parameters considered for calibration and comparison purposes includes time to peak in minutes (Table A-2), total runoff in inches (Table A-3), and peak flow in cfs (Table A-4).

Sediment Yield parameters considered for calibration and comparison purposes include sediment yield in tons (Table A-5) and sediment yield in tons/acre (Table A-6). It should be noted that the observed sediment yield includes upland erosion, bank failure, and channel erosion processes, while the computed sediment yield only consists of upland erosion processes.

Simulated results for each of the selected storms is included below. Storm event 1 was used to calibrate the roughness and USLE coefficients. Storm events 2 and 3 were used to verify that the coefficients were accurately simulating flow and sediment discharge within acceptable ranges at the watershed outlet and at various points within the watershed. In verifying storm events 2 and 3, only the infiltration parameters were adjusted to take into account the antecedent moisture conditions. For illustration purposes, rainfall gage 54 located near the middle of the watershed was selected for plots of the storm rainfall hyetograph. This gage was considered to closely represent an average of the seventeen gages within the watershed.

For all of the input grids (i.e., elevation, land use, and soil texture) the grid cell resolution was set to be 400 feet in height and 400 feet in width. In computing the output grids, the same grid cell resolution was used.

#### **5.2.1 - Sensitivity Analysis**

In performing this analysis, the storm event of October 17, 1981 was applied over the Goodwin Creek Watershed. Infiltration and channel routing were turned off so that the effects of changes in land use and changes in soil texture could be evaluated.

	Sand K=0.12	Silt K=0.48	Clay K=0.28
Forest C=0.008	Case 1	Case 2	Case 3
Idle Land C=0.07	Case 4	Case 5	Case 6
Row Crop C=0.65	Case 7	Case 8	Case 9

Figure 5.9 - Sensitivity Analysis

Case 1 assumed a uniform land use of forest and a uniform soil texture of sand. The maximum flow depth was computed to be 1.26 meters. The maximum sediment flux out of a grid cell was computed to be 0.63 cubic meters per second. The maximum suspended volume of sediment within a cell was computed to be 0.0 cubic meters. The maximum volume of sediment eroded off of a cell was 1998.9 cubic meters while the average volume of sediment eroded, off of the cells showing erosion, was computed to be 44.0 cubic meters for an average erosion depth of 2.96 millimeters. The maximum volume of sediment deposited on a cell was 1449.8 cubic meters while the average volume of sediment deposited, on the cells showing deposition, was 10.7 cubic meters for an average deposition depth of 0.72 millimeters.

Case 2 assumed a uniform land use of forest and a uniform soil texture of silt. The maximum flow depth was computed to be 1.26 meters. The maximum sediment flux out of

a grid cell was computed to be 2.54 cubic meters per second. The maximum suspended volume of sediment within a cell was computed to be 2.3 cubic meters. The maximum volume of sediment eroded off of a cell was 7995.5 cubic meters while the average volume of sediment eroded, off of the cells showing erosion, was computed to be 93.4 cubic meters for an average erosion depth of 6.3 millimeters. The maximum volume of sediment deposited on a cell was 5799.0 cubic meters while the average volume of sediment deposited, on the cells showing deposition, was 58.8 cubic meters for an average deposition depth of 3.95 millimeters.

Case 3 assumed a uniform land use of forest and a uniform soil texture of clay. The maximum flow depth was computed to be 1.26 meters. The maximum sediment flux out of a grid cell was computed to be 1.48 cubic meters per second. The maximum suspended volume of sediment within a cell was computed to be 276.8 cubic meters. The maximum volume of sediment eroded off of a cell was 4664.2 cubic meters while the average volume of sediment eroded, off of the cells showing erosion, was computed to be 67.3 cubic meters for an average erosion depth of 4.5 millimeters. The maximum volume of sediment deposited on a cell was 3382.5 cubic meters while the average volume of sediment deposited, on the cells showing deposition, was 29.8 cubic meters for an average deposition depth of 2.0 millimeters.

Case 4 assumed a uniform land use of idle land and a uniform soil texture of sand. The maximum flow depth was computed to be 1.22 meters. The maximum sediment flux out of a grid cell was computed to be 12.65 cubic meters per second. The maximum suspended volume of sediment within a cell was computed to be 0.0 cubic meters. The maximum volume of sediment eroded off of a cell was 25039.7 cubic meters while the

average volume of sediment eroded, off of the cells showing erosion, was computed to be 214.3 cubic meters for an average erosion depth of 14.4 millimeters. The maximum volume of sediment deposited on a cell was 18020.3 cubic meters while the average volume of sediment deposited, on the cells showing deposition, was 240.1 cubic meters for an average deposition depth of 16.1 millimeters.

Case 5 assumed a uniform land use of idle land and a uniform soil texture of silt. The maximum flow depth was computed to be 1.22 meters. The maximum sediment flux out of a grid cell was computed to be 50.6 cubic meters per second. The maximum suspended volume of sediment within a cell was computed to be 54.9 cubic meters. The maximum volume of sediment eroded off of a cell was 100159.0 cubic meters while the average volume of sediment eroded, off of the cells showing erosion, was computed to be 687.2 cubic meters for an average erosion depth of 46.2 millimeters. The maximum volume of sediment deposited on a cell was 72080.1 cubic meters while the average volume of sediment deposited, on the cells showing deposition, was 1466.3 cubic meters for an average deposition depth of 98.6 millimeters.

Case 6 assumed a uniform land use of idle land and a uniform soil texture of clay. The maximum flow depth was computed to be 1.22 meters. The maximum sediment flux out of a grid cell was computed to be 29.5 cubic meters per second. The maximum suspended volume of sediment within a cell was computed to be 5392.3 cubic meters. The maximum volume of sediment eroded off of a cell was 58426.8 cubic meters while the average volume of sediment eroded, off of the cells showing erosion, was computed to be 425.4 cubic meters for an average erosion depth of 28.6 millimeters. The maximum volume of sediment deposited on a cell was 42044.2 cubic meters while the average

volume of sediment deposited, on the cells showing deposition, was 742.1 cubic meters for an average deposition depth of 49.9 millimeters.

Case 7 assumed a uniform land use of row crop and a uniform soil texture of sand. The maximum flow depth was computed to be 1.15 meters. The maximum sediment flux out of a grid cell was computed to be 204.5 cubic meters per second. The maximum suspended volume of sediment within a cell was computed to be 0.1 cubic meters. The maximum volume of sediment eroded off of a cell was 289777.0 cubic meters while the average volume of sediment eroded, off of the cells showing erosion, was computed to be 1903.4 cubic meters for an average erosion depth of 128.0 millimeters. The maximum volume of sediment deposited on a cell was 206863.0 cubic meters while the average volume of sediment deposited, on the cells showing deposition, was 4741.3 cubic meters for an average deposition depth of 318.8 millimeters.

Case 8 assumed a uniform land use of row crop and a uniform soil texture of silt. The maximum flow depth was computed to be 1.15 meters. The maximum sediment flux out of a grid cell was computed to be 817.8 cubic meters per second. The maximum suspended volume of sediment within a cell was computed to be 987.4 cubic meters. The maximum volume of sediment eroded off of a cell was 1159110.0 cubic meters while the average volume of sediment eroded, off of the cells showing erosion, was computed to be 7524.6 cubic meters for an average erosion depth of 506.0 millimeters. The maximum volume of sediment deposited on a cell was 827444.0 cubic meters while the average volume of sediment deposited, on the cells showing deposition, was 19704.9 cubic meters for an average deposition depth of 1325.0 millimeters.



Case 9 assumed a uniform land use of row crop and a uniform soil texture of clay. The maximum flow depth was computed to be 1.15 meters. The maximum sediment flux out of a grid cell was computed to be 477.0 cubic meters per second. The maximum suspended volume of sediment within a cell was computed to be 78109.6 cubic meters. The maximum volume of sediment eroded off of a cell was 676154.0 cubic meters while the average volume of sediment eroded, off of the cells showing erosion, was computed to be 4393.2 cubic meters for an average erosion depth of 295.4 millimeters. The maximum volume of sediment deposited on a cell was 482655.0 cubic meters while the average volume of sediment deposited, on the cells showing deposition, was 11459.2 cubic meters for an average deposition depth of 770.5 millimeters.

The final total net volume grids (Figure 5.10), for cases 1 through 9, show the general pattern of erosion and deposition that one would expect to see. In the upland areas, there are different degrees of erosion taking place depending upon the land use and soil texture. In areas of mild slopes, different degrees of deposition take place depending upon the land use and soil texture. From the results discussed above, the relative order of magnitude of erosion between the different cases was expected. However, the amount of deposition, when the uniform sediment size was clay, was not expected. Examining the trap efficiency formulation (equation 3.25), the fall velocity of the fine grain sediments (i.e., clay) needs to be modified to take into account the turbulent nature of the overland flow and the re-suspension of the fine grain sediment particles into the flow field.

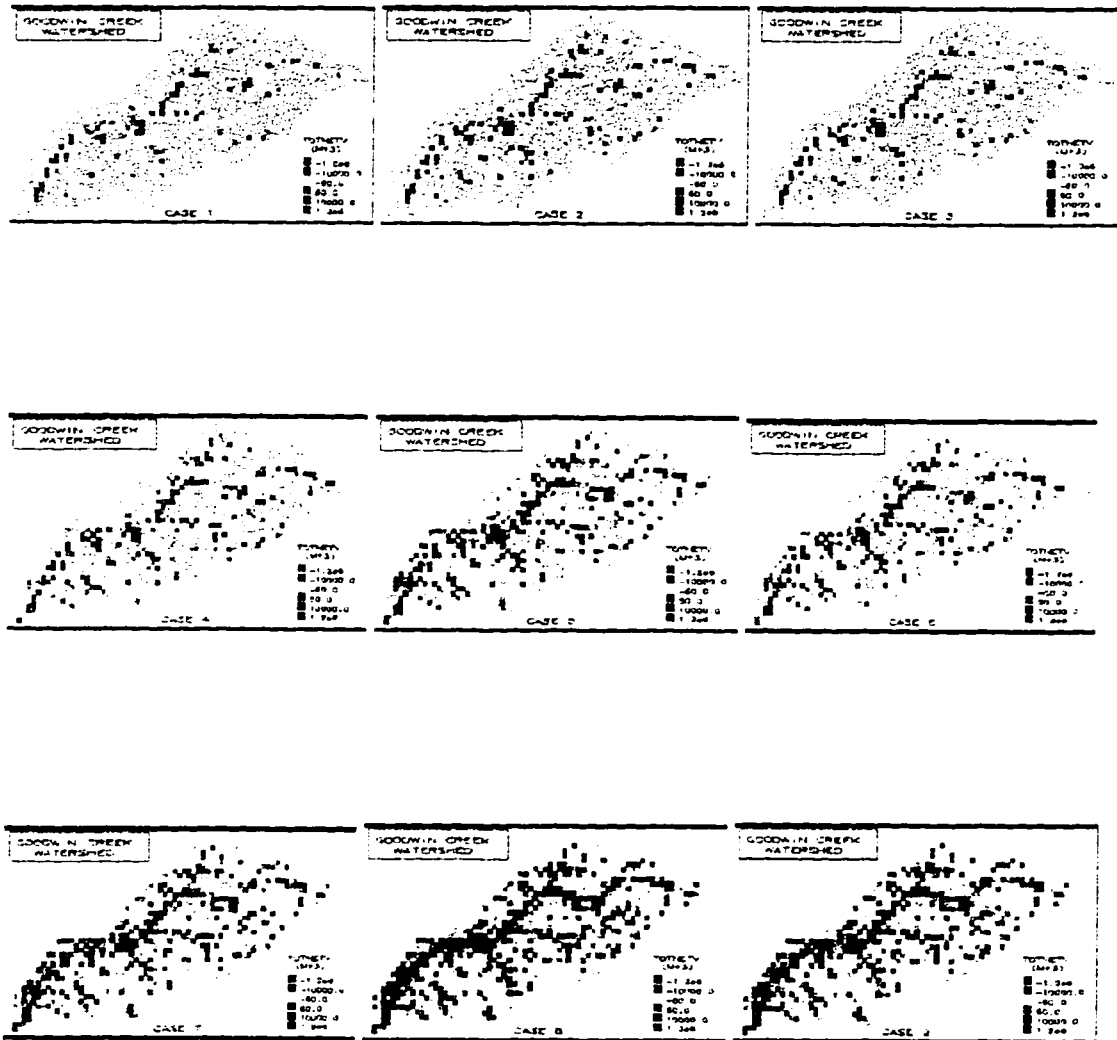


Figure 5.10 - Final Total Net Volume Grids for the Goodwin Creek Watershed Sensitivity Analysis.

### 5.2.2 - Storm Event 1

The storm event of October 17, 1981 began at 9:19 pm and had a total rainfall duration of 3.5 hours with very little rainfall preceding this event. The actual rainfall hyetograph for rain gage 54 is shown in Figure A-4. Total rainfall for this event varied from 2.55 to 3.11 inches with an average value of 2.85 inches (Table A-1). Total runoff varied from 0.87 inches at the upper streamflow gage to 0.64 inches at the downstream gaging location (Table A-3).

A comparison of the hydrograph plots (Figure A-5 to Figure A-7) and the hydrograph parameters (Table A-2 to Table A-4) show that CASC2D had a varying degree of simulation success. CASC2D was able to consistently simulate the overall shape and rate of rise. The time to peak was simulated within 3% at some places (gage 8 and gage 5), but was off by approximately 15% at gages 2 and 4. CASC2D simulated the total volume of runoff low by approximately 20% across the watershed. The peak flows were within 1% to 8% throughout the watershed except at gage 3, which was off by 26%.

A comparison of the sediment discharge plots (Figure A-8 to Figure A-12) and the sediment yield parameters (Table A-5 to Table A-6) show that CASC2D was able to predict upland erosion off of the Goodwin Creek Watershed within an acceptable range of -50% to 200% of the actual upland erosion. This range (-50% to 200%) is generally accepted by sedimentation engineers as being acceptable when comparing computed sediment yields versus actual sediment yields.

The CASC2D output grids (Appendix C) show various grids (i.e., rainfall, infiltration, depth, sediment flux, suspended sediment volume, and total net volume) changing with

time for this simulation. Figure 5.11 to Figure 5.15, show the CASC2D output grids changing with time for this event. The maximum overland depth was computed to be 0.16 meters while the maximum channel depth was computed to be 2.0 meters. The maximum infiltration depth was computed to be 0.13 meters and the maximum rainfall intensity for this event was 7.2 inches/hour. Evaluating the total net volume grids, the maximum sediment deposited on a cell was 1362.2 cubic meters, which results in a deposition depth of 91.6 millimeters. The average volume of sediment deposited, for all the grid cells showing deposition, was 9.5 cubic meters, resulting in an average deposition depth of 0.64 millimeters. The maximum sediment eroded from a grid cell was 1363.1 cubic meters, which results in an erosion depth of 91.7 millimeters. The average volume of sediment eroded, for all the grid cells showing erosion, was 18.3 cubic meters, resulting in an average erosion depth of 1.2 millimeters. From evaluating the total net volume grids, as the overland flow moves towards the crop lands, between gages 2 and 3, some of the eroded material starts to deposit. From the field trip taken on November 13, 1996, Figures 4.8 to 4.11, this general pattern of erosion and deposition was observed for the uplands and the row crops. However, as the flow exits the fields and enters the channel network system, rill and gully formations start to occur at selected locations. Comparing the total sediment yield (tons) versus upland erosion (tons) (Table A-5) and the total sediment yield (tons/acre) versus upland erosion (tons/acre) (Table A-6), one can see that the per cent of upland erosion as a component of total sediment yield is within acceptable ranges (20% to 40%) for the Goodwin Creek Watershed. From field observations and data collection activities over a number of years (1981 to 1997), the ARS has estimated the contribution of upland erosion to the total sediment yield, at the outlet of the Goodwin Creek

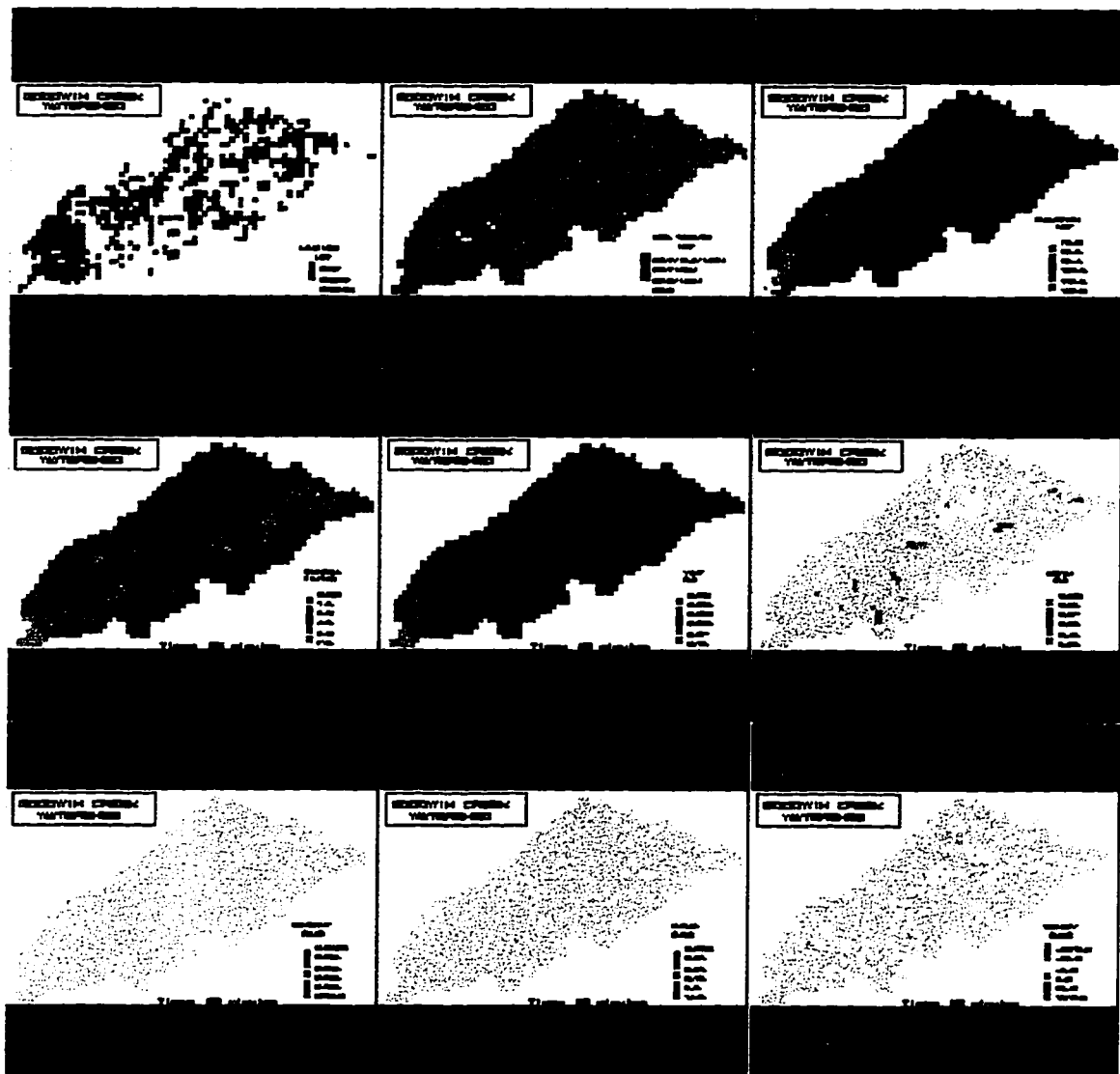


Figure 5.11 - October 17-18, 1981 at Time = 80.0 minutes.

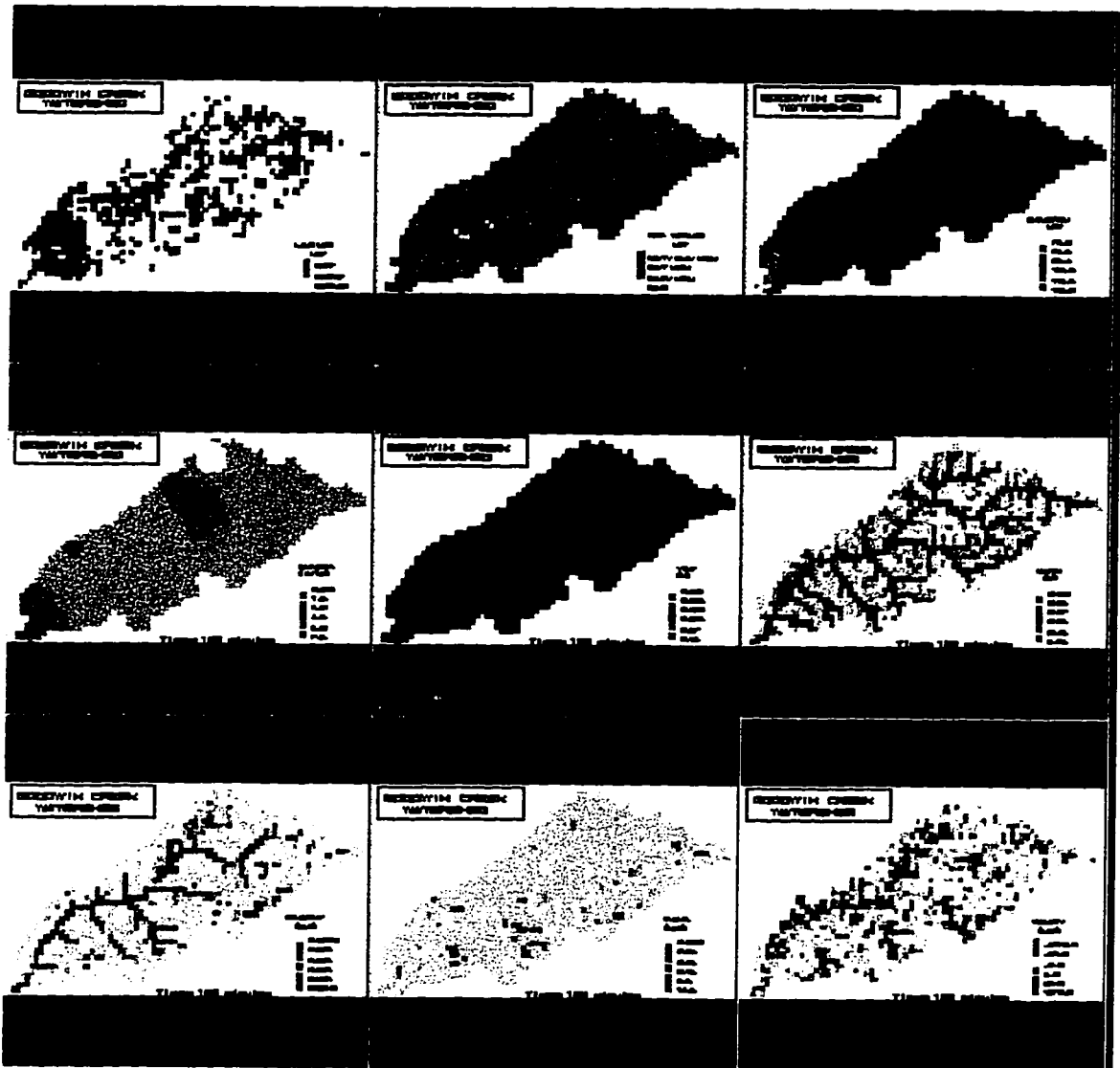


Figure 5.12 - October 17-18, 1981 at Time = 180.0 minutes.

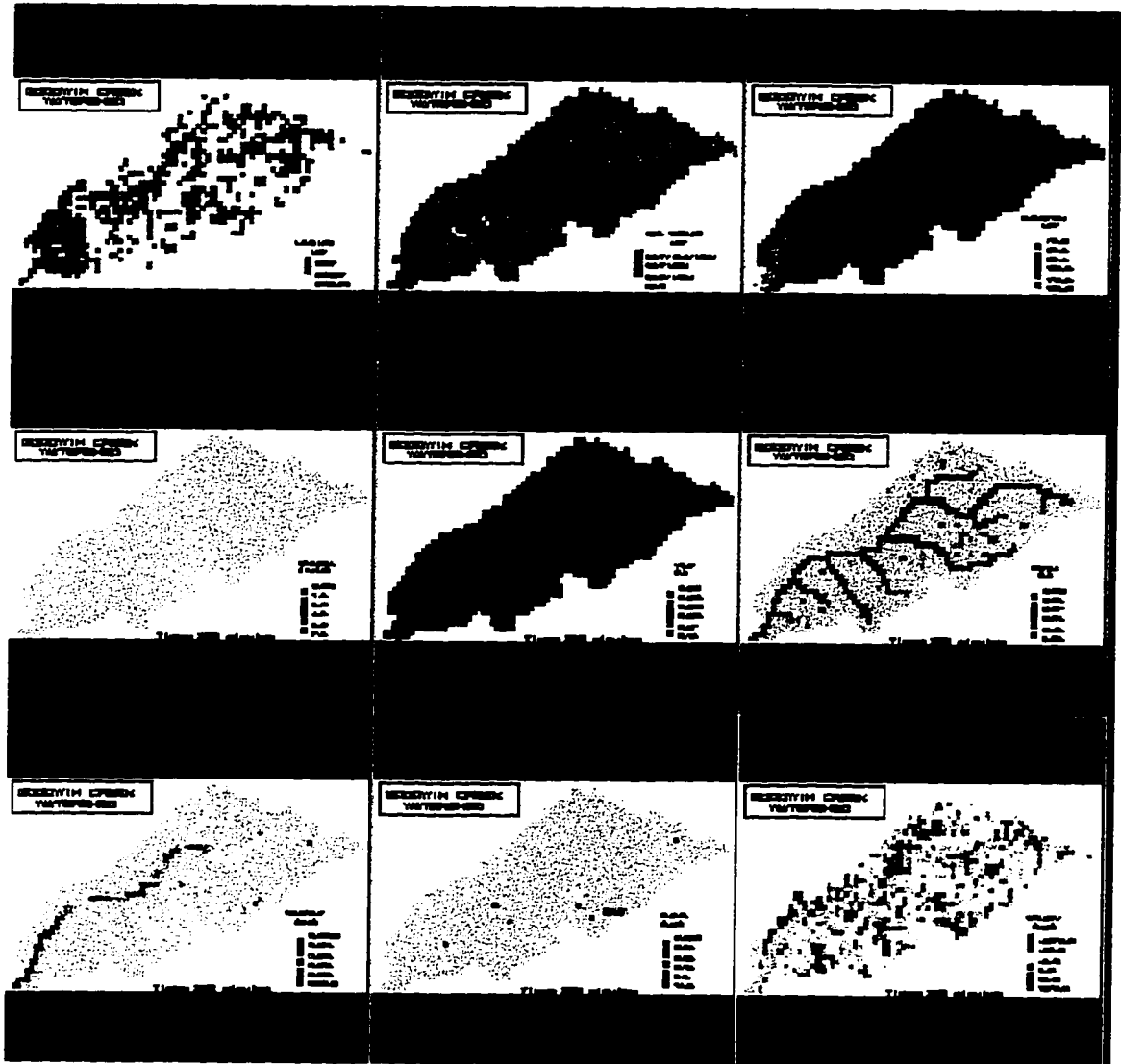


Figure 5.13 - October 17-18, 1981 at Time = 280.0 minutes.

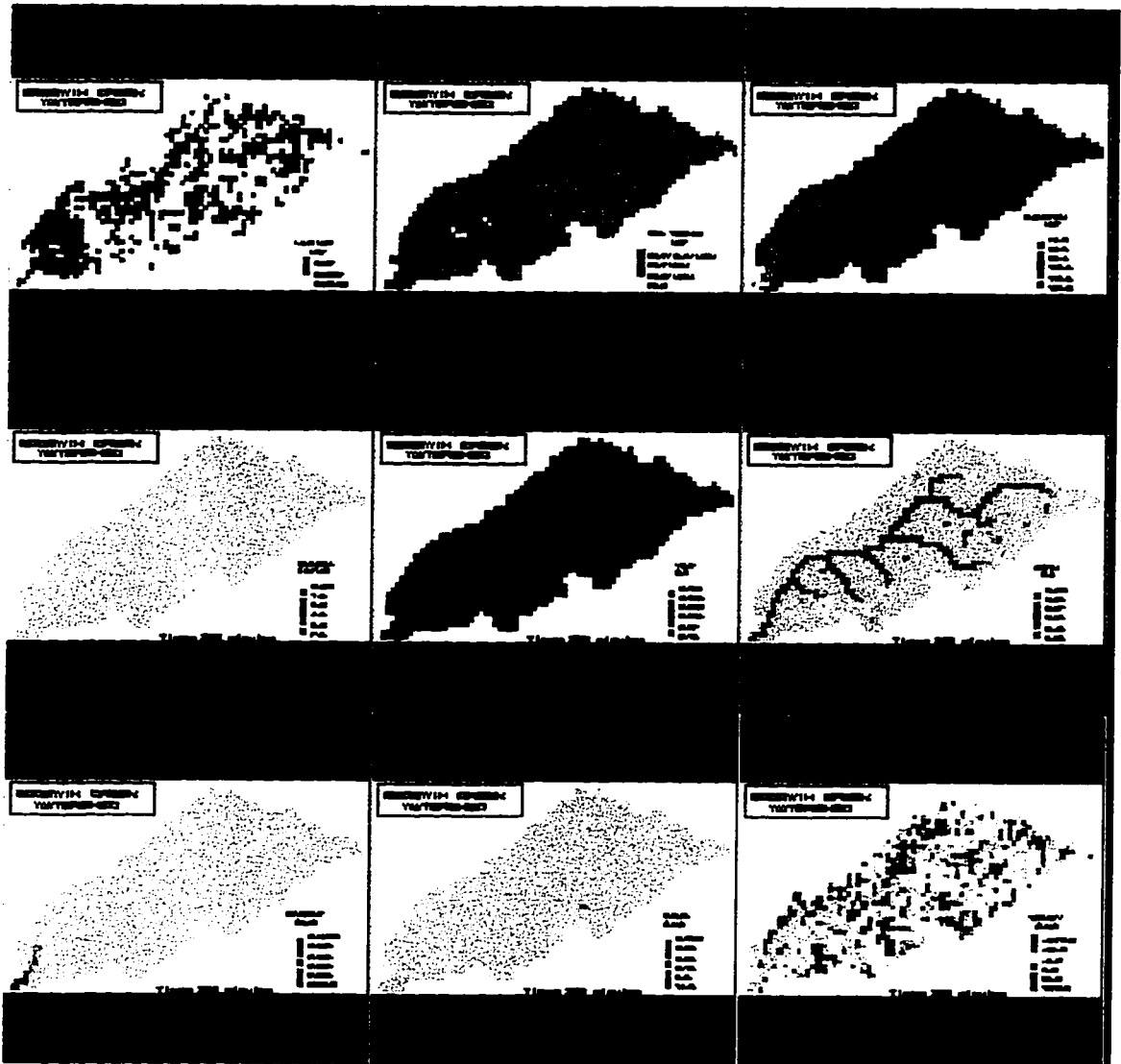


Figure 5.14 - October 17-18, 1981 at Time = 380.0 minutes.



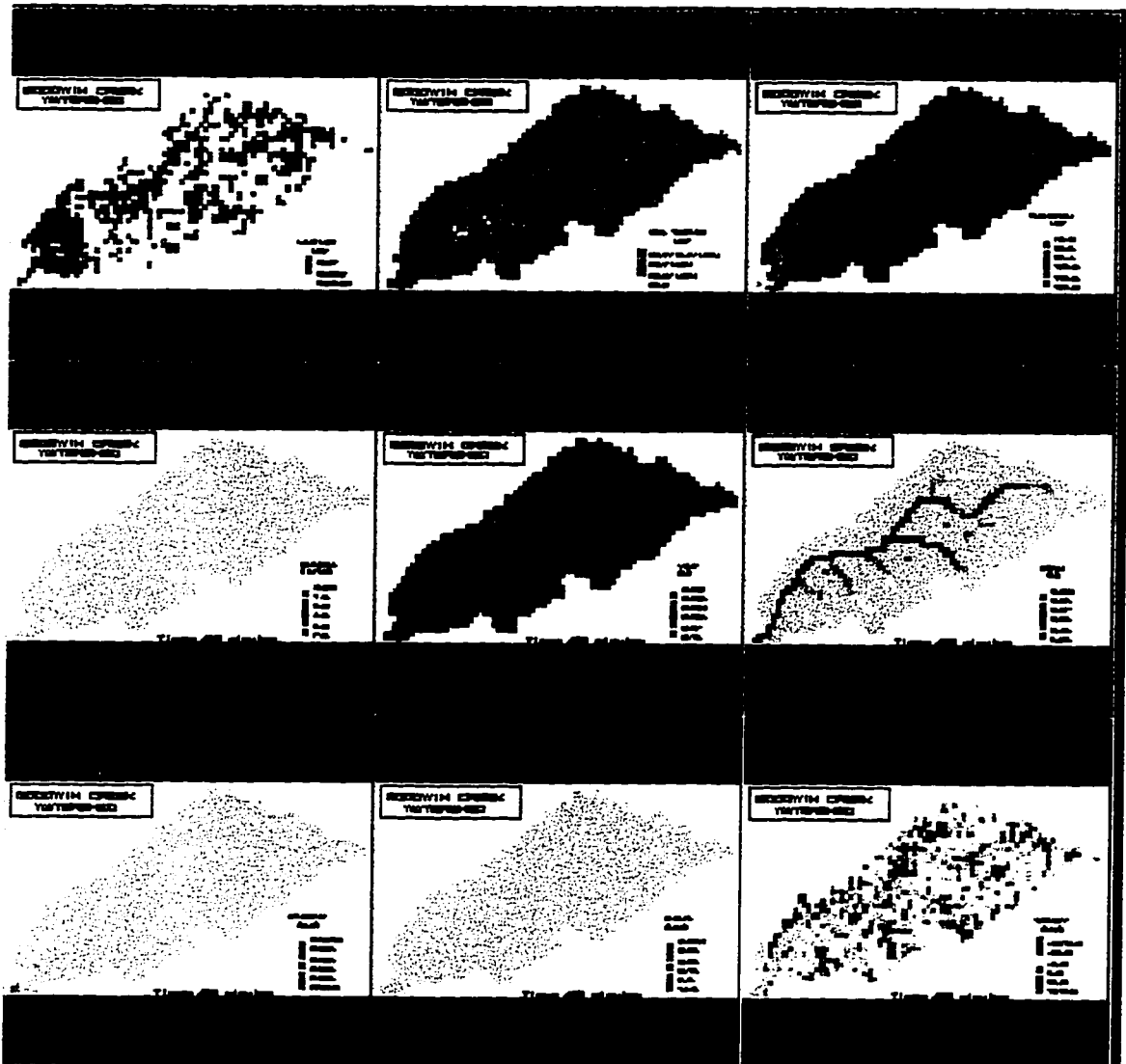


Figure 5.15 - October 17-18, 1981 at Time = 480.0 minutes.

Watershed, to be 20% to 40%. The total sediment yield at the outlet was 1394.4 tons and 0.26 tons/acre while CASC2D computed upland erosion, at the outlet, to be 420.6 tons and 0.08 tons/acre. This resulted in the volume of sediment passing the outlet due to upland erosion being 30.2% of the total volume of sediment. For this simulation, gages 4 and 14 showed the highest per cent of upland erosion at 95.3% and 106.5% with gage 5 showing the lowest at 15.6%.

Some of the gages showed a low percent of sediment yield due to upland erosion (i.e., 2, 3, 5, 9, and 12). From field observations (Figure 4.16 to Figure 4.19) there was evidence of significant channel processes taking place at isolated locations within the watershed. This introduction of sediment from the channel banks and the channel bed would cause a significant decrease in the percent of total sediment yield due to upland erosion.

### **5.2.3 - Storm Event 2**

The storm event of December 2, 1983 began at 12:00 am and had a total rainfall duration of 30 hours. There was significant rainfall preceding this event, therefore infiltration rates can be expected to be low. The hyetograph of observed rainfall for rain gage 54 is shown in Figure A-4. Total rainfall varied from 5.64 to 6.00 inches with an average of 5.82 inches (Table A-1). Total runoff varied from 4.88 inches at gage 8 to 4.85 inches at gage 1 (Table A-3).

A comparison of the hydrograph plots (Figure A-13 to Figure A-15) and the hydrograph parameters (Tables A-2 to A-4) show that CASC2D was able to simulate the overall shape and rate of rise. However, this simulation produced time to peaks

consistently too fast (12 minutes to 36 minutes) when compared to observed time to peaks throughout the watershed.

A comparison of the sediment discharge plots (Figure A-16 to Figure A-20) and the sediment yield parameters (Table A-5 to Table A-6) show that CASC2D was able to compute sediment yield to within 65% of the observed sediment yield at the outlet. However, some of the gages within the watershed showed a rather high volume of computed upland erosion when compared to the total observed sediment yield (400%). Figure 5.16 to Figure 5.20, show the CASC2D output grids changing with time for this event.

The crop management factors used for this simulation reflect values associated with high land disturbance. Since this event occurred in December, when farming practices were at a minimum, a reduction in the crop management factor for the row crop and pasture seems to be in order.

The maximum overland depth was computed to be 1.1 meters and the maximum channel depth was computed to be 3.1 meters. The maximum infiltration depth was computed to be 0.2 meters with the maximum rainfall intensity being 10.8 inches/hour. Evaluating the total net volume grids, the maximum sediment deposited on a grid cell was 4816.7 cubic meters, which results in a sediment deposition depth of 323.9 millimeters. The average volume of sediment deposited, over the grid cells showing deposition, was 76.9 cubic meters, resulting in an average deposition depth of 5.2 millimeters. The maximum sediment eroded off of a grid cell was computed to be 4612.1 cubic meters,

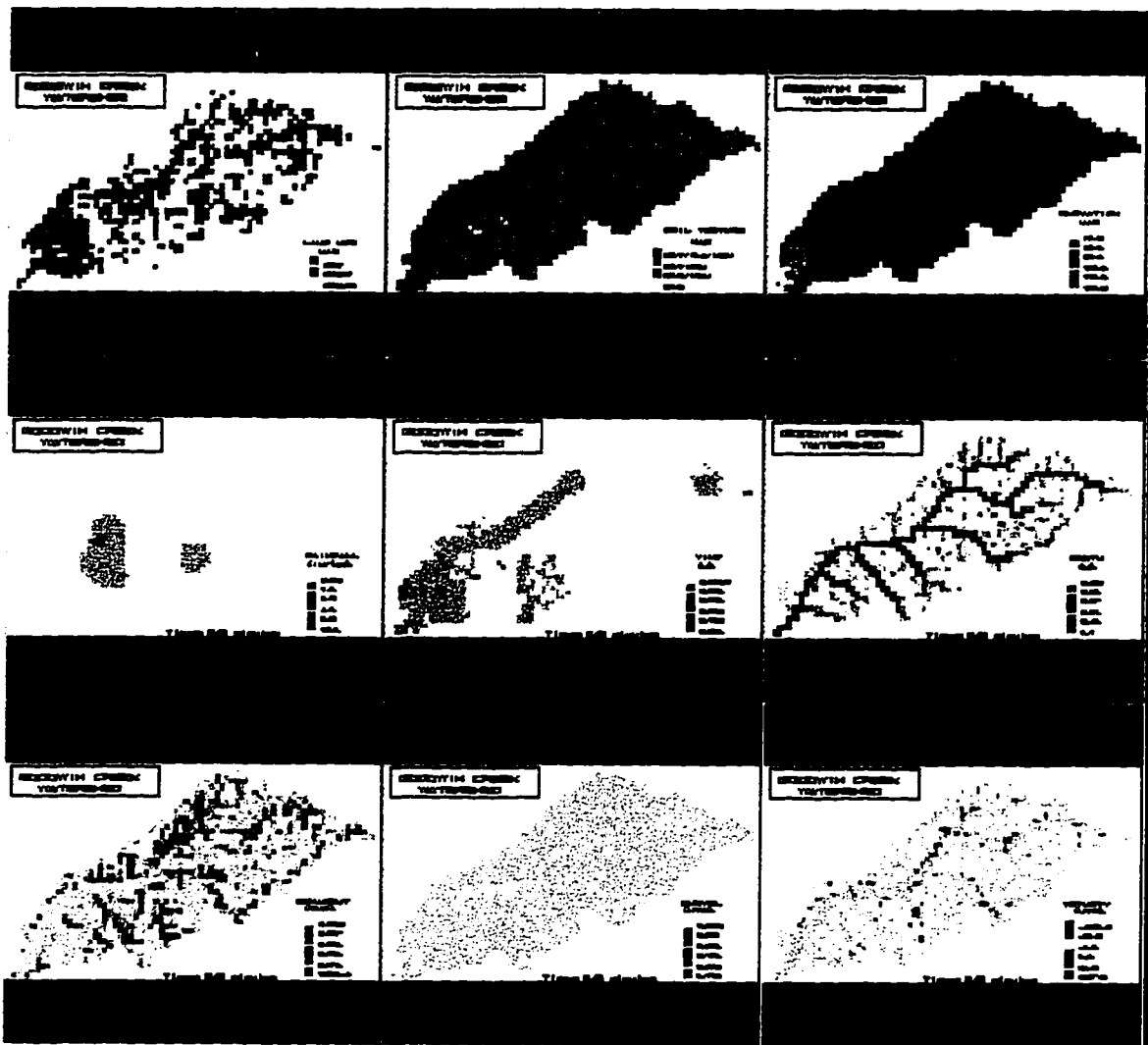


Figure 5.16 - December 2-3, 1983 at Time = 840.0 minutes.

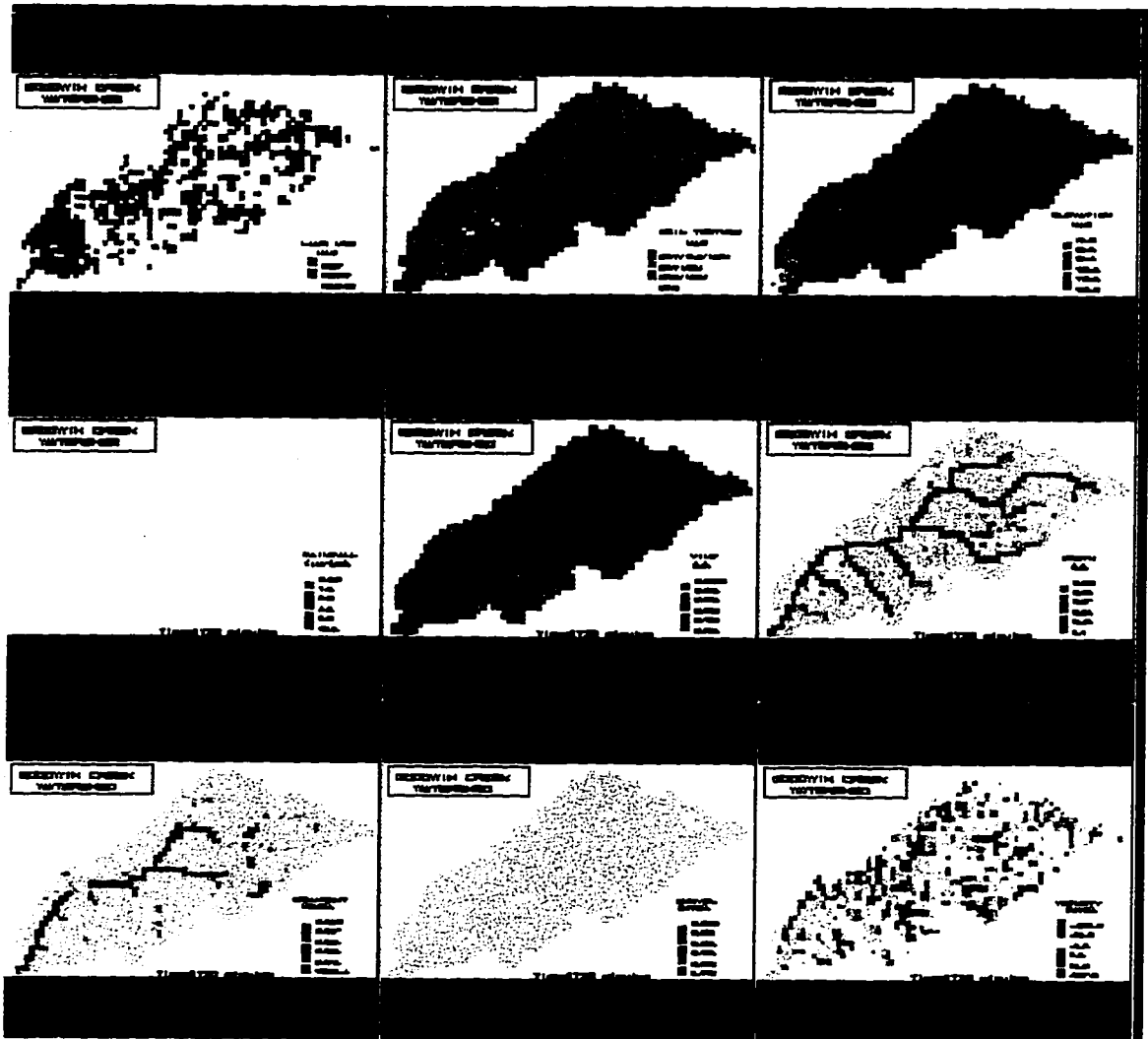


Figure 5.17 - December 2-3, 1983 at Time = 1720.0 minutes.

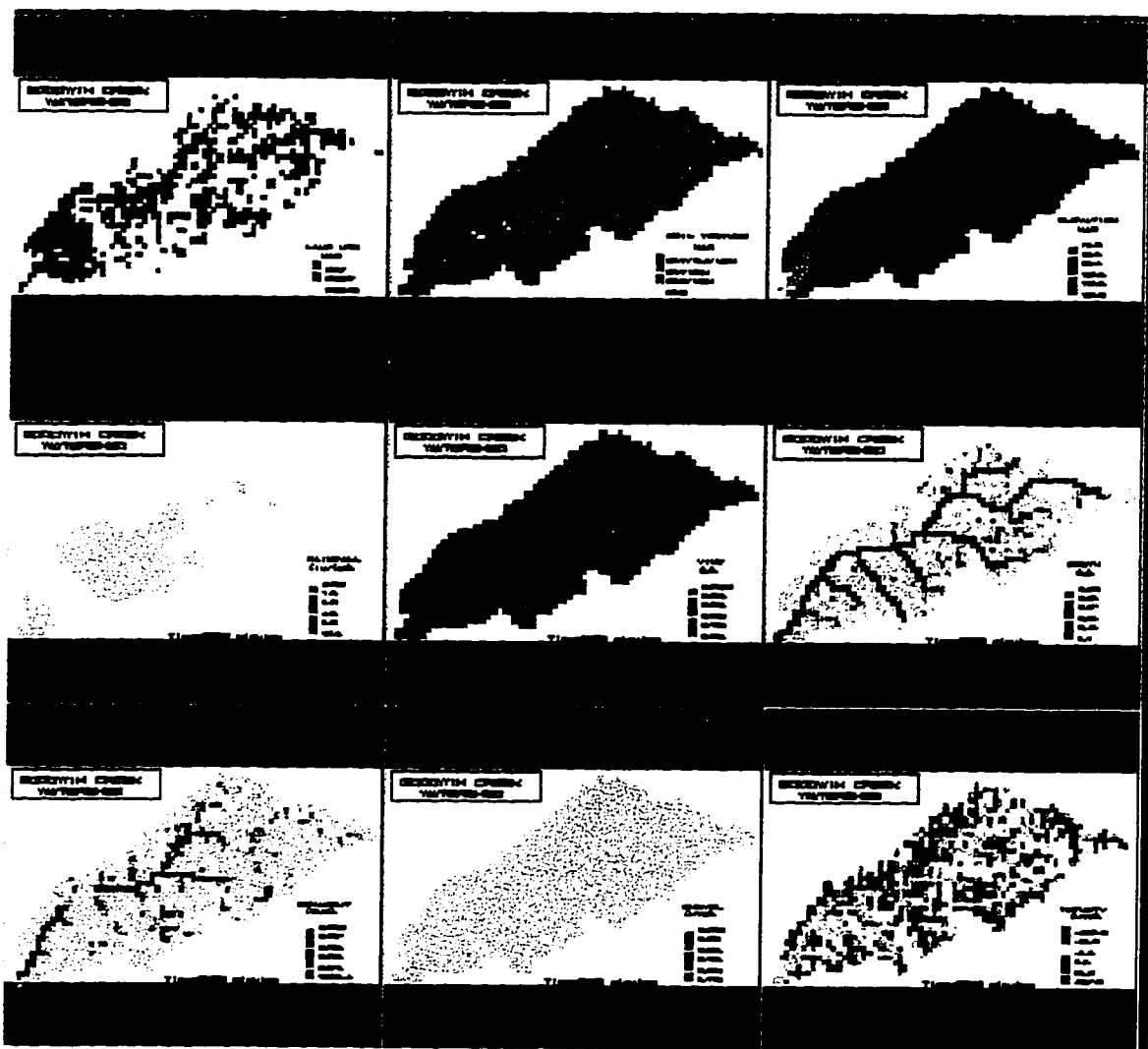


Figure 5.18 - December 2-3, 1983 at Time = 2600.0 minutes.

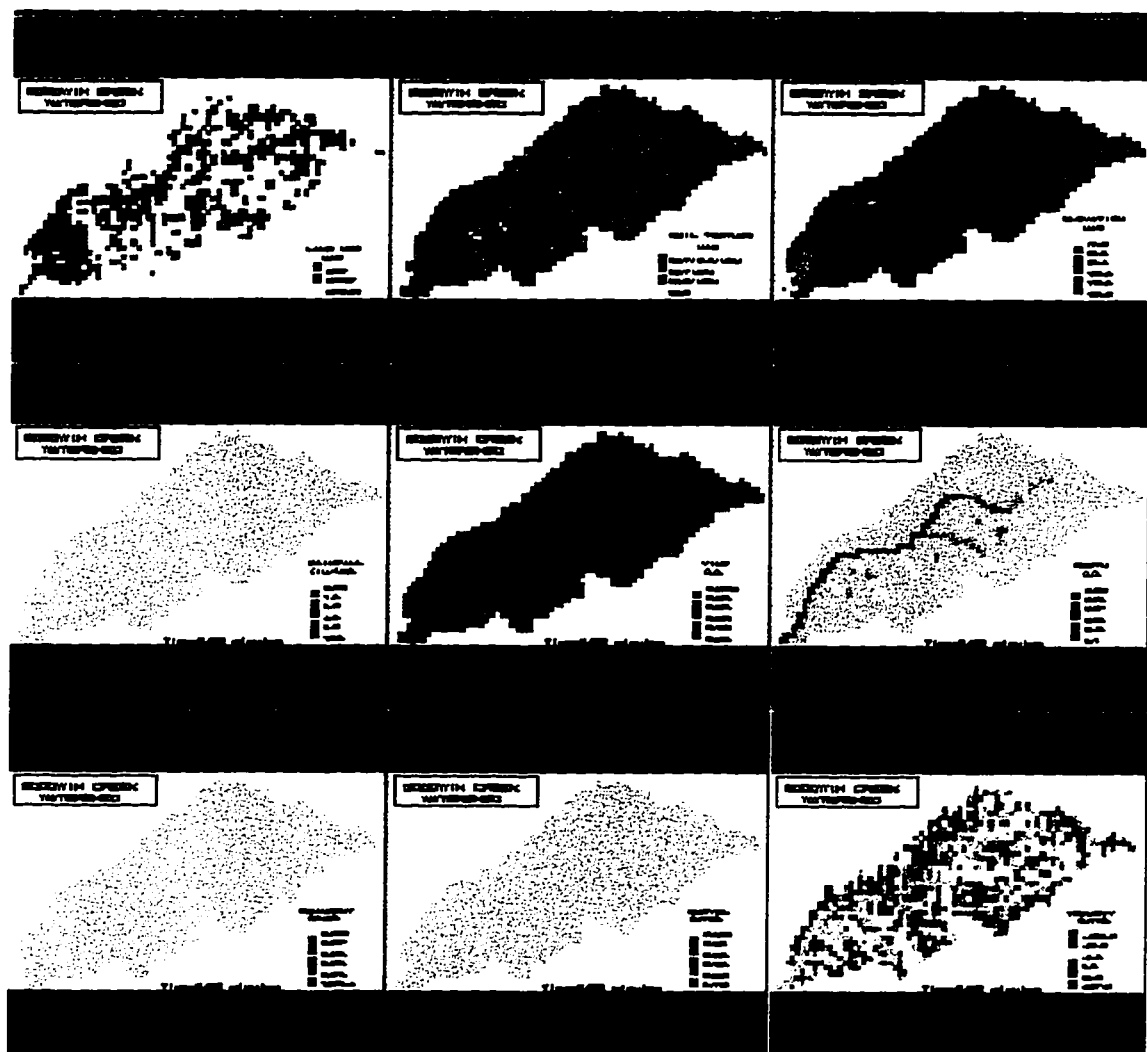


Figure 5.19 - December 2-3, 1983 at Time = 3480.0 minutes.

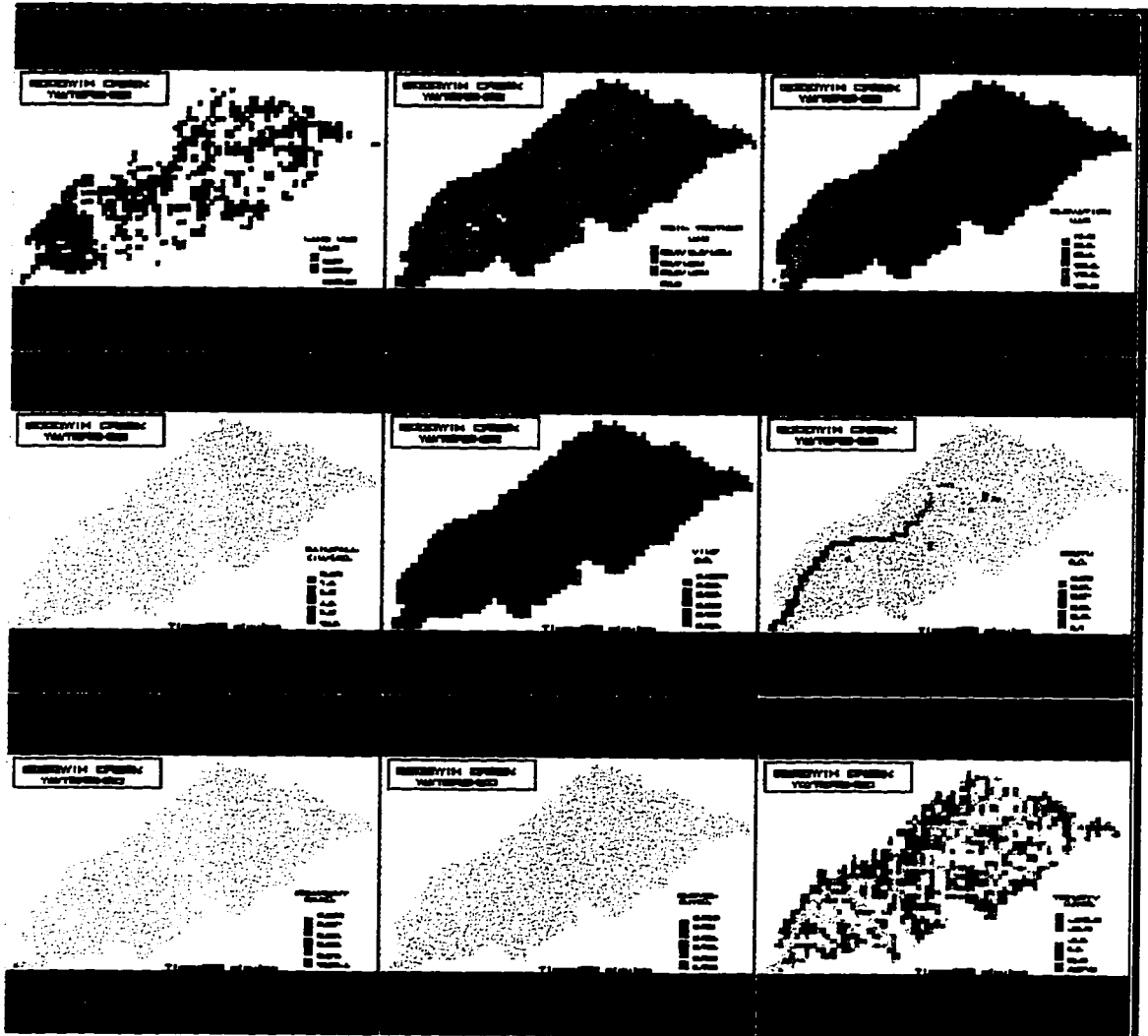


Figure 5.20 - December 2-3, 1983 at Time = 4320.0 minutes.



which results in an erosion depth of 310.1 millimeters. The average volume of sediment eroded, over the grid cells showing erosion, was 42.2 cubic meters, resulting in an average erosion depth of 2.8 millimeters.

#### **5.2.4 - Storm Event 3**

The storm event of May 2-3, 1984 began at 12:00 am and had a total rainfall duration of 28 hours. There was a moderate amount of rainfall preceding this event, therefore the infiltration rates can be expected to be low in some areas. The actual rainfall hyetograph for rain gage 54 is shown in Figure A-4. Total rainfall for this event varied from 4.46 to 4.90 inches with an average value of 4.65 inches (Table A-1). Total runoff varied from 3.76 inches at gage 8 to 3.66 inches at gage 1.

A comparison of the hydrograph plots (Figure A-21 to Figure A-23) and the hydrograph parameters (Table A-2 to Table A-4) show that the model was able to simulate the overall shape, rate of rise, and the total volume of runoff. However, for this simulation, CASC2D was off at selected locations on the time to peak and the peak flow. At the outlet, the measured peak flow was 3662.3 and CASC2D computed the peak flow to be 3743.5, so CASC2D estimated the peak flow at the watershed outlet to within 2.2%. At gage 3, the measured peak flow was estimated to be 3193.7 and CASC2D computed a peak flow of 1936.5. Since all of the other gages seemed to compare relatively well (1% to 30%) with the observed peak flow measurements, the difference at gage 3 seems to be out of place and may suggest some error in the instrumentation at this gage site.

The time to peak was off by a rather large amount at the outlet, with the difference between measured and computed being 46 minutes. In the upper portion of the watershed,

the time to peak was too fast by approximate 15 minutes with the difference increasing as the flow moved down the watershed.

A comparison of the sediment discharge plots (Figure A-24 to Figure A-28) and the sediment yield parameters (Table A-5 to Table A-6) show CASC2D computing upland erosion within acceptable ranges at most of the gages (-50% to 200%). Gages 4, 9, and 14 show upland erosion amounts to be a little high (125% to 265%), but again, since the model is using average annual crop management factors and not taking into account seasonal variations, this can be expected. At the outlet, the observed sediment yield was 10487.6 tons and 1.98 tons/acre, while CASC2D computed the upland erosion component to be 3647.0 tons and 0.69 tons/acre. This results in a per cent of total sediment yield due to upland erosion being 34.8%.

Figure 5.21 to Figure 5.25, show the CASC2D output grids changing with time for this event. The maximum overland depth was computed to be 0.9 meters with the maximum channel depth being computed to be 3.5 meters. The maximum infiltration depth was computed to be 0.13 meters and the maximum rainfall intensity was 15.6 inches/hour. Evaluating the total net volume grids, the maximum sediment deposited on a grid cell was computed to be 6054.7 cubic meters, resulting in a deposition depth of 407.1 millimeters. The average volume of sediment deposited, over all the grid cells showing deposition, was 109.8 cubic meters, resulting in an average deposition depth of 7.4 millimeters. The maximum volume of sediment eroded off of a grid cell was 6058.0 cubic meters, which results in an erosion depth of 407.3 millimeters. The average volume of sediment eroded, over all the grid cells showing erosion, was 62.7 cubic meters, resulting in an average erosion depth of 4.2 millimeters.

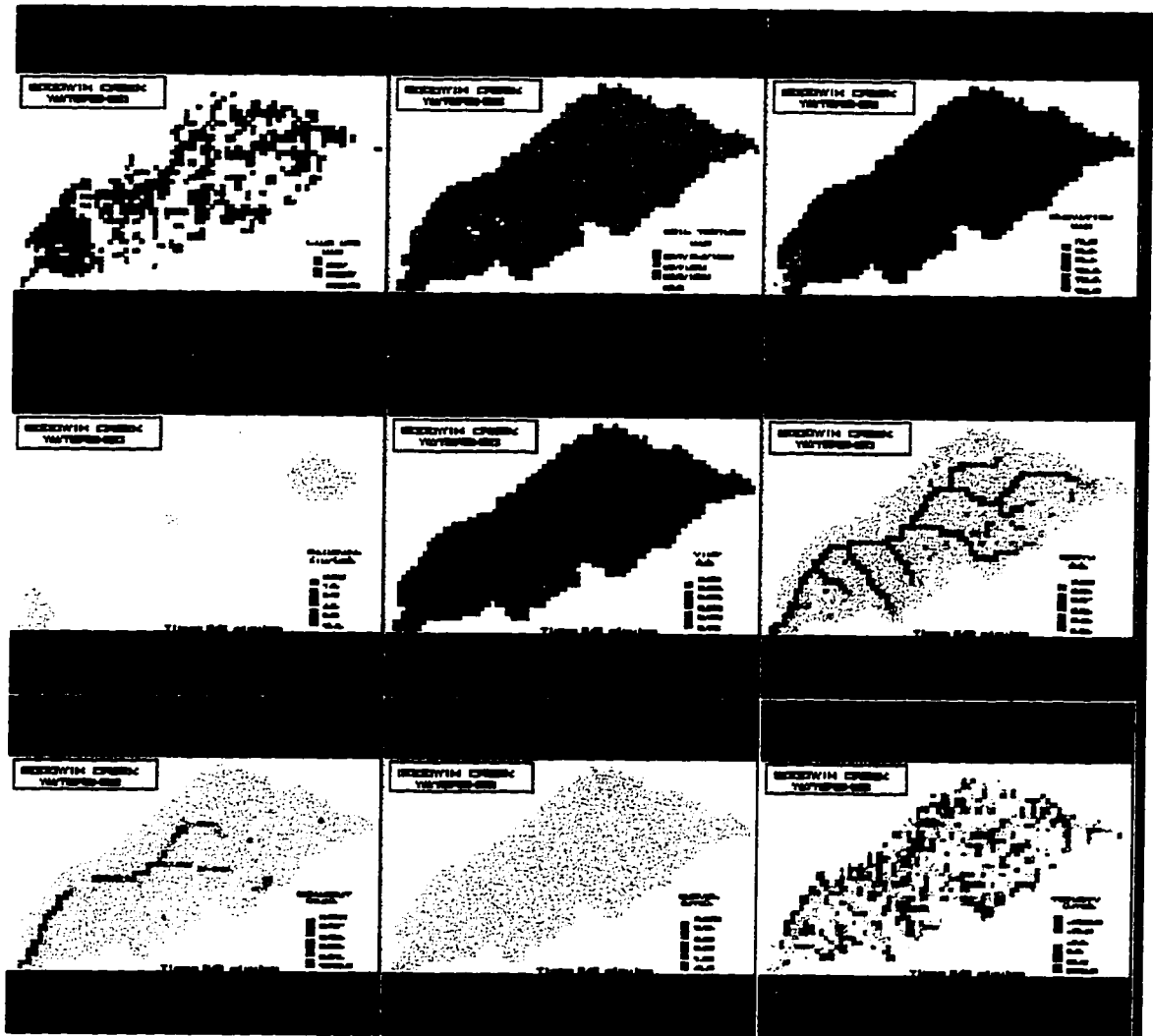


Figure 5.21 - May 2-3, 1984 at Time = 840.0 minutes.

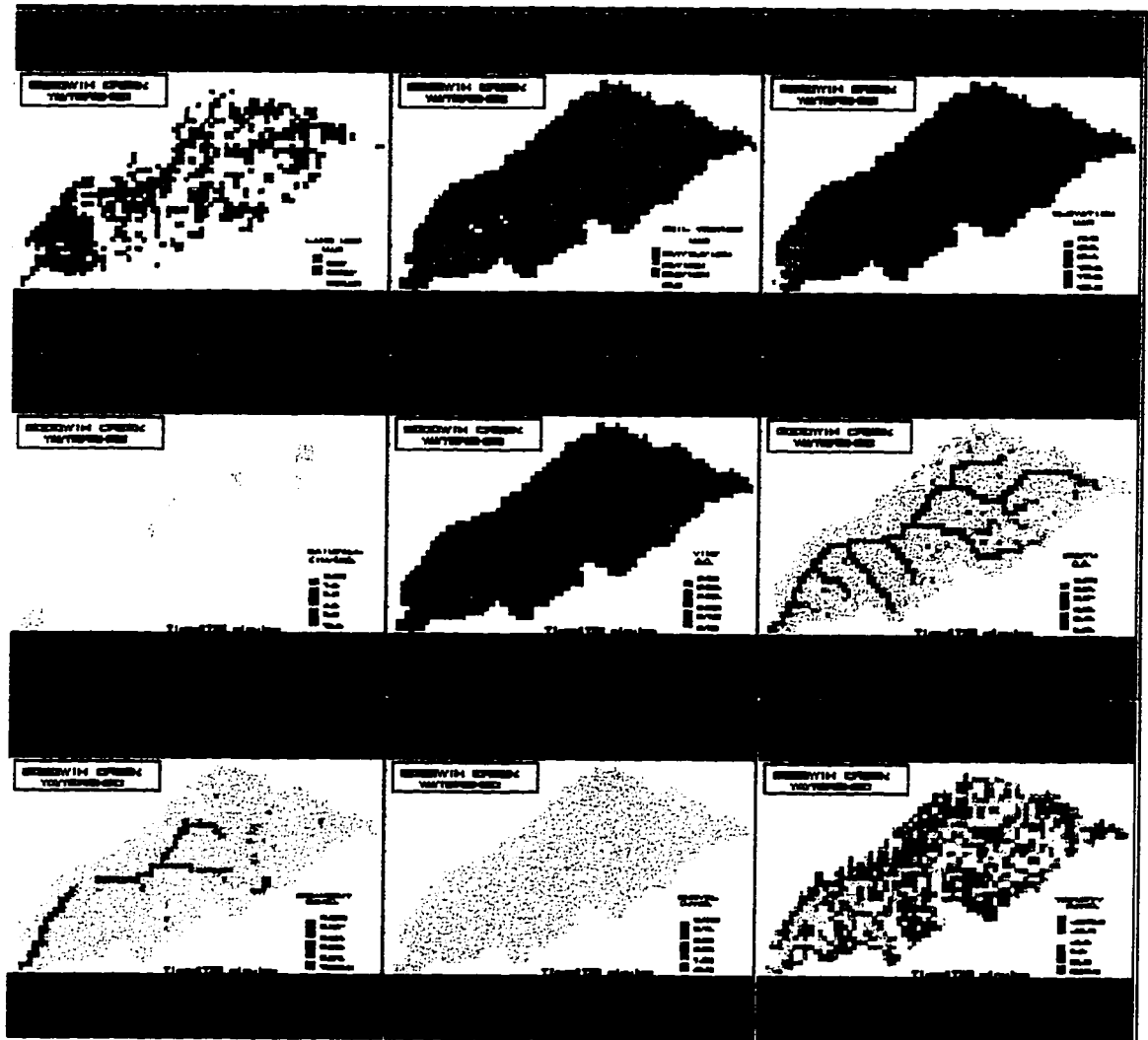


Figure 5.22 - May 2-3, 1984 at Time = 1720.0 minutes.

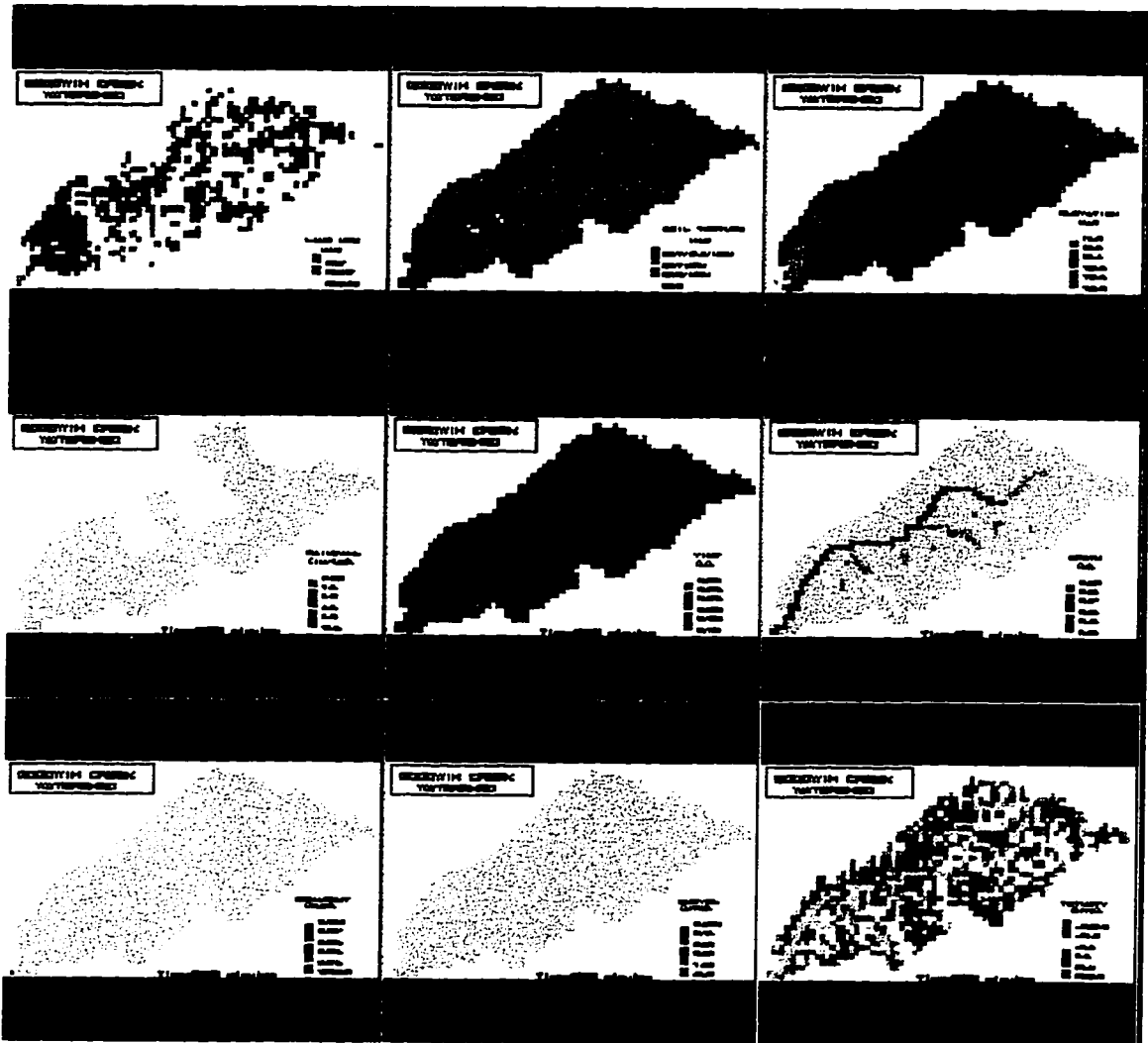


Figure 5.23 - May 2-3, 1984 at Time = 2600.0 minutes.

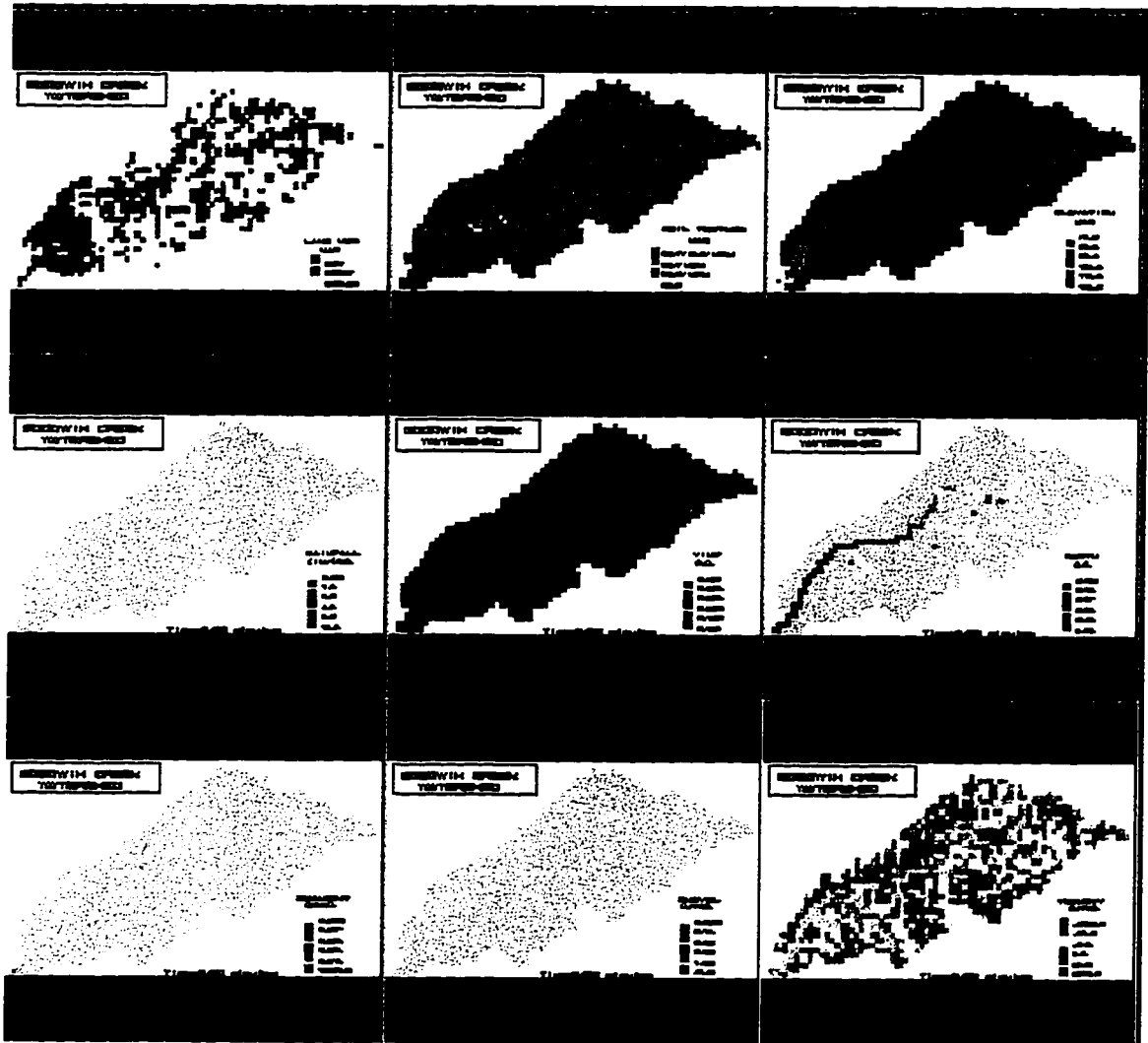


Figure 5.24 - May 2-3, 1984 at Time = 3480.0 minutes.

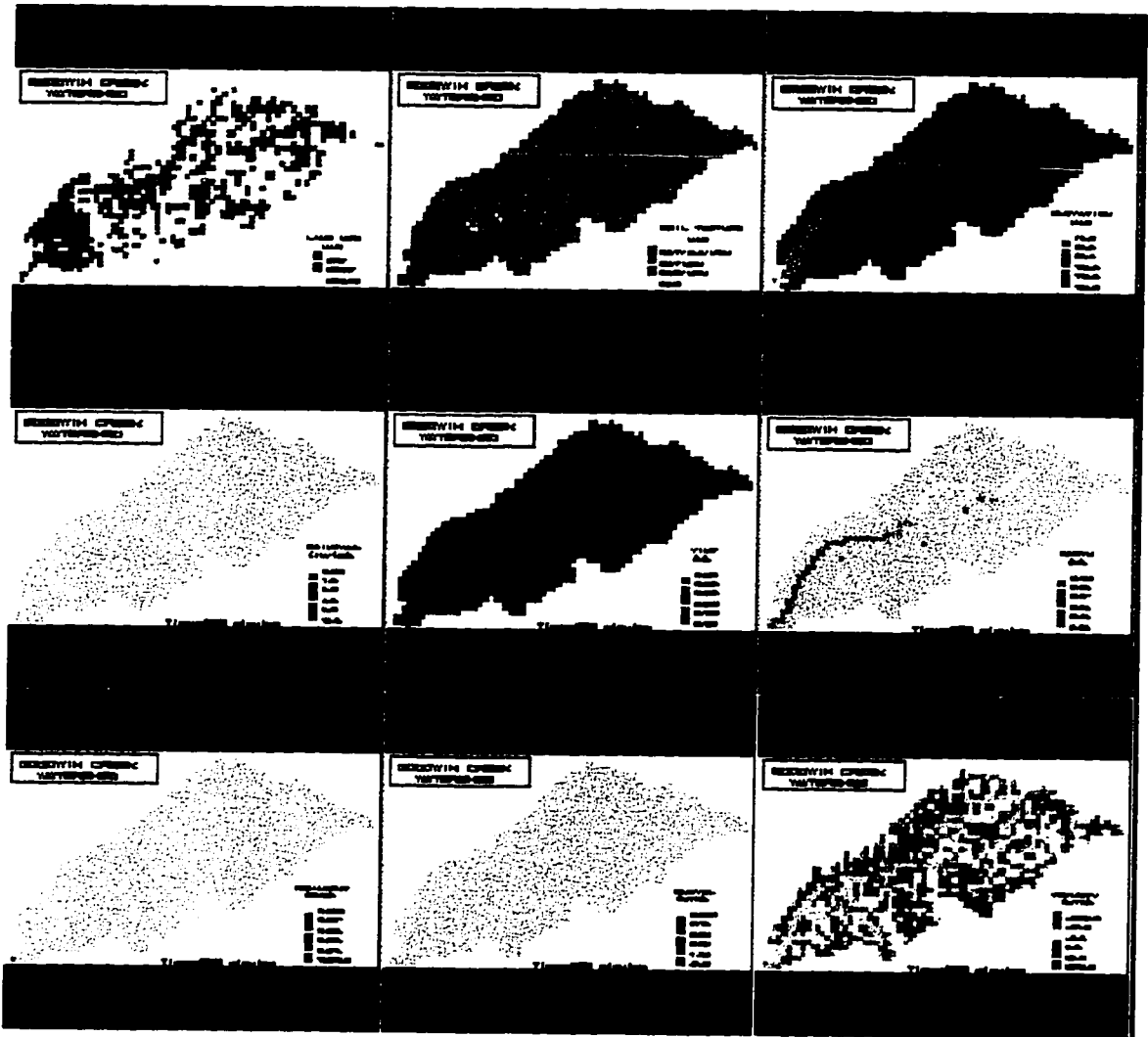


Figure 5.25 - May 2-3, 1984 at Time = 4320.0 minutes.

## **CHAPTER 6**

### **Summary, Conclusions, and Recommendations**

#### **6.1 - Summary**

In performing this research, the main goal was to develop a storm event based upland erosion scheme for the two dimensional hydrology model, CASC2D. An erosion scheme was developed where by three size classes (i.e., sand, silt, and clay) can be transported, in both the x-direction and the y-direction, from one grid cell (outgoing cell) to an adjacent grid cell (receiving cell).

In order to demonstrate that the scheme was computing sediment yield within reasonable ranges, simulations were run for both the test plot scale (5.2 acres) and the watershed scale (8.2 square miles).

On the test plot scale, the Nelson Farm Test Plot #2 was used. In performing the analysis on the test plot, single events (i.e., February 1991 and June 1992) and various hypothetical events (annual yield analysis) were simulated.

The watershed used in this research was the Goodwin Creek Watershed located in North Mississippi. There were three storm events (i.e., October 17-18, 1981, December 2-3, 1983, and May 2-3, 1984) used to calibrate and verify the erosion scheme on a single event basis. There was also a sensitivity analysis performed whereby various scenarios of uniform land use and uniform soil texture were evaluated.



## 6.2 - Conclusions

From the watershed and the test plot results, the following conclusions can be drawn:

1.) CASC2D accurately simulated the rainfall-runoff processes for both the watershed scale and the test plot scale.

2.) The erosion and deposition patterns computed by the upland sediment scheme is accurate when compared to field observations made on the Goodwin Creek Watershed.

3.) The upland sediment scheme implemented within the CASC2D model computed sediment yield from upland erosion on both the watershed scale and on the test plot scale, within reasonable limits (-50% to 200%) on a single event basis (Goodwin Creek and Nelson Farm) and an annual basis (Nelson Farm).

4.) The linkage of the GRASS GIS with CASC2D did help in the manipulation of input grids and the animation of output grids. In the calibration and verification of the model, the lack of animation tools would have made it very difficult to evaluate the results.

5.) In the upland drainage areas (Goodwin Creek Watershed), the upland sediment scheme was able to compute sediment yield well within an acceptable range (-50% to 200%). In the channel system, there are other components (gully erosion, bank failure, and bed erosion) that contribute to the total sediment yield. The contribution of upland sediments to the total sediment yield, at the watershed outlet, is generally accepted to be 20% to 40%, by the ARS. From the model results, the upland sediment scheme was able to compute the upland erosion contribution within an acceptable range.

### **6.3 - Recommendations**

The principal objective to this study was to develop and evaluate an upland erosion scheme for the two dimensional hydrology model, CASC2D. The simulation results from this study, for both the watershed scale and the test plot scale, show that the model can adequately simulate sediment yield due to upland erosion. Also, the model can adequately predict areas of erosion and areas of deposition.

At the present, CASC2D can only compute sediment yield due to upland erosion. In order to perform a study where the goal is to compute the total sediment yield off of a watershed, the upland erosion amounts would need to be fed into another model (i.e., HEC-6) in order to compute channel erosion. Even this method does not take into account sediment introduced to the system due to bank failures, so it is recommended that a channel erosion and bank failure scheme be added to CASC2D so that total sediment yield can be simulated. As a part of this work, a scheme would need to be added where by the channel cross-section could be changed during the simulation since there may be cases where there is significant erosion or deposition that could change the hydraulic conditions.

Another limitation is not so much with the model as with the USLE coefficients. Until recently, sediment yield computations were done on an annual basis, so average values of crop management factor could be used in the analysis. Now that more attention is being given to performing single event analysis, research needs to be done on how the crop management factor changes on an event basis. If the model is to be used in long term simulations, there is a strong need to be able to vary the crop management factor at least on a seasonal basis.

In this analysis, both the watershed and the test plot were capacity limited. That is to say that there was more soil than could be eroded. In real world applications, the model will have to be able to read in a soil profile for each grid cell. This would allow the model to change the soil erodibility factor over time and to stop erosion if a hard point is reached, such as bed rock.

The GRASS GIS turned out to be a very useful tool. However, GRASS is not a very user friendly GIS. It requires that the user spend a considerable amount of time learning how to use the various tools. In order for distributive modeling to become widely used, graphical user interfaces (GUI) will have to be written to help the novice read in data, manipulate the data, and visualize the model output. One example of this is the Watershed Modeling System (WMS) being developed by Brigham Young University in association with the Waterways Experiment Station (WES). This system uses a windows based approach to allow the user to easily load data of various formats into the system, edit and manipulate the data, run various hydrologic and hydraulic models using the same data set, animate the output grids, and save frames for inclusion into reports. Work has already begun to incorporate a version of CASC2D, which only performs the rainfall-runoff processes, into the WMS. Once this work is completed, incorporation of the upland erosion scheme will take place. The recommendation is that future development of CASC2D should be done in such a way as to incorporate the new schemes into the WMS.

### **Bibliography**

Abrahams, A. D., et al. (1991). The Effects of Spatial Variability in Overland Flow on the Downslope Pattern of Soil Loss on a Semiarid Hillslope, Southern Arizona. *Catena*, Vol. 18, 255-270.

Alonzo, C. V., et al. (1981). Estimating Sediment Transport Capacity in Watershed Modeling. *Transactions of the ASAE*. 1211-1226.

Anderson, M. G., et al. (1988). A review of the bases of geomorphological modeling. In M. G. Anderson (ed) : *Modeling Geomorphological Systems*. John Wiley & Sons Ltd. Chapter 1, 1-32.

Anderson, M. G. & Rogers, C. C. M. (1990). Catchment scale distributed hydrological models ; a discussion of research directions. *Progress in Physical Geography*. 28-51.

Apmann, R. P. And Rumer, R. R. Jr. (1970). Diffusion of sediment in developing flow. *Journal of the Hydraulics Division, Proc. of the ASCE* 96(HY1) : 109-123.

Band, L. E. and Moore. I. D. (1995). Scale : Landscape Attributes and Geographical Information Systems. *Hydrological Processes*, Vol. 9, 401-422.

Barfield, B. J., et al. (1996). The Sedimot III - Model of Watershed Hydrology and Sedimentology. *Proceedings of the Sixth Federal Interagency Sedimentation Conference*. Volume 2, Section IX, 54-61.

Bennett, J. P. (1974). Concepts of Mathematical Modeling of Sediment Yield. *Water Resources Research* 10 (3) : 485-492.

Bergstrom, S. (1991). Principles and Confidence in Hydrological Modeling. *Nordic Hydrology*, 22, 123-136.

Beven, K. (1985). Distributed Models. Chapter 13 in *Hydrologic Forecasting*, Edited by M. G. Anderson and T. P. Burt. John Wiley & Sons, Chichester, UK.

Beven, K. (1989). Changing Ideas in Hydrology - The Case of Physically based Models. *Journal of Hydrology*, 105, 157-172.

Blackmarr, W. A. (1995). Documentation of Hydrologic, Geomorphic, and Sediment Transport Measurements on the Goodwin Creek Experimental Watershed, North Mississippi, for the period 1982-1993 – Preliminary Release. National Sedimentation Laboratory - Research Report No. 3 - October 1995.

Boardman, J. (1984a). A morphometric approach to soil erosion on agricultural land near Lewes, East Sussex. In T. Lakehurst and R. L. Gant (eds) : Issues in Countryside Research. Kingston/Brighton Research Paper. Brighton Polytechnics. 1-10.

Boardman, J. (1984b). The context of soil erosion. In : C. P. J. Burham and J. I. Pitman (eds) : SEESOIL, The Journal of the South East England Soils Discussion Group, Volume 3 (for 1986). 1-13.

Boardman, J., et al. (1990). Soil Erosion Studies : Some Assessments. In J. Boardman, I. D. L. Foster and J. A. Dearing (eds) : Soil Erosion on Agricultural Land. John Wiley & Sons Ltd., 659-672.

Bork, H. R. And Rohdenburg, H. (1986). Transferable Parameterization Methods for Distributed Hydrological and Agroecological Catchment Models. *Catena*. Vol. 13, 99-117.

Bouraoui, F. And Dillaha, T. A. (1996). ANSWERS 2000 : Runoff and Sediment Transport Model. *Journal of Environmental Engineering*, June 1996, Vol. 122, No. 6, 493-502.

Brubaker, S. C., et al. (1994). Regression Models for Estimating Soil Properties by Landscape Position. *Soil Sci. Soc. Am. J.* 58 : 1763-1767.

Bruneau, P., et al. (1995). Sensitivity to Space and Time Resolution of a Hydrological Model Using Digital Elevation Data. *Hydrological Processes*. Vol. 9, 69-81.

Burrough, P. A. (1986). Principles of Geographical Information Systems for Land Resources Assessment. Clarendon Press, Oxford.

Burrough, P. A. (1989). Matching spatial databases and quantitative models in land resources assessment. *Soil Use and Management*, Vol. 5, No. 1, 3-8.

Burt, T. P. and Butcher D. P. (1986). Development of Topographic Indices for use in semi-distributed hillslope runoff models. *Z. Geomorph. N. F., Suppl-Bd.* 58, 1-19.

Carrara, A., et al. (1991). GIS-Techniques and Statistical Models in Evaluating Landslide Hazard. *Earth Surface Processes and Landforms*. Vol. 16, 427-445.

Chang, K. T. And Tsai, B. W. (1991). The Effects of DEM Resolution on Slope and Aspect Mapping. *Cartography and Geographic Information Systems*, Vol. 18, No. 1, 69-77.

Chansheng, H., et al. (1993). Integration of Geographic Information Systems and a Computer Model to Evaluate Impacts of Agricultural Runoff on Water Quality. *Water Resources Bulletin*. AWRA. Vol. 29, No. 6, 891-900.

Chesier, R. (1996). Sediment Budgets - Their Preparation and use in Watershed Planning. *Proceedings of the Sixth Federal Interagency Sedimentation Conference*. Vol. 2, Section X, 22-29.

Costa-Cabral, M. C. And Burges, S. J. (1994). Digital Elevation Model Networks (DEMON) : A model of flow over hillslopes for computation of contributing and dispersal areas. *Water Resources Research*, Vol. 30, No. 6, 1681-1692.

Curtis, D. C. (1976). A Deterministic Urban Storm Water and Sediment Discharge Model. In : *Proc. of National Symposium on Urban Hydrology, Hydraulics, and Sediment Control*. University of Kentucky, Lexington, KY., 151-162.

Dabney, S. M., et al. (1997). Runoff and Sediment Yield from Conventional and Conservation Cropping Systems. (Report in Progress).

Davis, S. S. (1978). Deposition of Nonuniform Sediment by Overland Flow on Concave Slopes. M.S. Thesis. Purdue University, West Lafayette, IN., 137.

De Roo, A. P. J., et al. (1989). Soil Erosion Modeling Using ANSWERS and Geographical Information Systems. *Earth Surface Processes and Landforms*, Vol. 14, 517-532.

De Roo, A. P. J. (1993). Modeling Surface Runoff and Soil Erosion in Catchments Using Geographical Information Systems : Validity and Applicability of the ANSWERS Model in Two Catchments in the Loess Area of South Limburg (The Netherlands) and One in Devon (UK) - *Nederlandse Geografische Studies*, ISSN 0169-4839 157.

De Roo, A. P. J. and Walling, D. E. (1994). Validating the ANSWERS Soil Erosion Model Using 137Cs. In R. J. Rickson (ed) : *Conserving Soil Resources : European Perspectives*. CAB International. Chapter 24. 246-263.

Desmet, P. J. J. and Govers, G. (1995). GIS-based Simulation of Erosion and Deposition Patterns in an Agricultural Landscape : A Comparison of Model Results with Soil Map Information. *Catena* 25, No. 1-4, 389-401.

Dietrich, W. E., et al. (1995). A Processes-based Model for Colluvial Soil Depth and Shallow Landsliding Using Digital Elevation Data. *Hydrological Processes*, Vol. 9, 383-400.

Dikau, R. (1989). Chapter 5 : The application of a digital relief model to landform analysis in geomorphology. In J. Raper (ed) : *Three Dimensional Applications in Geographical Information Systems*. 51-77.

Drayton, R. S., et al. (1992). *Geographical Information System Approach to Distributed Modeling*. *Hydrological Processes*, Vol. 6, 361-368.

Dymond, J. R., et al. (1995). Automated Mapping of Land Components from Digital Elevation Data. *Earth Surface Processes and Landforms*. Vol. 20, 131-137.

Eash, D. A. (1994). A Geographic Information System Procedure to Quantify Drainage-Basin Characteristics. *Water Resources Bulletin*. AWRA. Vol. 30, No. 1, 1-8.

Einstein, H. A. (1968). Deposition of Suspended Particles in a Gravel Bed. *Journal of the Hydraulics Division, Proc. of the ASCE 94 (HY5)* : 1197-1205.

Elliott, W. J., et al. (1989). Effect of Soil Properties on Soil Erodibility. Paper No. 89-2150, Am. Soc. Agric. Eng. Summer Meeting, Quebec, Canada. ASAE, St. Joseph, MI.

Elliott, W. J., et al. (1996). Predicting Sedimentation from Timber Harvest Areas with the WEPP Model. *Proceedings of the Sixth Federal Interagency Sedimentation Conference*. Vol. 2, Section IX, 46-53.

Engel, B. A., et al. (1993). A Spatial Support Decision Support System for Modeling and Managing Agricultural Non-Point Source Pollution. In : M. F. Goodchild, B. O. Parks, L. T. Steyaert (eds) : *Environmental Modeling with GIS*. New York, Oxford University Press, Inc. 231-237.

Evans, R. (1980a). Chapter 4 : Mechanics of Water Erosion and their Spatial and Temporal Controls : An Empirical viewpoint. In M. J. Kirkby and R. P. C. Morgan (eds) : *Soil Erosion*. 109-117.

Everaert, W. (1991). Empirical Relations for the Sediment Transport Capacity of Interrill Flow. *Earth Surface Processes and Landforms*, Vol.16, 513-532.

Fairfield, J. (1991). Drainage Networks from Grid Digital Elevation Models. *Water Resources Research*, Vol. 27, No. 5, 709-717.

Flacke, W., et al. (1990). Combining a Modified Universal Soil Loss Equation with a Digital Terrain Model for Computing High Resolution Maps of Soil Loss resulting from Rain Wash. *Catena*, Vol. 17, 383-397.

Flanagan, D. C., et al. (1995). WEPP Reference Manual - Chapter 1 - Overview of the WEPP Erosion Prediction Model.

Foster, G. R. And Meyer, L. D. (1972a). A Closed-Form Soil Erosion Equation for Upland Areas. In : Sedimentation (Einstein). H. W. Shen (ed. ). Colorado State University, Fort Collins, CO. Chapter 12.

Foster, G. R. And Meyer, L. D. (1972b). Transport of Soil Particles by Shallow Flow. TRANSACTIONS of the ASAE 15 (1) : 99-102.

Foster, G. R. And Wischmeier, W. H. (1974). Evaluating Irregular Slopes for Soil Loss Prediction. Transactions of the ASAE. Paper No. 73, 227.

Foster, G. R. And Huggins, L. F. (1977). Deposition of Sediment by Overland Flow on Concave Slopes. In : Soil Erosion Prediction and Control. Special Publication No. 21. Soil Conservation Society of America, Ankeny, IA., 167-182.

Foster, G. R. (1982). Chapter Eight of Hydrologic Modeling of Small Watersheds, Edited by C. T. Haan, H. P. Johnson, and D. L. Brakensiek. American Society of Agricultural Engineers. International Standard Book Number : 0-916150-44-5.

Foster, G. R., et al. (1987). User Requirements : USDA-Water Erosion Prediction Project (WEPP). Written for Presentation at the 1987 International Winter Meeting of the American Society of Agricultural Engineers. Paper No. 87-2539.

Foster, G. R. (1990). Process based Modeling of Soil Erosion by Water on Agricultural Land. In J. Boardman, I. D. L. Foster and J. A. Dearing (eds) : Soil Erosion on Agricultural Land. John Wiley & Sons, Ltd. 429-446.

Freeman, T. G. (1991). Calculating Catchment Area with Divergent Flow based on a Regular Grid. Computers & Geosciences, Vol. 17, No. 3, 413-422.

Frenette, M. And Julien, P. Y. (1987). Computer Modeling of Soil Erosion and Sediment Yield from Large Watersheds. International Journal of Sediment Research, No. 1, Nov. 1987, 39-68.

Gagliuso, R. A. (1994). Surface Analysis Differences Between Lattice and TIN Derived Terrain Models. Proceedings of the Fourteenth Annual ESRI User Conference, 1267.

Gandoy-Bernasconi, W. and Palacios-Velez, O. L. (1990). Automatic Cascade Numbering of Unit Elements in Distributed Hydrological Models. Journal of Hydrology, Vol. 112, 375-393.

Gardner, T. W., et al. (1990). Automated Extraction of Geomorphometric Properties from Digital Elevation Data. Z. Geomorph. N. F. Suppl.-Bd.80, 57-68.



- Garg, P. K. And Harrison, A. R. (1992). Land Degradation and Erosion Risk Analysis in S. E. Spain : A Geographic Information System Approach. *Catena*. Vol. 19, 411-425.
- Gee, Michael D. And MacArthur, R. C. (1996). Use of Land Surface Erosion Techniques with Stream Channel Sedimentation Models. *Proceedings of the Sixth Federal Interagency Sedimentation Conference*, Vol. 2, Section IX, 17-25.
- Gessler, P. E., et al. (1995). Soil-Landscape Modeling and spatial Prediction of Soil Attributes. *Int. J. Geographical Information Systems*, Vol. 9, No. 4, 421-432.
- Govers, G. And Poesen, J. (1988). Assessment of the Interrill and Rill Contributions to Total Soil Loss from an Upland Field Plot. *Geomorphology*, 1, 343-354.
- Govers, G. (1990). Empirical Relationships for the Transport Capacity of Overland Flow, Erosion, Transport, and Deposition Processes. (*Proceedings of the Jerusalem Workshop, March-April, 1987*). IAHS Publ. No. 189, 45-63.
- Grayson, R. B. And Moore, I. D. (1992). Chapter 7 - Effect of Land Surface Configuration on Catchment Hydrology. In : *Overland Flow : Hydraulics and Erosion Mechanics* (eds A. J. Parsons and A. D. Abrahams), University College London Press Ltd, London, 147-175.
- Grayson, R. B., et al. (1992a). Physically based Hydrologic Modeling : I. A terrain based model for investigation purposes. *Water Resources Research* 28 (10) : 2639-2658.
- Grayson, R. B., et al (1992b). Physically based Hydrologic Modeling : II. Is the concept realistic? *Water Resources Research* 28 (10) : 2659-2666.
- Grissinger, E. H. and Murphree, C. E. Jr. (1991). Instrumentation for Upland Erosion Research. *Proceedings of the Fifth Interagency Sedimentation Conference*, volume 2, ps-24 to ps-31.
- Higgit, D. (1991). Soil Erosion and Soil Problems. *Progress in Physical Geography* 15, 1, 91-100.
- Higgit, D. (1993). Soil Erosion and Soil Problems. *Progress in Physical Geography* 17, 4, 461-472.
- Holmgren, P. (1994). Multiple Flow Direction Algorithms for Runoff Modeling in Grid Based Elevation Models : An Empirical Evaluation. *Hydrological Processes*, Vol. 8, No. 4, 327-335.
- Howes, S. and Anderson, M. G. (1988). Computer Simulation in Geomorphology. In M. G. Anderson (ed) : *Modeling Geomorphological Systems*. John Wiley & Sons Ltd. Chapter 15, 421-441.

Hudson, N. (1995). *Soil Conservation - Fully Revised and Updated Third Edition*. Iowa State University Press. Ames, Iowa.

Hutchinson, M. F. and Dowling, T. I. (1991). A Continental Hydrological Assessment of a New Grid based Digital Elevation Model of Australia. *Hydrological Processes*, Vol. 5, 45-58.

Inter-Agency Committee on Water Resources (IACWR). (1957). *The Development and Calibration of the Visual Accumulation Tube. Measurements and Analysis of Sediment Loads in Streams*. Report No. 11. Minneapolis, Minn. : St. Anthony Falls Hydraulic Laboratory.

Jackson, S. J. (1984a). *The Role of Slope Form on Soil Erosion at Different Scales as a Possible Link between Soil Erosion Surveys and Soil Erosion Models*. Unpublished Ph.D Thesis. Cranfield Institute of Technology, National College of Agricultural Engineering.

Jenson, K. H. And Mantoglou, A. (1991). Future of Distributed Modeling. *Hydrological Processes*. Vol. 6, 255-264.

Jenson, S. K. and Domingue, J. O. (1988). Extracting Topographic Structure from Digital Elevation Data for Geographic Information Analysis. *Photogrammetric and Remote Sensing*. Vol. 54, No. 11, 1593-1600.

Jenson, S. K. (1991). Applications of Hydrologic Information Automatically Extracted from Digital Elevation Models. *Hydrological Processes*, Vol. 5, 31-44.

Johnson, B. E. (1993). *Comparison of Distributed versus Lumped Rainfall-Runoff Modeling Techniques*. Master's Thesis, Memphis State University.

Julien, P. Y. And Frenette, M. (1987). Macroscale Analysis of Upland Erosion. *Hydrological Sciences Journal des Sciences Hydrologiques*, 32, 3, 347-358.

Julien, P. Y. and Tanago, M. G. D. (1991a). Spatially Varied Soil Erosion under Different Climates. *Hydrological Sciences Journal des Sciences Hydrologiques*, 36, 6, 511-524.

Julien, P. Y. and Saghafian, Bahram (1991b). *CASC2D User's Manual - A Two-Dimensional Watershed Rainfall-Runoff Model*. Center for Geosciences - Hydrologic Modeling Group, Colorado State University (CER90-91PYJ-BS-12).

Julien, P. Y. (1995a). *Erosion and Sedimentation*. Press Syndicate of the University of Cambridge, New York, NY.

Julien, P. Y. and Saghafian, Bahram, et al. (1995b). Raster-Based Hydrologic Modeling of Spatially-Varied Surface Runoff. *Water Resources Bulletin*, Vol. 31, No. 3, 523-536.

Kilinc, M. and Richardson, E. V. (1973). *Mechanics of Soil Erosion from Overland Flow Generated by Simulated Rainfall*. Hydrology Papers No. 63, Colorado State University.

Kirkby, M. J. (1969). Hillslope process response models based on the continuity equation.

Kirkby, M. J. (1990). The Landscape viewed through Models. *Z. Geomorph. N. F., Suppl.-Bd. 79*, 63-81.

Kreznor, W., et al. (1992). Field Evaluation of Methods to Estimate Soil Erosion. *Soil Science*. Vol. 153, No. 1, 69-81.

Laflen, J. M. (1996). WEPP - The New Generation of Water Erosion Prediction Technology. *Proceedings of the Sixth Federal Interagency Sedimentation Conference*. Vol. 2, Section IX, 90-97.

Lal, R. (1994). *Second Edition Soil Erosion Research Methods*. Soil and Water Conservation Society, St. Lucie Press, Delray Beach, FL.

Lane, L. J., et al. (1988). Modeling Erosion on Hillslopes. In M. G. Anderson (ed) : *Modeling Geomorphological Systems*. John Wiley & Sons Ltd. Chapter 10, 287-307.

Langhaar, E. M. (1967). *Dimensional Analysis and Theory of Models*. 8<sup>th</sup> Printing, John Wiley & Sons, Inc., New York, London, Sydney, 166.

Lee, J., et al. (1992). Modeling the Effect of Data Errors on Feature Extraction from Digital Elevation Models. *Photogrammetric Engineering & Remote Sensing*, Vol. 58, No. 10, 1461-1467.

Maidment, D. R. (1993). *Handbook of Hydrology*, McGraw-Hill Inc., New York, NY.

Martz, L. W. and De Jong, E. (1985). The Relationship between Land Surface Morphology and Soil Erosion and Deposition in a Small Saskatchewan Basin. *Proceedings of Canadian Society for Civil Engineering Annual Conference*, May 27-31, 1985 Saskatchewan, SK.

Martz, L. W. and Garbrecht, J. (1992). Numerical Definition of Drainage Networks and Subcatchment Area from Digital Elevation Models. *Computers and Geosciences* 18 (6) : 747-761.

Martz, L. W. and Garbrecht, J. (1993). Automated Extraction of Drainage Network and Watershed Data from Digital Elevation Models. *Water Resources Bulletin*. AWRA. Vol. 29, No. 6, 901-908.

Mathier, L., et al. (1989). The Effect of Slope Gradient and Length on the Parameters of a Sediment Transport Equation for Sheetwash. *Catena*, Vol. 16, 545-558.

- Mathier, L. and Roy, A. G. (1993). Temporal and Spatial Variations of Runoff and Rainwash Erosion on an Agricultural Land. *Hydrological Processes*, Vol. 7, No. 1, 1-18.
- McCool, D. K., et al. (1987). Revised Slope Steepness Factor for the Universal Soil Loss Equation. *Transactions of the ASAE*, Vol. 30 (5) : 1387-1396.
- Mellerowicz, K. T., et al. (1994). Soil Conservation Planning at the Watershed Level using the Universal Soil Loss Equation with GIS and microcomputer technology : A case study. *Journal of Soil and Water Conservation*, Vol. 49 (2) : 194-200.
- Merot, P., et al. (1995). Mapping Waterlogging of Soils using Digital Terrain Models. *Hydrological Processes*. Vol. 9, 27-34.
- Meyer, L. D. And Wischmeier, W. H. (1969). Mathematical Simulation of the Process of Soil Erosion by Water. *TRANACTIONS of the ASAE* 12 (6) : 754-758, 762.
- Meyer, D. L. (1984). Evolution of the Universal Soil Loss Equation. *Journal of Soil and Water Conservation*. March-April. 99-105.
- Meyer, D. L., et al. (1992). Size Characteristics of Sediment from Agricultural Soils. *Journal of Soil and Water Conservation*. 47 (1), 107-111.
- Meyer, D. L., et al. (1995). Sediment Trapping Effectiveness of Stiff Grass Hedges. *TRANSACTIONS of the ASAE*, 38 (3), 809-815.
- Mitasova, H., et al. (1995). Modeling Spatially and Temporally Distributed Phenomena : New Methods and Tools for GRASS GIS. *Int. J. Geographical Information Systems*, Vol. 9, No. 4, 433-446.
- Mitchell, J. K. and Bubenzer, G. D. (1980). Chapter 2 - Soil Loss Estimation. In M. J. Kirkby and R. P. C. Morgan (eds) : *Soil Erosion*. 17-39.
- Mitchell, J. K., et al. (1993). Validation of AGNPS for Small Watersheds using an Integrated AGNPS/GIS System. *Water Resources Bulletin*. AWRA. Vol. 29, No. 5, 833-846.
- Montoro, J. A. and Stocking, M. A. (1989). Comparative Evaluation of Two Models in Predicting Storm Soil Loss from Erosion Plots in Semi-Arid Spain. *Catena*, Vol. 16, 227-236.
- Moore, I. D. and Burch, G. J. (1986a). Modeling Erosion and Deposition : Topographic Effects. *TRANSACTIONS of the ASAE*, Vol. 29 (6), 1624-1630.
- Moore, I. D., et al. (1988a). A Contour-based Topographic Model for Hydrological and Ecological Applications. *Earth Surface Processes and Land Forms*. Vol. 13, 305-320.

- Moore, I. D., et al. (1988b). Topographic Effects on the Distribution of Surface Soil Water and the Location of Ephemeral Gullies. *TRANSACTIONS of the ASAE*, Vol. 31 (4), July-August, 1098-1107.
- Moore, I. D. and Grayson, R. B. (1991a). Terrain-based catchment partitioning and runoff prediction using vector elevation data. *Water Resources Research*, Vol. 27 (6), 1177-1191.
- Moore, I. D., et al. (1991b). Digital Terrain Modeling - A Review of Hydrological, Geomorphological, and Biological Applications. *Hydrological Processes*, Vol. 5, 3-30.
- Moore, I. D. (1992). Terrain Analysis Programs for the Environmental Sciences - TAPES. *Agricultural Systems & Information Technology*, Vol. 4, No. 2, 37-39.
- Moore, I. D., et al. (1993a). GIS and Land-Surface-Subsurface Process Modeling. In : M. F. Goodchild, B. O. Parks, L. T. Steyaert (eds) : *Environmental Modeling with GIS*. New York, Oxford University Press, Inc. 196-230.
- Moore, I. D., et al. (1993b). Soil Attributes Prediction using Terrain Analysis. *Soil Sci. Soc. Am. J.* Vol. 57, 443-452.
- Moore, R. F. and Thornes, J. B. (1976). LEAP - A suite of FORTRAN IV programs for generating erosional potentials of land surfaces from topographic information. *Computers & Geosciences*, Vol. 2, 493-499.
- Morgan, R. P. C. (1980b). Field studies of Sediment Transport by Overland Flow. *Earth Surface Processes and Landforms*, Vol. 5, 307-316.
- Morgan, R. P. C. And Morgan, D. D. V. (1982). Predicting Hillslope Runoff and Erosion in the United Kingdom - Preliminary Trial with the CREAMS Model. In : V. Svetlosanov and W. G. Knisel (eds) : *European and United States Case Studies in Application of the CREAMS Model*. 83-97.
- Morgan, R. P. C. (1986). The relative significance of splash, rainwash, and wash as processes of soil erosion. *Z. Geomorph. N. F.*, Vol. 30, No. 3, 329-337.
- Morgan, R. P. C. (1992). A Soil Erosion Prediction Model for the European Community, Chapter 12, in *Soil Conservation for Survival*, edited by H. Hurni and K. Tato, Soil and Water Conservation Society, Ankeny, Iowa.
- Mutchler, C. K., et al. (1994). Chapter 2 - Laboratory and Field Plots for Erosion Research. In R. Lal (ed) : *Soil Erosion Research Methods (Second Edition)*. 11-37.
- Nearing, M. A., et al. (1990). Prediction Technology for Soil Erosion by Water : Status and Research Needs. *Soil Sci. Soc. Am. J.*, Vol. 54, 1702-1711.

Nearing, M. A., et al. (1994). Chapter 6 - Modeling Soil Erosion. In R. Lal (ed) : Soil Erosion Research Methods (Second Edition). 127-156.

Nelson, J. (1994). WMS - Watershed Modeling System (Reference and Tutorial Manuals). Engineering Computer Graphics Laboratory, Brigham Young University, Provo, Utah.

Noss, D. K. (1995). Estimating Upland Erosion using the Universal Soil Loss Equations - Application to Goodwin Creek, Panola County, MS., Essays on River Mechanics (1995), Colorado State University.

Overton, D. E. (1992). Soil Erosion and Sediment Yield - Modeling, Simulation, and Prediction. Stormwater Publications, Inc., Knoxville, TN.

Palacios-Velez, O. L.. and Cuevas-Renaud, B.(1986). Automated River-Course, Ridge and Basin Delineation from Digital Elevation Data. Journal of Hydrology, Vol. 86, 299-314.

Palacios-Velez, O. L.. and Cuevas-Renaud, B. (1992). SHIFT - A Distributed Runoff Model using Irregular Triangular Facets. Journal of Hydrology, Vol. 134, 35-55.

Panuska, J. C., et al. (1991). Terrain Analysis - Integration into the Agricultural Nonpoint Source (AGNPS) Pollution Model. Journal of Soil and Water Conservation. January-February, 59-64.

Philip, J. R. (1983). Infiltration in One, Two, and Three Dimensions. Proceedings of the National Conference on Advances in Infiltration. American Society of Agricultural Engineers. St. Joseph, MI., 1-13.

Pickup, G. (1988). Hydrology and Sediment Models. In M. G. Anderson (ed) : Modeling Geomorphological Systems. John Wiley & Sons Ltd., Chapter 7, 153-165.

Ponce, V. M. (1989). Engineering Hydrology - Principles and Practices, Prentice Hall Inc., Englewoods Cliffs, NJ.

Price, C. V. and Pierce, R. R. (1994). GIS Applications to Hydrological Modeling in the U. S. Geological Survey, Water Resources Division - Past and Future. Proceedings of the Fourteenth Annual ESRI User Conference, 1163-1167.

Quinn, P. F., et al. (1991). The Prediction of Hillslope Flow Paths for Distributed Hydrological Modeling using Digital Terrain Models. Hydrological Processes, Vol. 5, 59-79.

Quinton, J. N. and Morgan, R. P. C. (1993). Description of the European Soil Erosion Model and an Example of its Validation, Paper presented at the International Workshop on Soil Erosion in Steep Lands ; Evaluation and Modeling, Merida, Venezuela, May 1993.

- Quinton, J. N. (1994). Validation of Physically based Erosion Models, with Particular Reference to EUROSEM. In R. J. Rickson (ed) : *Conserving Soil Resources : European Perspectives*. CAB International. Chapter 28, 300-313.
- Renard, K. G., et al. (1991). RUSLE - Revised Universal Soil Loss Equation. *Journal of Soil and Water Conservation*, January-February, 30-33.
- Risse, L. M., et al. (1993). Error Assessment in the Soil Loss Equation. *Soil Sci. Soc. Am. J.*, Vol. 57, 825-833.
- Ritchie, J. C. and McHenry, J. R. (1985). A Comparison of Three Methods for Measuring Recent Rates of Sediment Accumulation. *Water Resources Bulletin*. AWRA. Vol.. 21, No. 1, 99-103.
- Romkens, M. J. M., et al. (1996). Sediment Concentration in Relation to Surface and Subsurface Hydrologic Soil Conditions, *Proceedings of the Sixth Federal Interagency Sedimentation Conference*, Vol. 2, Section IX, 9-16.
- Simons, D. B., et al. (1977). A Simple Procedure for Estimating On-Site Erosion. In : *Proc. of International Symposium on Urban Hydrology, Hydraulics, and Sediment Control*. University of Kentucky, Lexington, KY., 95-102.
- Simons, D. B. And Senturk, F. (1992). *Sediment Transport Technology - Water and Sediment Dynamics*. Water Resources Publication, Littleton, CO.
- Smith, R. E. (1976). Field Test of a Distributed Watershed Erosion/Sedimentation Model, *Soil Erosion - Prediction and Control*, Special Publication 21, Soil Conservation Society of America, Ankeny, IA., 201-209.
- Tachikawa, Y., et al. (1994). Development of a Basin Geographic Information System using a TIN-DEM Data Structure. *Water Resources Bulletin*, AWRA. Vol. 30, No. 1, 9-18.
- Tarboton, D. G., et al. (1991). On the Extraction of Channel Networks from Digital Elevation Data. *Hydrological Processes*, Vol. 5, 81-100.
- Thomas, W. A. (1976). *Scour and Deposition in Rivers and Reservoirs*. HEC-6. Hydrologic Engineering Center, U. S. Army Corps of Engineers.
- Thorne, C. R., et al. (1987). Terrain Analysis for Quantitative Description of zero-order basin. *Erosion and Sedimentation in the Pacific Rim (Proceedings of the Corvallis Symposium, August, 1987)*. IAHS Publ., No. 165, 121-130.
- Thornes, J. B. (1980). Chapter 5 - Erosion Processes of Running Water and their Spatial and Temporal Controls : A Theoretical Viewpoint. In M. J. Kirkby and R. P. C. Morgan (eds) : *Soil Erosion*. 158-167.

Toffaleti, F.B. (1966). A Procedure for Computation of Total River Sand Discharge and Detailed Distribution, Bed to Surface. Committee on Channel Stabilization, U. S. Army Corps of Engineers.

Version 94.7 User Summary for Water Erosion Prediction Project : Erosion Prediction Model. NSERL Report No. 9. USDA - Agricultural Research Service, National Soil Erosion Research Laboratory, West Lafayette, Indiana, USA, August 1994.

Vertessy, R. A., et al. (1990). Predicting Erosion Hazard Areas using Digital Terrain Analysis. Research Needs and Applications to Reduce Erosion and Sedimentation in Tropical Steeplands (Proceedings of the Fiji Symposium, June 1990) : IAHS-AISH Publ. No. 192, 298-308.

Vieux, B. E. (1991). Geographic Information Systems and Non-Point Source Water Quality and Quantity Modeling. Hydrological Processes, Vol. 5, 101-113.

Walling, D. E. (1990). Linking the Field to the River - Sediment Delivery from Agricultural Land. In J. Boardman, I. D. L. Foster and J. A. Dearing (eds) : Soil Erosion on Agricultural Land. John Wiley & Sons Ltd. 129-152.

Walling, D. E. (1993). Erosion and Sediment Yield Research : Current Status and Needs. In : Runoff and Sediment Yield Modeling (Proceedings of the Warsaw Symposium, September 1993). Department of Hydraulic Structures - SGGW, 23-42.

Wang, Menghua and Hjelmfelt, Allen (1996). A DEM Based Hydrologic and Sediment Transport Model. North American Water and Environment Congress & Destructive Water Conference Proceedings : Edited by Chenchayya T. Bathala. American Society of Civil Engineers (ASCE). Section C-126. Anaheim, CA.

Weibel, R. and Heller, M. (1991). Digital Terrain Modeling. In : D. J. Maguire, M. F. Goodchild, and D. W. Rhind (eds) : Geographic Information Systems : Principles and Application. Longman Group UK Ltd. 269-297.

Young, R. A. and Mutcher, C. K. (1969). Effect of Slope Shape on Erosion and Runoff. TRANSACTIONS of the ASAE, St. Joseph, Michigan, Vol. 12, No. 2, 231-233, 239.

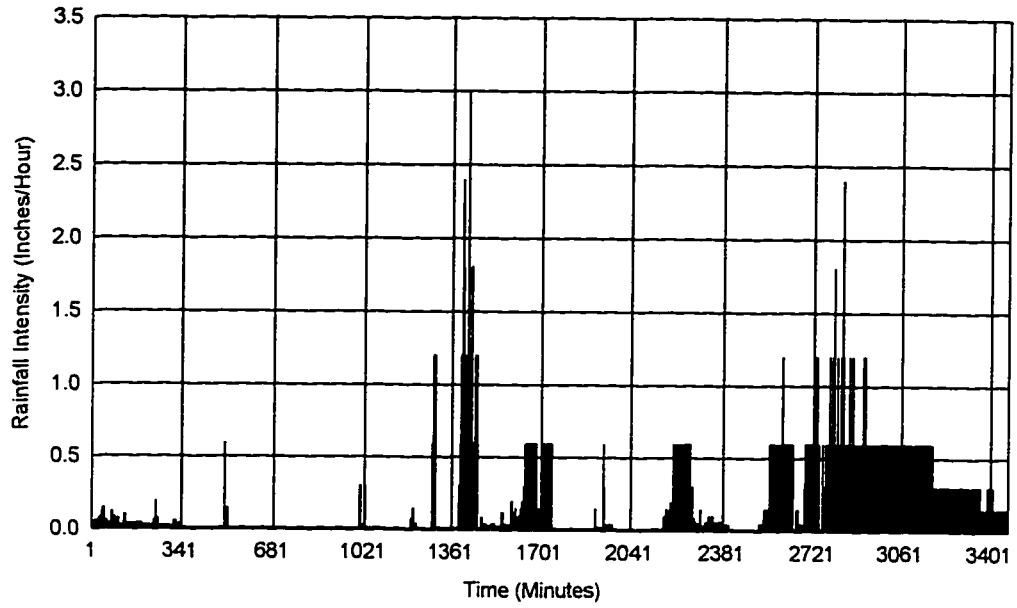
Zevenbergen, L. W. and Thorne, C. R. (1987). Quantitative Analysis of Land Surface Topography. Earth Surface Processes and Landforms, Vol. 12, 47-56.



**Appendix A**

**Tables and Gage Plots  
for Nelson Farm Test #2 and  
Goodwin Creek Watershed**

Nelson Farm Test Plot #2  
February 17-19, 1991



Nelson Farm Test Plot #2  
June 3, 1992

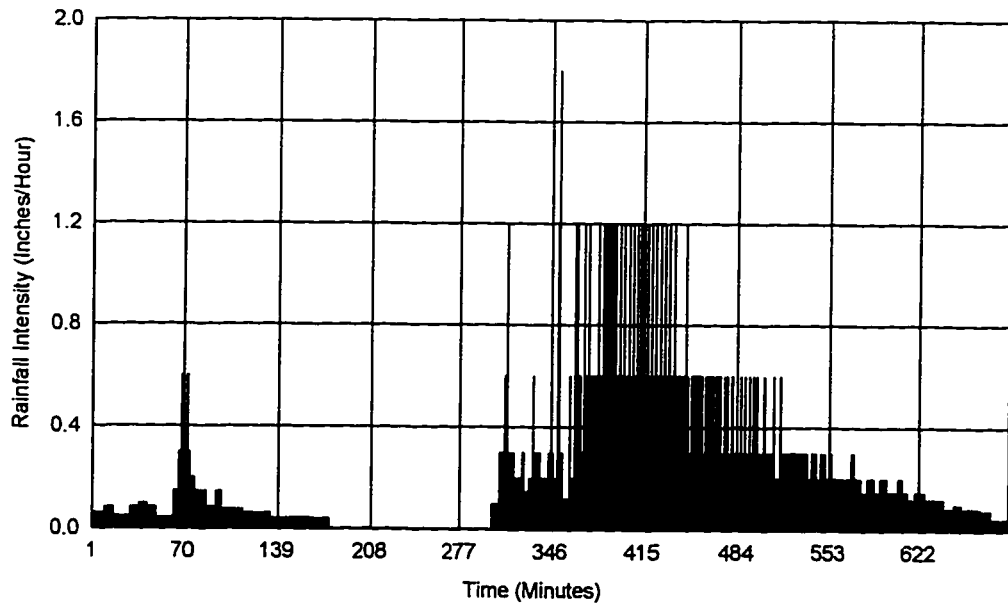


Figure A-1 - Rain Hyetographs for Nelson Farm Test Plot #2.

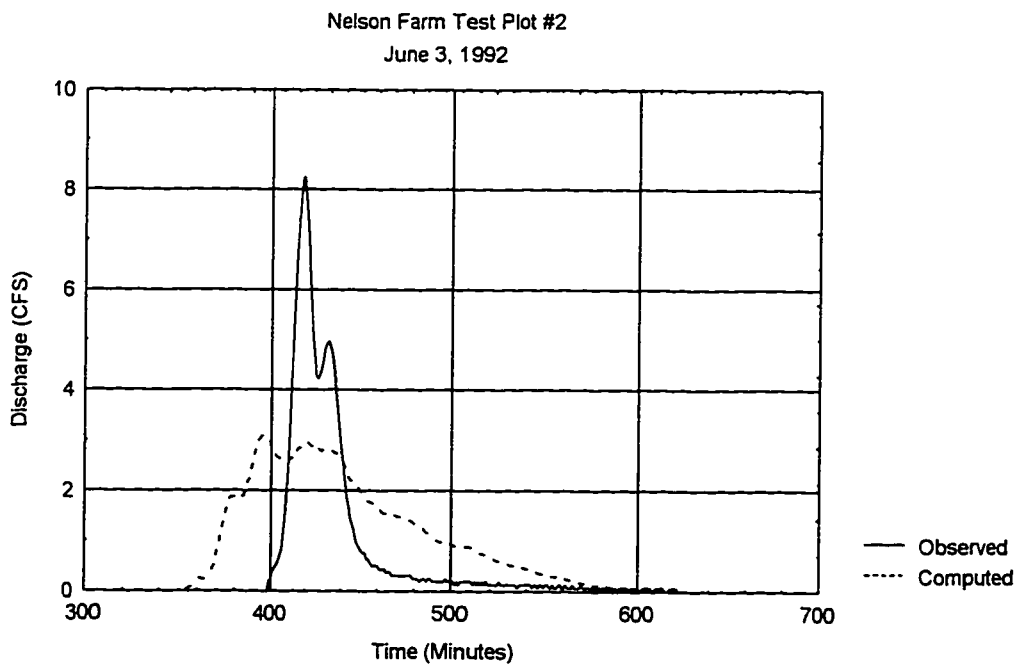
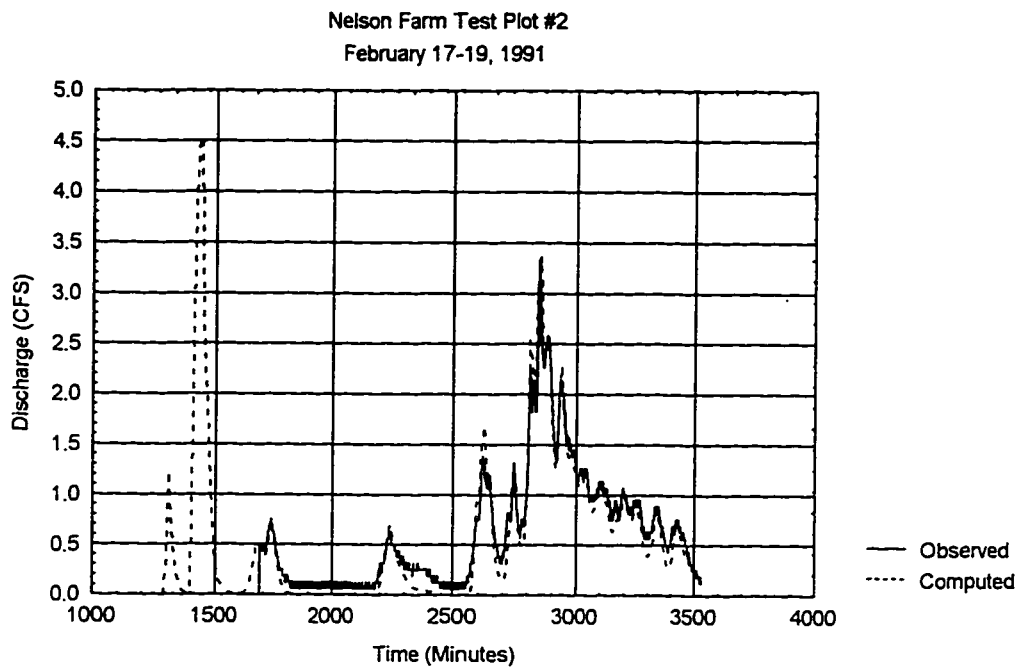


Figure A-2 - Flow Hydrographs for Nelson Farm Test Plot #2.

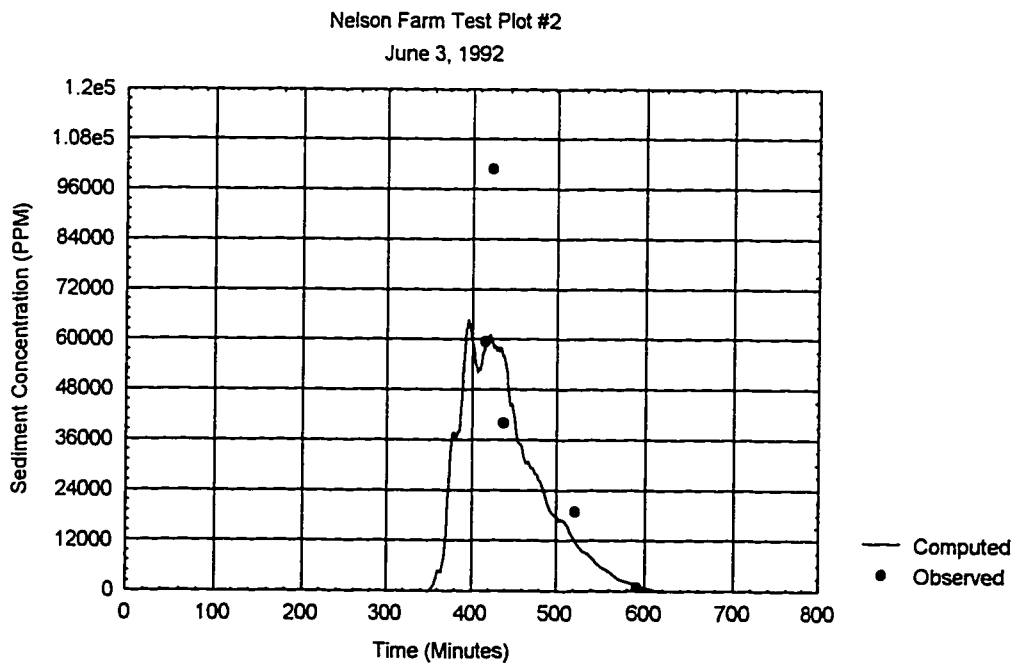
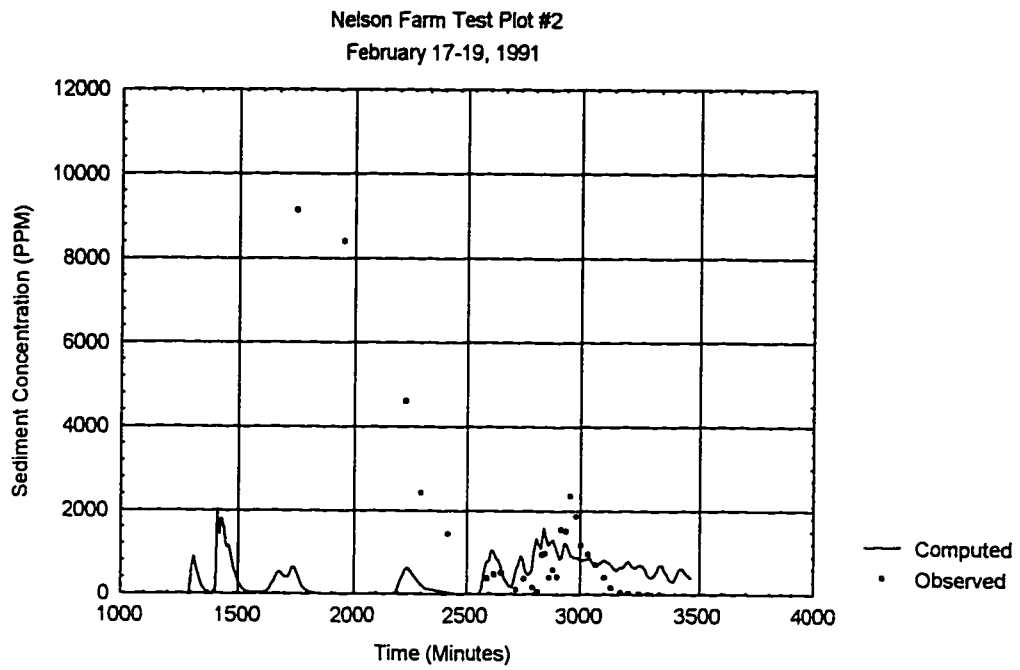


Figure A-3 - Sediment Concentrations for Nelson Farm Test Plot #2.

Table A-1 - Goodwin Creek Watershed - Total Rainfall (Inches)

Rain Gage I.D.	October 17-18 1981		December 2-3 1983		May 2-3 1984	
	1	2.66		5.83		4.65
2	2.81		5.89		4.46	
4	2.91		5.79		4.62	
5	3.01		5.72		4.51	
6	2.66		5.83		4.48	
7	2.96		5.68		4.50	
8	2.90		5.87		4.89	
10	3.04		5.85		4.64	
11	2.97		5.73		4.64	
13	2.69		6.00		4.59	
14	2.79		5.81		4.64	
50	3.04		5.80		4.90	
51	2.81		5.93		4.73	
52	2.75		5.88		4.78	
53	2.55		5.86		4.69	
54	2.84		5.83		4.76	
55	3.11		5.64		4.64	
Average	2.85		5.82		4.65	

Table A-2 - Goodwin Creek Watershed - Time to Peak (Minutes)

Gage I.D.	October 17-18 1981			December 2-3 1983			May 2-3 1984		
	Obs.	Comp.	Diff	Obs.	Comp.	Diff	Obs.	Comp.	Diff
1	266	254	12	2126	2092	34	1466	1420	46
2	239	223	16	2116	2080	36	1420	1392	28
3	207	213	6	2104	2088	16	1415	1396	19
4	195	181	14	2091	2064	27	1399	1364	35
5	191	188	3	2096	2084	12	1397	1384	13
8	181	179	2	2096	2080	16	1386	1372	14

Table A-3 - Goodwin Creek Watershed - Total Runoff (Inches)

Gage I.D.	October 17-18 1981			December 2-3 1983			May 2-3 1984		
	Obs.	Comp.	% Diff	Obs.	Comp.	% Diff	Obs.	Comp.	% Diff
1	0.75	0.64	-14.7	4.26	4.85	13.8	3.35	3.66	9.3
2	0.71	0.70	-1.4	4.80	4.80	0.0	3.50	3.63	3.7
3	1.00	0.74	-26.0	4.81	4.86	1.0	3.52	3.68	4.5
4	0.77	0.66	-14.3	4.75	4.65	-2.1	3.80	3.49	-8.2
5	1.08	0.83	-23.1	5.17	4.90	-5.2	3.88	3.72	-4.1
8	1.08	0.87	-19.4	5.00	4.88	-2.4	3.79	3.76	-0.8

Table A-4 - Goodwin Creek Watershed - Peak Flow (CFS)

Gage I.D.	October 17-18 1981			December 2-3 1983			May 2-3 1984		
	Obs.	Comp.	% Diff	Obs.	Comp.	% Diff	Obs.	Comp.	% Diff
1	1405.1	1385.3	-1.4	3382.7	3347.8	-1.0	3662.3	3743.5	2.2
2	1286.5	1372.0	6.6	3256.1	2923.4	-10.2	3502.5	3547.5	1.3
3	1050.6	820.1	-21.9	1785.2	1562.9	-12.5	3193.7	1936.5	-39.4
4	347.2	376.4	8.4	670.9	599.5	-10.6	1076.0	993.2	-7.7
5	560.3	529.1	-5.6	915.8	802.9	-12.3	1492.1	1143.6	-23.4
8	260.2	248.7	-4.4	349.8	304.6	-12.9	761.3	535.2	-29.7

Table A-5 - Goodwin Creek Watershed - Sediment Yield (Tons)

Gage I.D.	October 17-18 1981			December 2-3 1983			May 2-3 1984		
	Obs.	Comp.	C/O %	Obs.	Comp.	C/O %	Obs.	Comp.	C/O %
1	1394.4	420.6	30.2	5181.5	3357.1	64.8	10487.6	3647.0	34.8
2	1104.0	181.5	16.4	3582.5	1852.9	51.7	4422.6	1883.4	42.6
3	733.0	136.3	18.6	1188.5	796.5	67.0	1111.4	672.2	60.5
4	445.2	424.1	95.3	690.3	2903.6	420.6	2840.3	3567.3	125.6
5	290.7	45.3	15.6	2162.9	290.4	13.4	1620.5	359.7	22.2
8	93.0	66.7	71.7	251.5	282.3	112.2	771.4	453.5	58.8
9	123.0	38.9	31.6	73.1	118.3	161.8	128.8	201.9	156.8
11	---	4.9	---	42.7	16.5	38.6	55.1	24.7	44.8
12	3.3	0.7	21.2	33.7	3.2	9.5	136.7	5.4	4.0
14	154.0	164.0	106.5	140.7	656.6	466.7	402.0	1063.2	264.5

Table A-6 - Goodwin Creek Watershed - Sediment Yield (Tons/Acre)

Gage I.D.	Drainage Area (Acres)	October 17-18 1981			December 2-3 1983			May 2-3 1984		
		Obs.	Comp.	C/O %	Obs.	Comp.	C/O %	Obs.	Comp.	C/O %
1	5286.4	0.26	0.08	30.2	0.98	0.64	64.8	1.98	0.69	34.8
2	4480.0	0.25	0.04	16.4	0.80	0.41	51.7	0.99	0.42	42.6
3	2176.0	0.34	0.06	18.6	0.55	0.37	67.0	0.51	0.31	60.5
4	889.6	0.50	0.48	95.3	0.78	3.26	420.6	3.19	4.01	125.6
5	1075.2	0.27	0.04	15.6	2.01	0.27	13.4	1.51	0.33	22.2
8	390.4	0.24	0.17	71.7	0.64	0.72	112.2	1.98	1.16	58.8
9	44.8	2.75	0.87	31.6	1.63	2.64	161.8	2.88	4.51	156.8
11	70.4	---	0.07	---	0.61	0.23	38.6	0.78	0.35	44.8
12	76.8	0.04	0.01	21.2	0.44	0.04	9.5	1.78	0.07	4.0
14	409.6	0.38	0.40	106.5	0.34	1.60	466.7	0.98	2.60	264.5

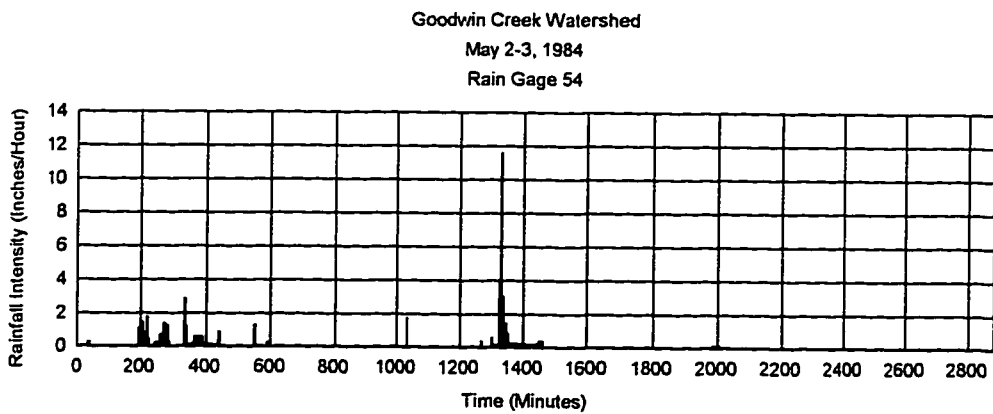
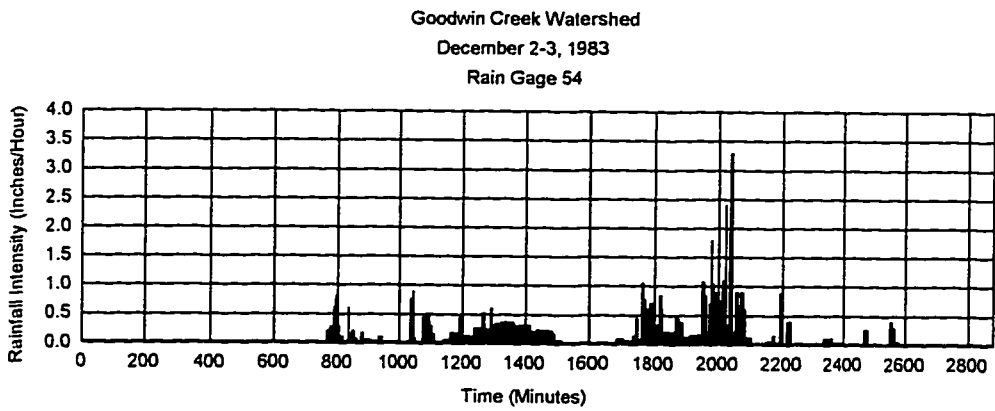
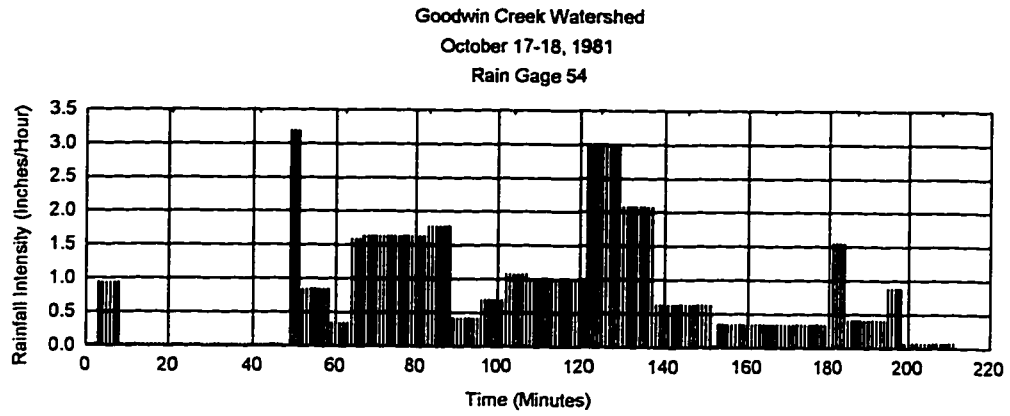


Figure A-4 - Rainfall Hyetographs at Raingage No. 54.



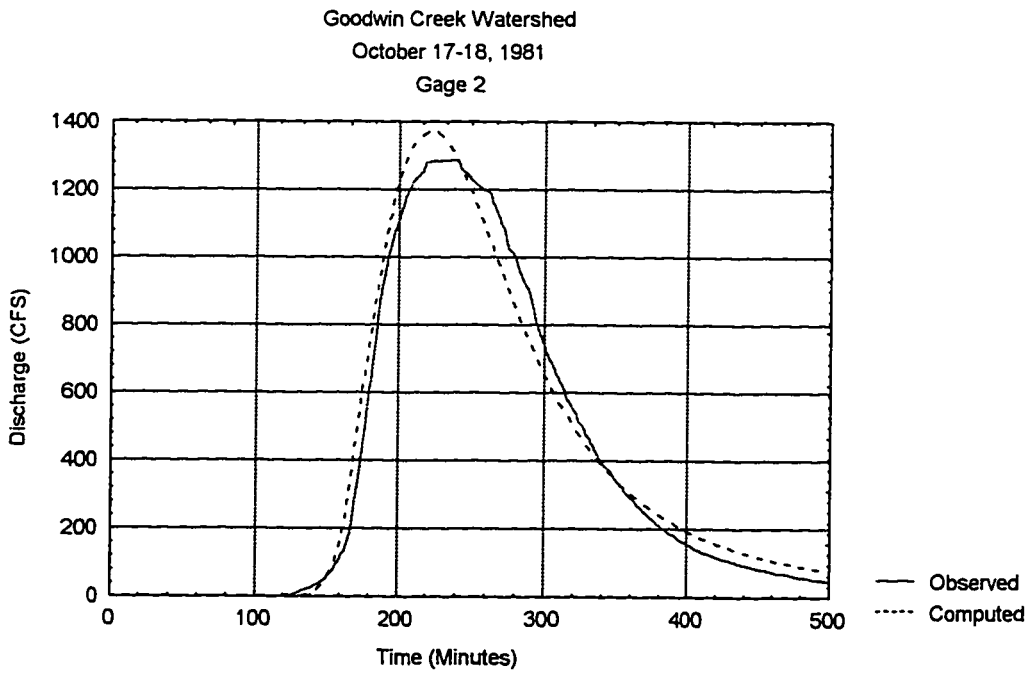
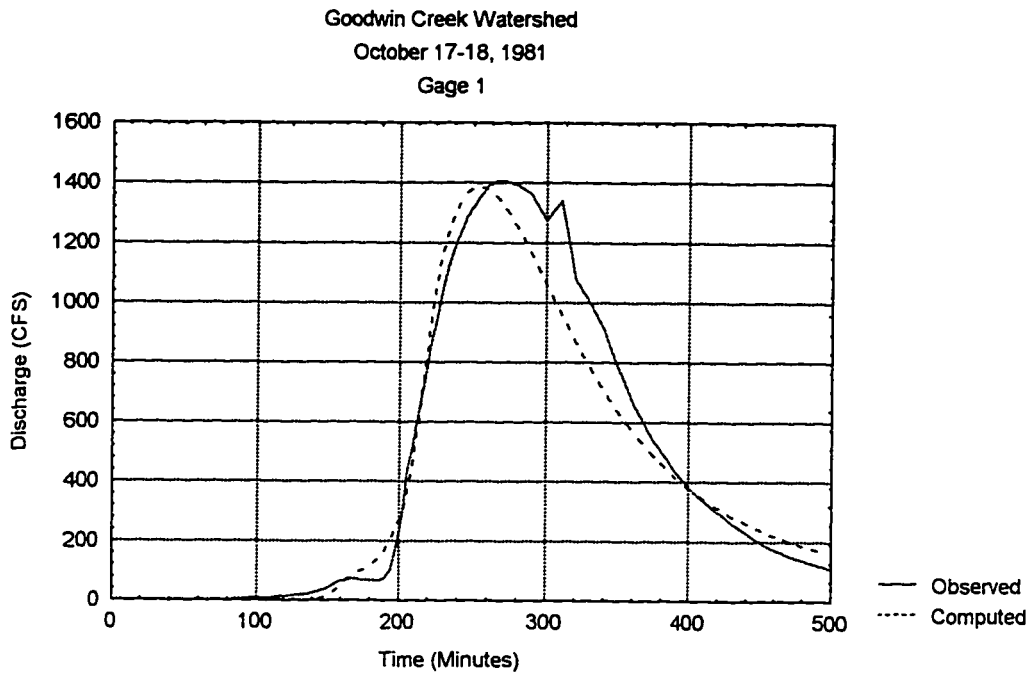


Figure A-5 - Flow Hydrographs for October 17-19, 1981.

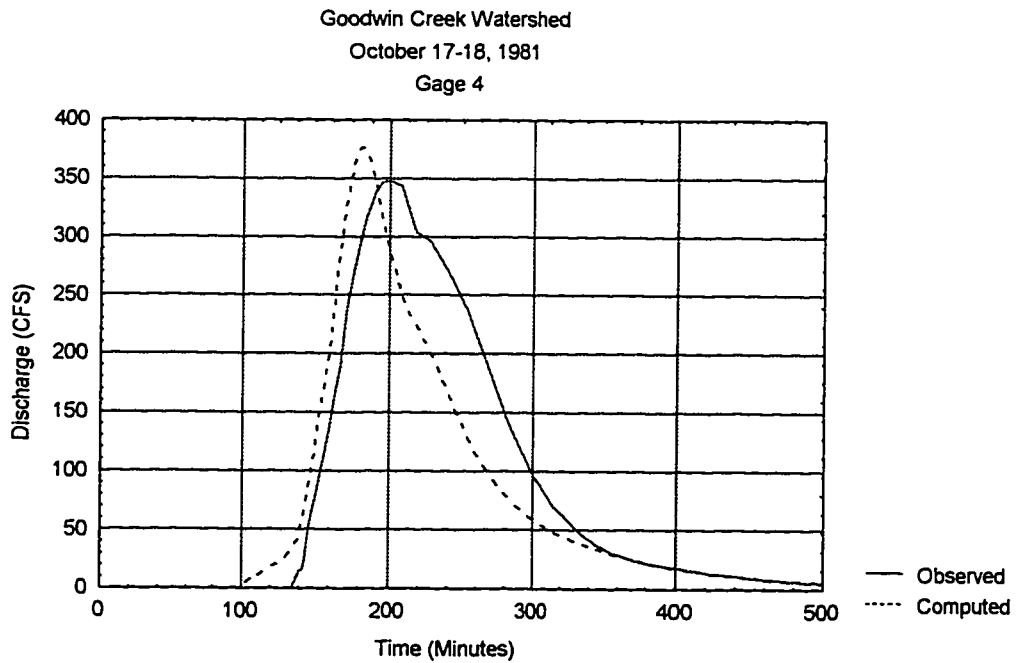
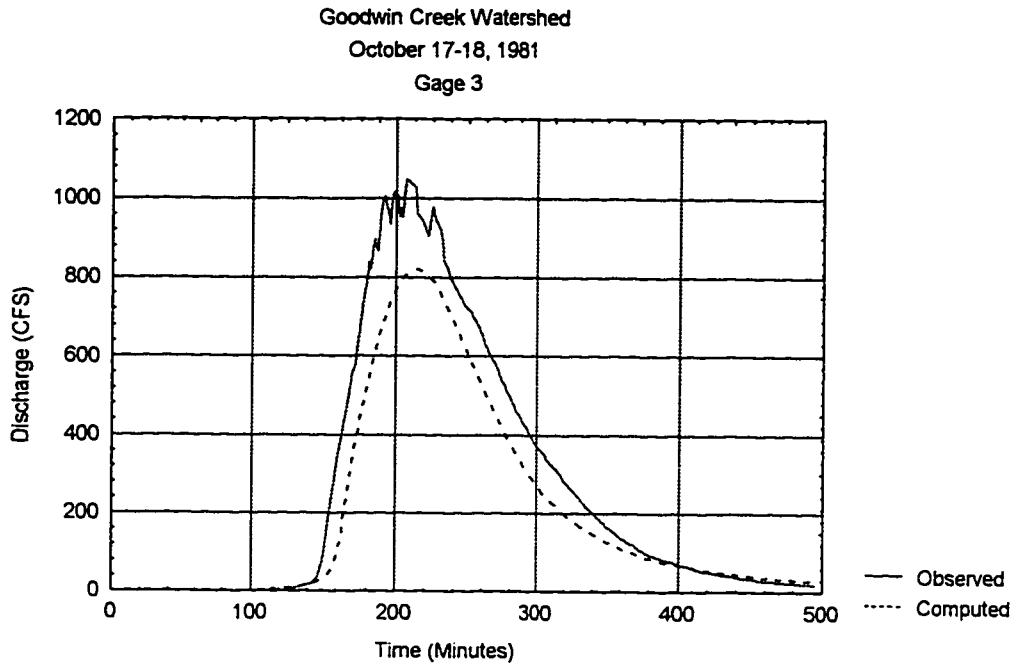


Figure A-6 - Flow Hydrographs for October 17-18, 1981 (Continued).

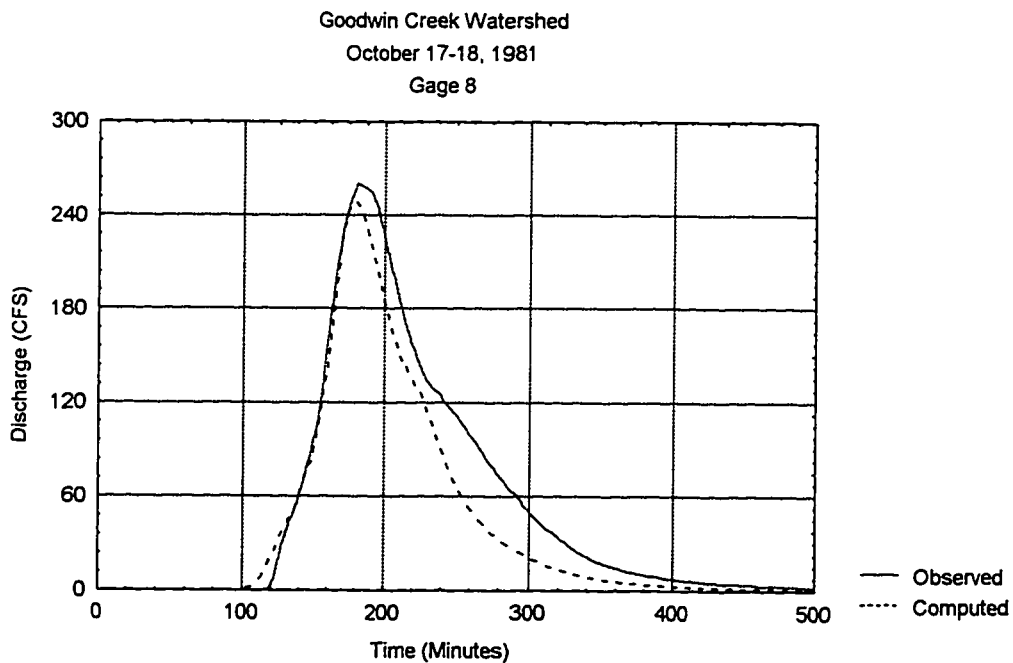
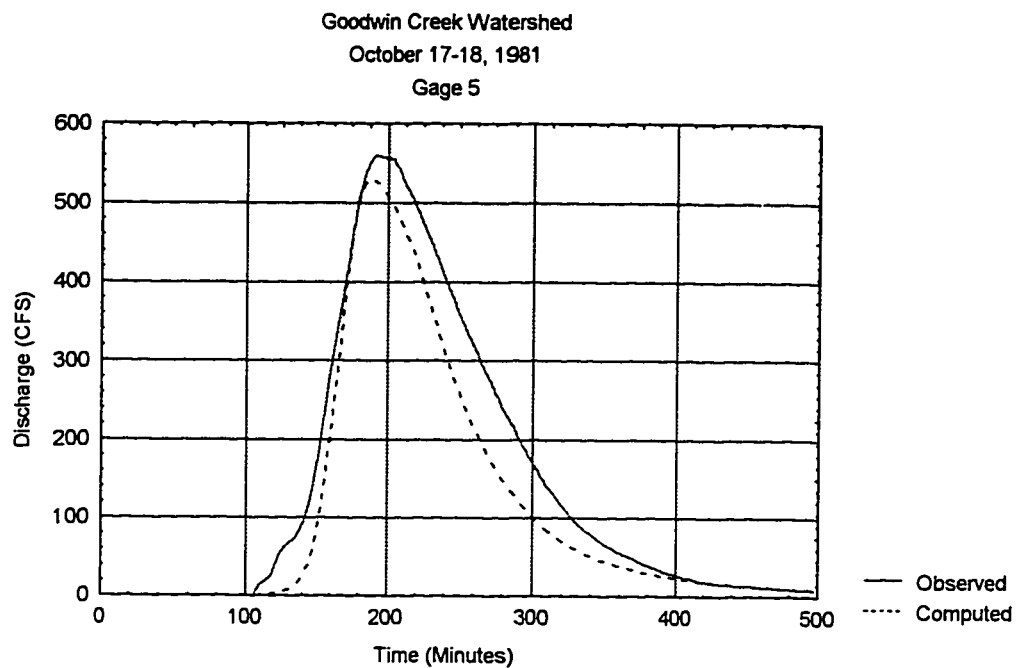


Figure A-7 - Flow Hydrographs for October 17-18, 1981 (Continued).

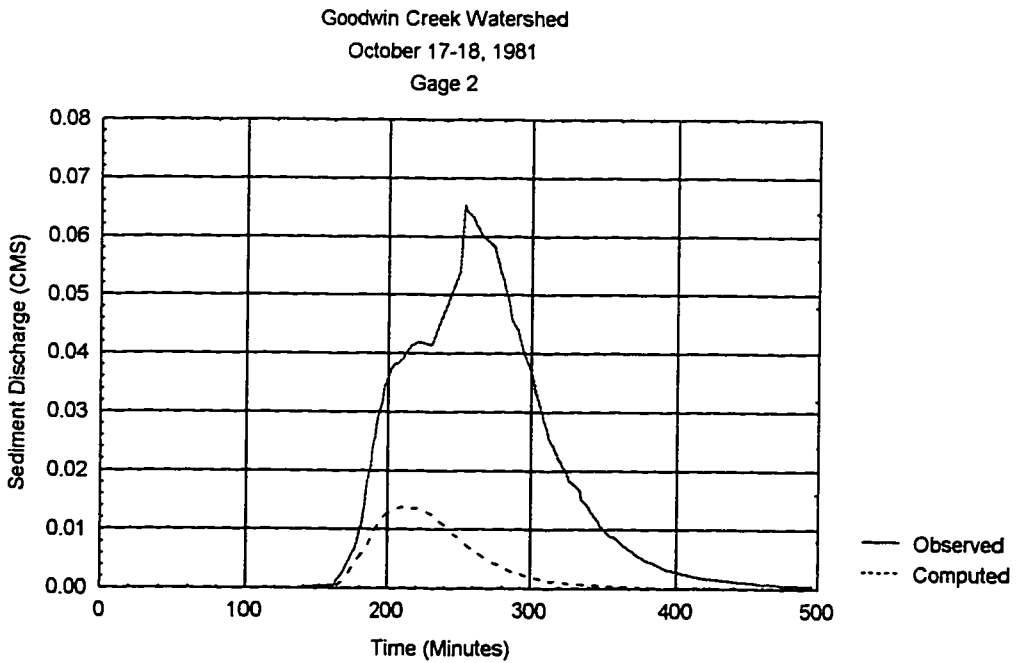
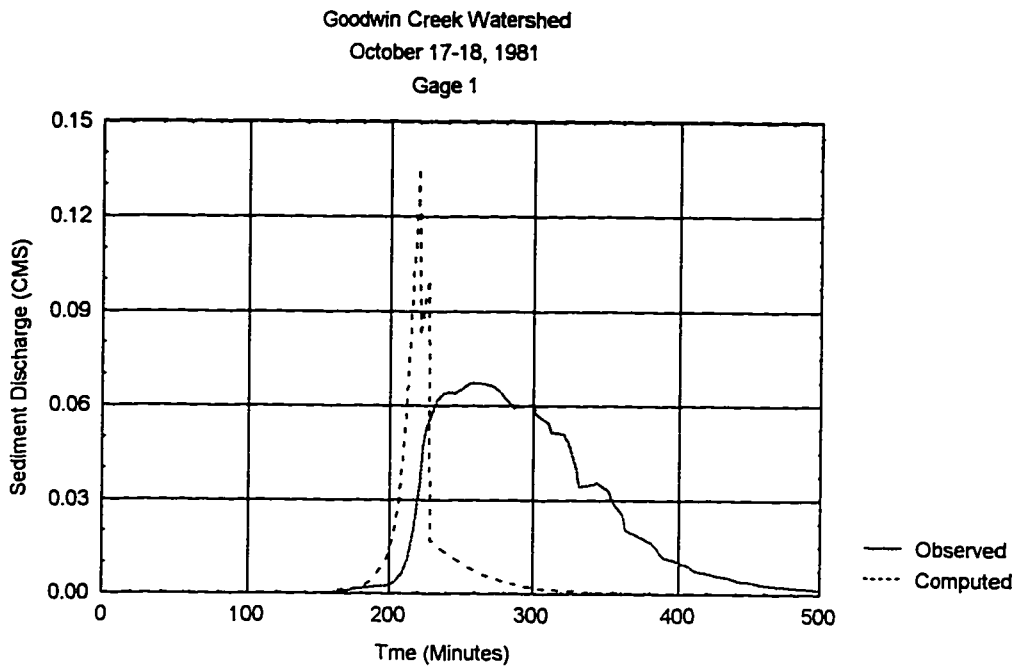


Figure A-8 - Sediment Discharge Hydrographs for October 17-18, 1981.

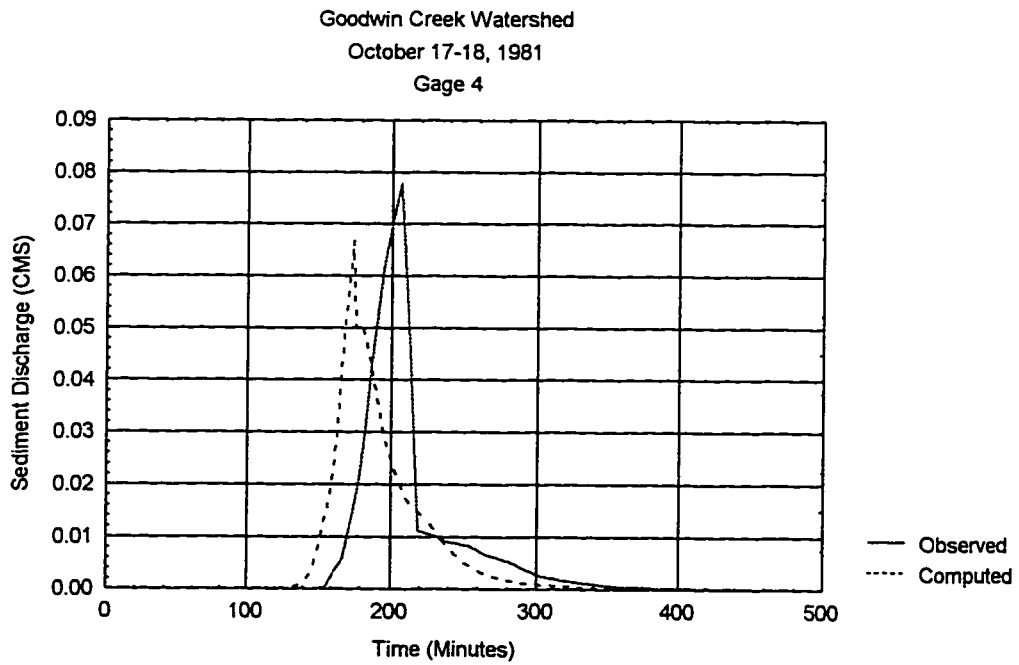
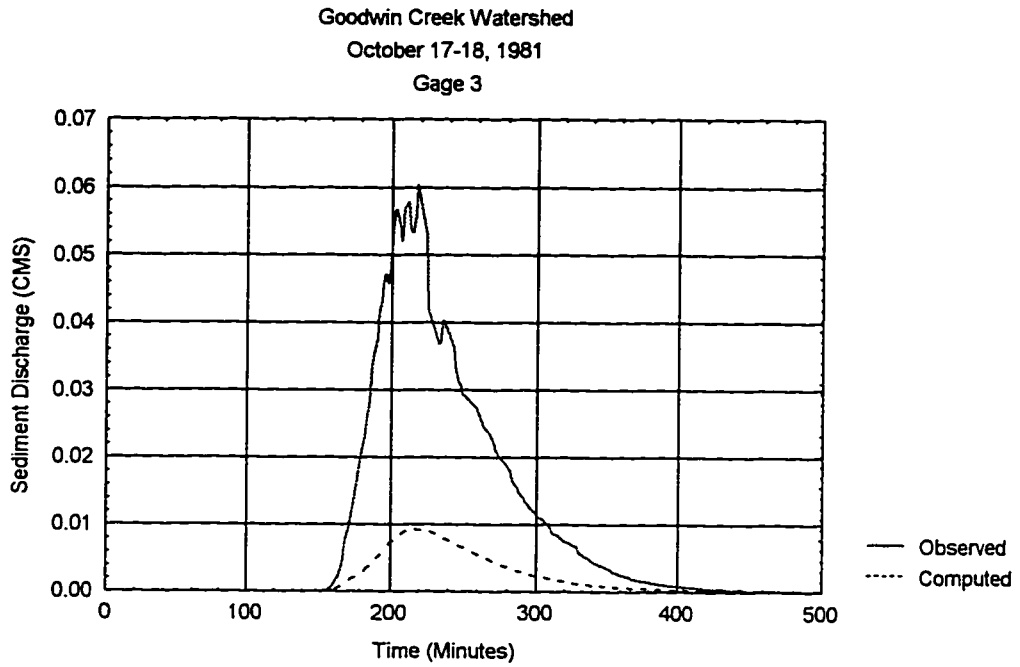


Figure A-9 - Sediment Discharge Hydrographs for October 17-18, 1981 (Continued.)

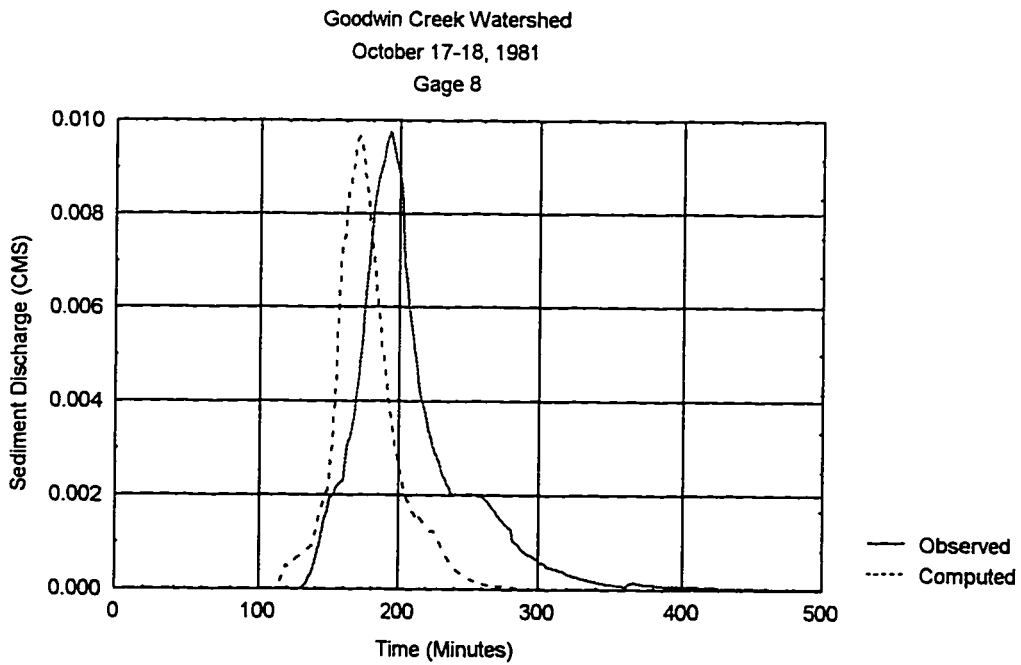
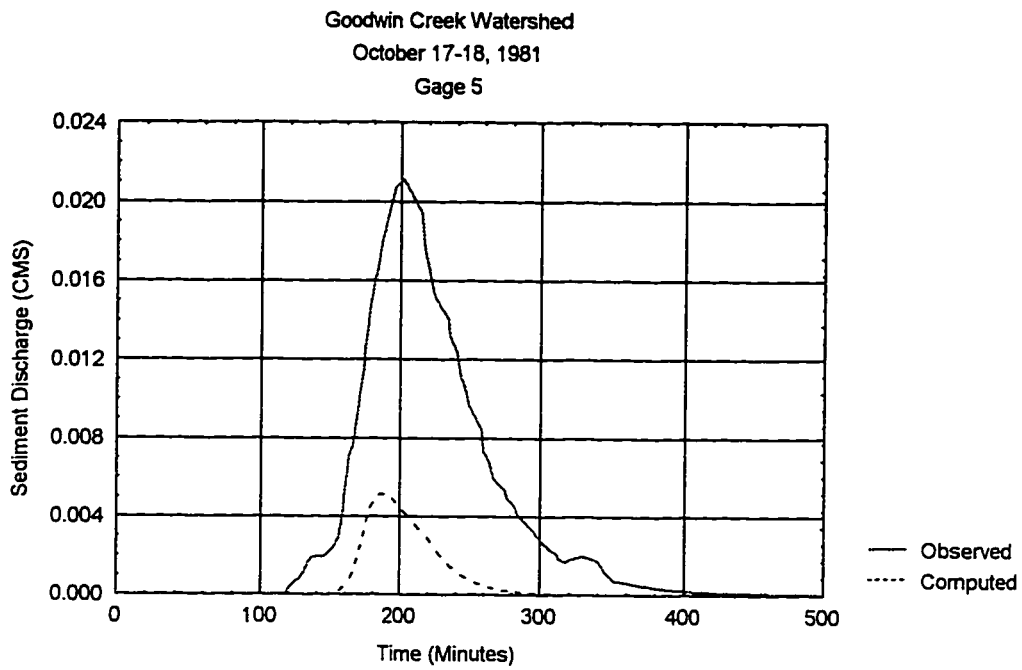


Figure A-10 - Sediment Discharge Hydrographs for October 17-18, 1981 (Continued).

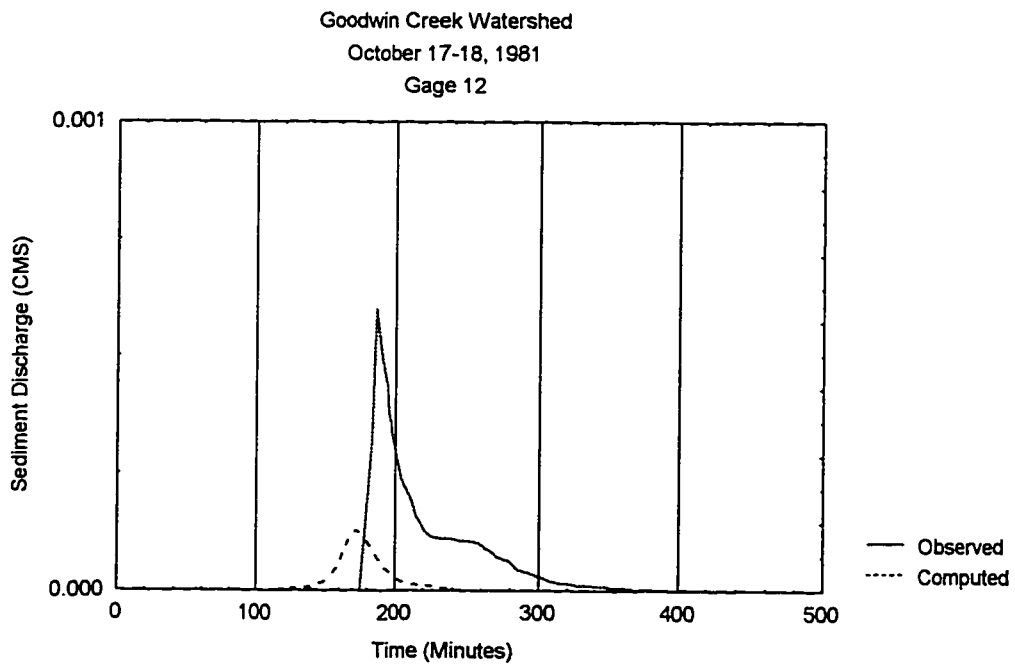
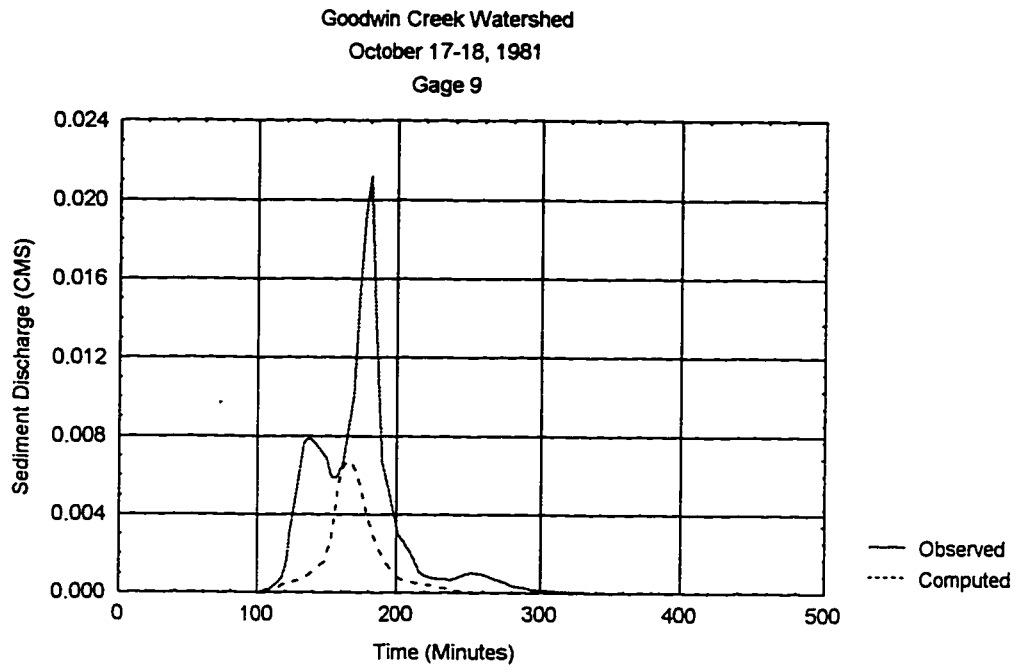


Figure A-11 - Sediment Discharge Hydrographs for October 17-18, 1981 (Continued).

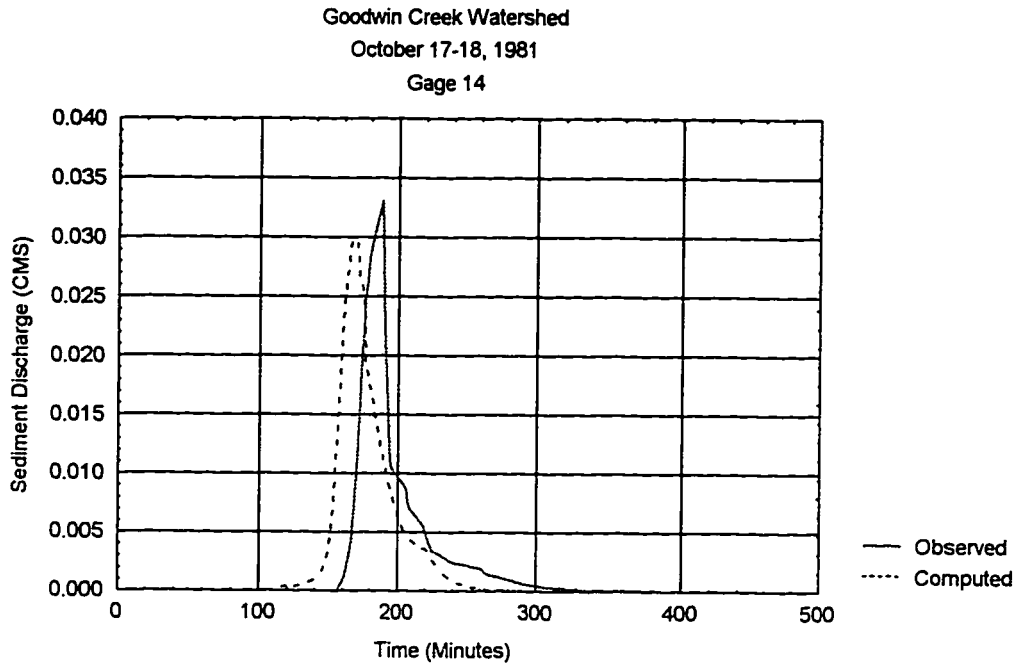


Figure A-12 - Sediment Discharge Hydrographs for October 17-18, 1981 (Continued).



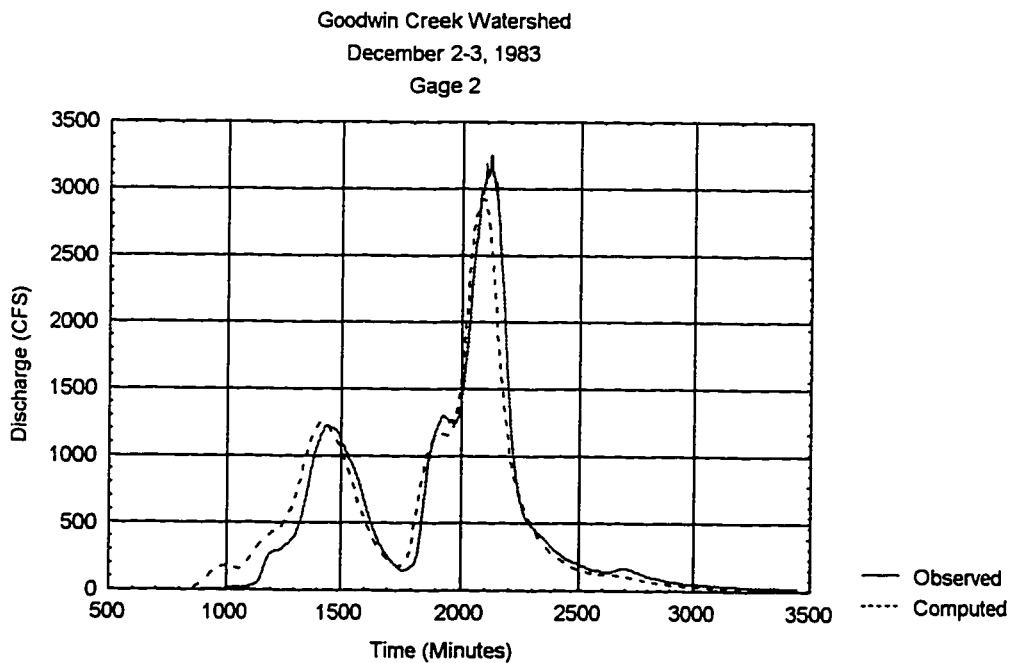
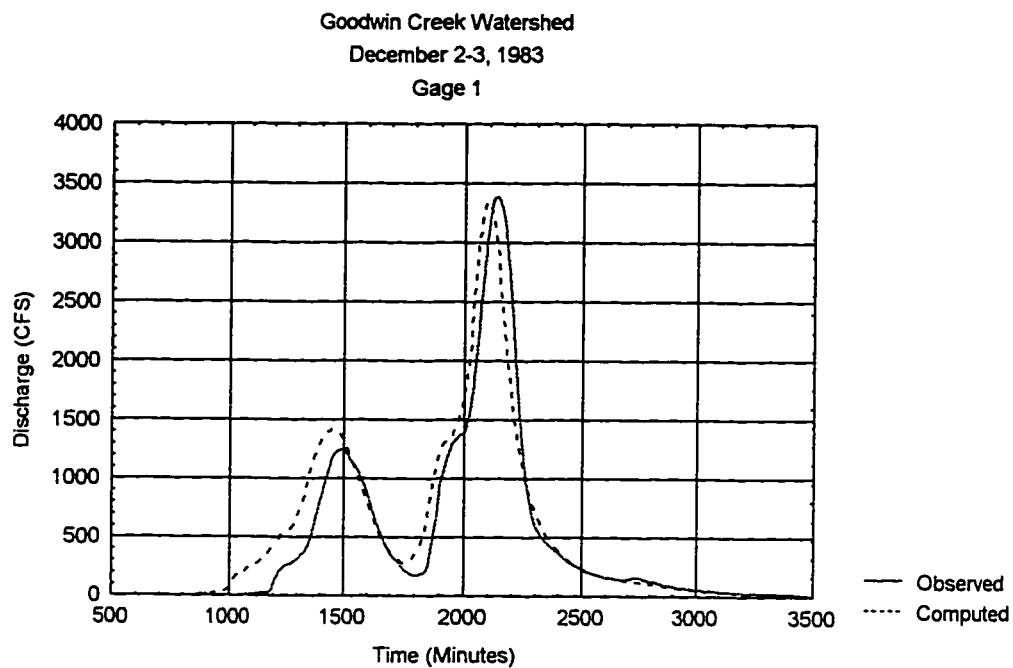


Figure A-13 - Flow Hydrographs for December 2-3, 1983.

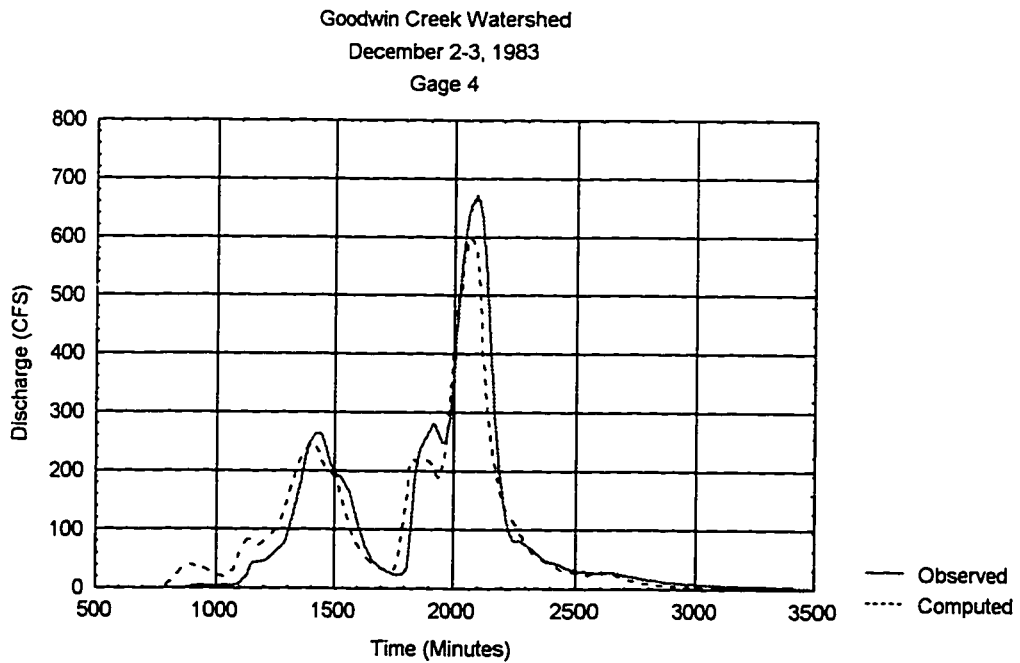
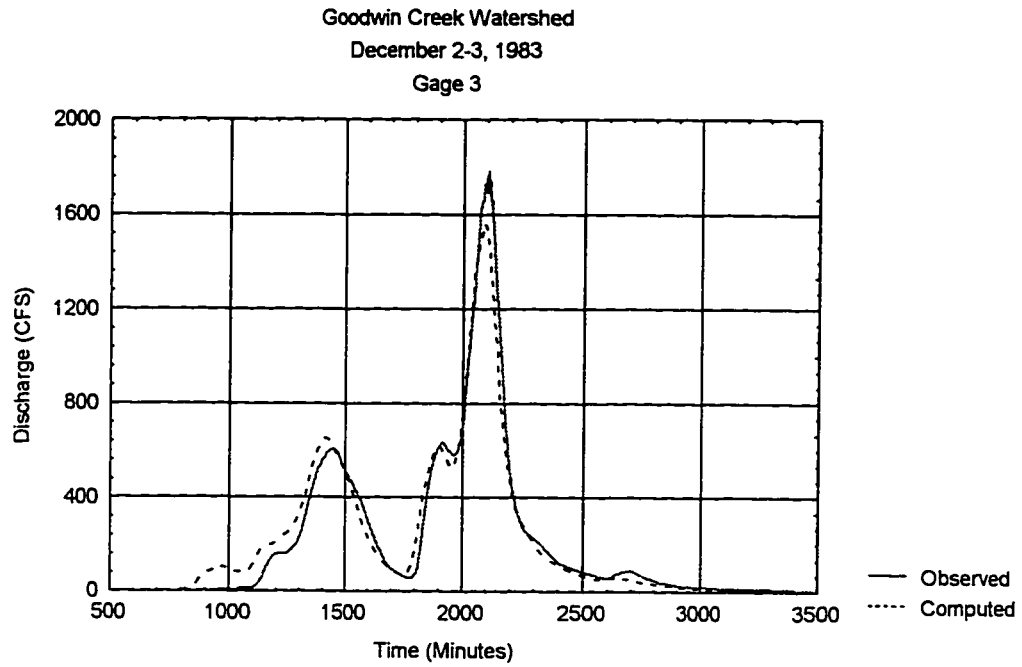


Figure A-14 - Flow Hydrographs for December 2-3, 1983 (Continued).

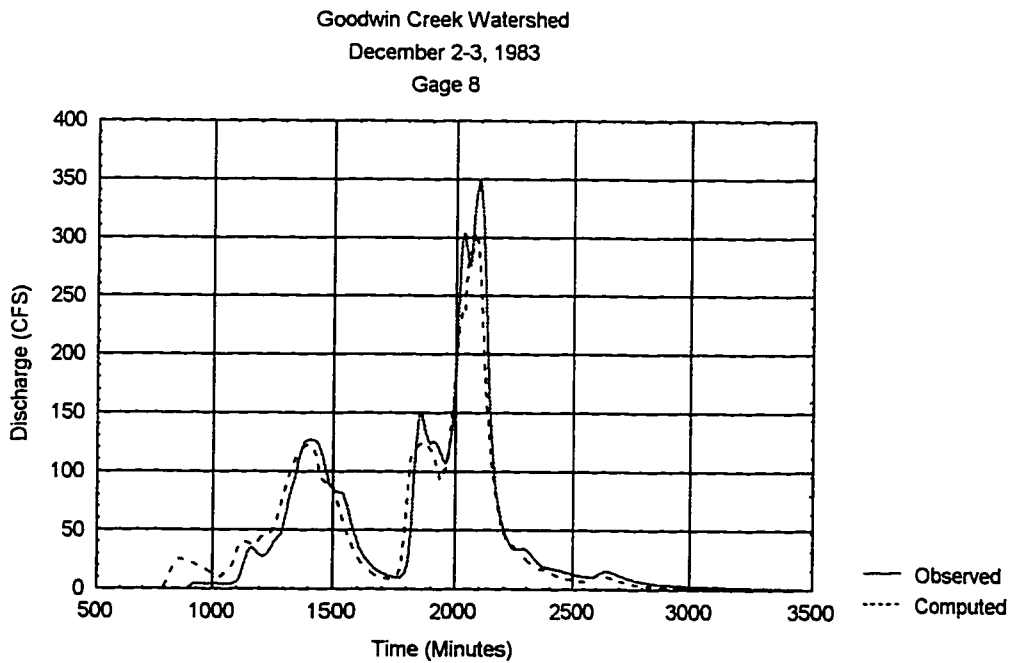
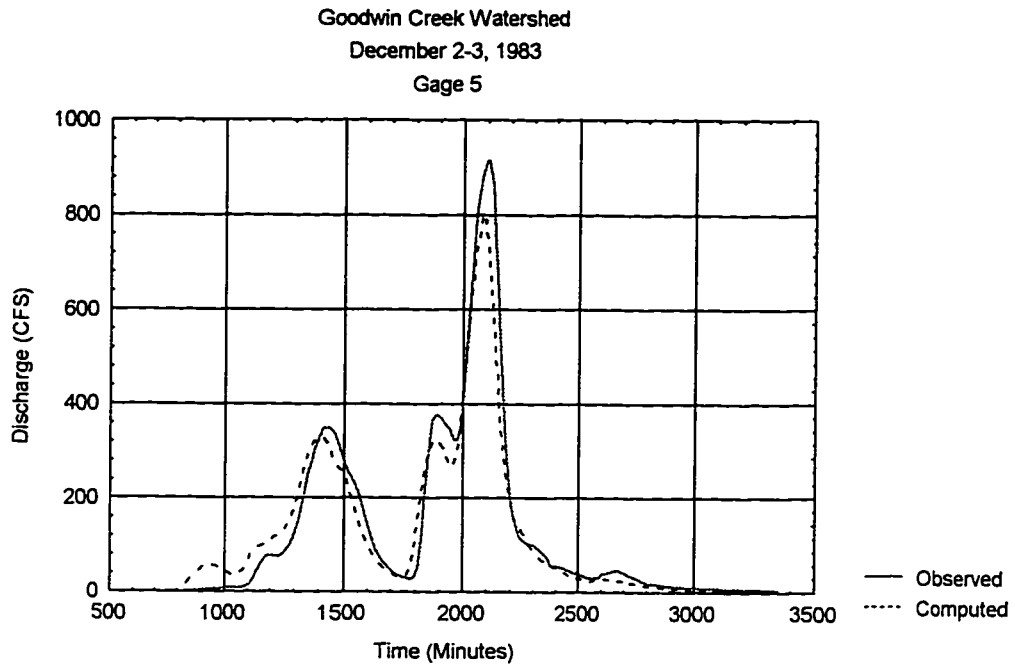


Figure A-15 - Flow Hydrographs for December 2-3, 1983 (Continued).

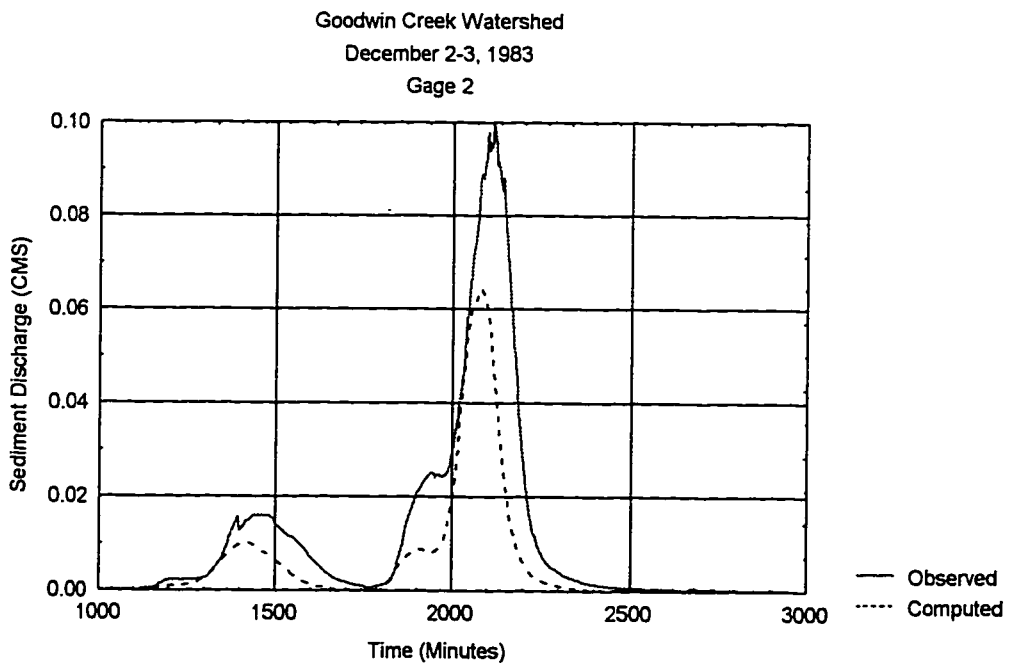
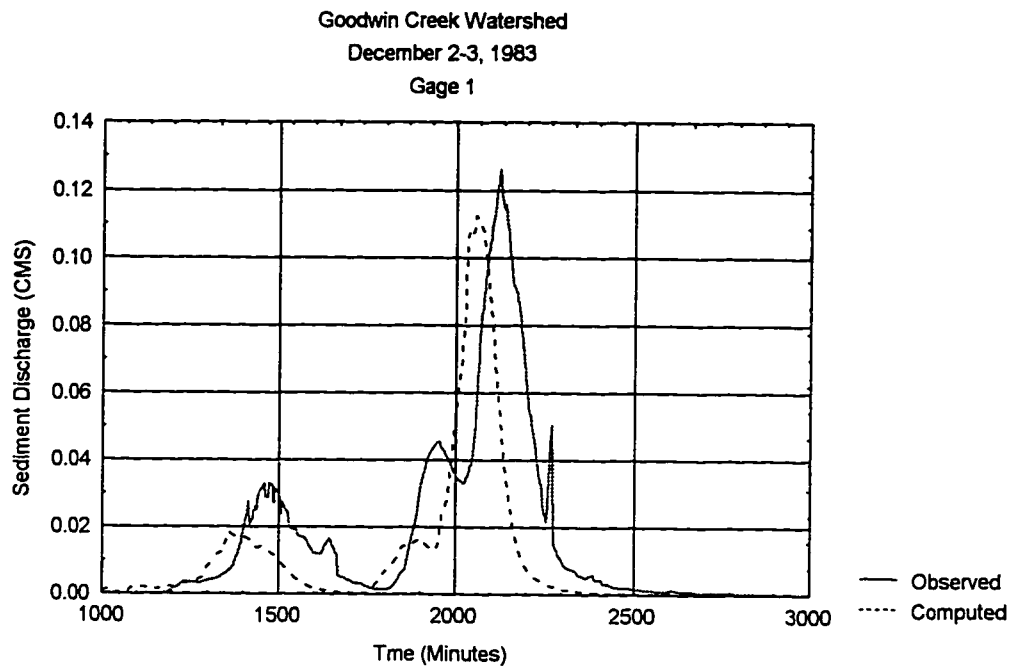


Figure A-16 - Sediment Discharge Hydrographs for December 2-3, 1983.

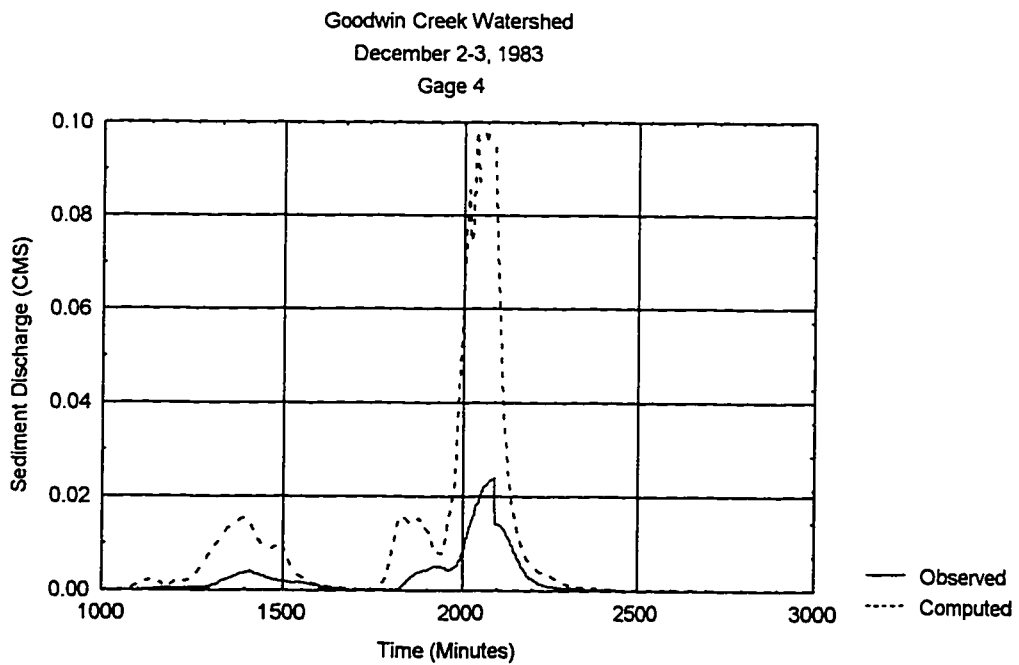
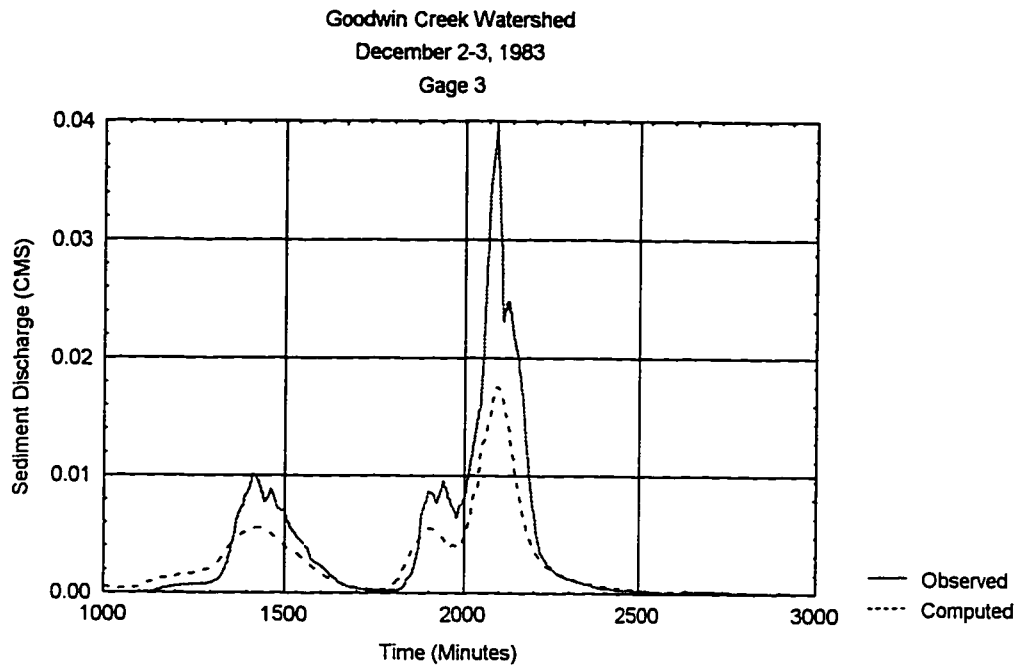


Figure A-17 - Sediment Discharge Hydrographs for December 2-3, 1983 (Continued).

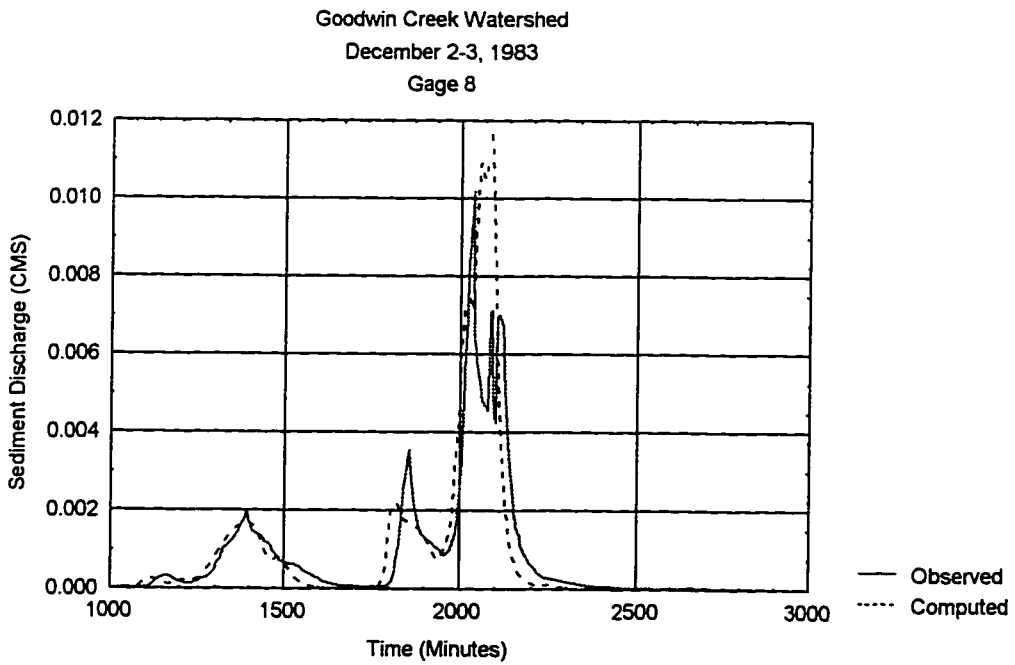
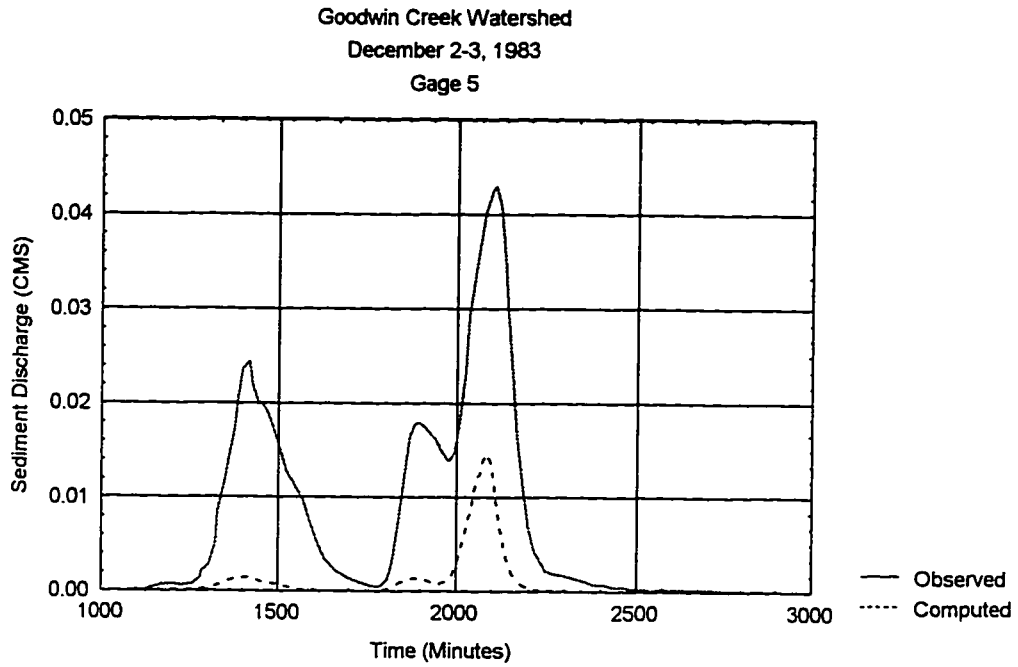


Figure A-18 - Sediment Discharge Hydrographs for December 2-3, 1983 (Continued).

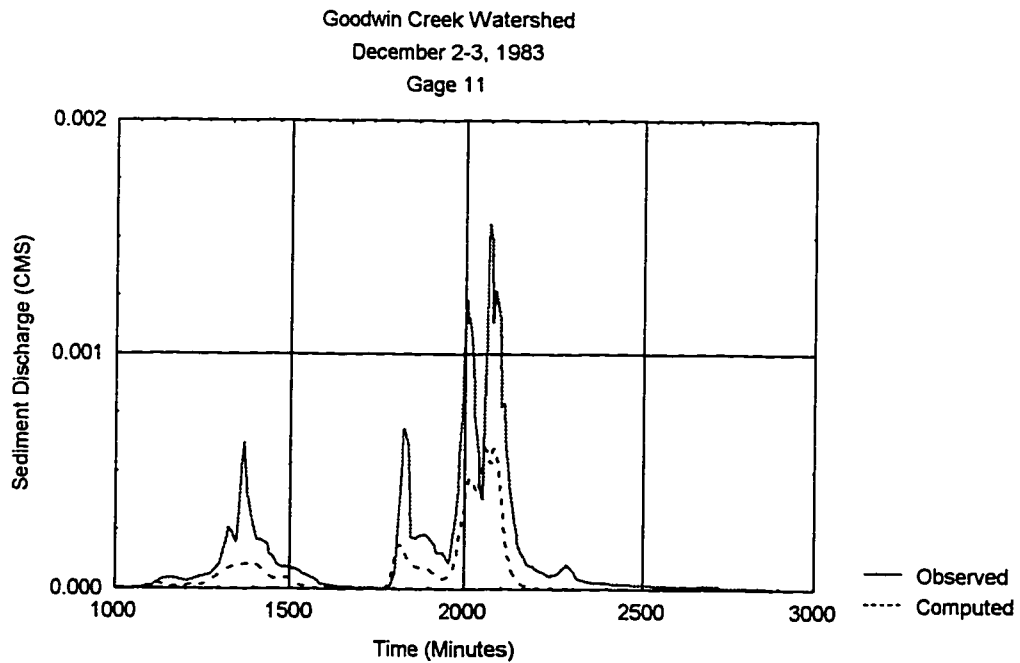
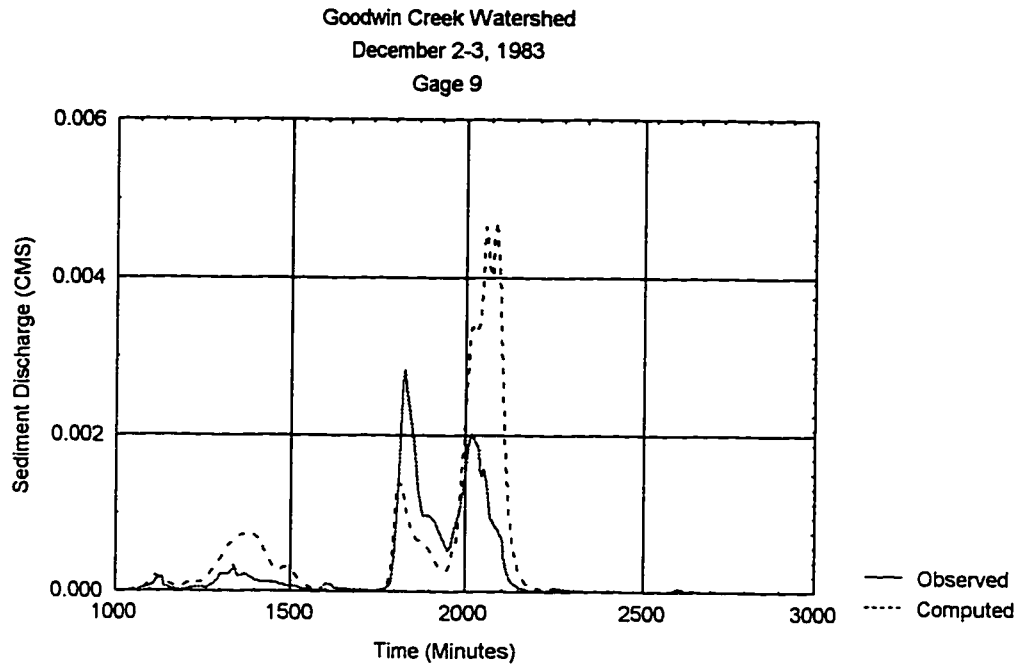


Figure A-19 - Sediment Discharge Hydrographs for December 2-3, 1983 (Continued).

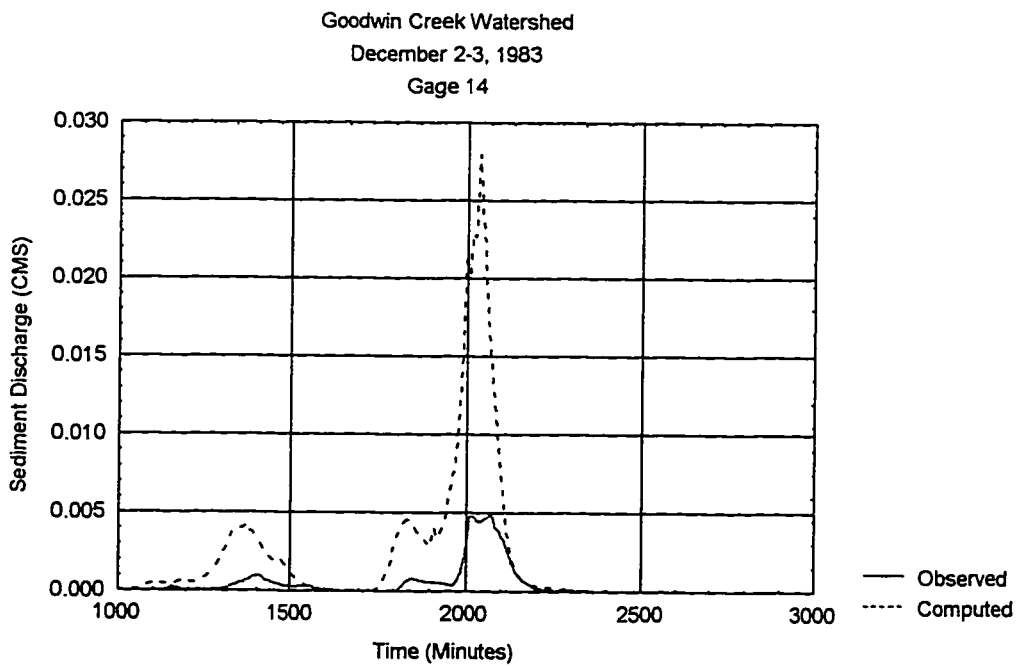
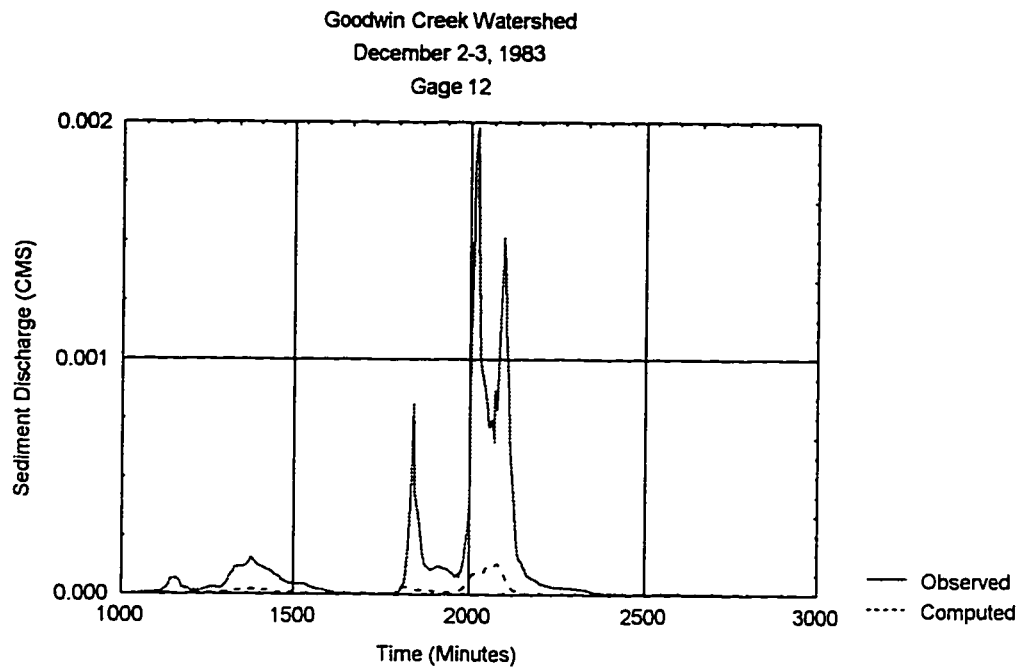


Figure A-20 - Sediment Discharge Hydrographs for December 2-3, 1983 (Continued).



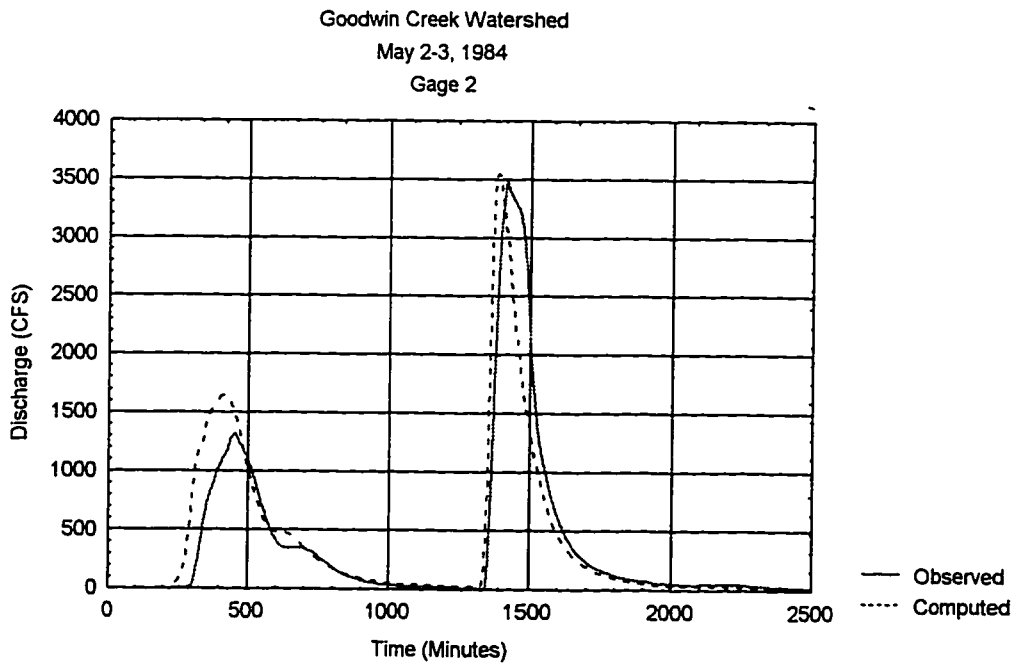
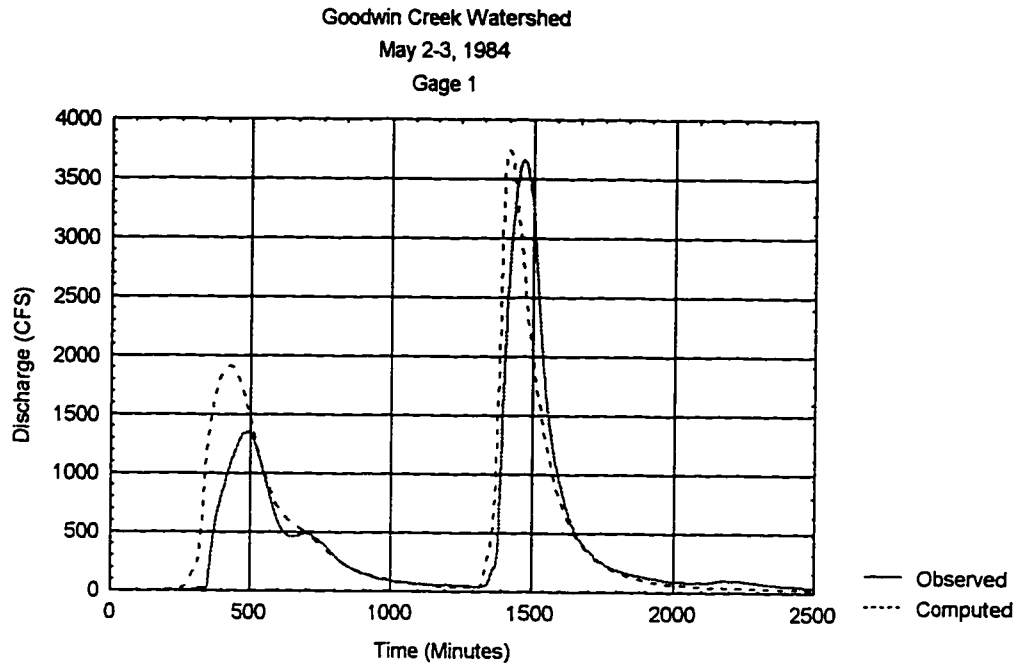


Figure A-21 - Flow Hydrographs for May 2-3, 1984.

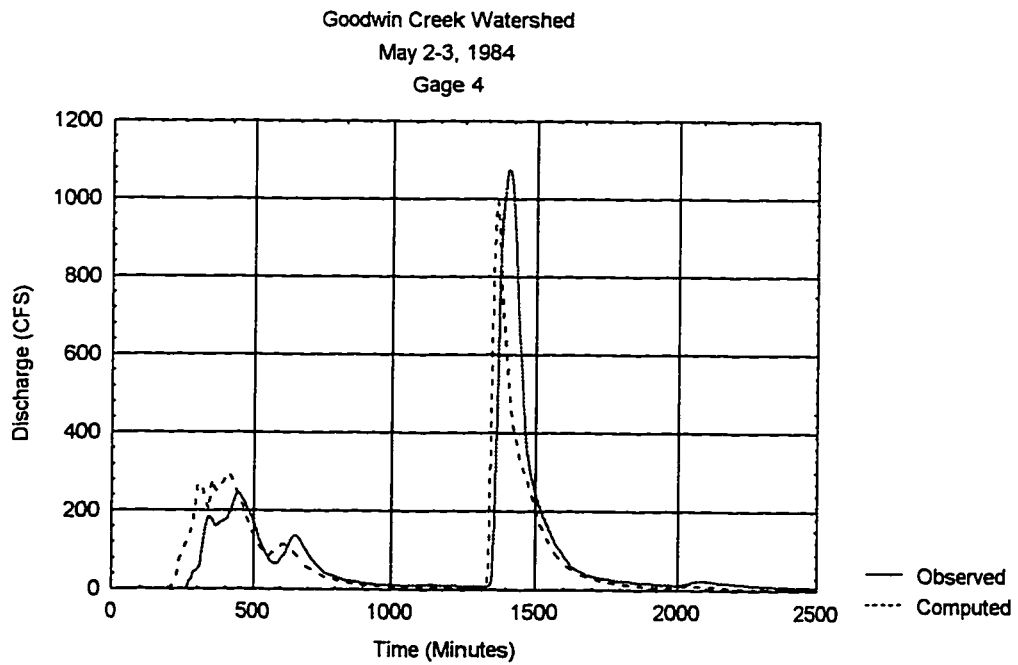
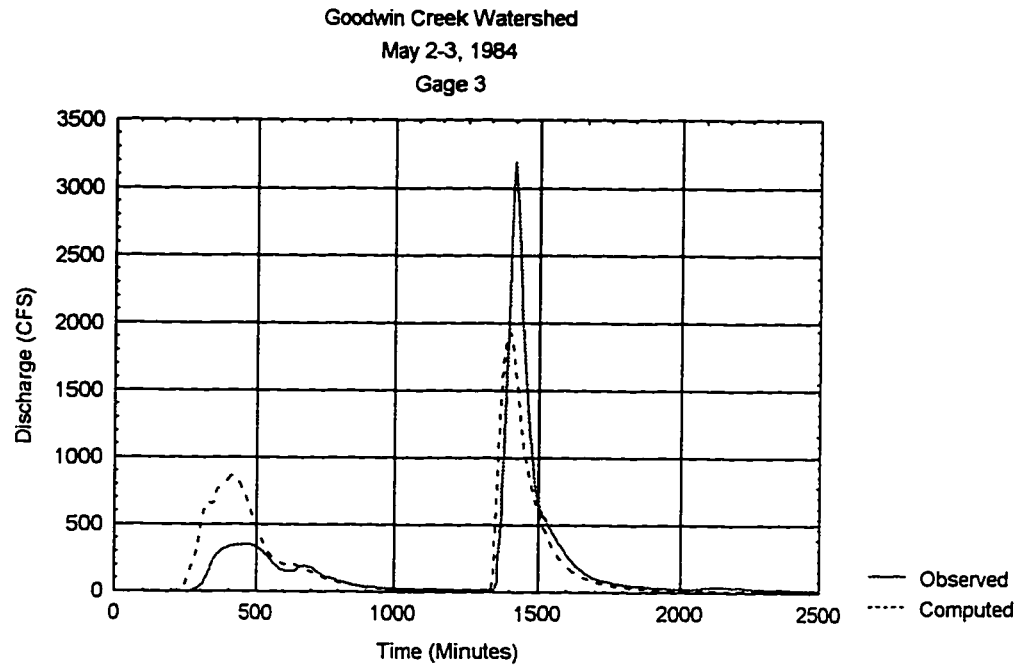


Figure A-22 - Flow Hydrographs for May 2-3, 1984 (Continued).

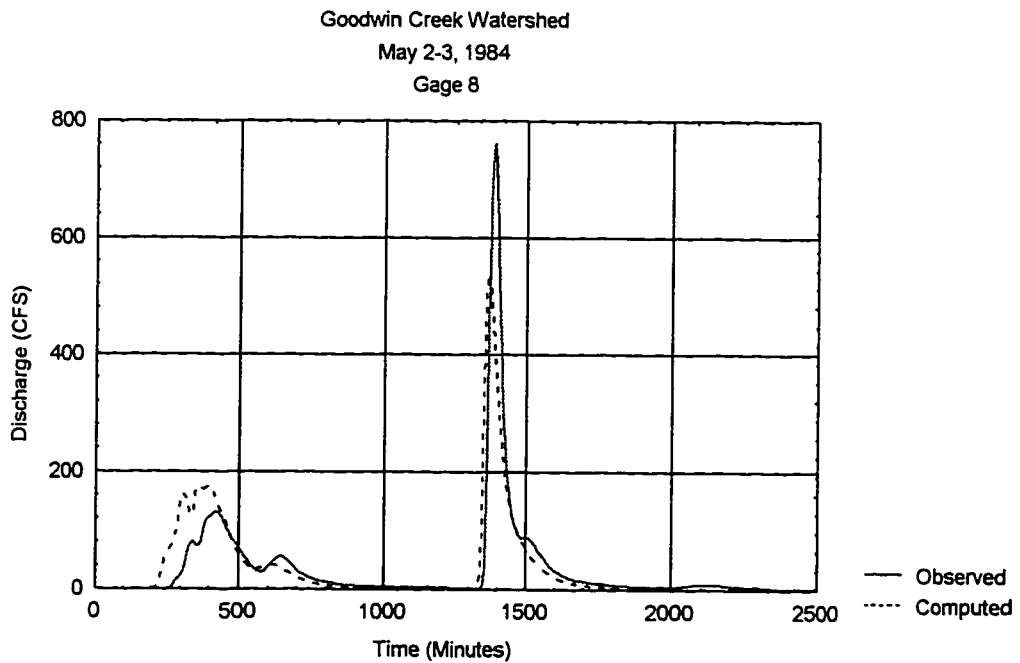
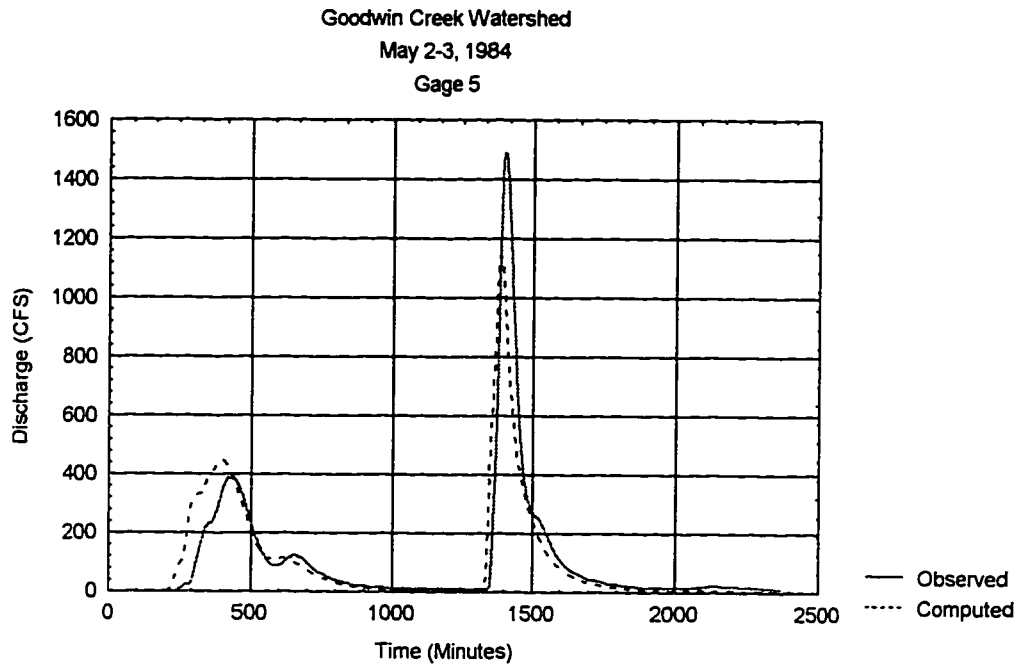


Figure A-23 - Flow Hydrographs for May 2-3, 1984 (Continued).

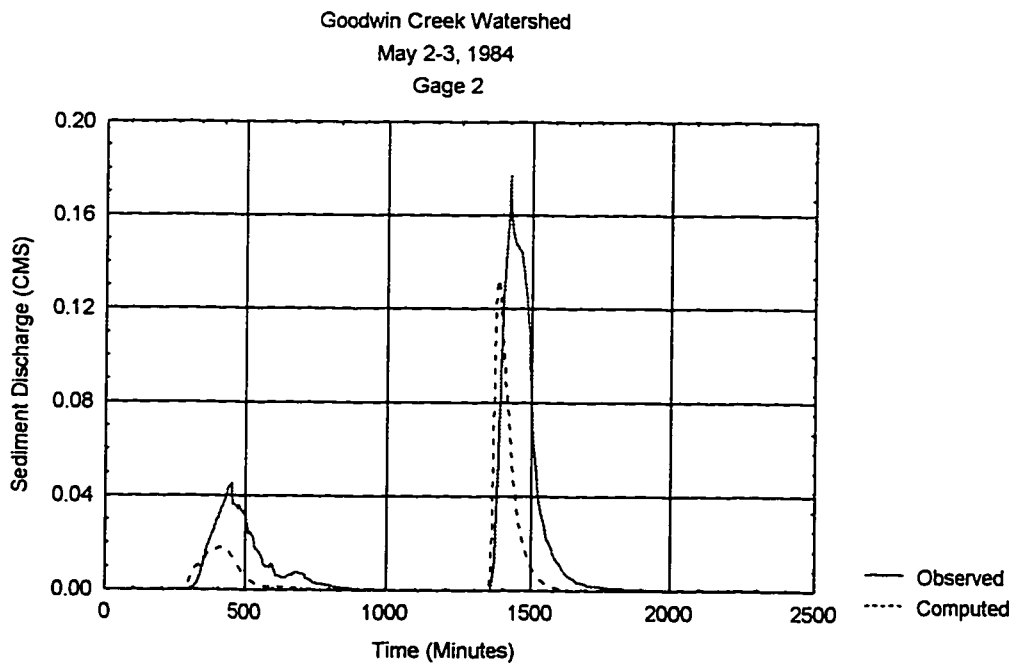
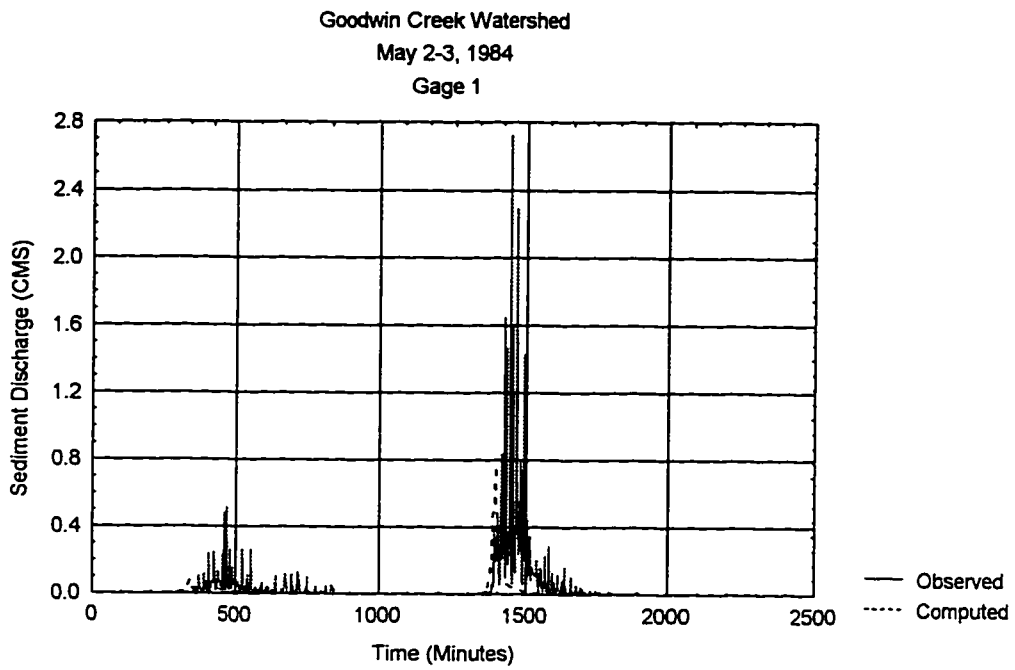


Figure A-24 - Sediment Discharge Hydrographs for May 2-3, 1984.

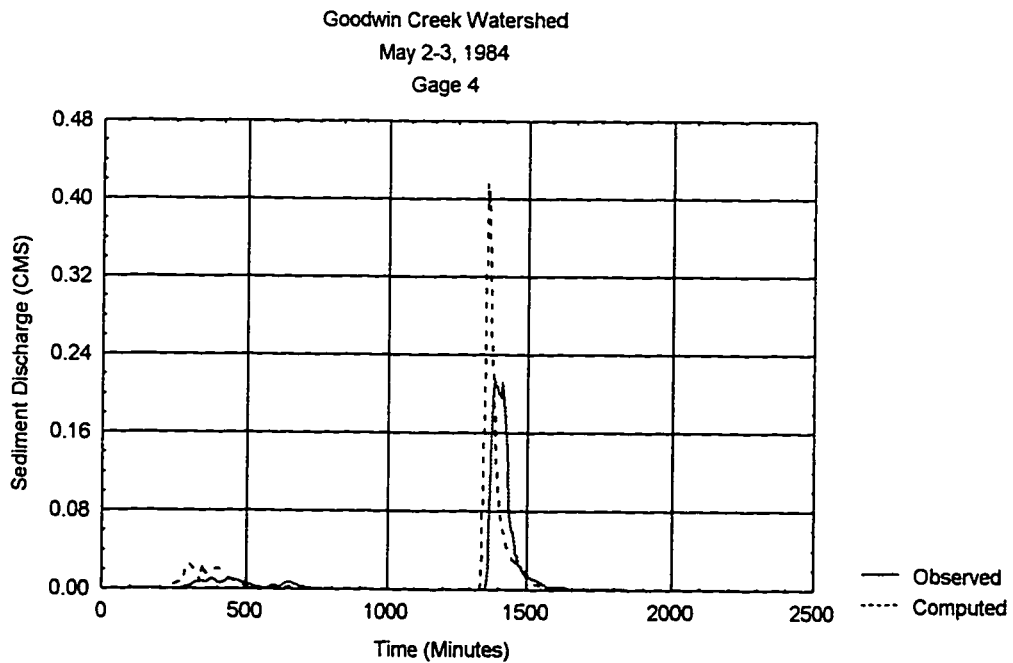
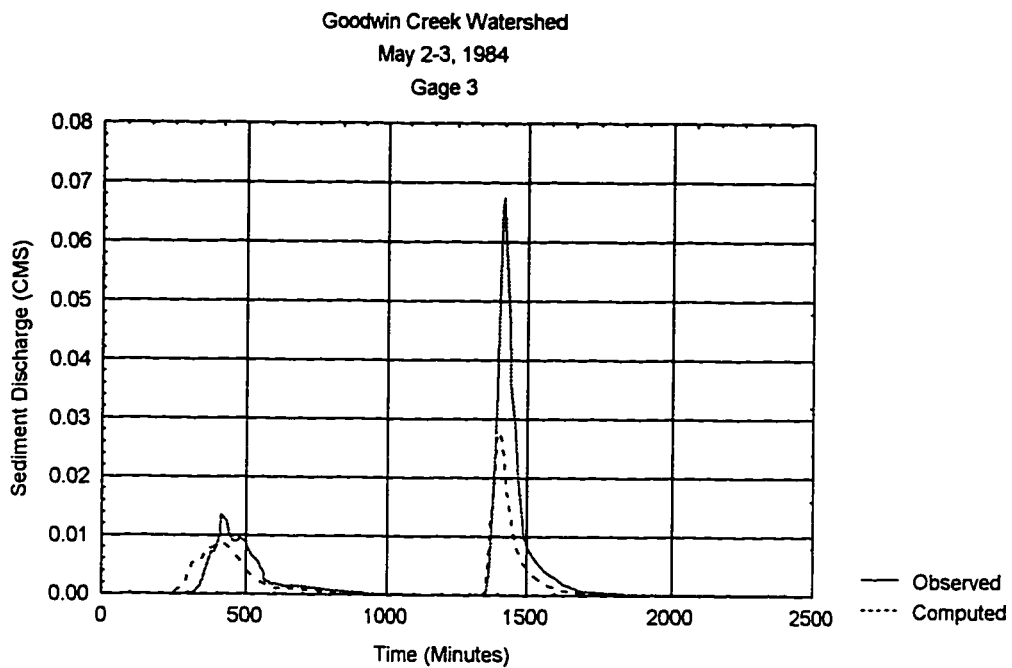


Figure A-25 - Sediment Discharge Hydrographs for May 2-3, 1984 (Continued).

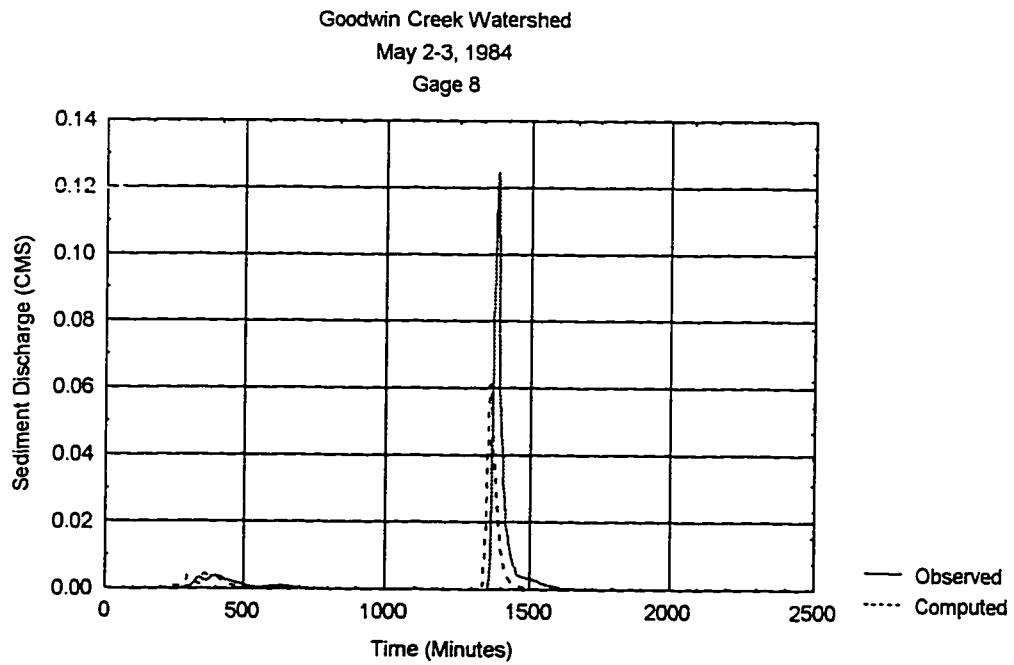
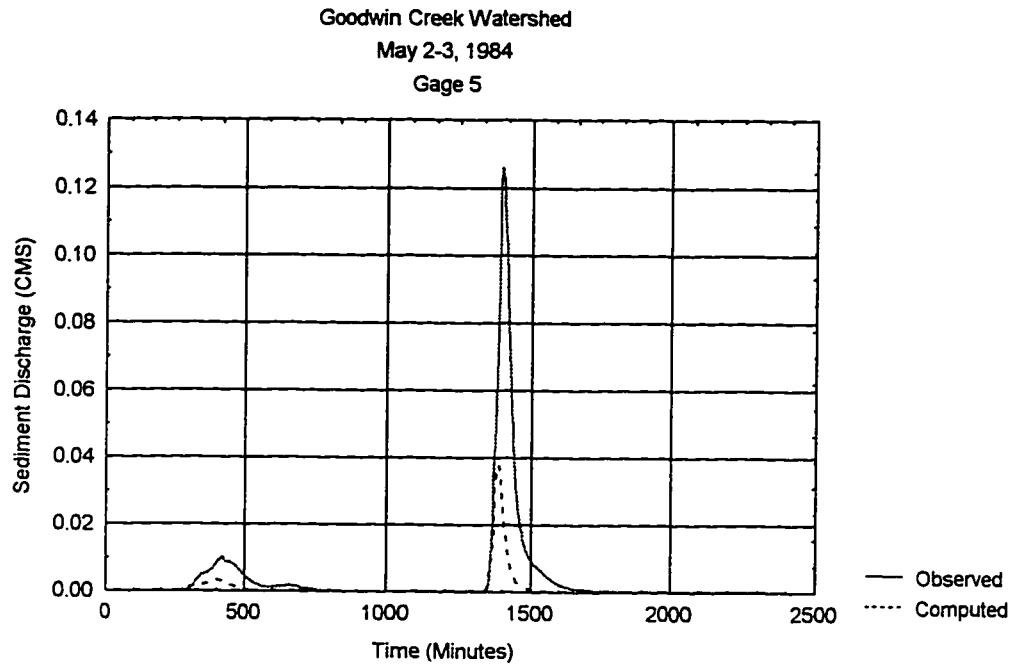


Figure A-26 - Sediment Discharge Hydrographs for May 2-3, 1984 (Continued).

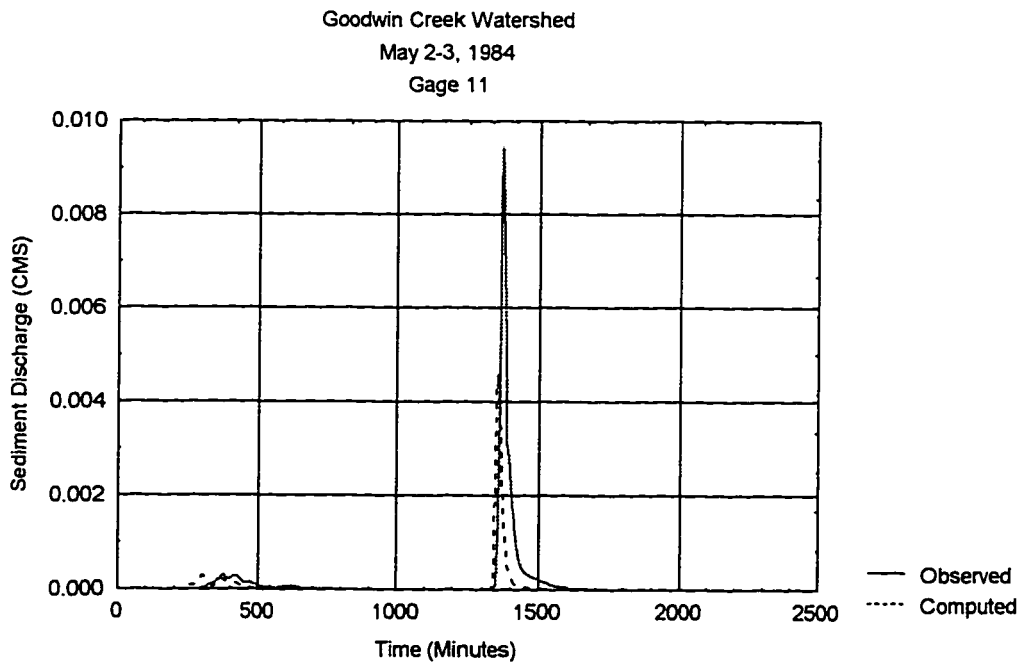
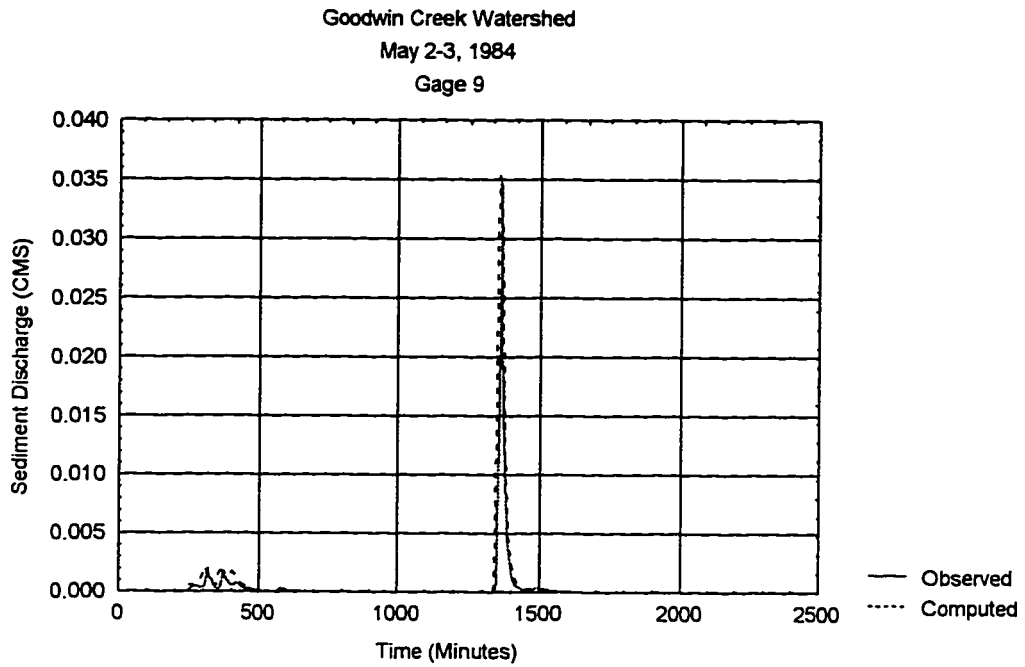


Figure A-27 - Sediment Discharge Hydrographs for May 2-3, 1984 (Continued).

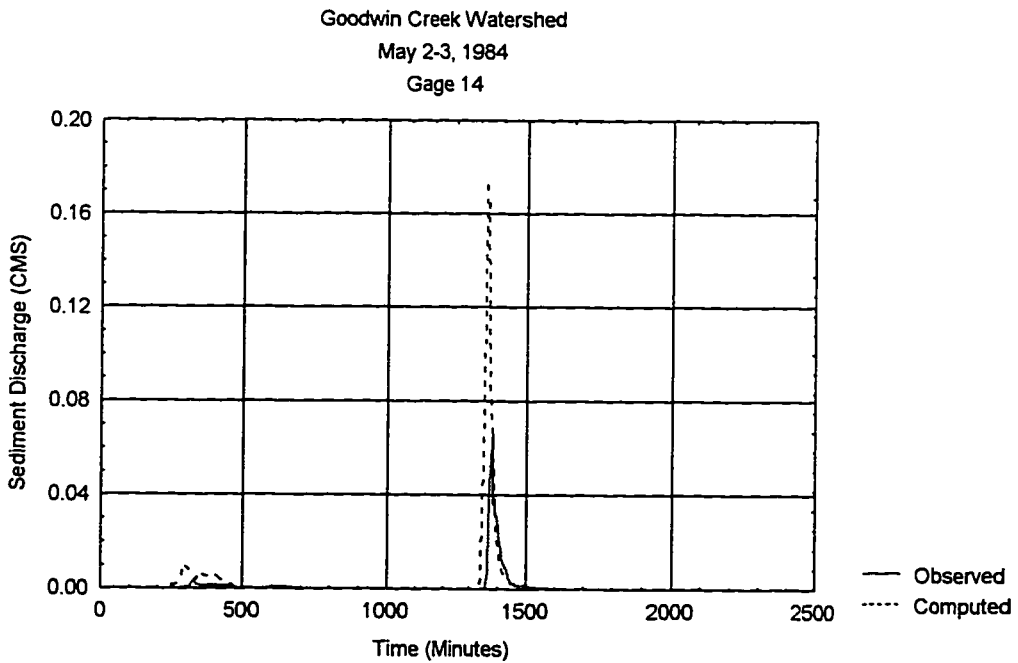
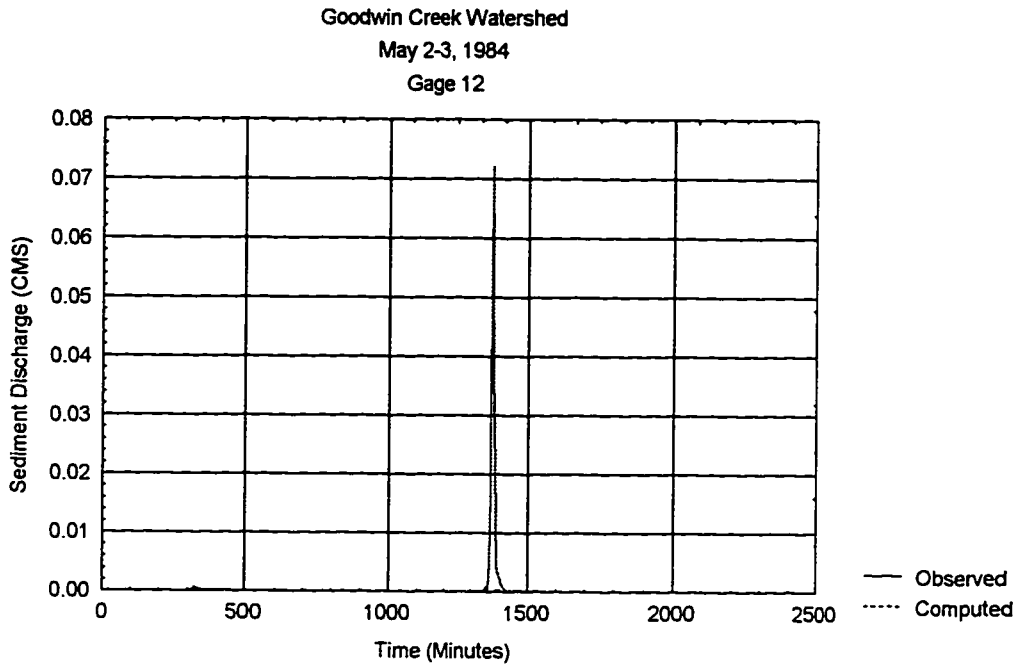


Figure A-28 - Sediment Discharge Hydrographs for May 2-3, 1984 (Continued).



**Appendix B**

**CASC2D Output Grids**

**Test Plot #2**

**February 17-19, 1991**

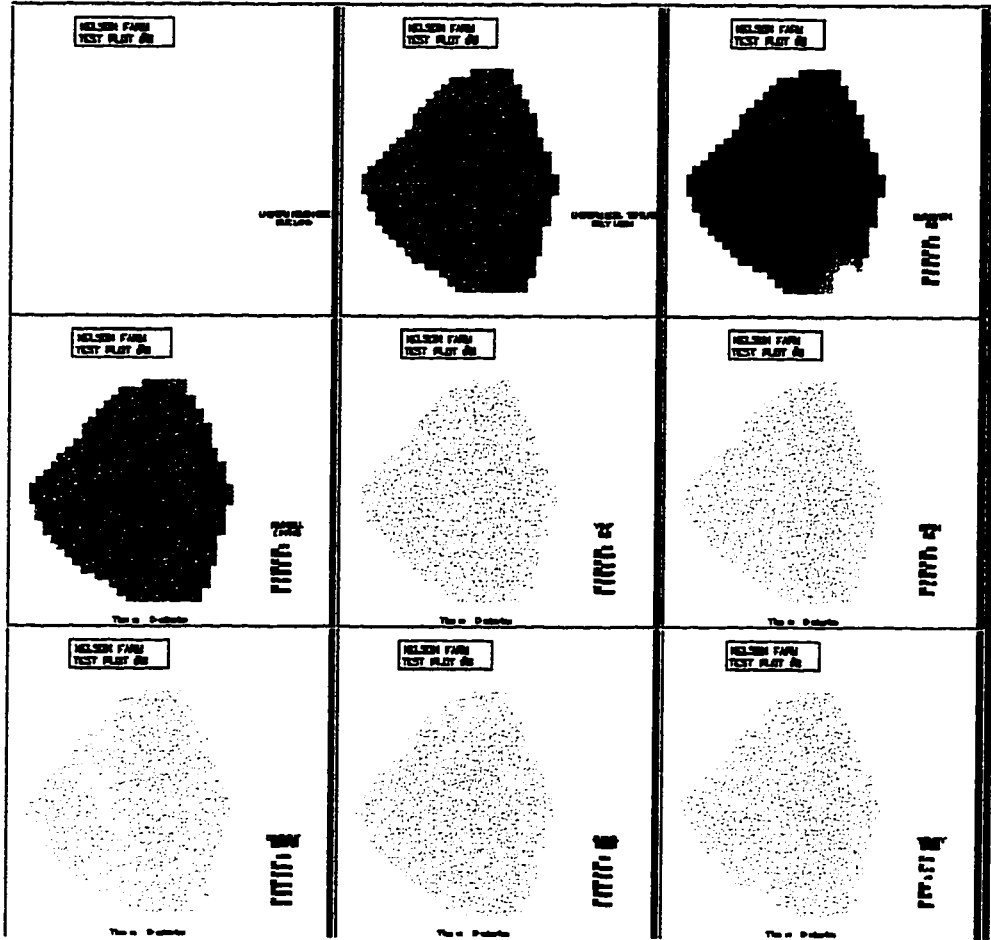


Figure B-1 - February 17-19, 1991 at Time = 0.0 minutes.

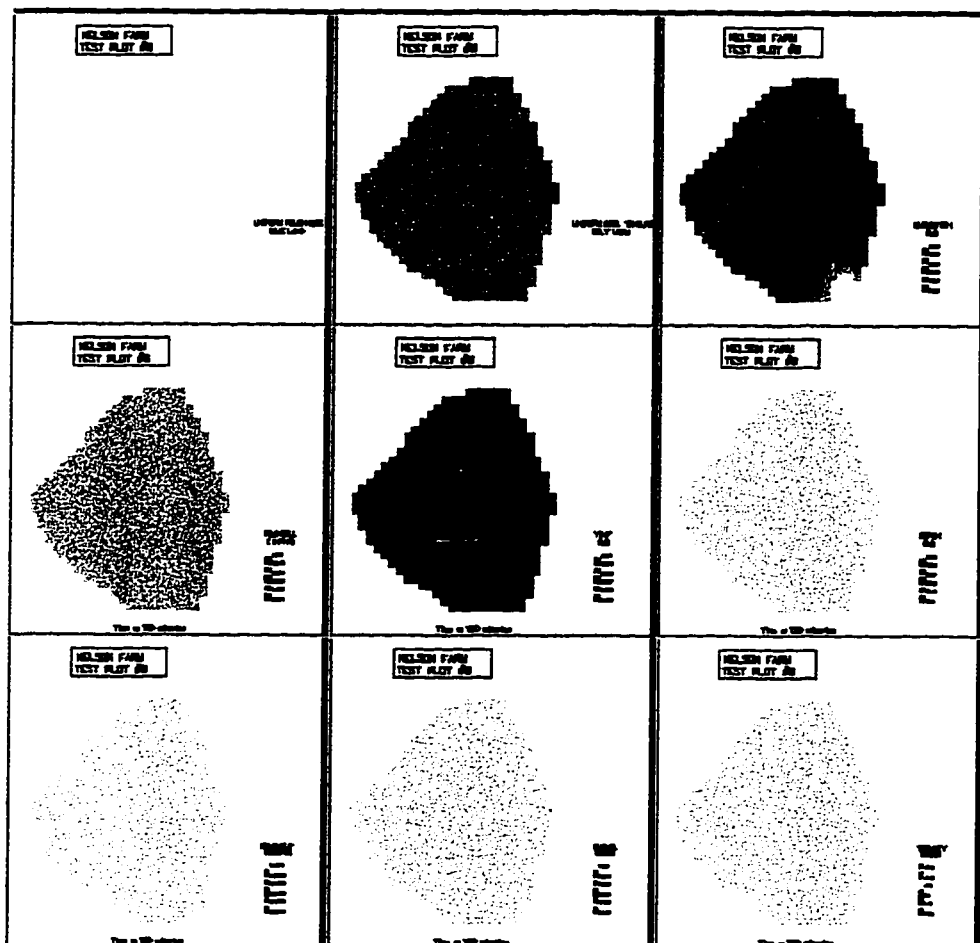


Figure B-2 - February 17-19, 1991 at Time = 120.0 minutes.

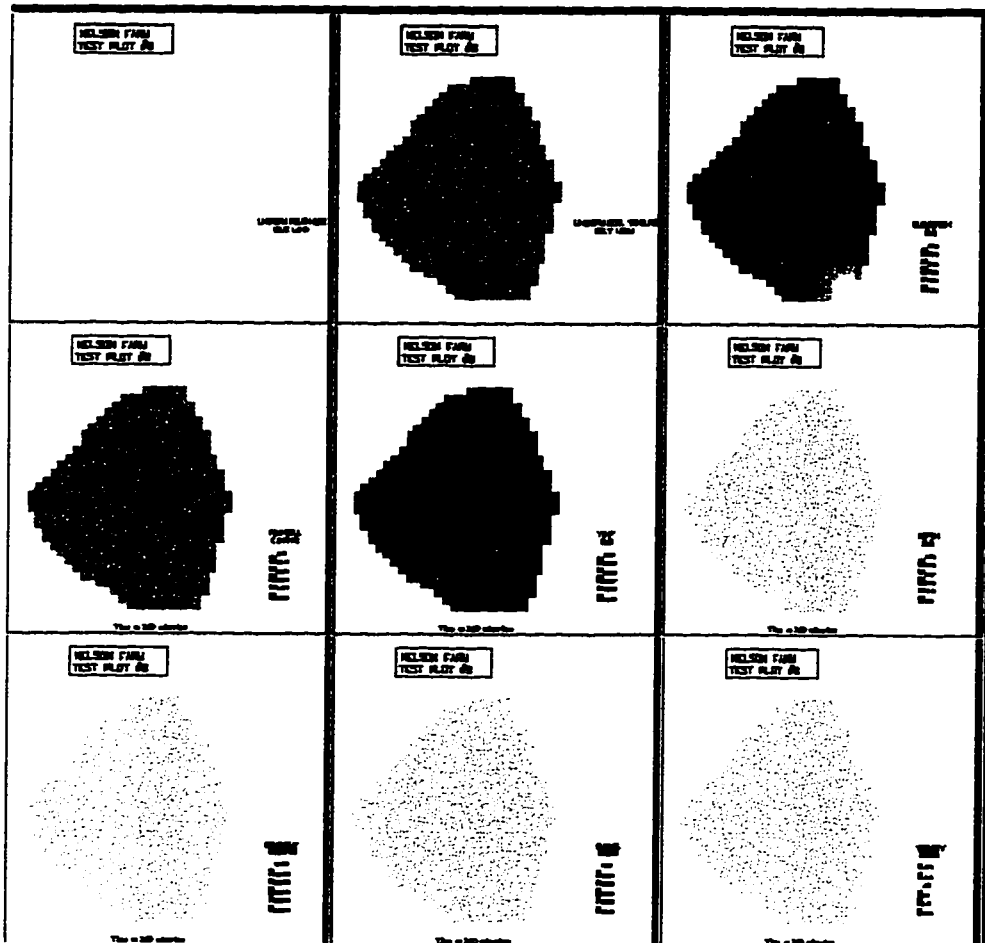


Figure B-3 - February 17-19, 1991 at Time = 240.0 minutes.

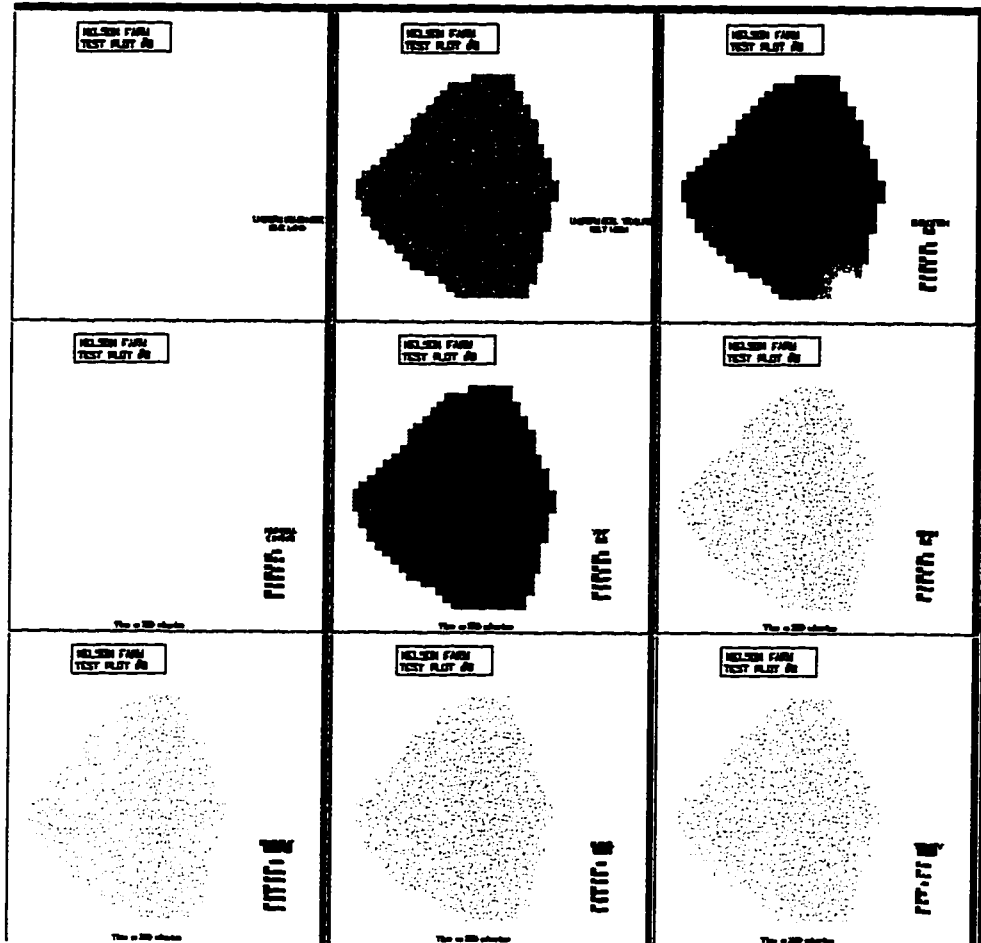


Figure B-4 - February 17-19, 1991 at Time = 360.0 minutes.

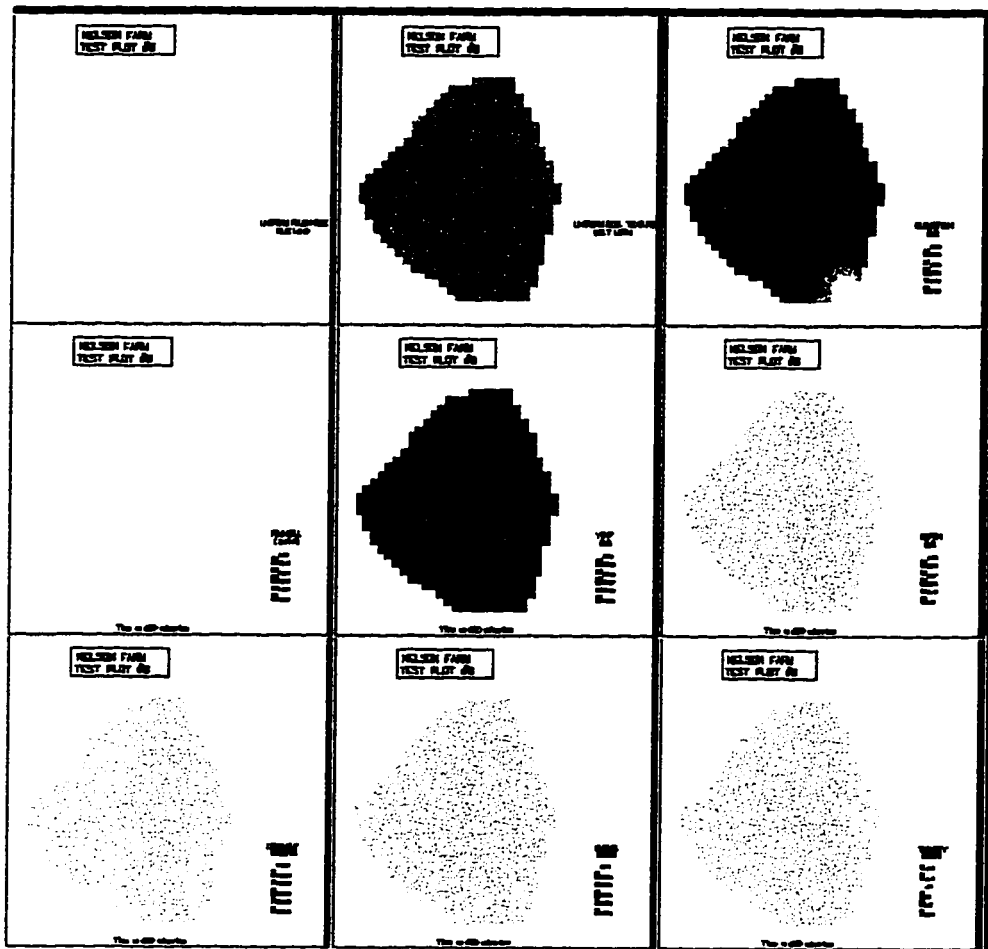


Figure B-5 - February 17-19, 1991 at Time = 480.0 minutes.

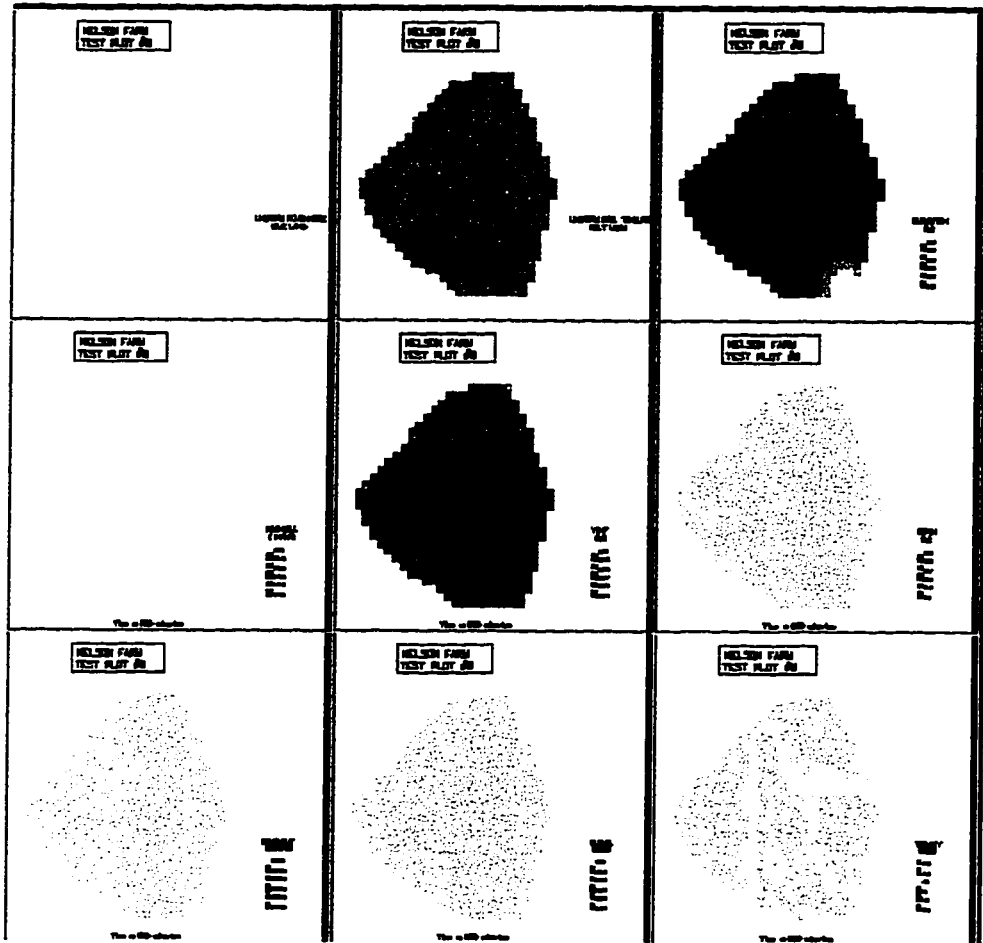


Figure B-6 - February 17-19, 1991 at Time = 600.0 minutes.

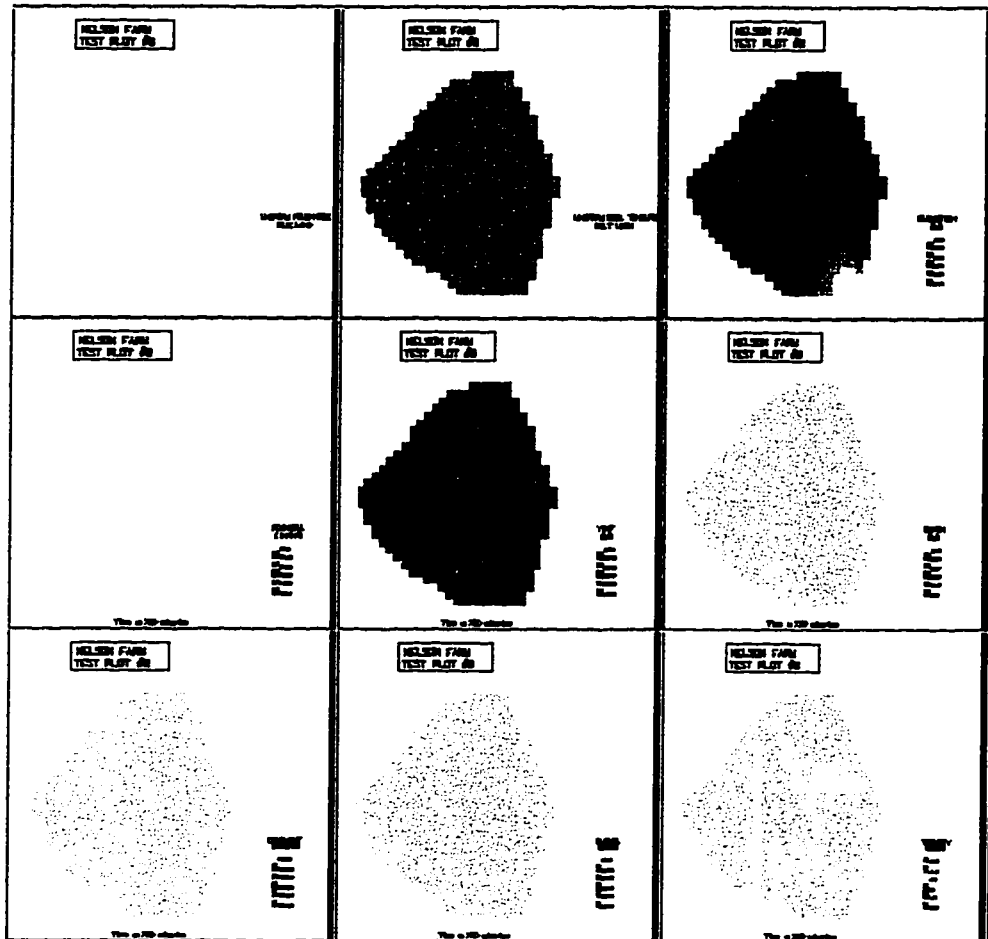


Figure B-7 - February 17-19, 1991 at Time = 720.0 minutes.



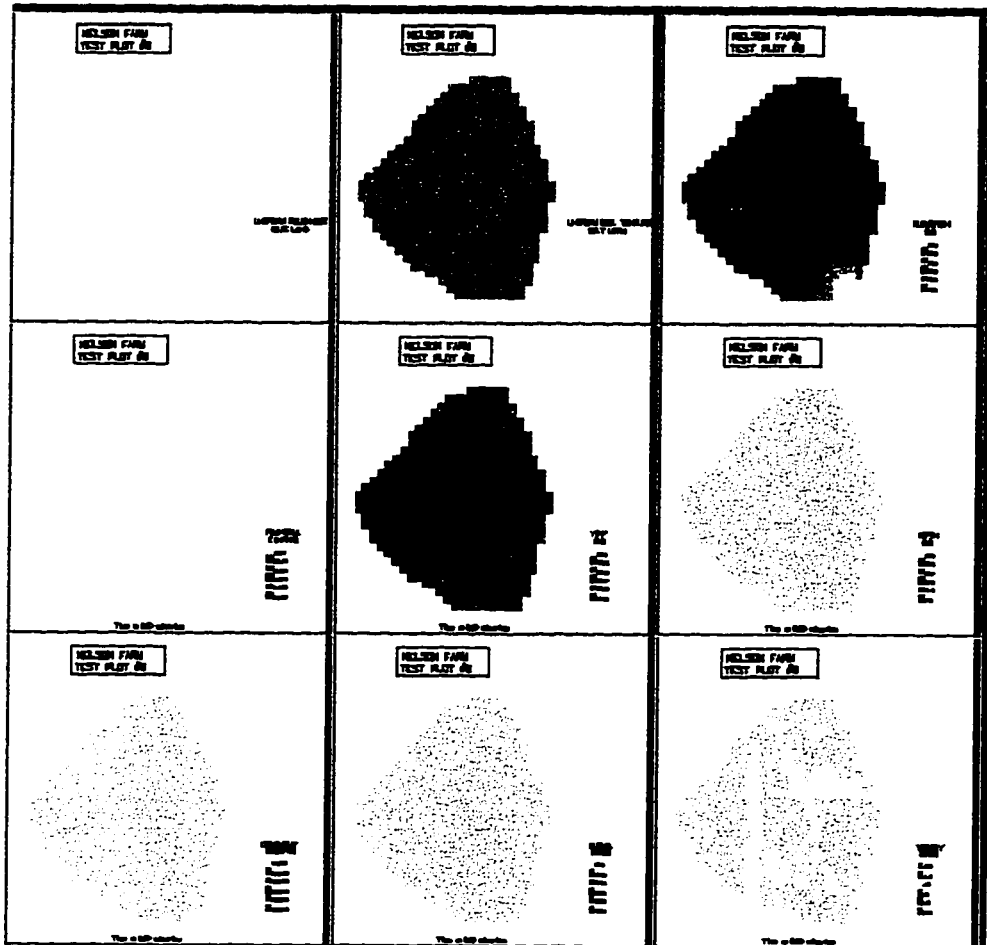


Figure B-8 - February 17-19, 1991 at Time = 840.0 minutes.

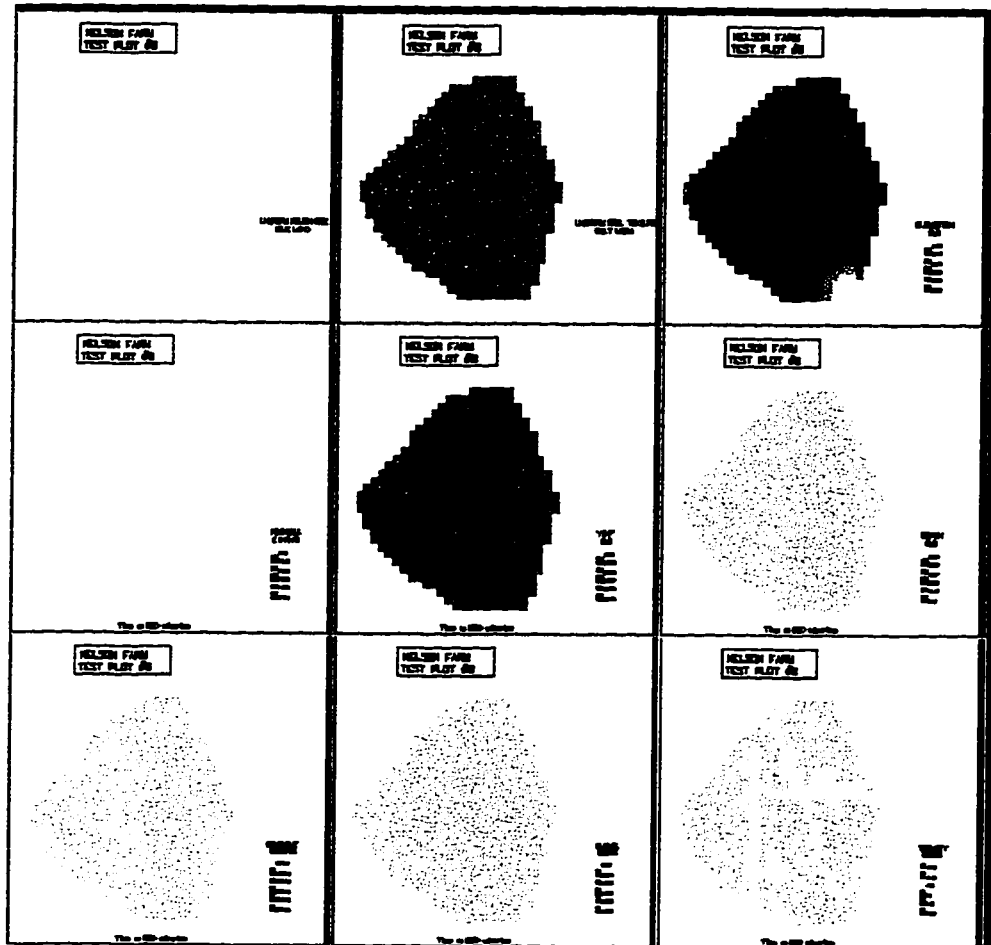


Figure B-9 - February 17-19, 1991 at Time = 960.0 minutes.

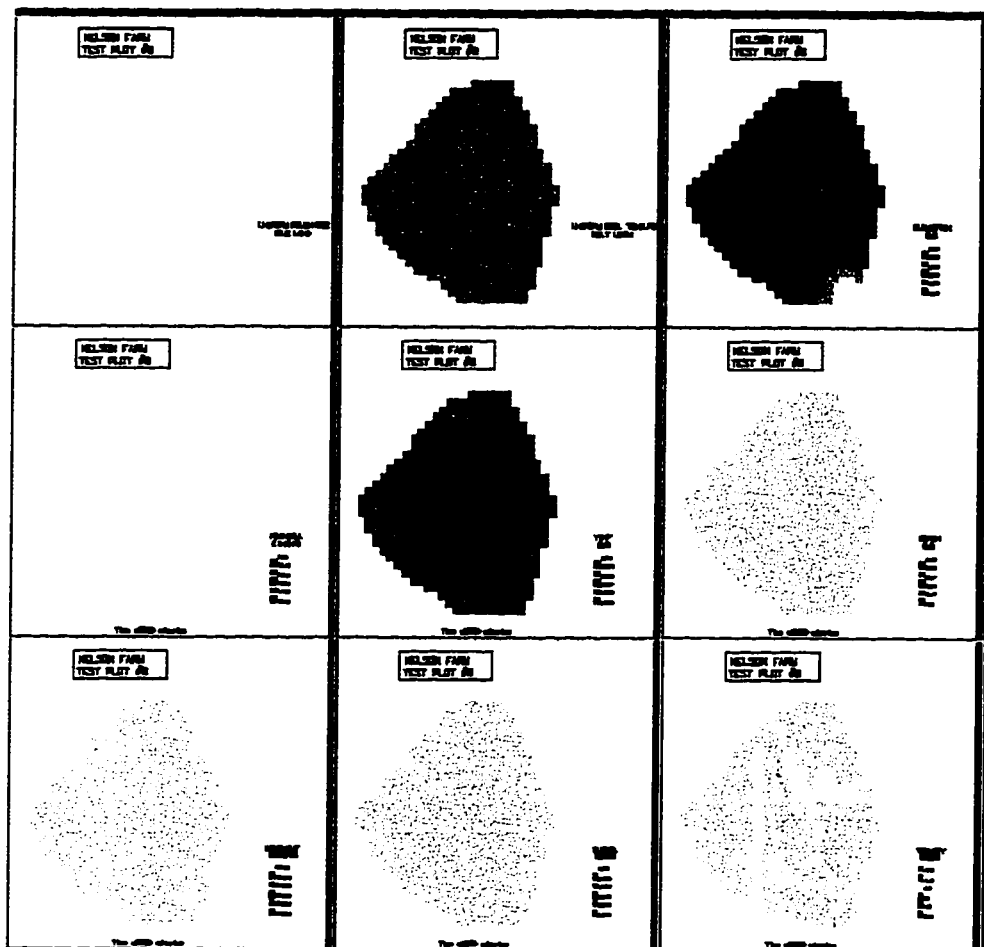


Figure B-10 - February 17-19, 1991 at Time = 1080.0 minutes.

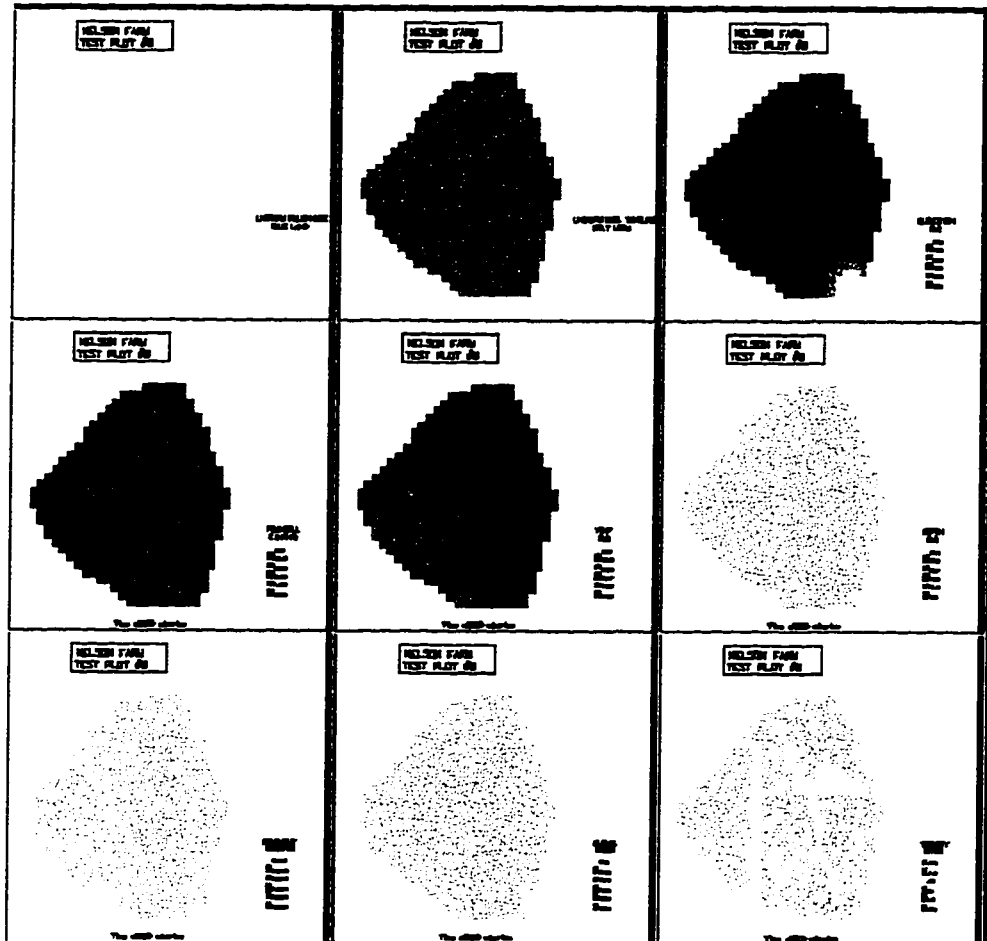


Figure B-11 - February 17-19, 1991 at Time = 1200.0 minutes.

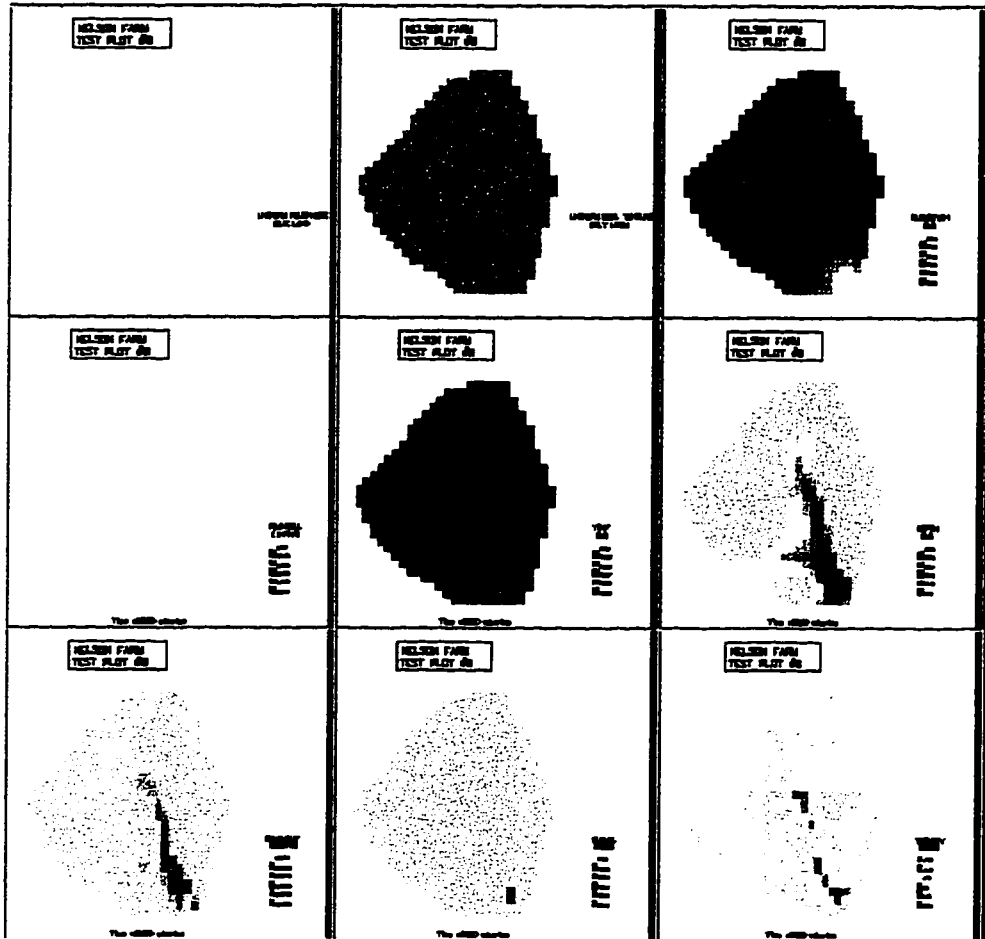


Figure B-12 - February 17-19, 1991 at Time = 1320.0 minutes.

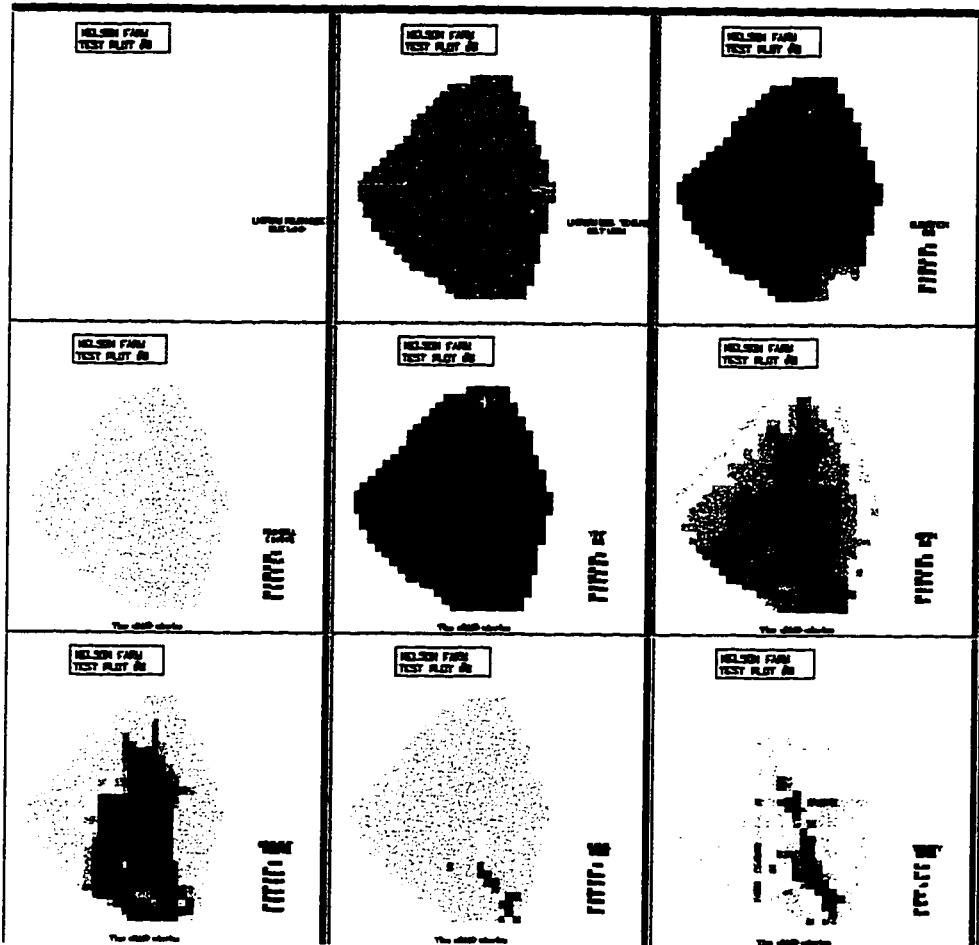


Figure B-13 - February 17-19, 1991 at Time = 1440.0 minutes.

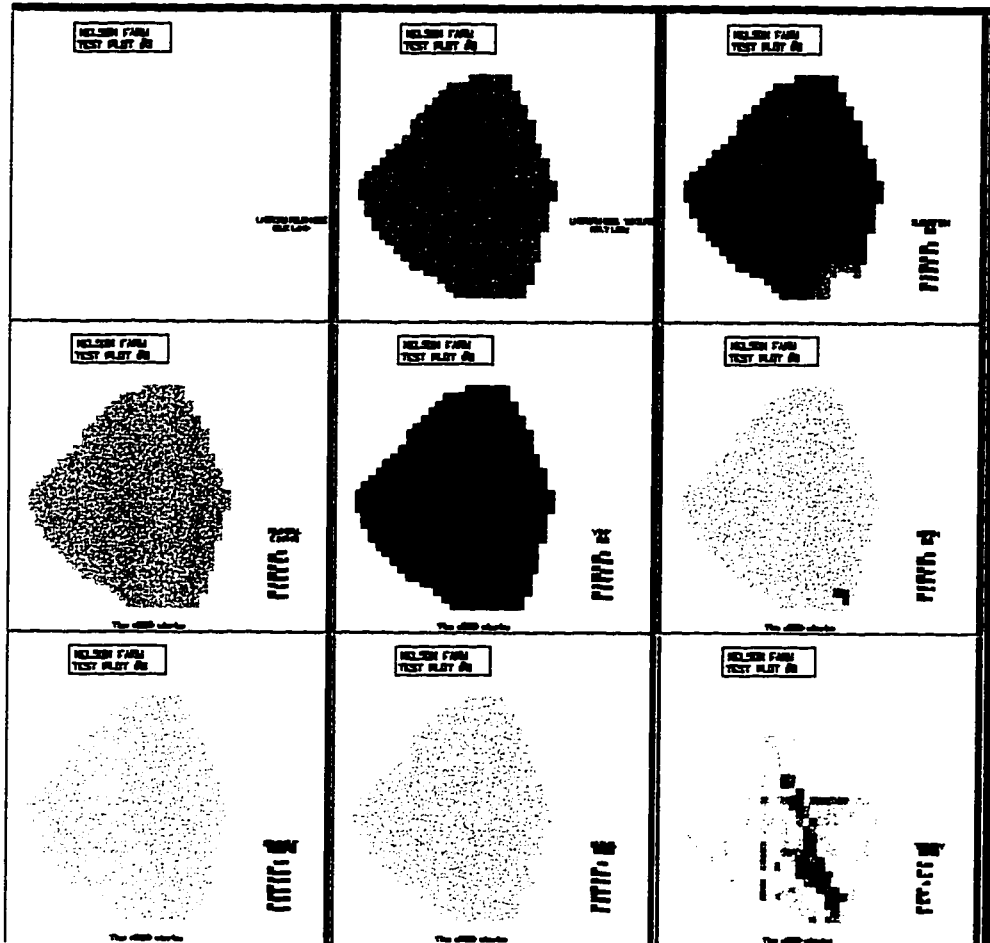


Figure B-14 - February 17-19, 1991 at Time = 1560.0 minutes.

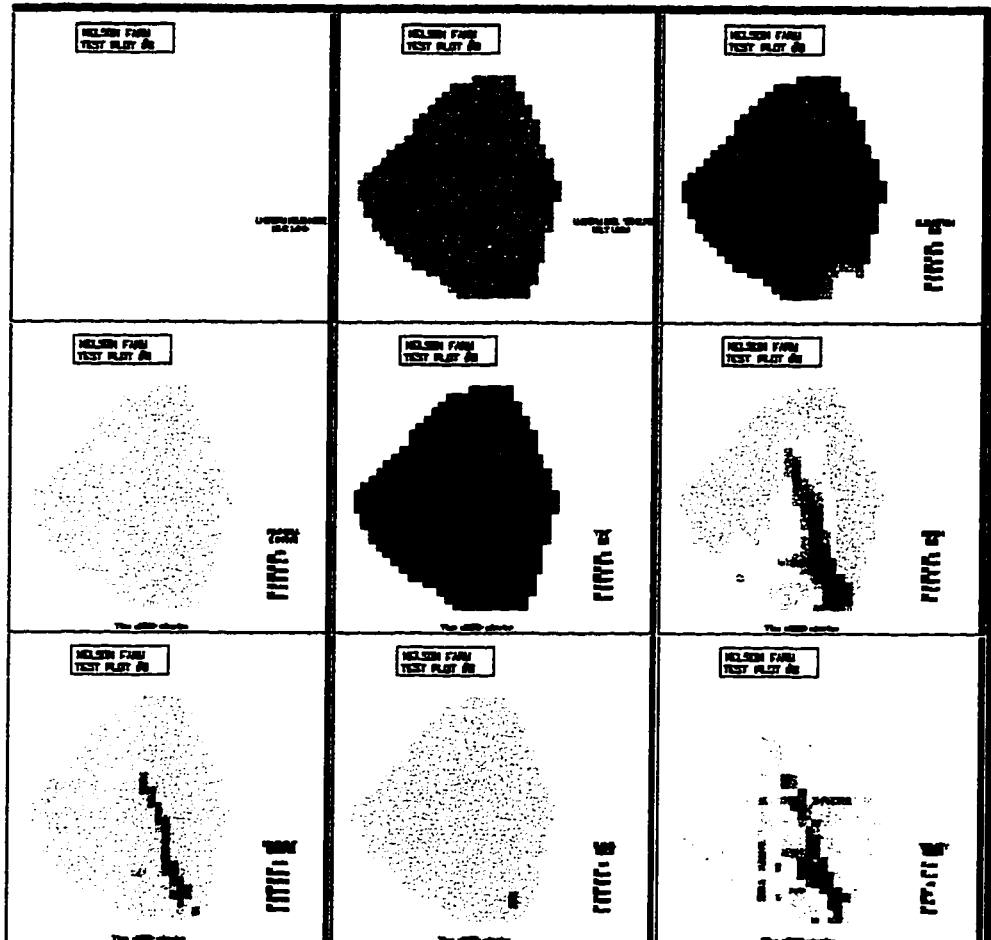


Figure B-15 - February 17-19, 1991 at Time = 1680.0 minutes.



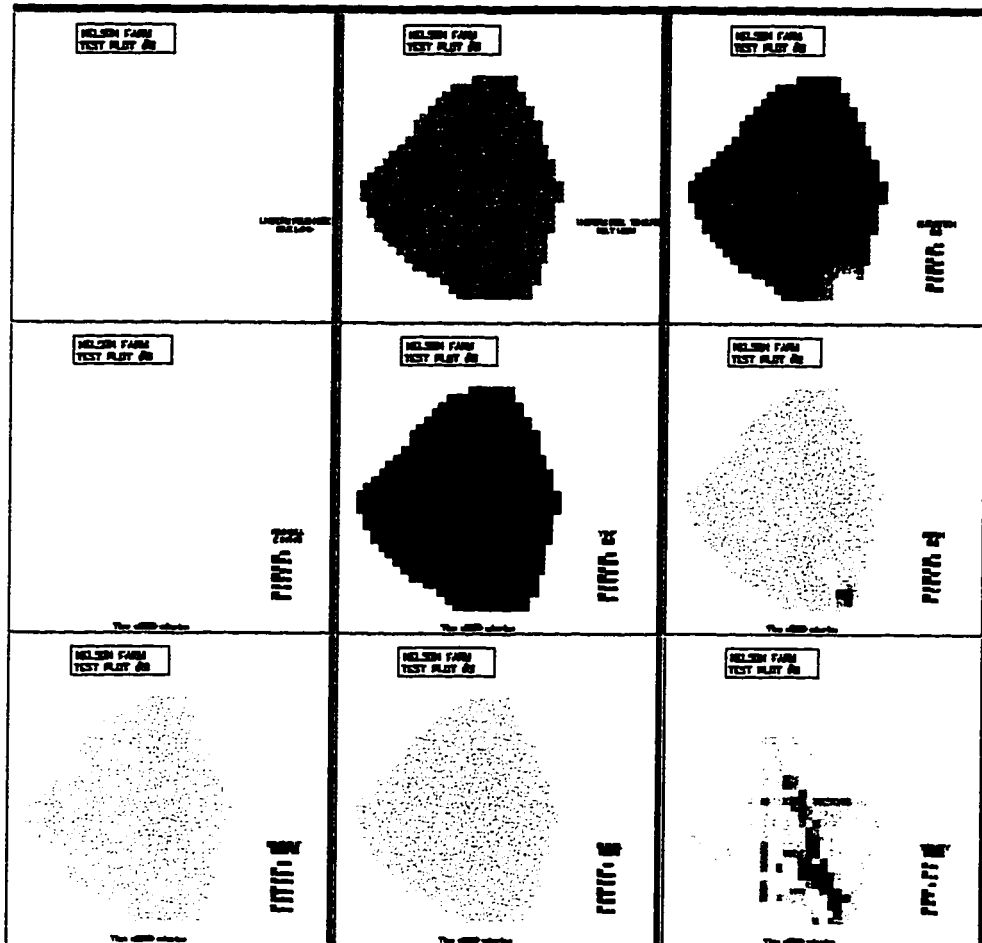


Figure B-16 - February 17-19, 1991 at Time = 1800.0 minutes.

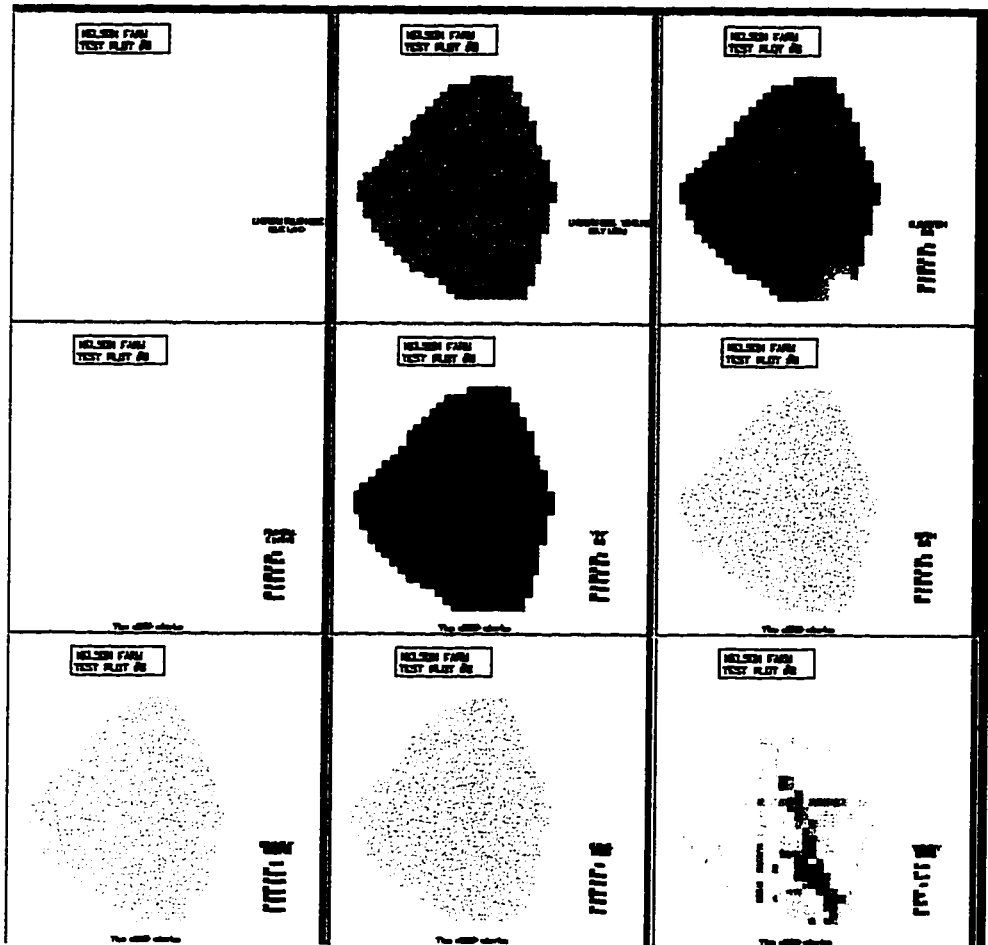


Figure B-17 - February 17-19, 1991 at Time = 1920.0 minutes.

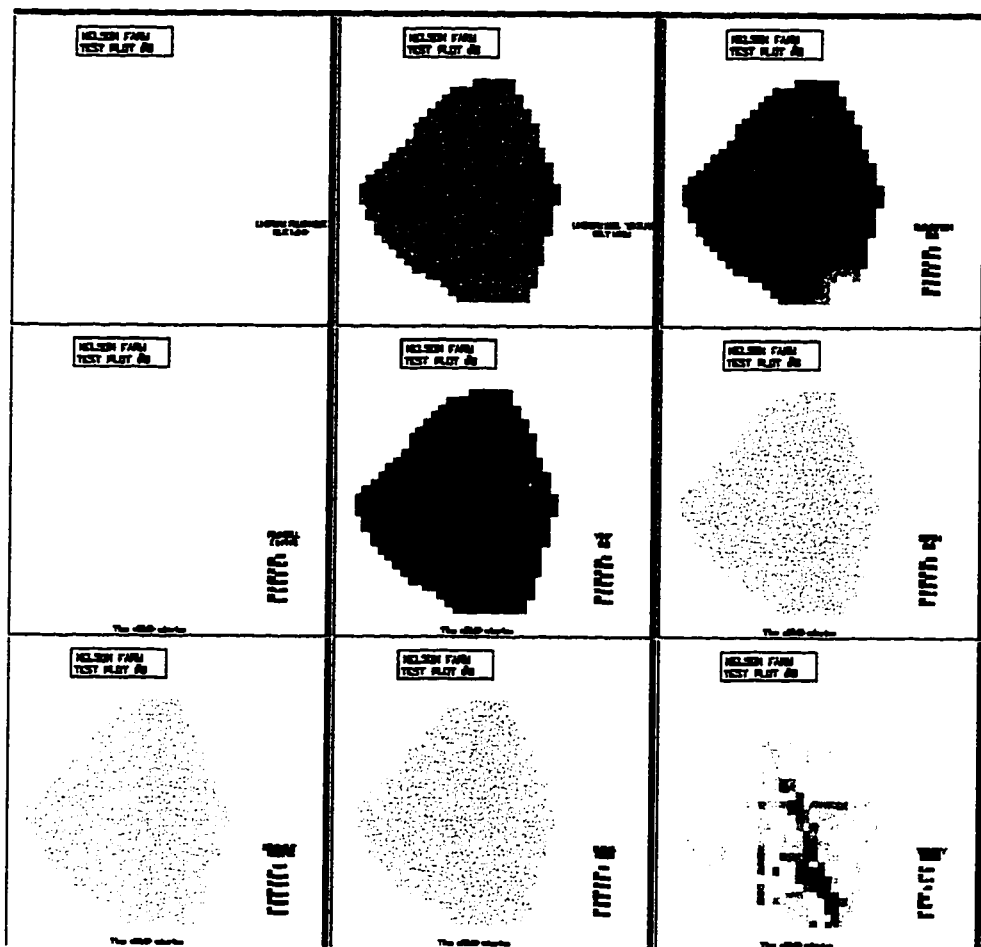


Figure B-18 - February 17-19, 1991 at Time = 2040.0 minutes.

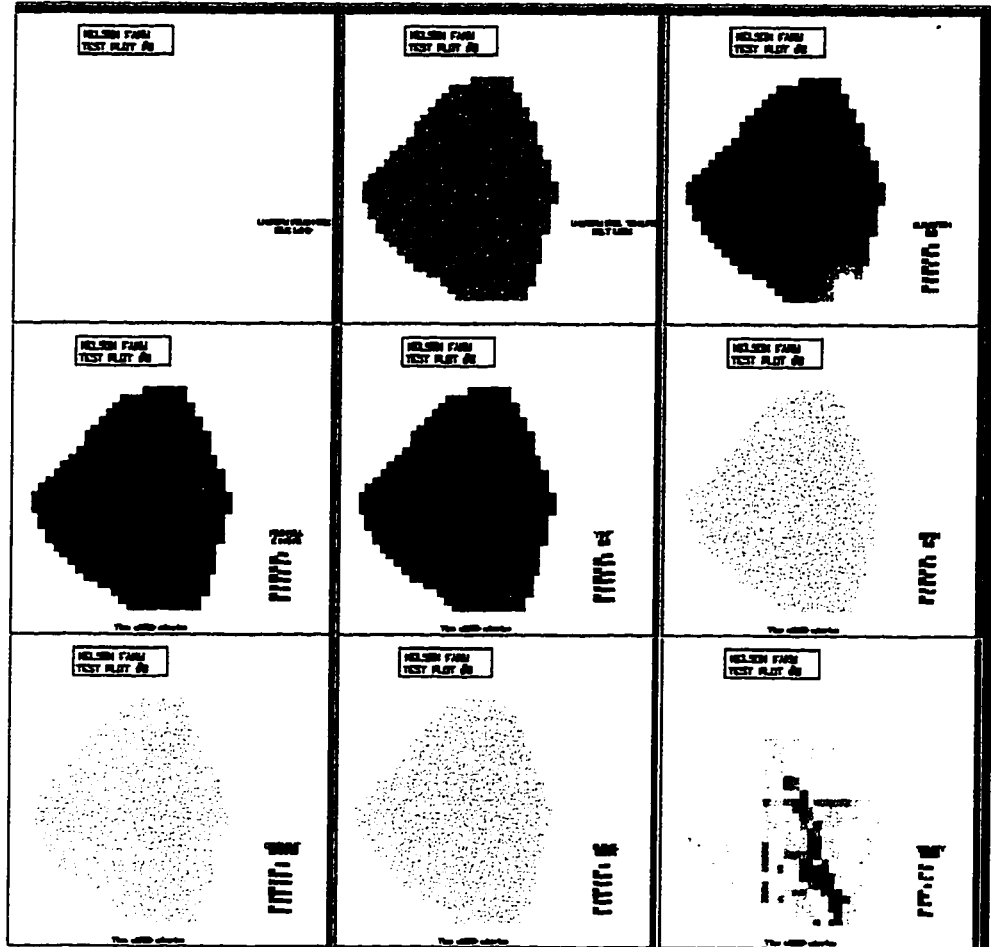


Figure B-19 - February 17-19, 1991 at Time = 2160.0 minutes.

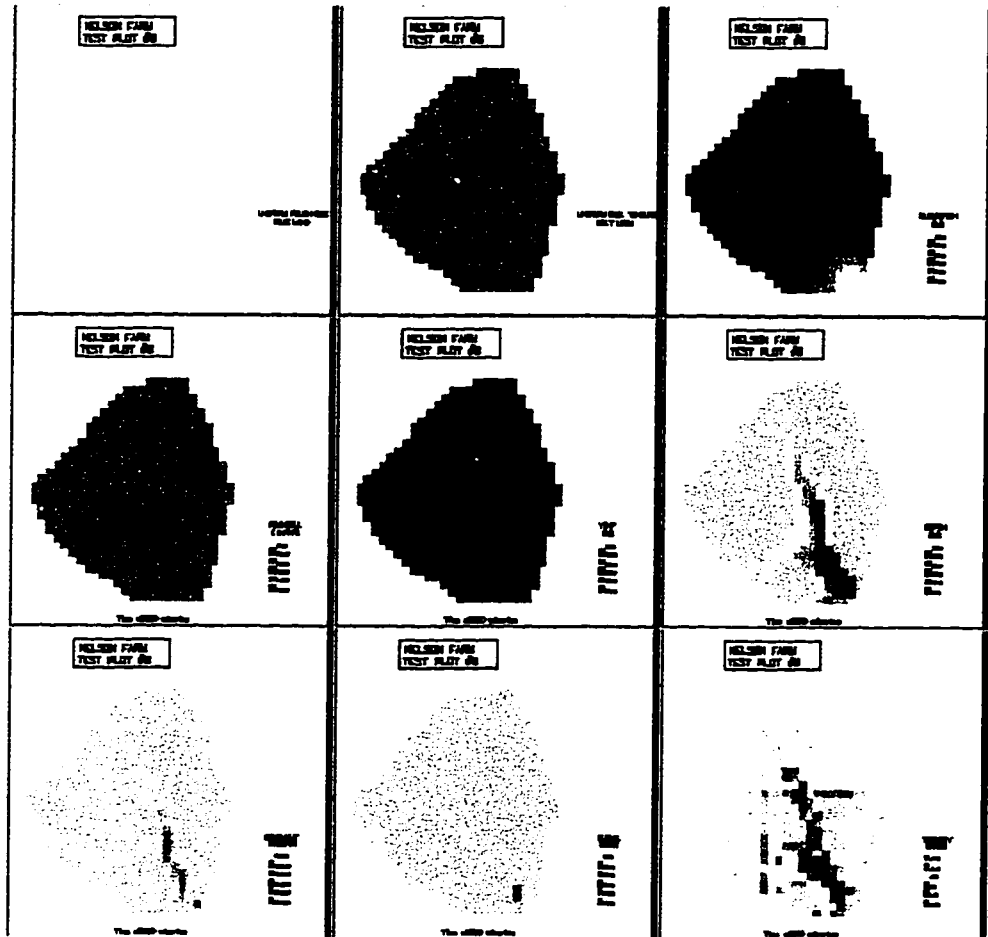


Figure B-20 - February 17-19, 1991 at Time = 2280.0 minutes.

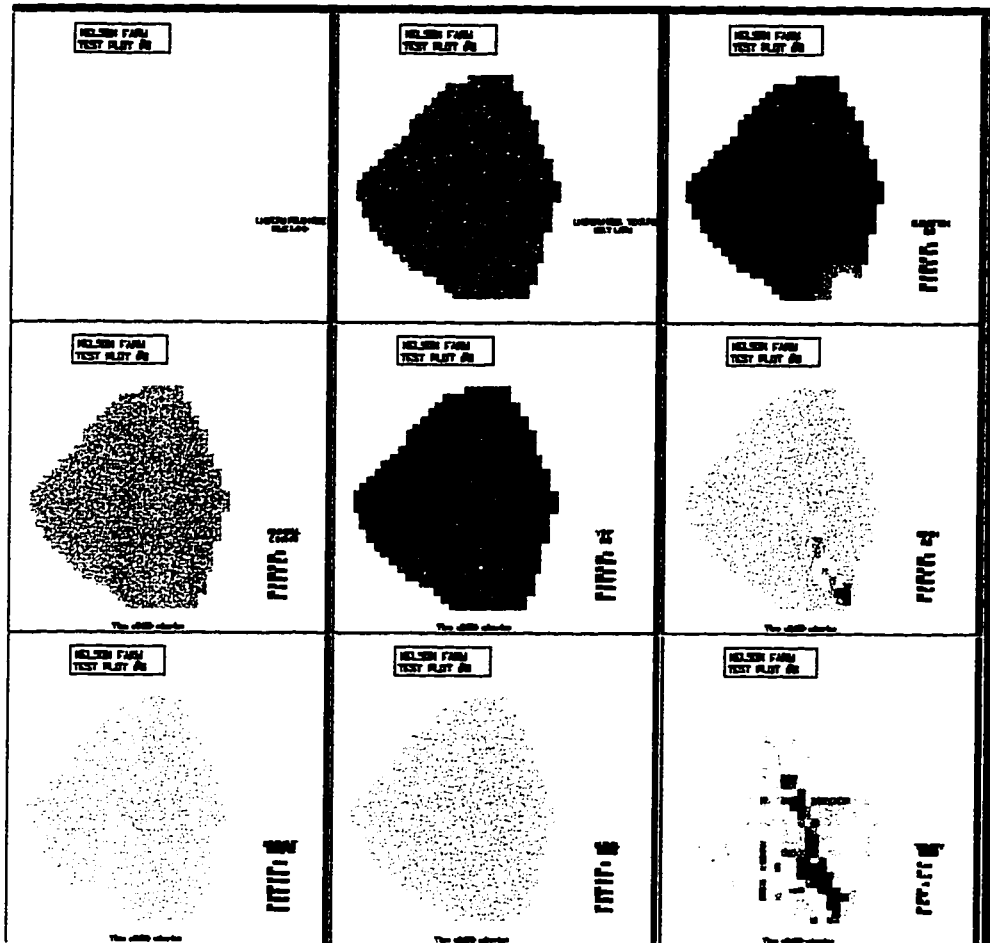


Figure B-21 - February 17-19, 1991 at Time = 2400.0 minutes.

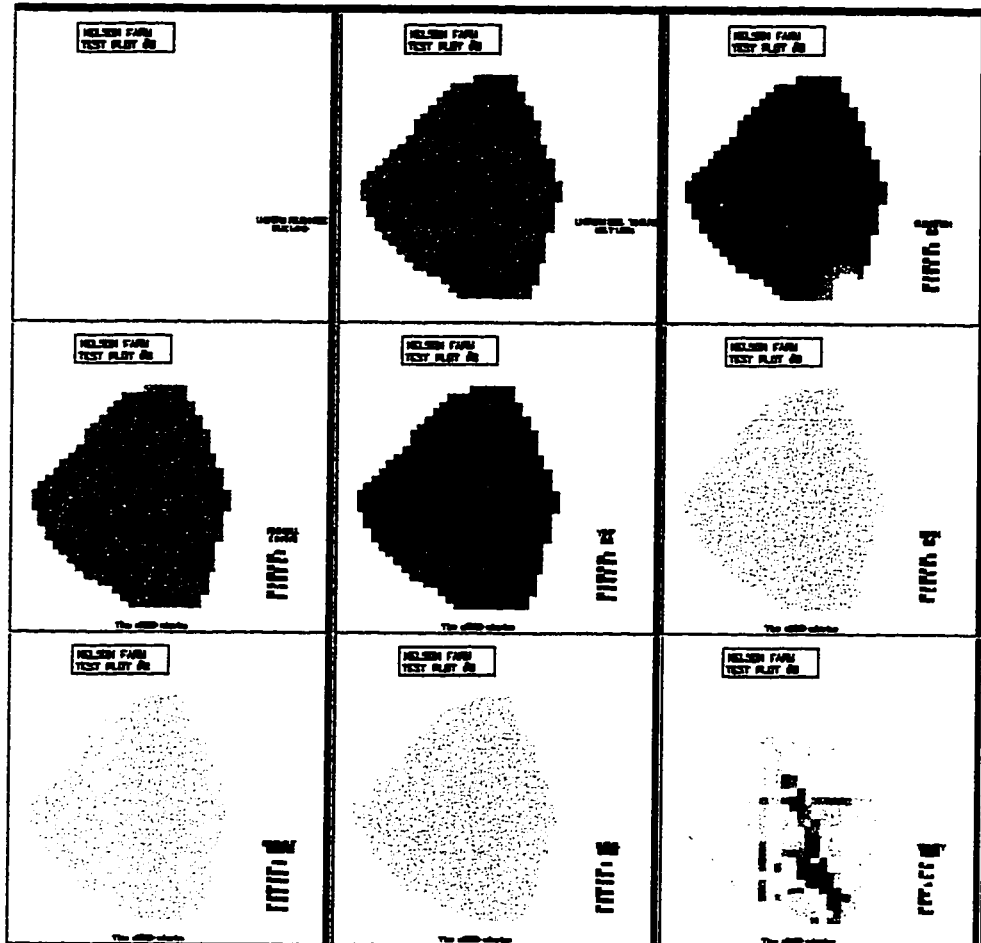


Figure B-22 - February 17-19, 1991 at Time = 2520.0 minutes.

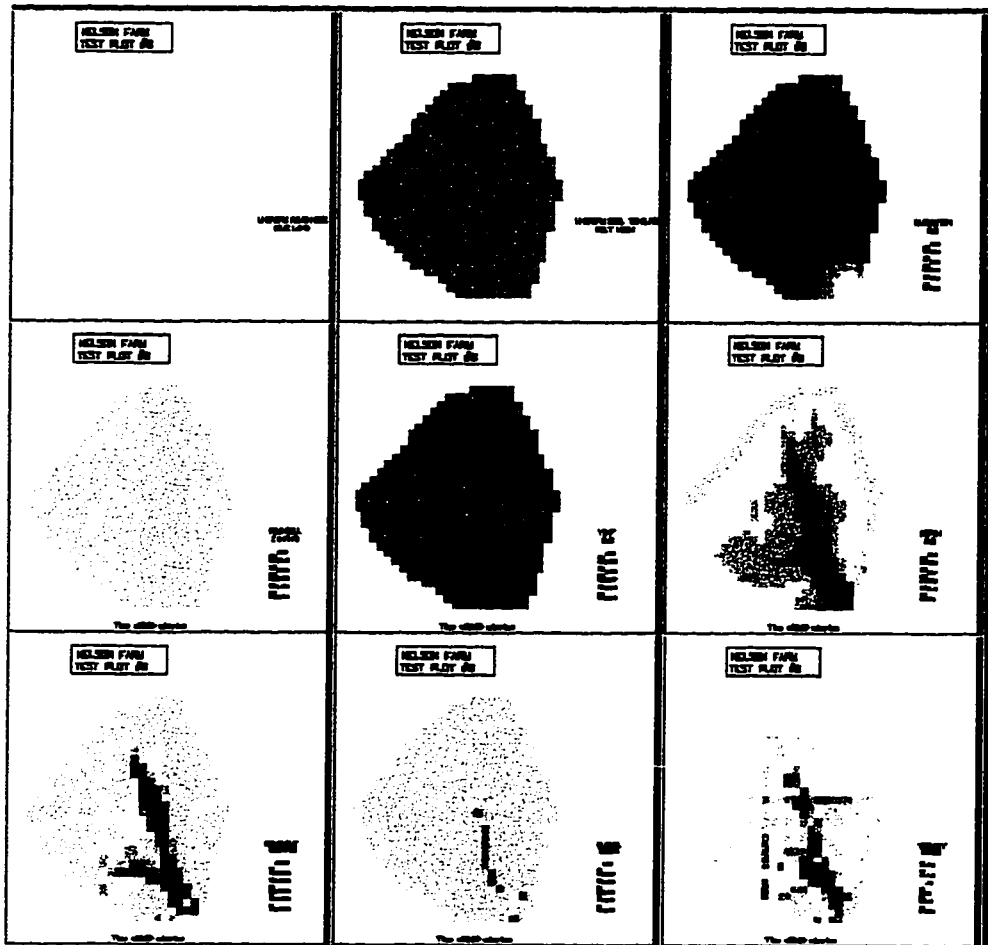


Figure B-23 - February 17-19, 1991 at Time = 2640.0 minutes.



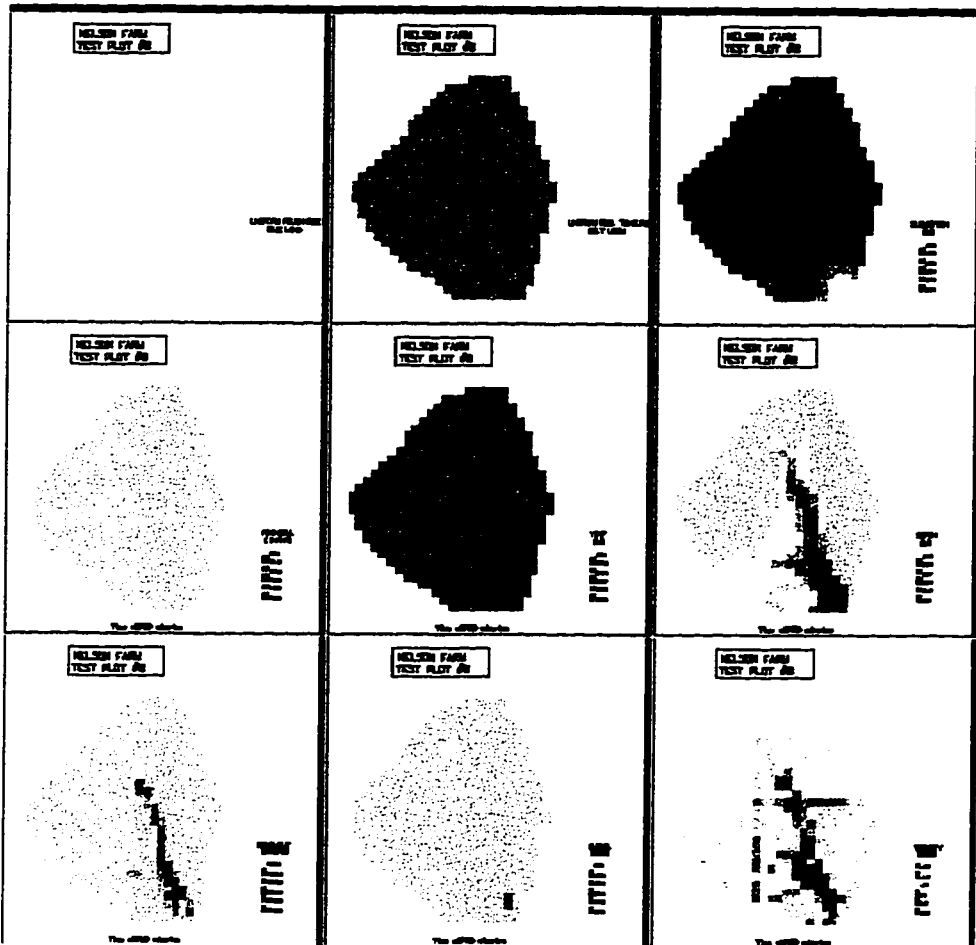


Figure B-24 - February 17-19, 1991 at Time = 2760.0 minutes.

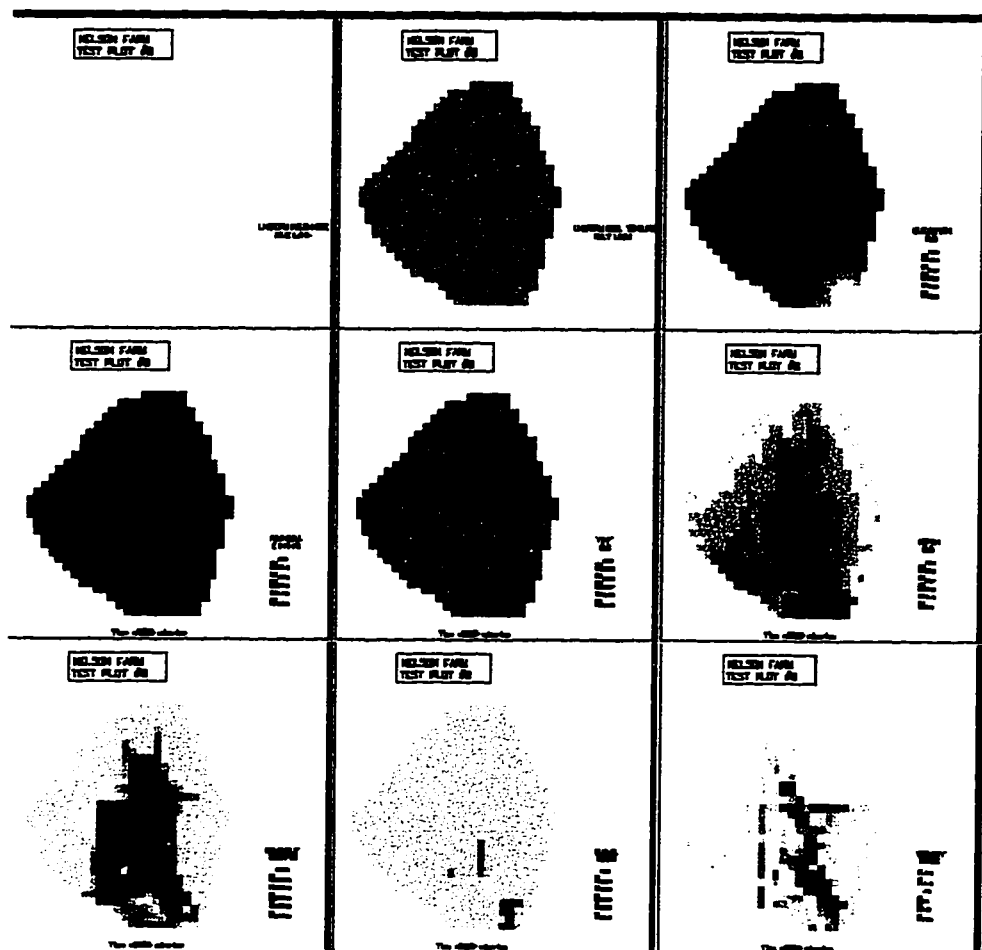


Figure B-25 - February 17-19, 1991 at Time = 2880.0 minutes.

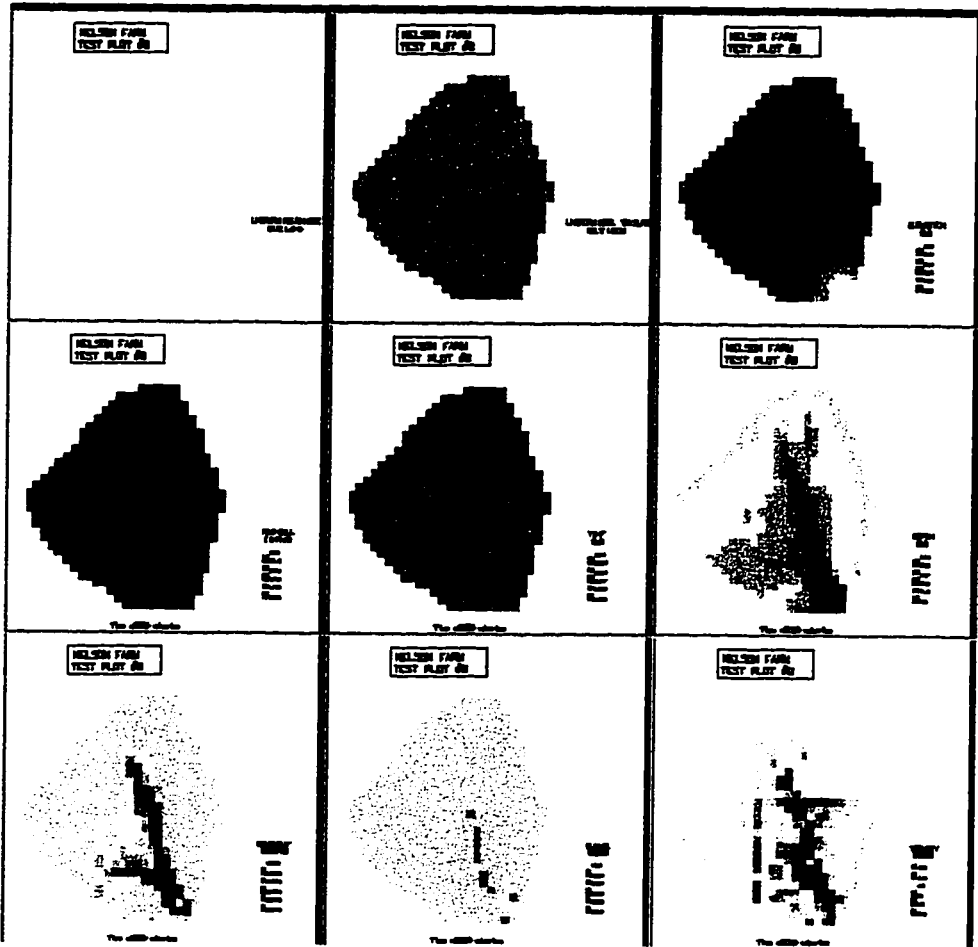


Figure B-26 - February 17-19, 1991 at Time = 3000.0 minutes.

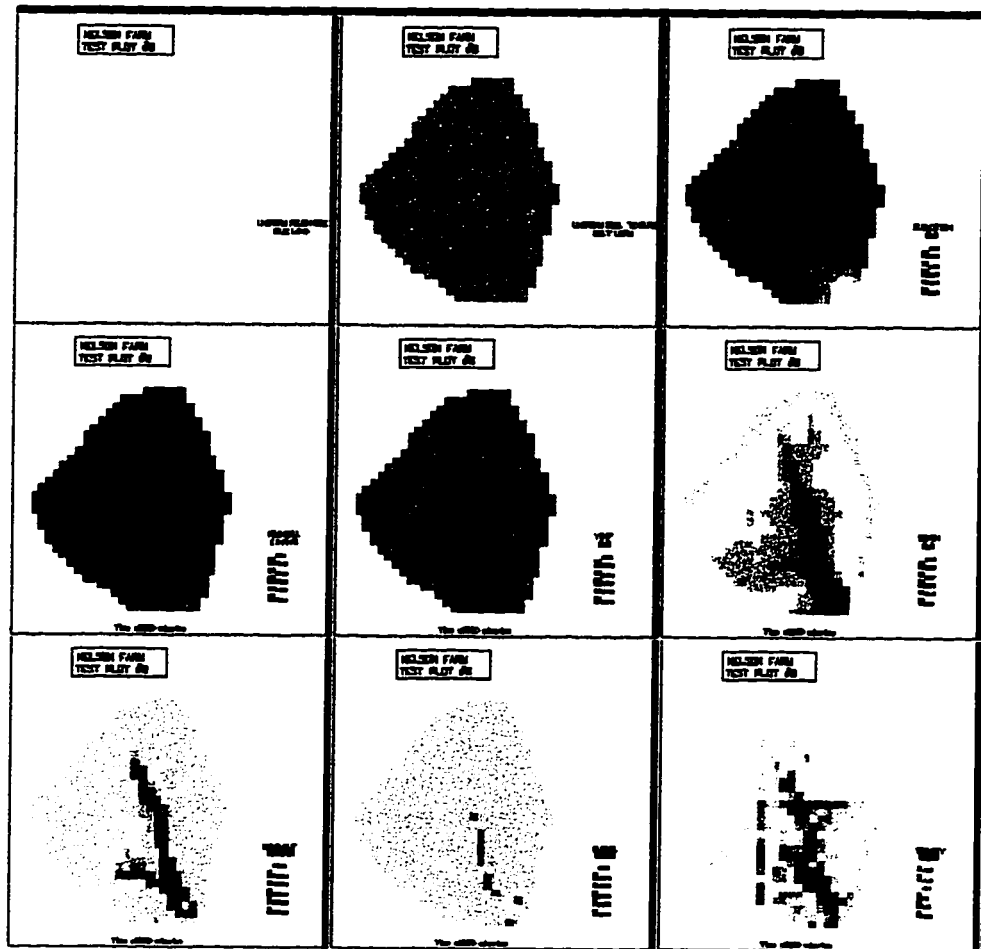


Figure B-27 - February 17-19, 1991 at Time = 3120.0 minutes.

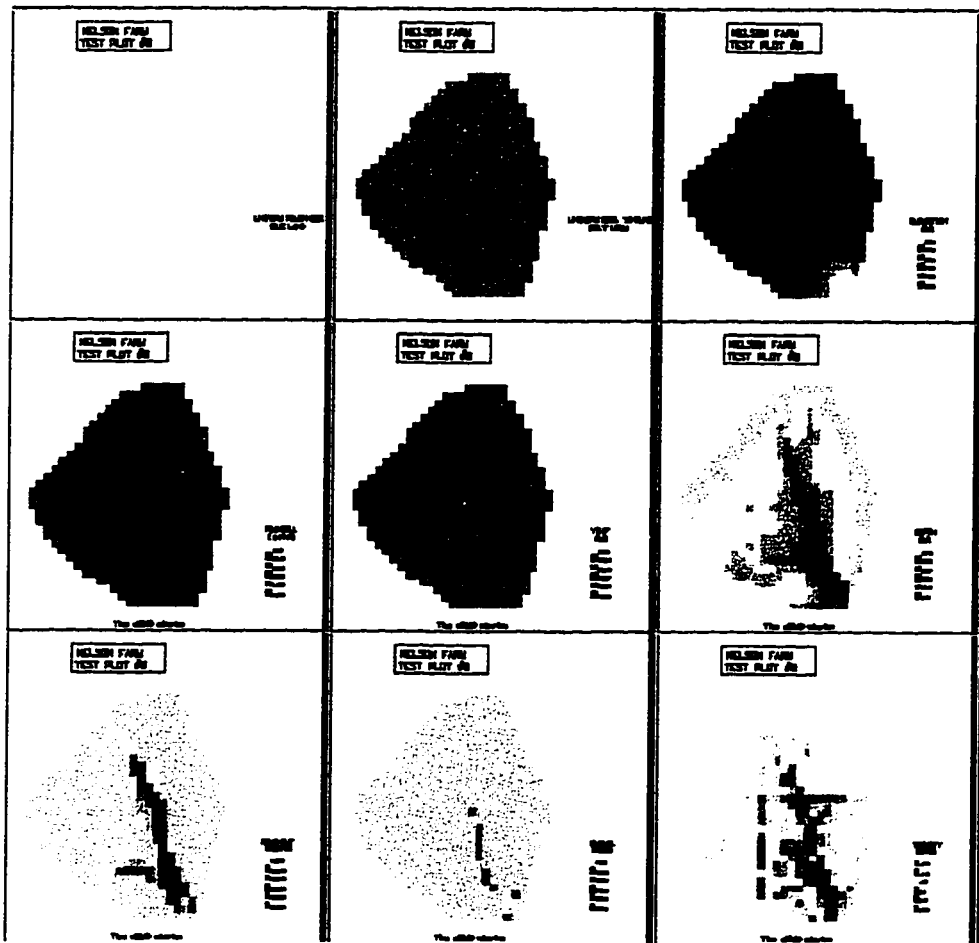


Figure B-28 - February 17-19, 1991 at Time = 3240.0 minutes.

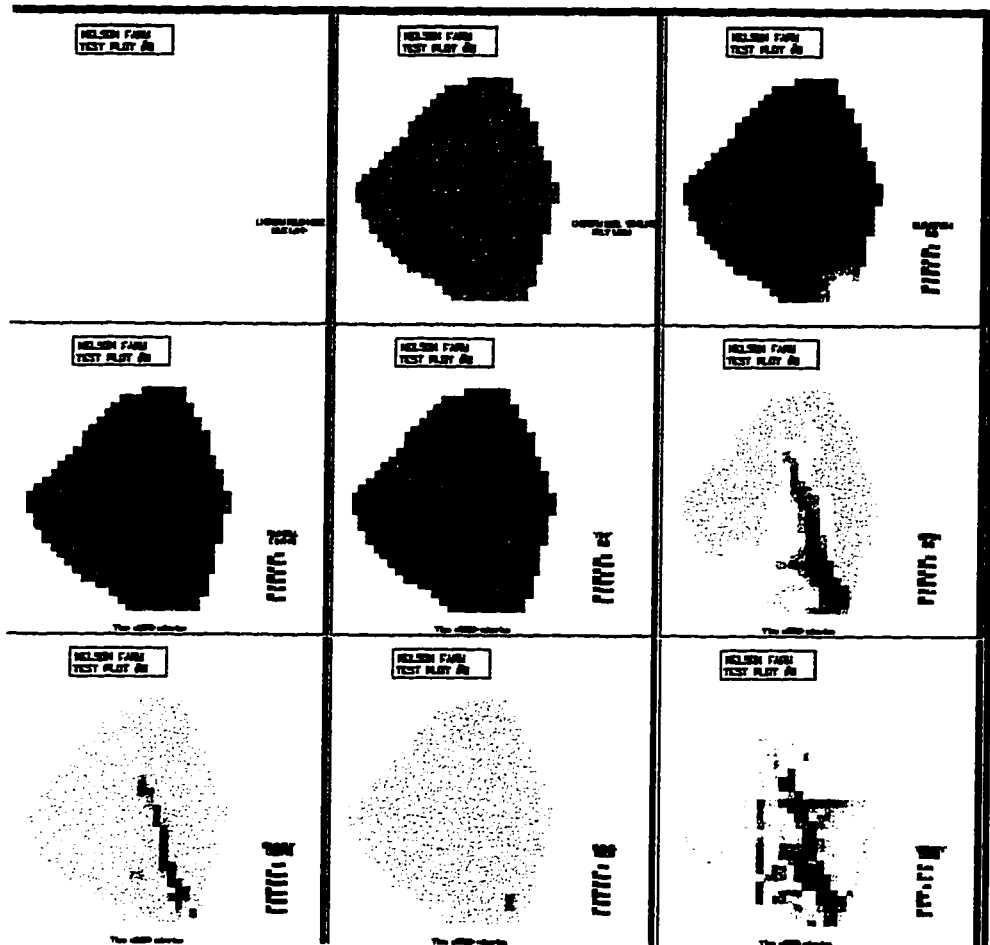


Figure B-29 - February 17-19, 1991 at Time = 3360.0 minutes.

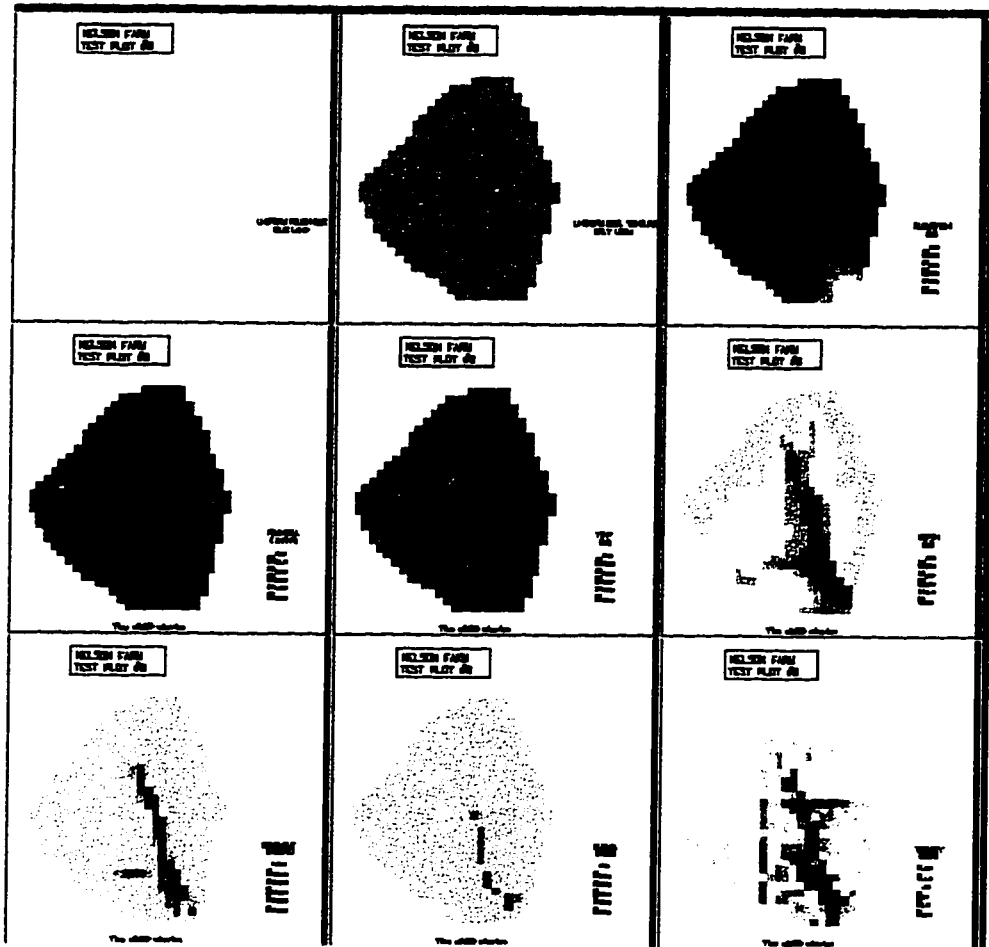


Figure B-30 - February 17-19, 1991 at Time = 3420.0 minutes.

**Appendix C**

**CASC2D Output Grids**

**Goodwin Creek Watershed**

**October 17-18, 1981**



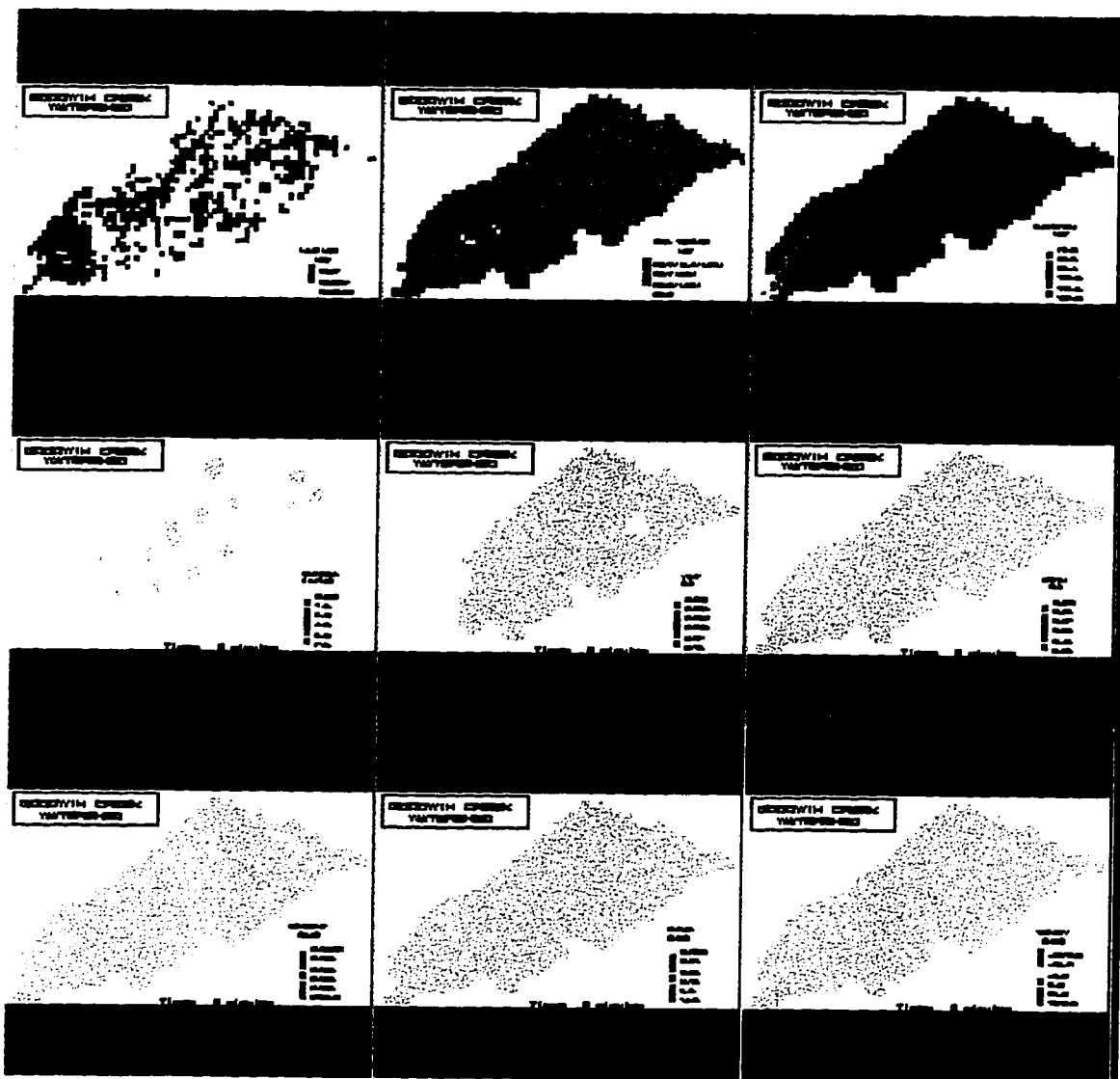


Figure C-1 - October 17-18, 1981 at Time = 0.0 minutes.

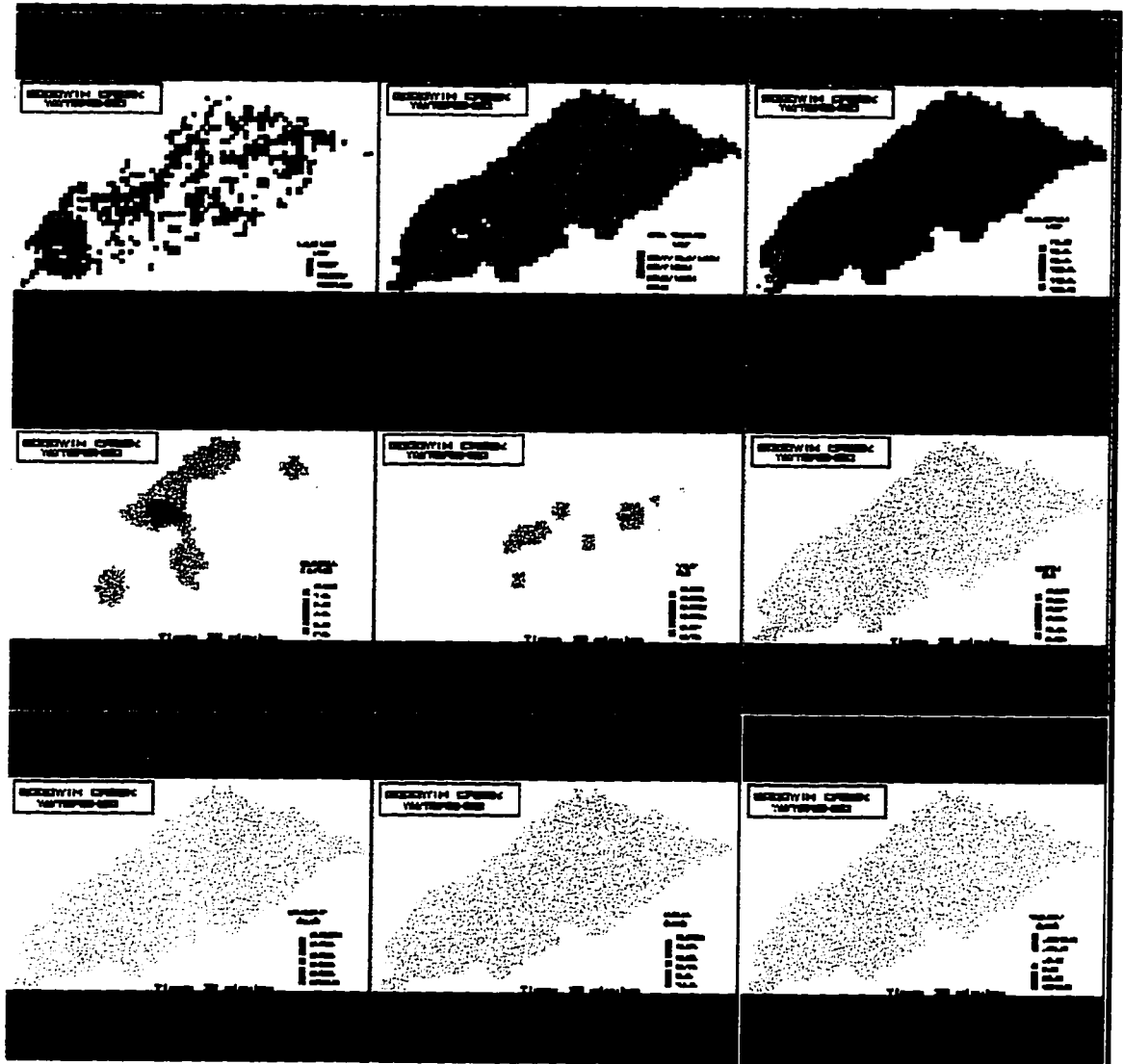


Figure C-2 - October 17-18, 1981 at Time = 20.0 minutes.

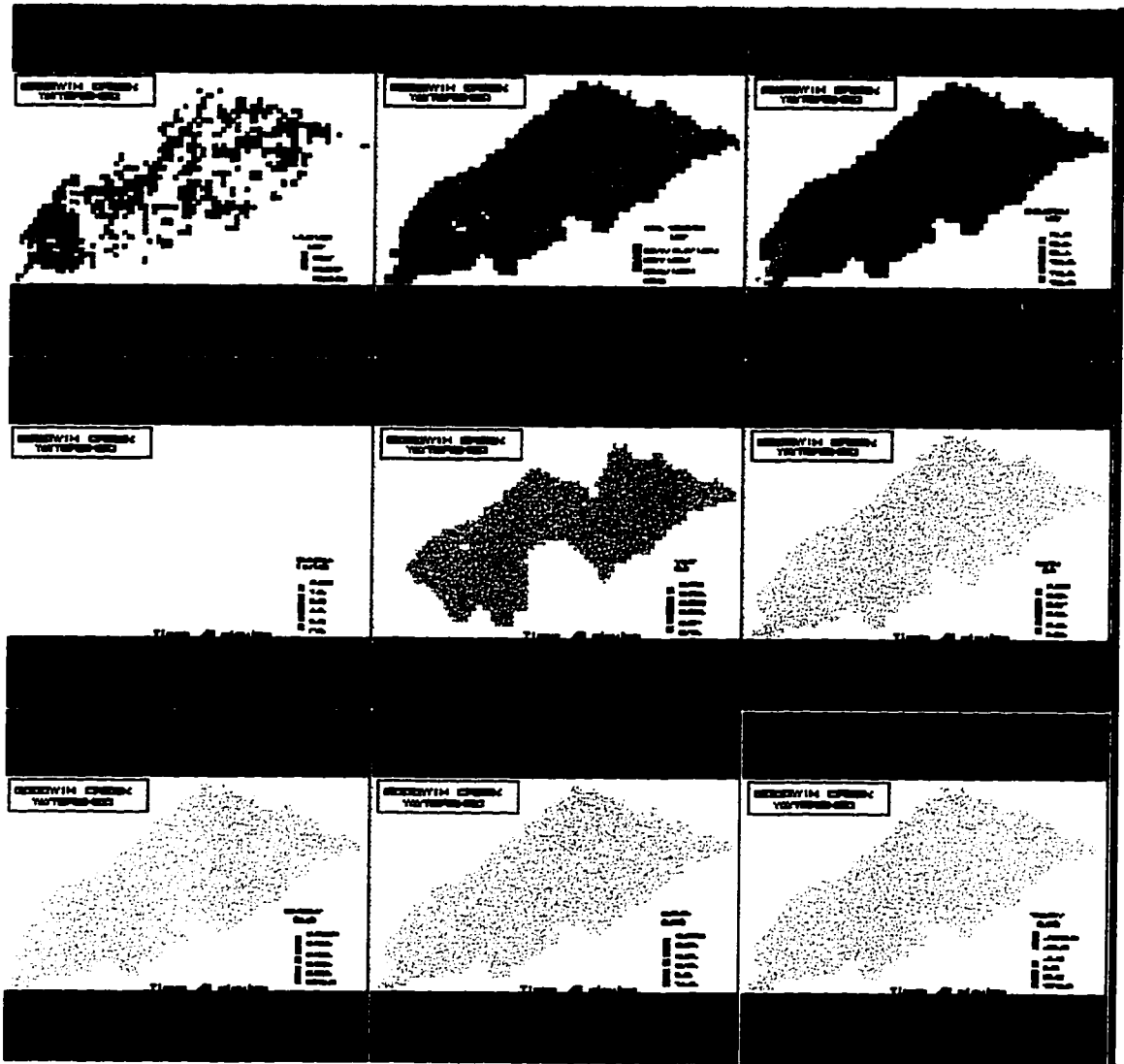


Figure C-3 - October 17-18, 1981 at Time = 40.0 minutes.

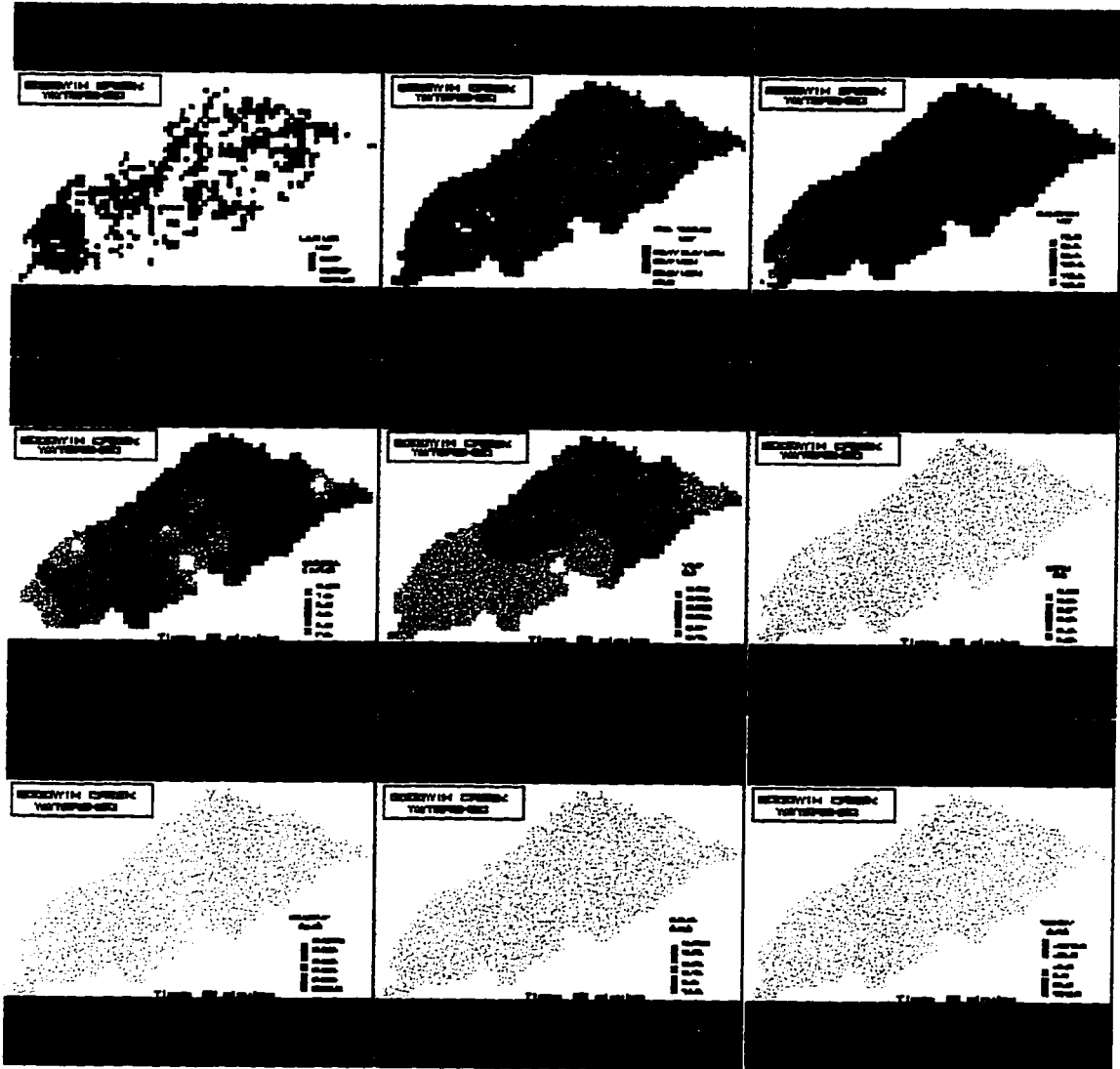


Figure C-4 - October 17-18, 1981 at Time = 60.0 minutes.

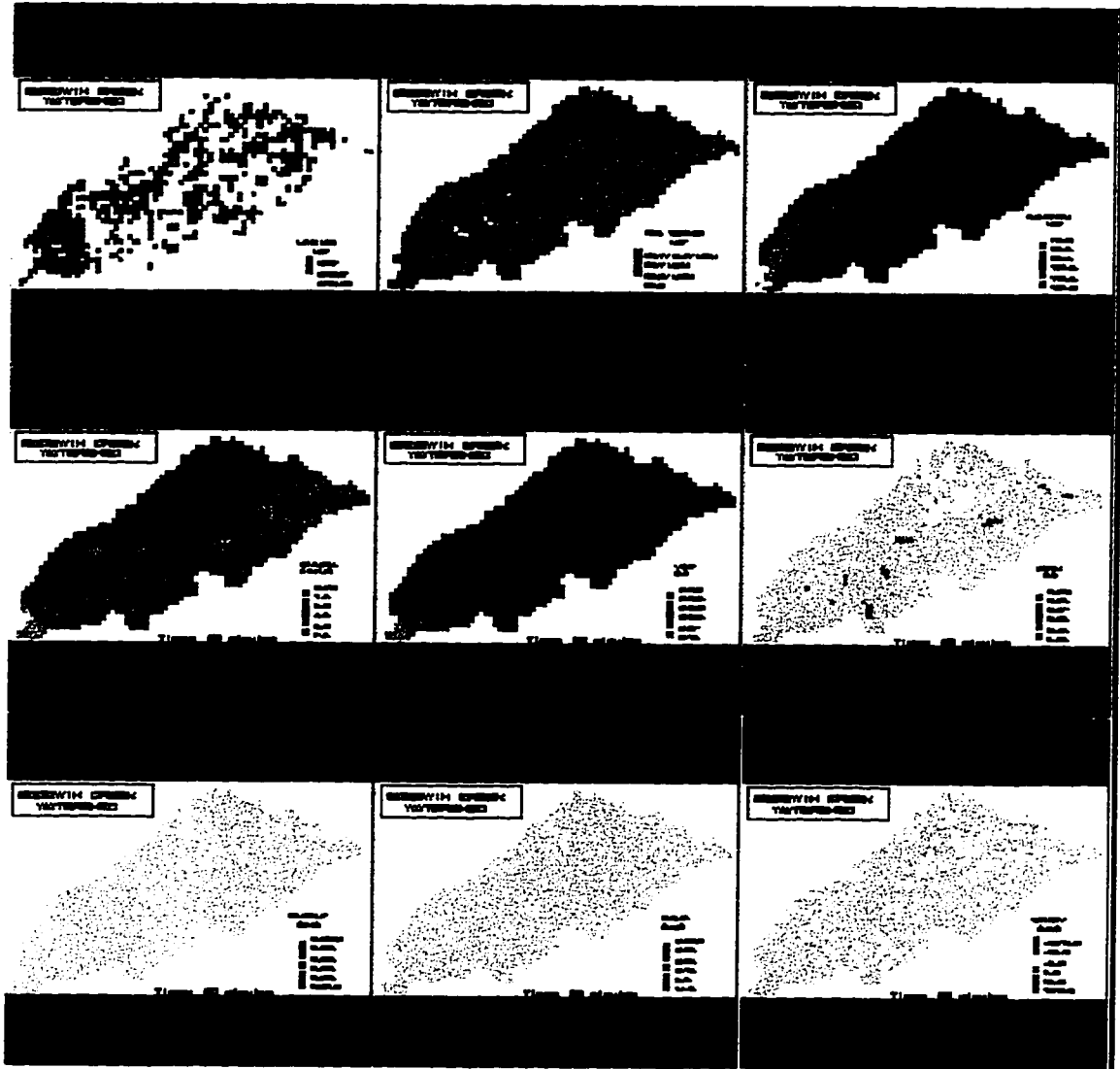


Figure C-5 - October 17-18, 1981 at Time = 80.0 minutes.

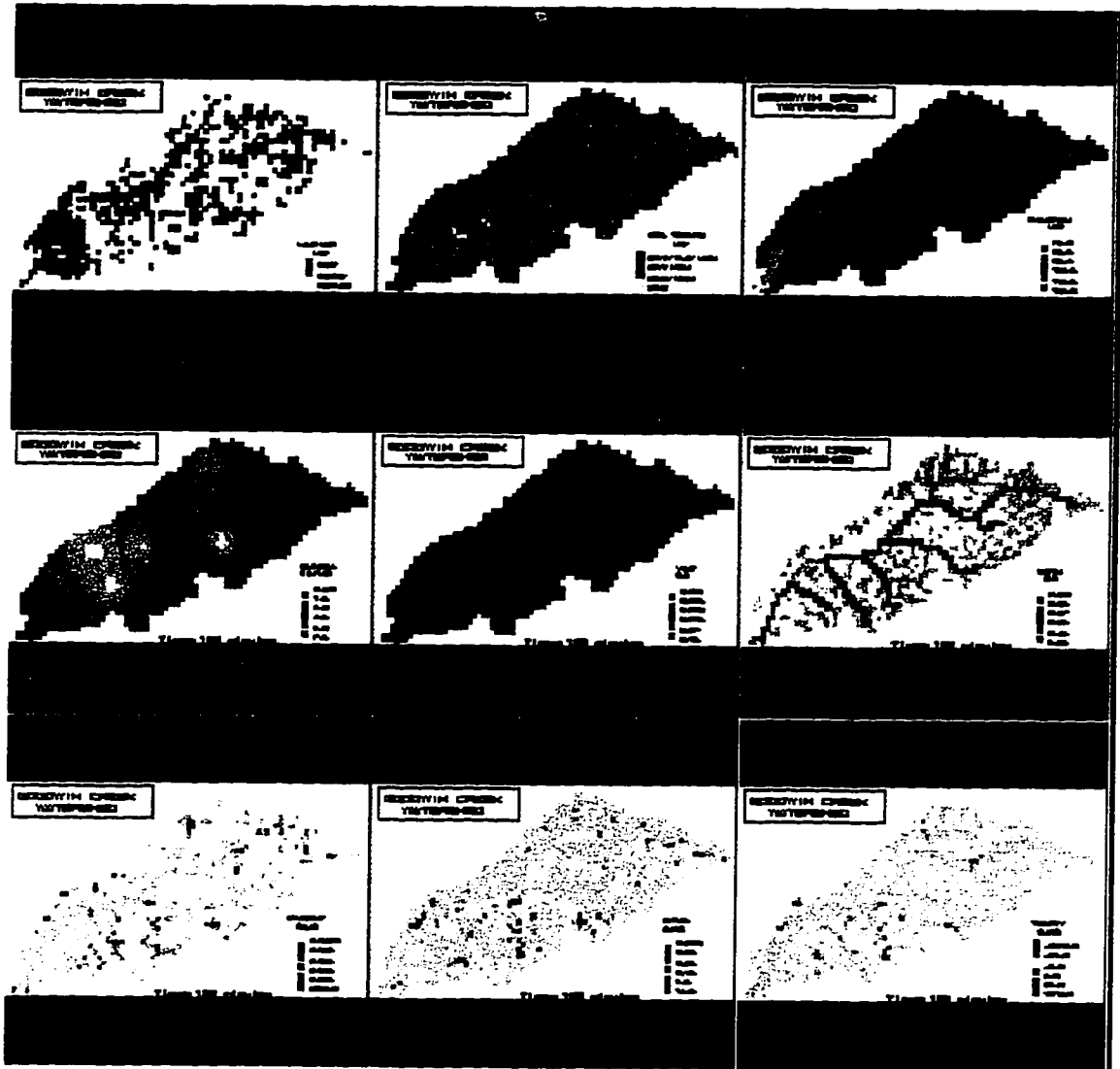


Figure C-6 - October 17-18, 1981 at Time = 100.0 minutes.

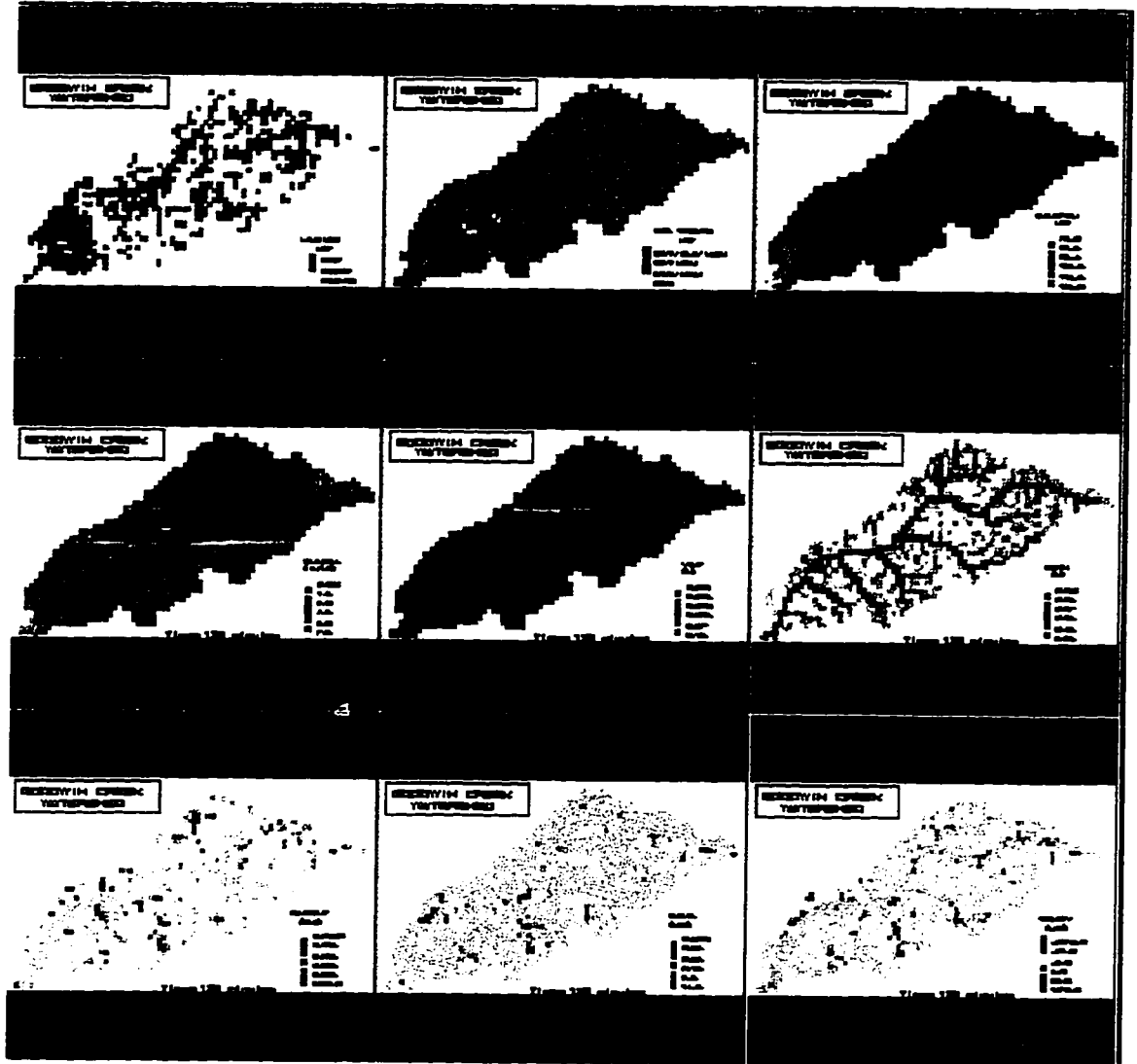


Figure C-7 - October 17-18, 1981 at Time = 120.0 minutes.

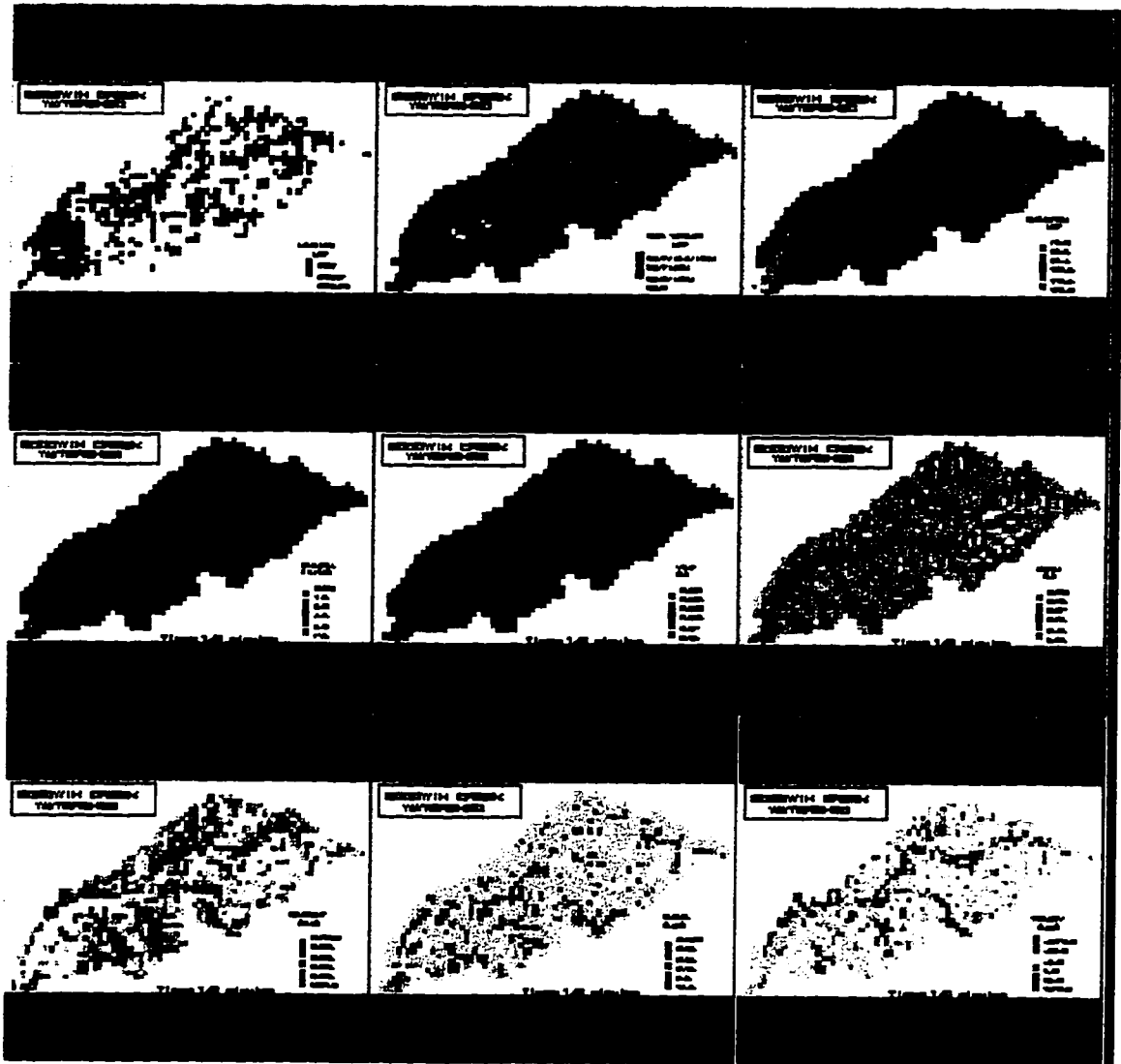


Figure C-8 - October 17-18, 1981 at Time = 140.0 minutes.



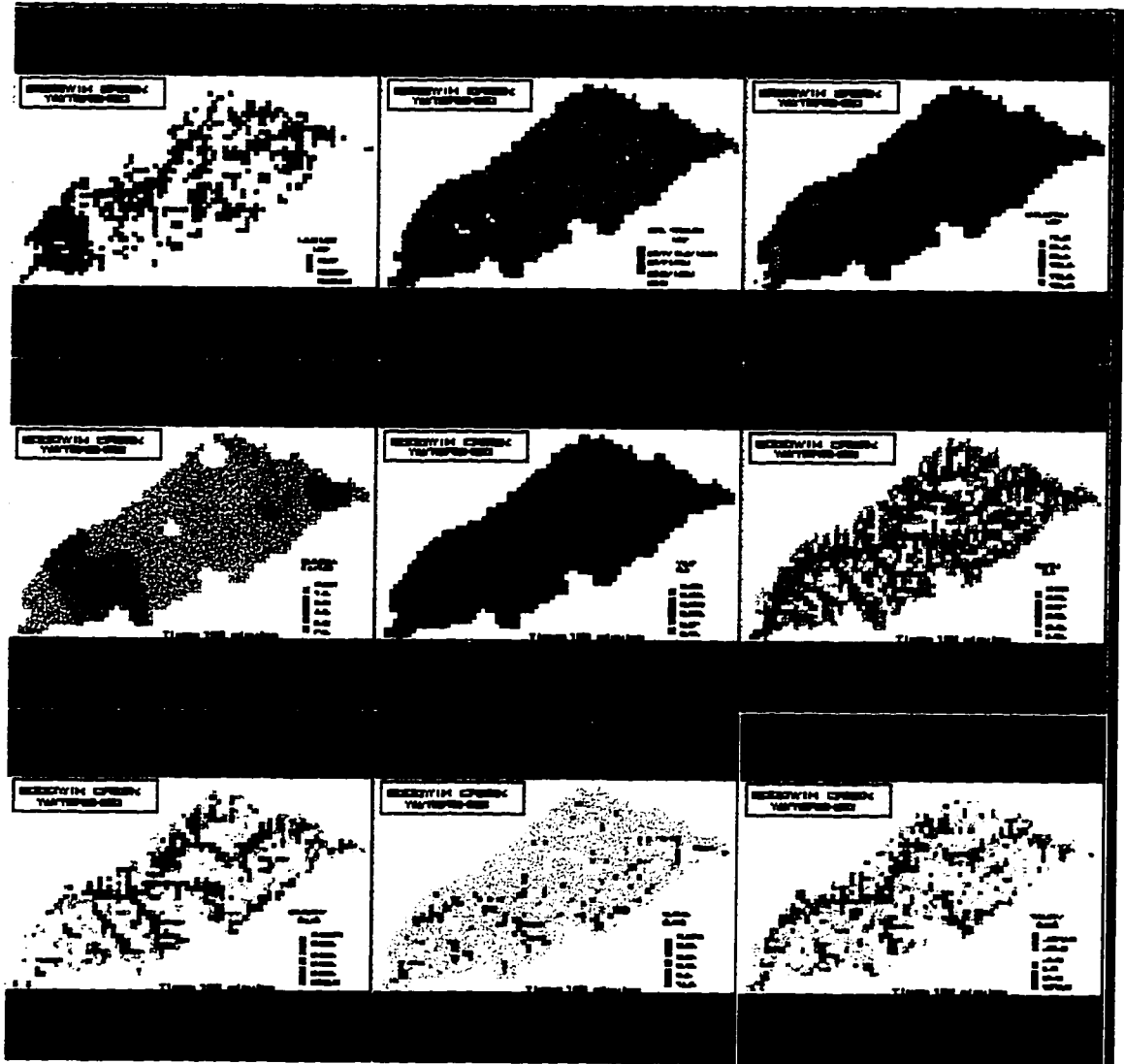


Figure C-9 - October 17-18, 1981 at Time = 160.0 minutes.

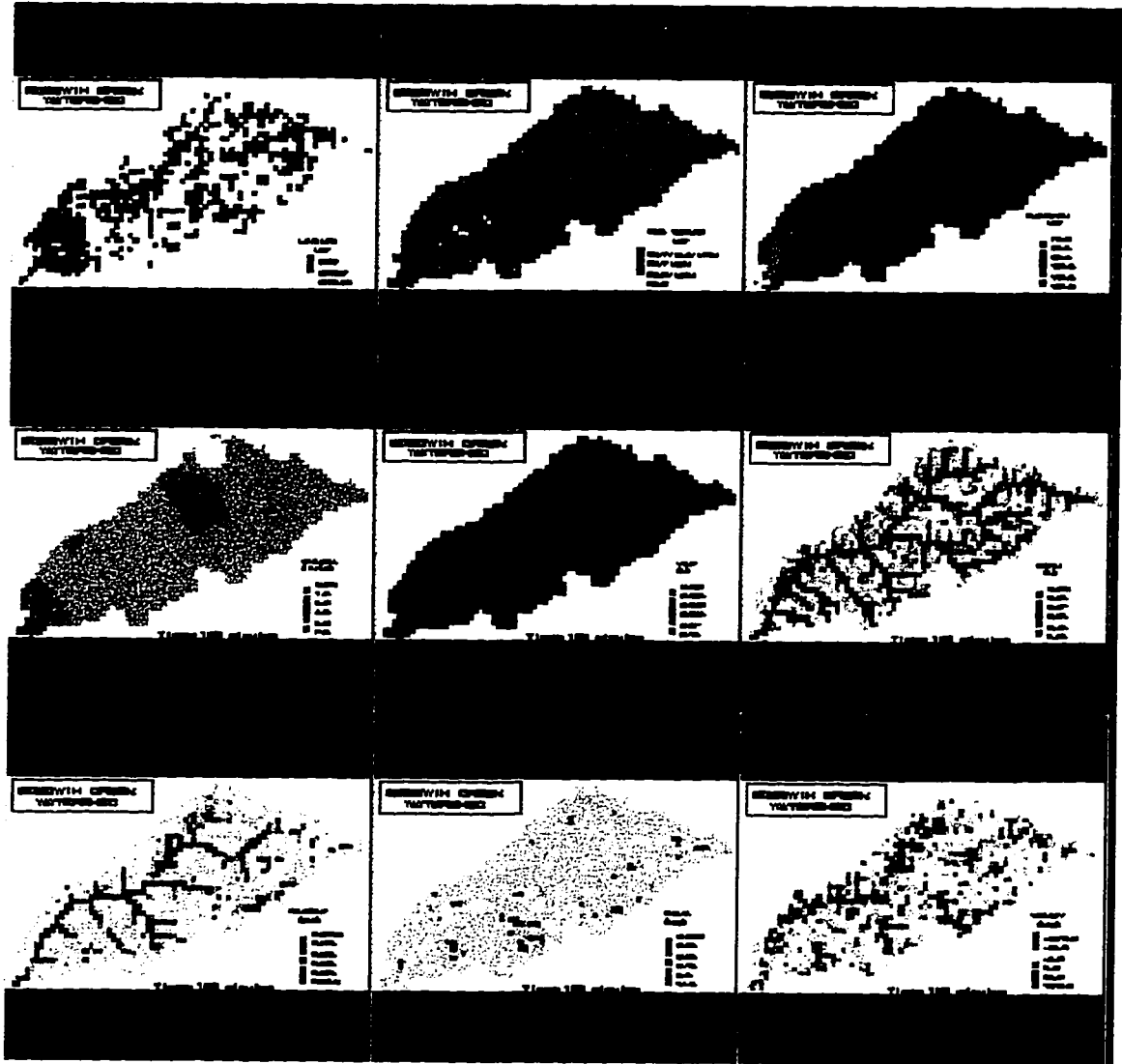


Figure C-10 - October 17-18, 1981 at Time = 180.0 minutes.

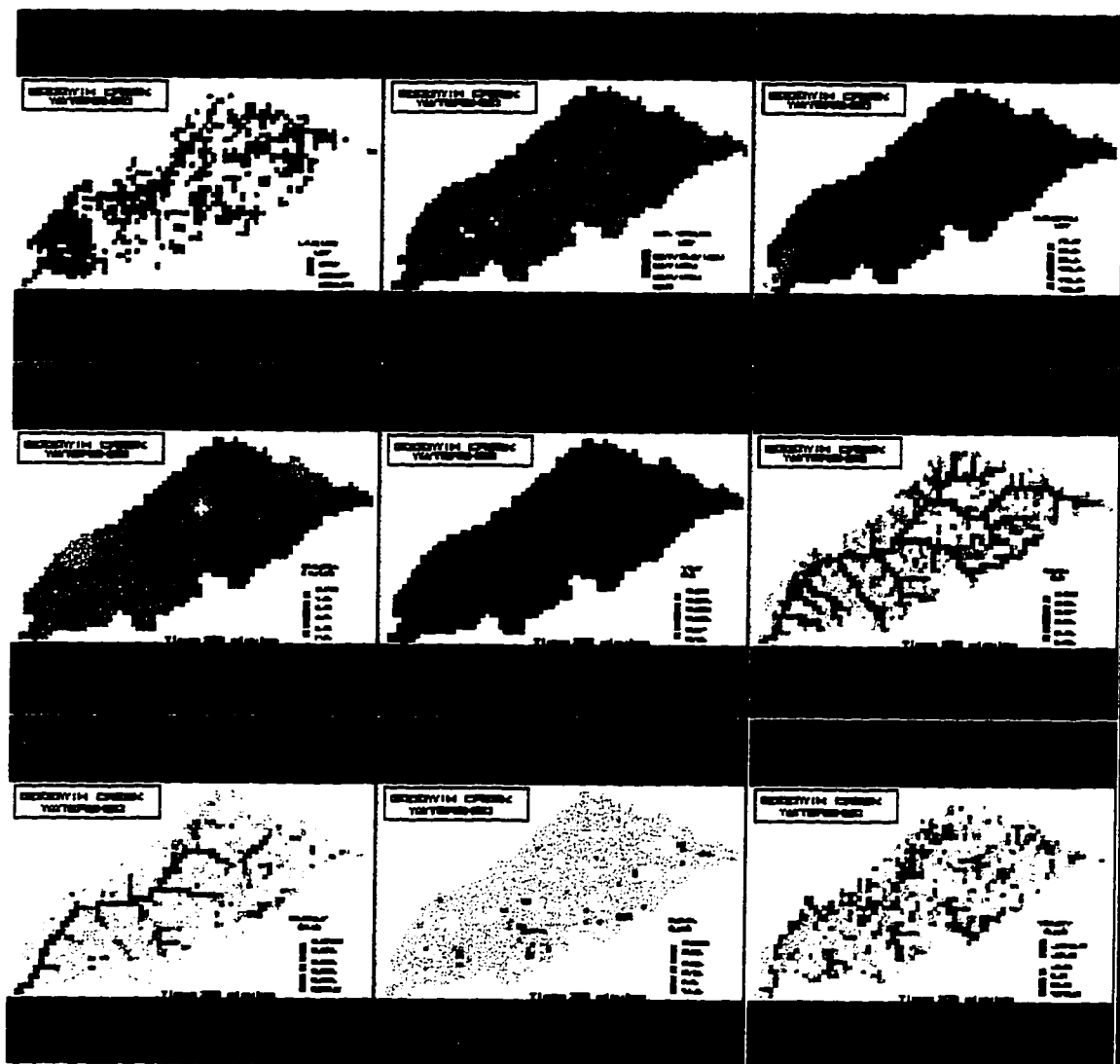


Figure C-11 - October 17-18, 1981 at Time = 200.0 minutes.

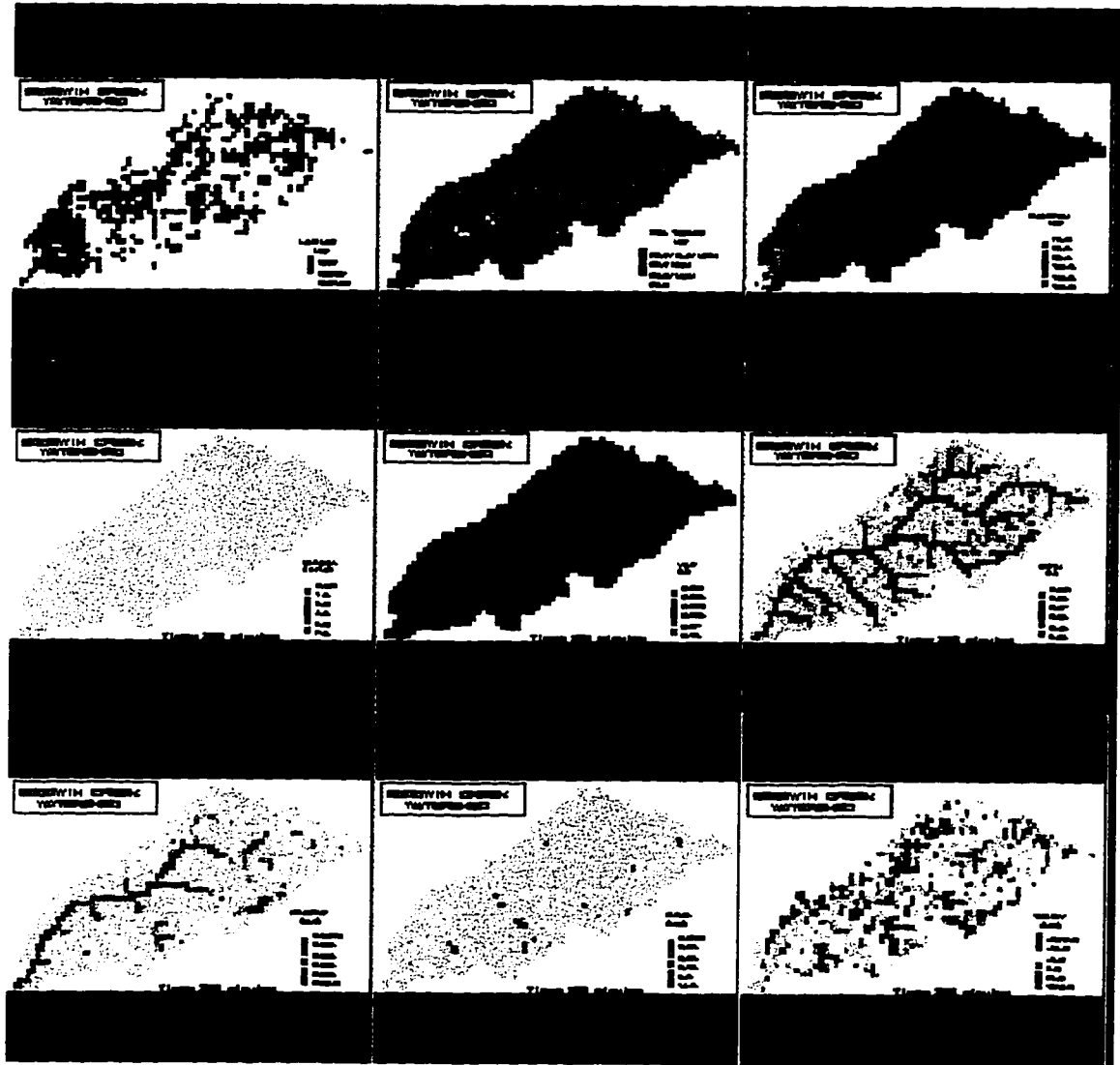


Figure C-12 - October 17-18, 1981 at Time = 220.0 minutes.

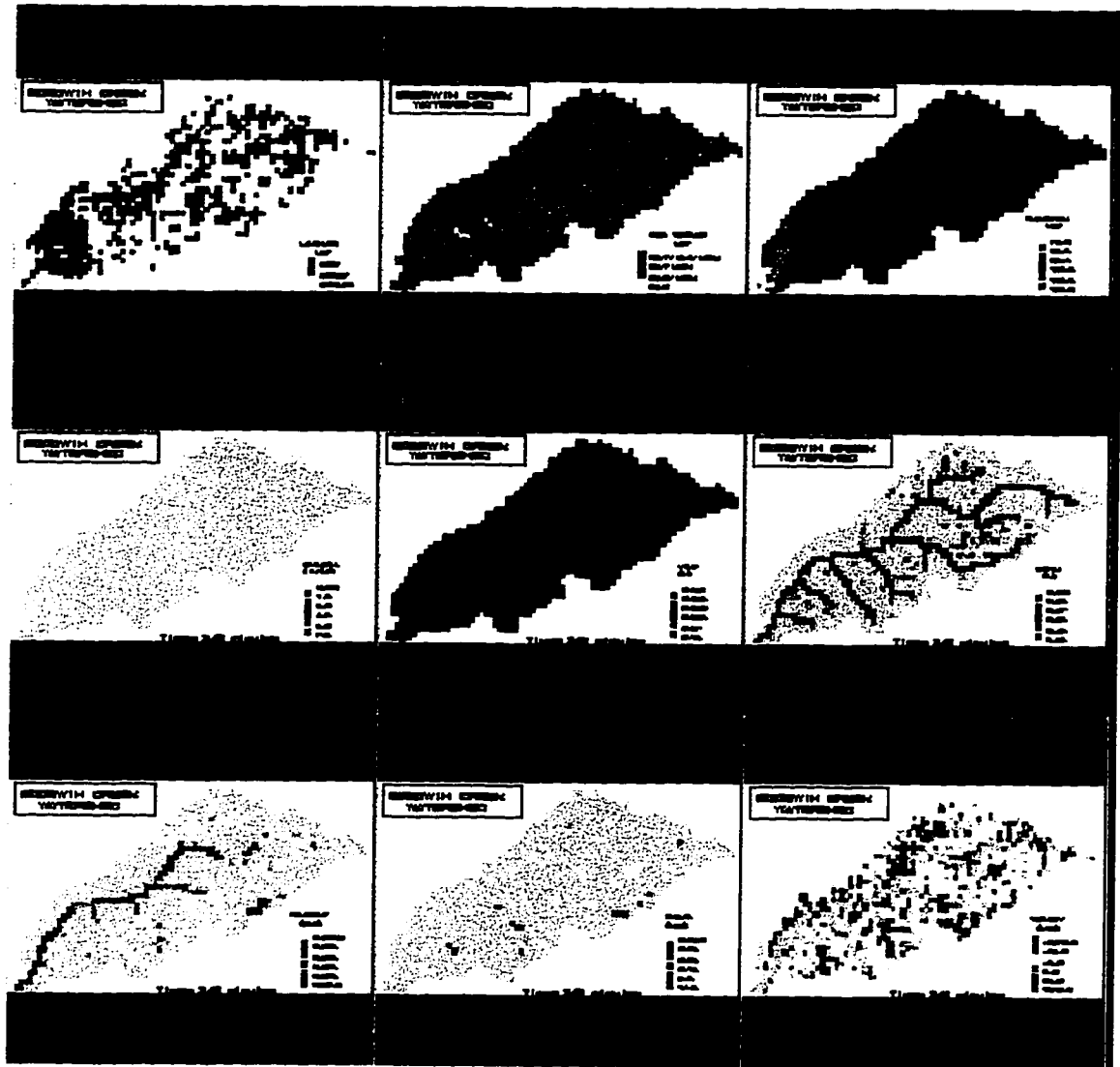


Figure C-13 - October 17-18, 1981 at Time = 240.0 minutes.

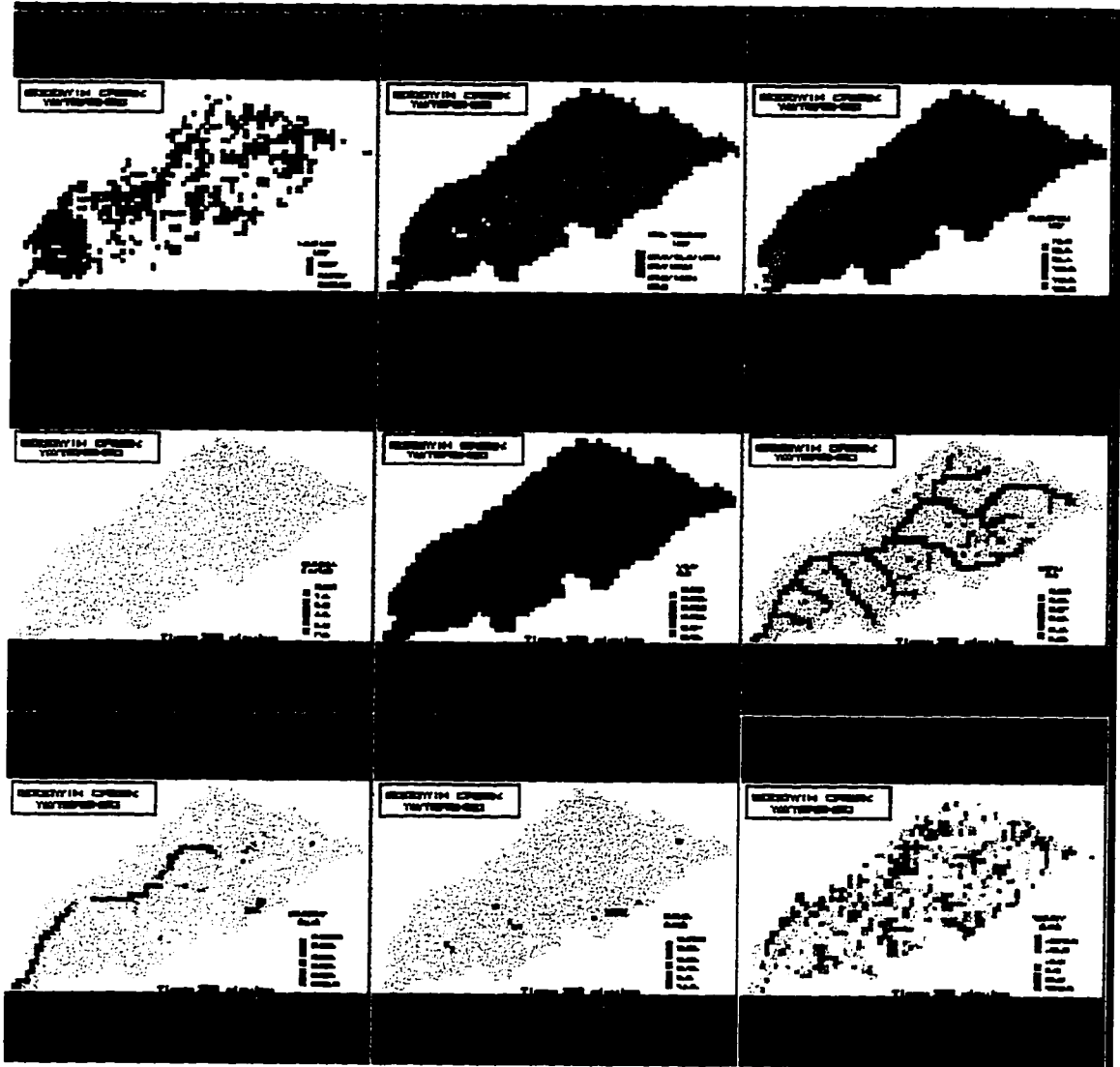


Figure C-14 - October 17-18, 1981 at Time = 260.0 minutes.

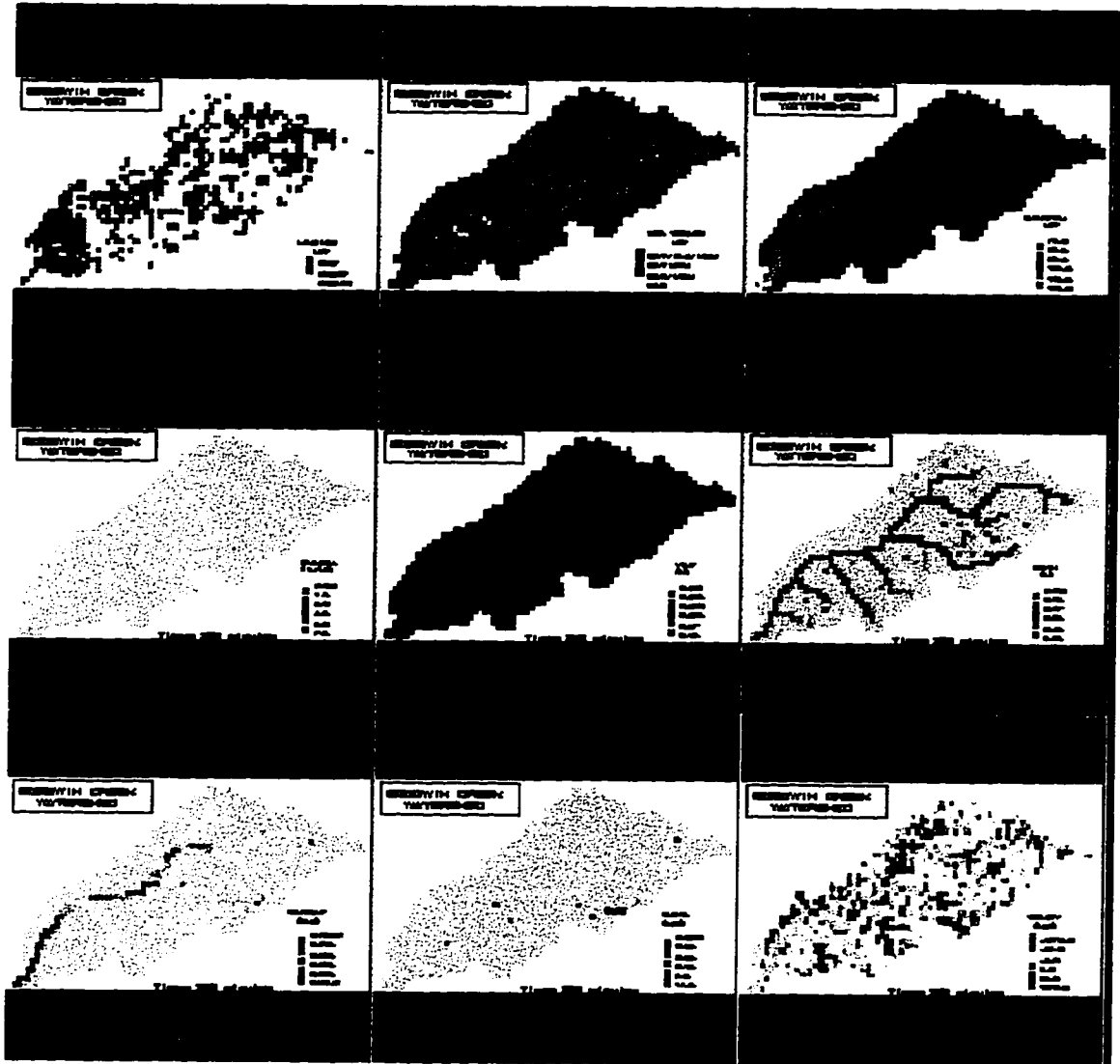


Figure C-15 - October 17-18, 1981 at Time = 280.0 minutes.

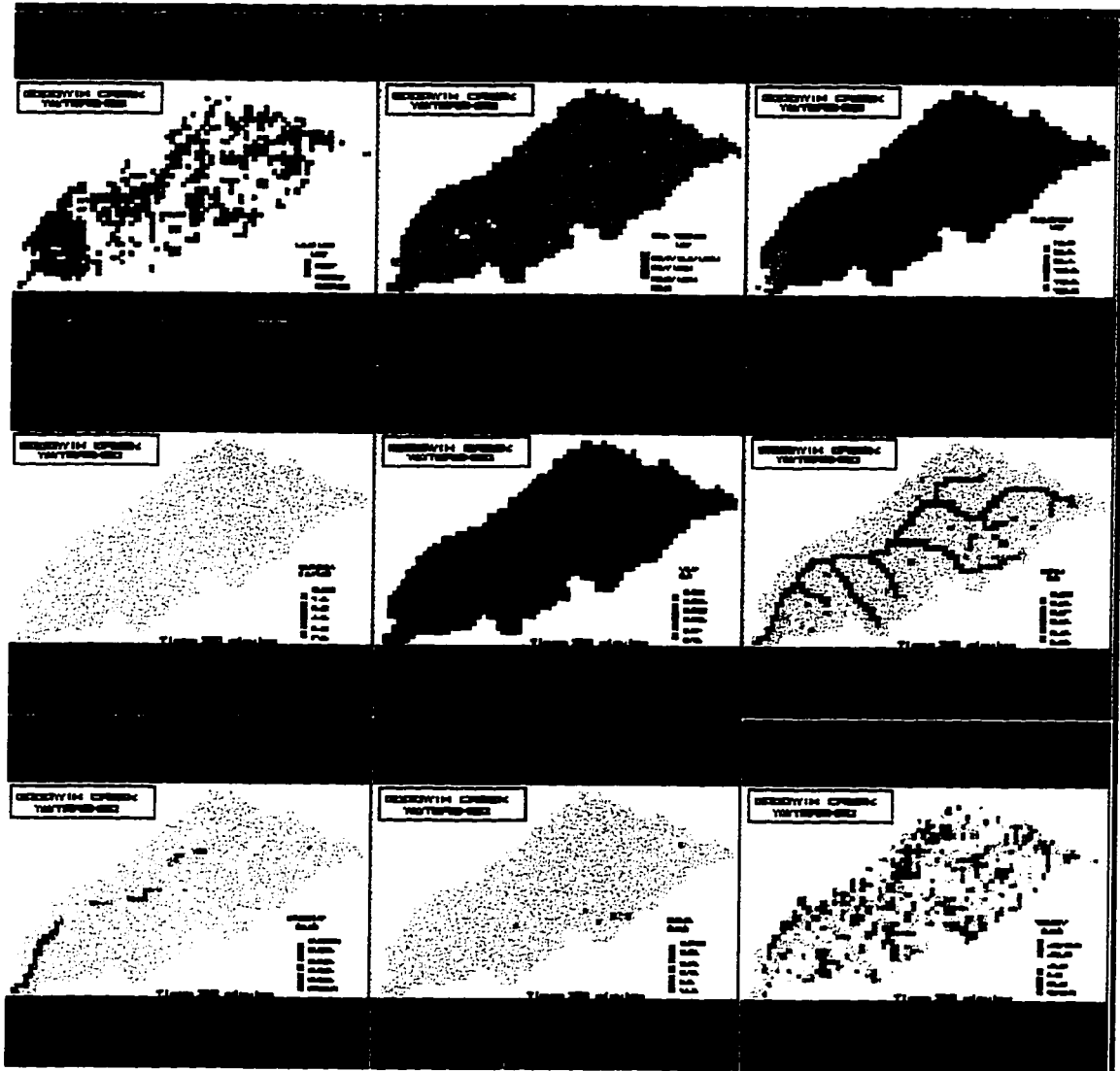


Figure C-16 - October 17-18, 1981 at Time = 300.0 minutes.



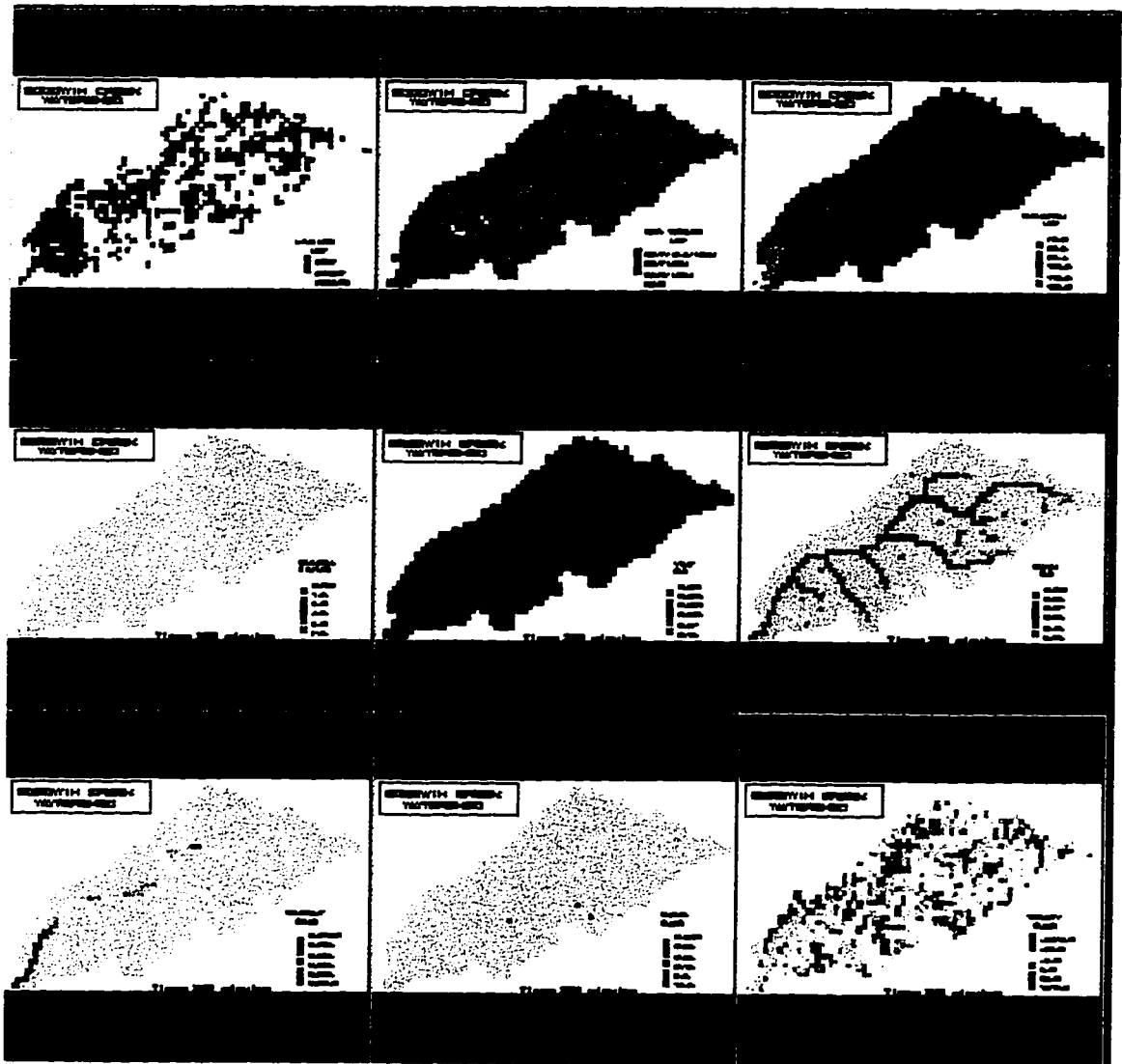


Figure C-17 - October 17-18, 1981 at Time = 320.0 minutes.

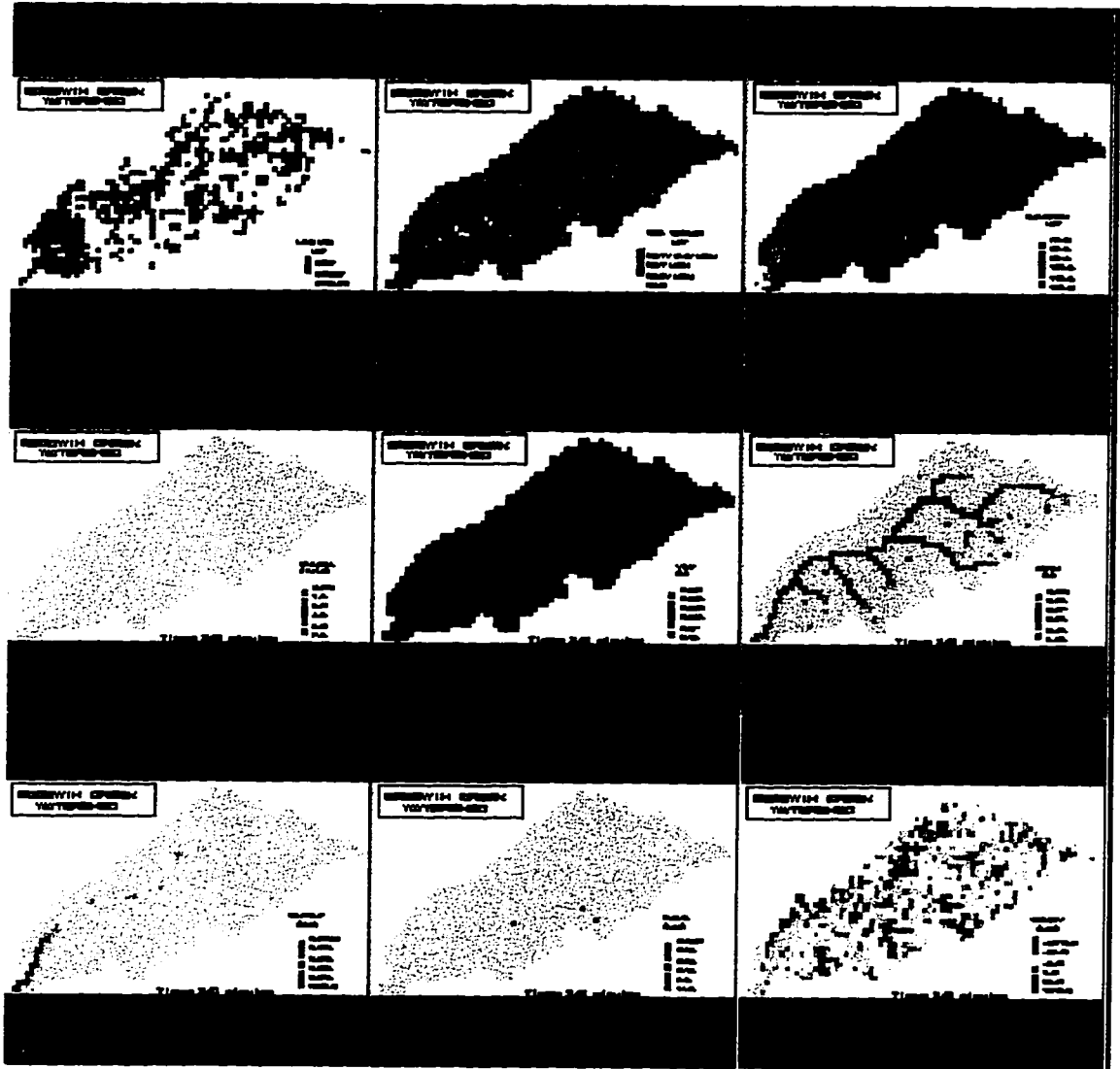


Figure C-18 - October 17-18, 1981 at Time = 340.0 minutes.

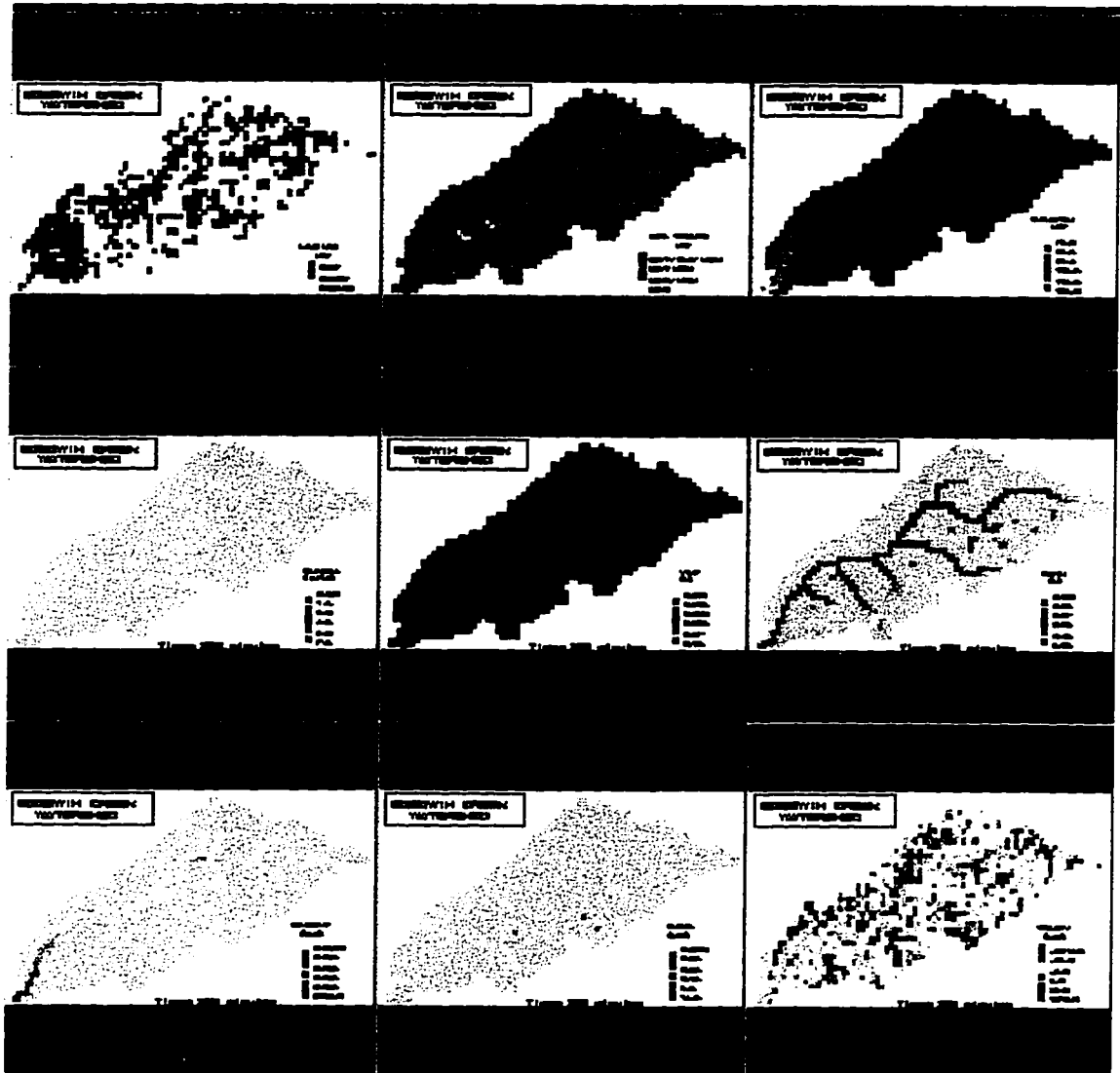


Figure C-19 - October 17-18, 1981 at Time = 360.0 minutes.

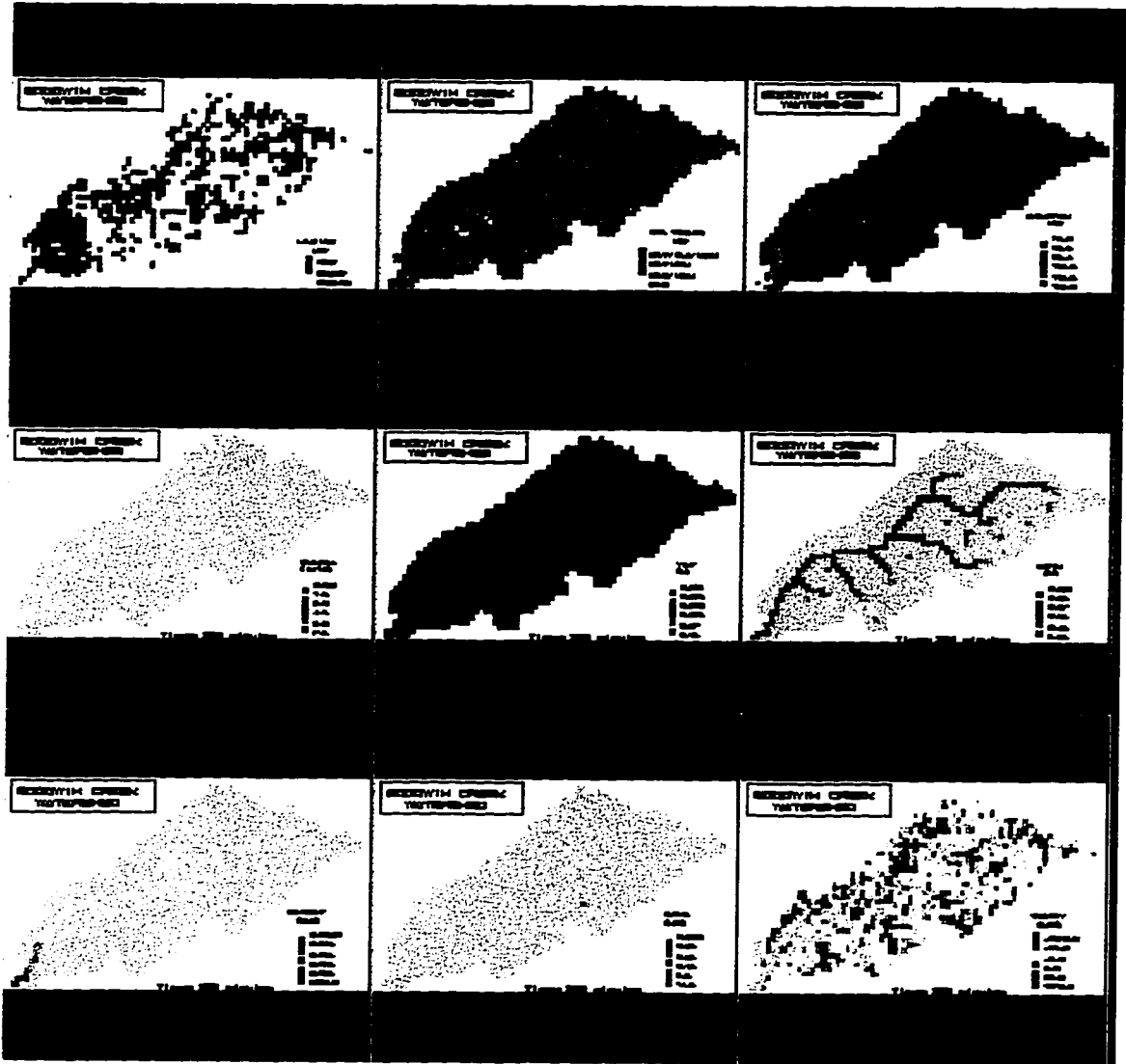


Figure C-20 - October 17-18, 1981 at Time = 380.0 minutes.

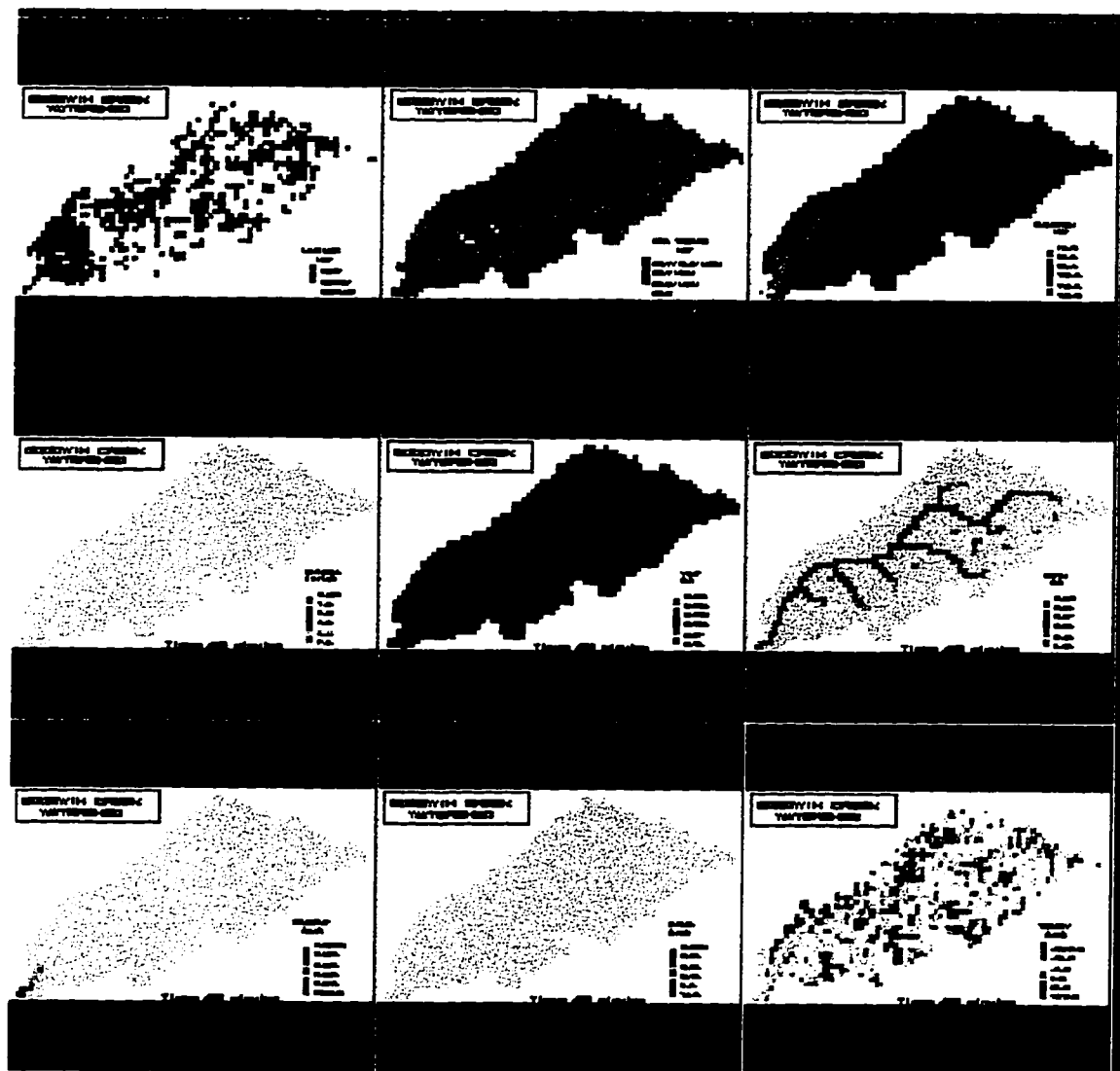


Figure C-21 - October 17-18, 1981 at Time = 400.0 minutes.

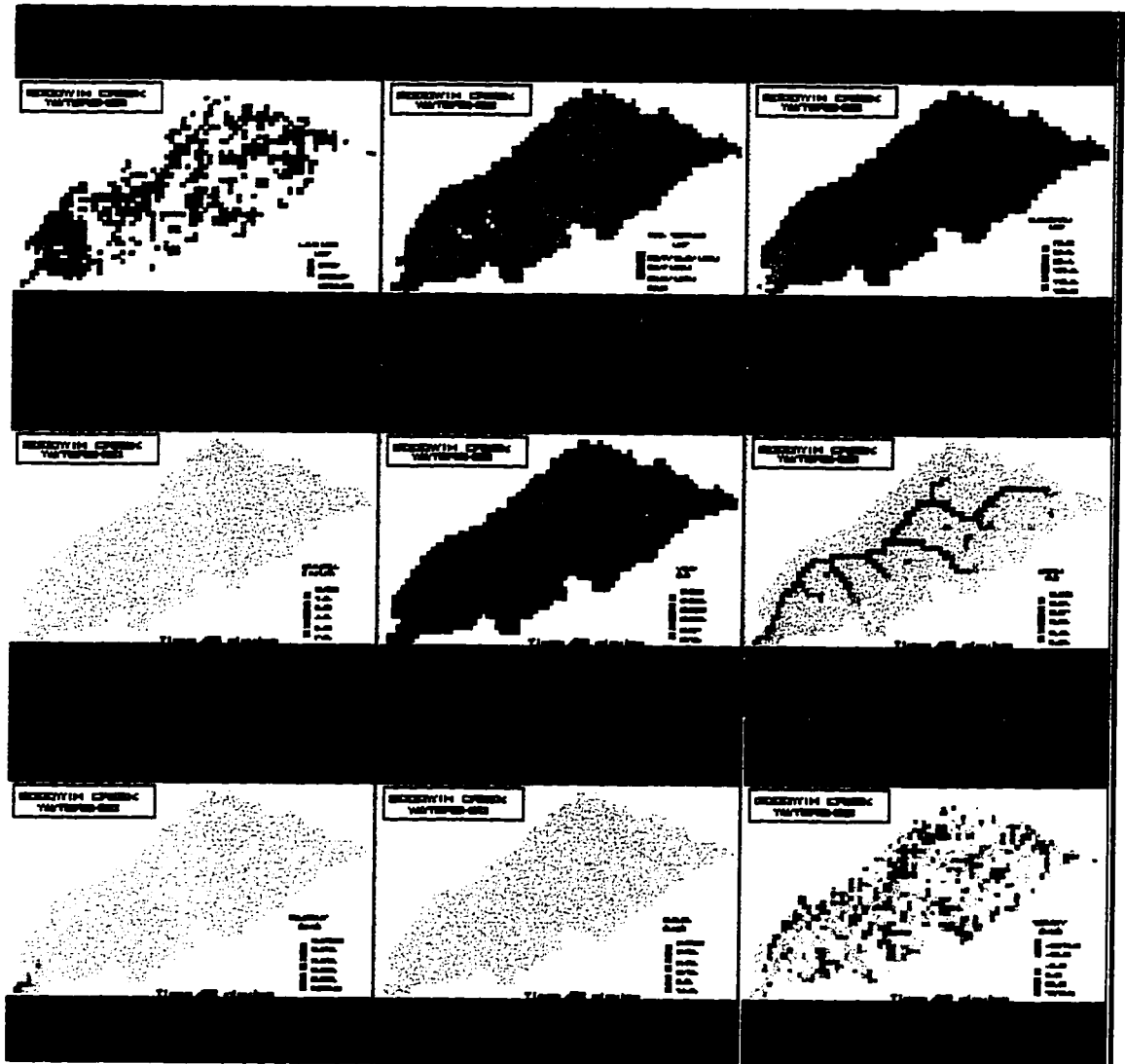


Figure C-22 - October 17-18, 1981 at Time = 420.0 minutes.

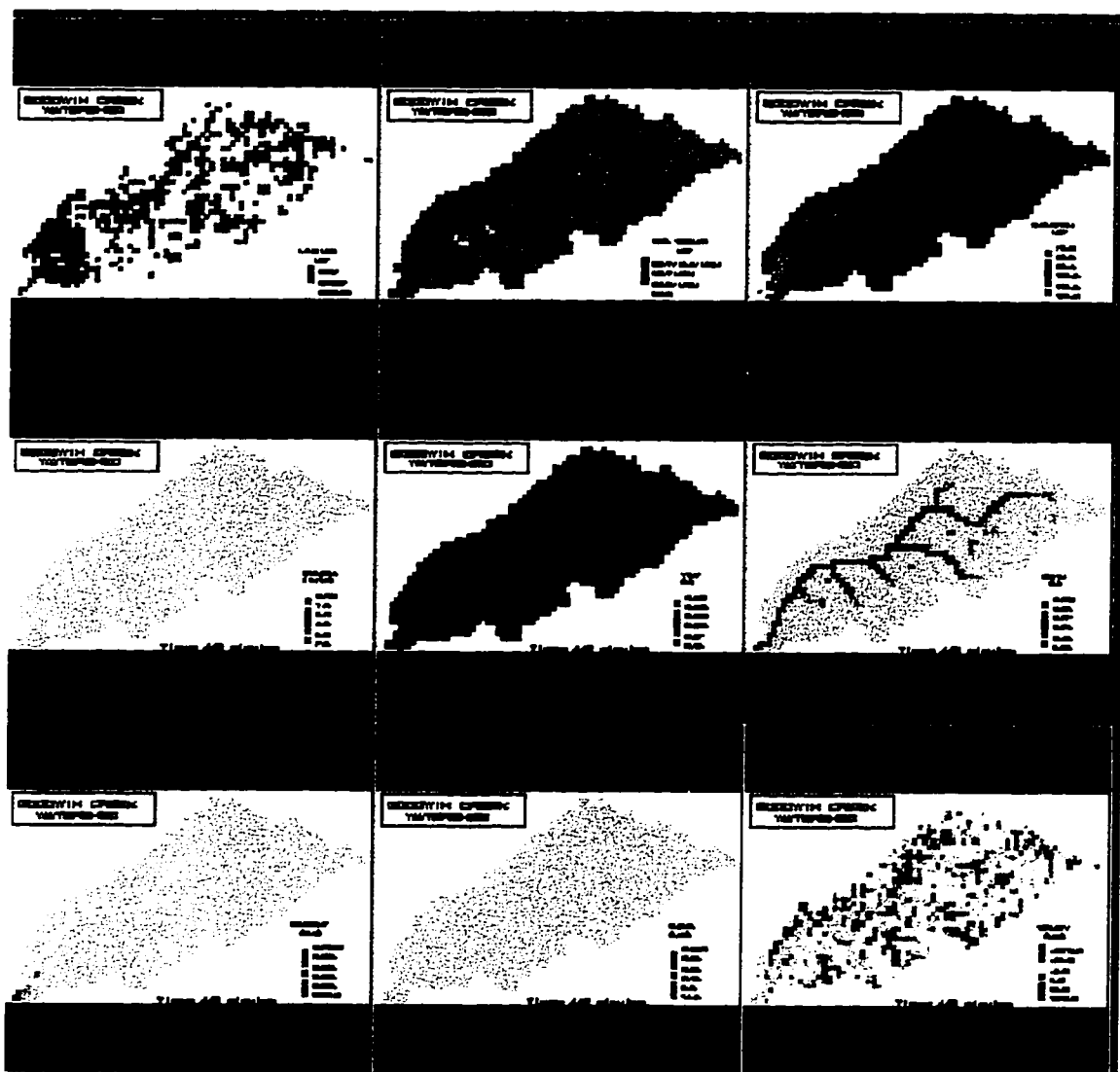


Figure C-23 - October 17-18, 1981 at Time = 440.0 minutes.

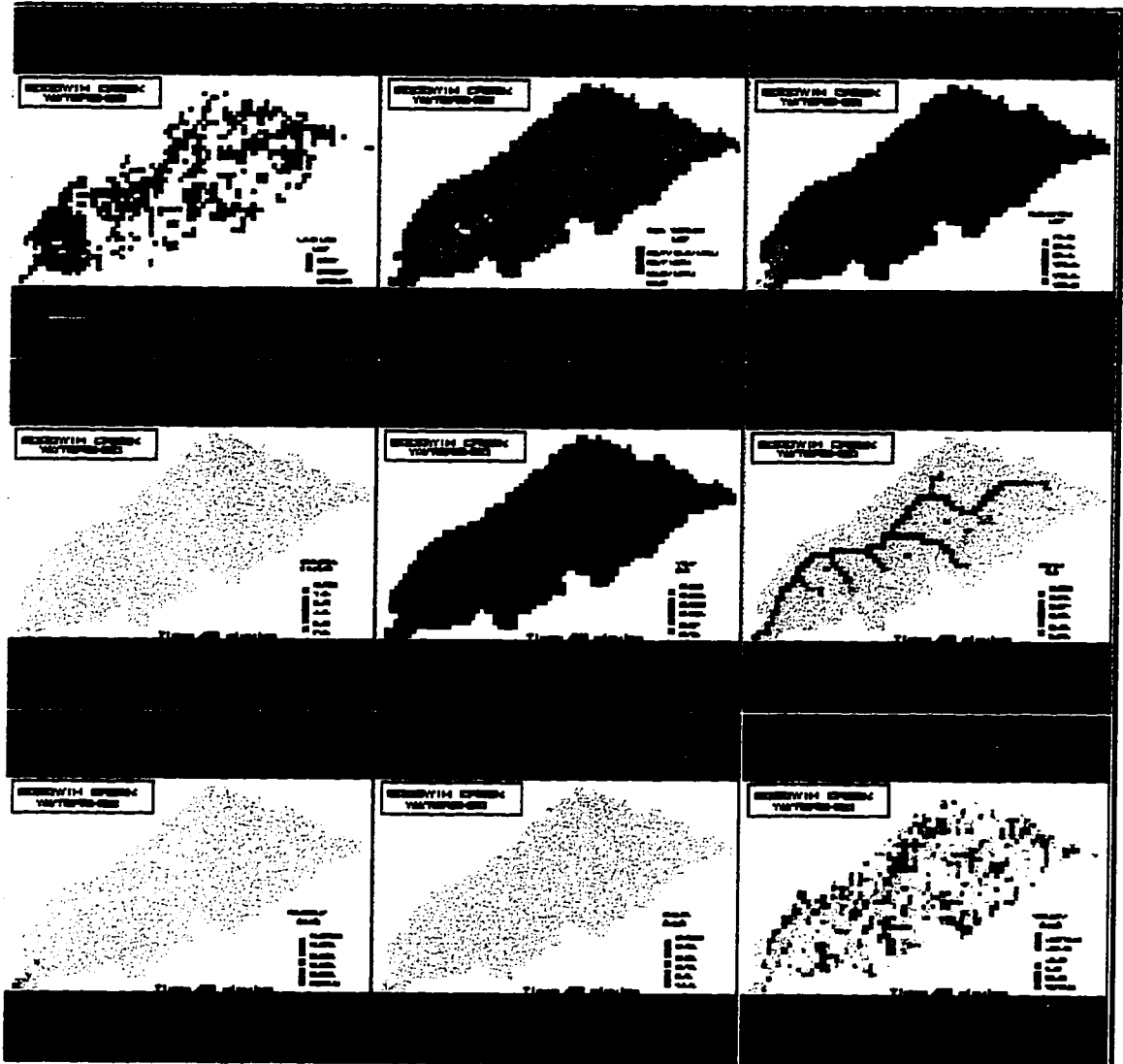


Figure C-24 - October 17-18, 1981 at Time = 460.0 minutes.



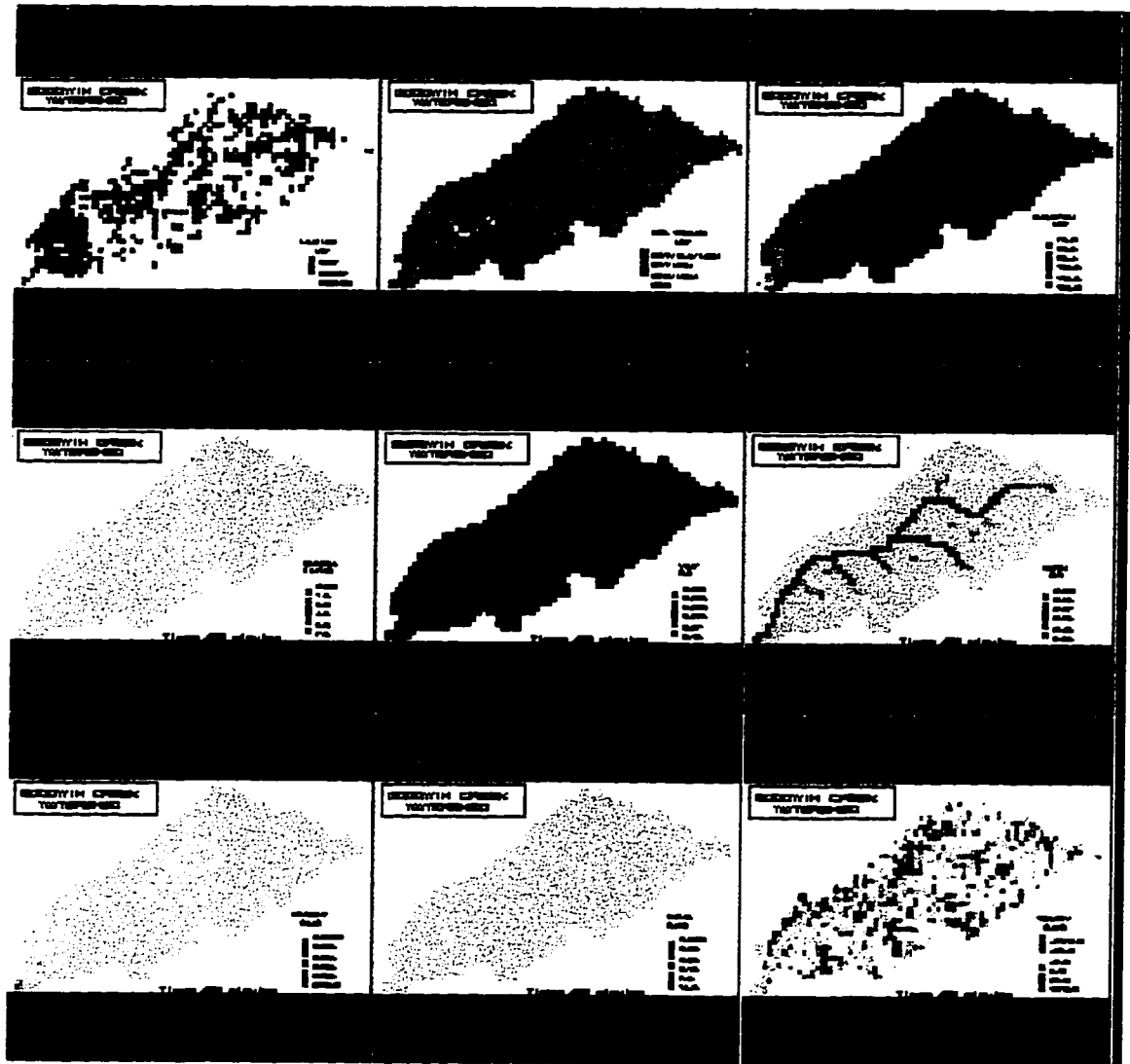


Figure C-25 - October 17-18, 1981 at Time = 480.0 minutes.

**Appendix D**

**Computer Program Listing for CASC2D  
and an Example of ASCII Input Data  
required for CASC2D simulations.**

**CASC2D Computer Listing**

```

C  CASC2D
C
C  Last Modified : 2/17/97
C
C  ISHP = Determines the shape of the watershed (1 if the grid cell
C         is within the watershed and 0 if the grid cell is
C         outside of the watershed)
C  IMAN = Manning's roughness grid
C  ISOIL = Soil index grid
C  E = Elevation grid (from the file ELAVG.DAT)
C  H = Overland depth
C  RINT = Rainfall intensity
C  VINF = Infiltration depth
C  DQOV = Overland flow rate
C  DQCH = Channel flow rate
C  HCH = Channel depth
C  XRG = Column position of each rainfall gage
C  YRG = Row position of each rainfall gage
C  RRG = Rainfall intensities at recorded gages
C  PMAN = Manning's roughness coefficients corresponding to each
C         roughness group
C  PINF = Infiltration parameters (Hydraulic Conductivity,
C         Capillary Suction Head, and Soil Moisture Deficit
C         respectively.)
C  ICHN = Channel element addresses
C  CHP = Channel parameters (width, depth, and Manning's 'n')
C  IQ = ???????
C  Q = ???????
C
C  character dname*20,tname*20,mname*20,qname*20,
+headline(6)*80,vinfname*20,susname*20
C  INTEGER  ISHP(70,75),IMAN(70,75),ISOIL(70,75)
C  DIMENSION E(70,75),H(70,75),RINT(70,75),VINF(70,75),
+          DQOV(70,75),DQCH(70,75),HCH(70,75),RTOT(70,75),
+          XRG(20),YRG(20),RRG(20),PMAN(10),PINF(10,7),
+          ICHN(50,50,2),CHP(29,4),IQ(20,2),Q(20),
+          VOLS(3,70,75),SSOIL(3,70,75),ised(20,3),
+          QOVS(3,70,75),QSMAXOUT(70,75),qsedppm(10),
+          TOTNETV(70,75),TOTSUS(70,75),cpfactor(2,10),
+          qss(70,75)
C
C  NOTE : QOVS(1,J,K) = VOLUME OF SUSPENDED SAND
C         QOVS(2,J,K) = VOLUME OF SUSPENDED SILT
C         QOVS(3,J,K) = VOLUME OF SUSPENDED CLAY
C         VOLS(1,J,K) = DEPOSITED VOLUME OF SAND

```

```

C      VOLS(2,J,K) = DEPOSITED VOLUME OF SILT
C      VOLS(3,J,K) = DEPOSITED VOLUME OF CLAY
C      SSOIL(1,70,75) = VOLUME OF SAND ERODED FROM THE SOIL
C      SSOIL(2,70,75) = VOLUME OF SILT ERODED FROM THE SOIL
C      SSOIL(3,70,75) = VOLUME OF CLAY ERODED FROM THE SOIL
C      PINF(J,1) = HYDRAULIC CONDUCTIVITY FOR SOIL J
C      PINF(J,2) = CAPILLARY SUCTION HEAD FOR SOIL J
C      PINF(J,3) = SOIL MOISTURE DEFICIT FOR SOIL J
C      PINF(J,4) = PERCENT SAND FOR SOIL J
C      PINF(J,5) = PERCENT SILT FOR SOIL J
C      PINF(J,6) = PERCENT CLAY FOR SOIL J
C
C
C      CALL GETTIM(IHR,IMIN,ISEC,I100)
C      -----
C      OPENING FILES
C      -----
C      OPEN(UNIT=21,FILE='SHAP.DAT',status='unknown')
C      OPEN(UNIT=22,FILE='ELAVG.DAT',status='unknown')
C      OPEN(UNIT=23,FILE='RAIN.DAT',status='unknown')
C      OPEN(UNIT=24,FILE='SOIL.DAT',status='unknown')
C      OPEN(UNIT=25,FILE='DATA1',status='unknown')
C      OPEN(UNIT=26,FILE='CHN.DAT',status='unknown')
C      OPEN(UNIT=27,FILE='OUT.PRN',status='unknown')
C      OPEN(UNIT=28,FILE='IMAN.DAT',status='unknown')
C      OPEN(UNIT=29,FILE='DISCHARGE.OUT',status='unknown')
C      OPEN(UNIT=36,FILE='DEPTH.OUT',status='unknown')
C      OPEN(UNIT=37,FILE='PLOT.OUT',STATUS='UNKNOWN')
C      OPEN(UNIT=54,FILE='SED.OUT',STATUS='UNKNOWN')
C
C      Reading Header file for Output Grids to be read into GRASS
C
C      open(unit=38,file='head',status='unknown')
C      do 1500 i=1,6
C      read(38,1501) headline(i)
C      1501 format(a80)
C      1500 continue
C      close(38)
C      -----
C      WRITE(27,(' Started at ",I2,".",I2,".",I2'))IHR,IMIN,ISEC
C      WRITE(27,222)
C
C      M = Maximum number of rows
C      N = Maximum number of columns
C      W = Grid Cell Resolution

```

```

C   NMAN = Total number of Manning 'n' values found in the overland
C   plane.
C   SDEP = Storage deposition
C   DT = Computational time step
C   NITER = Total number of time intervals for the runoff simulation
C   NITRN = Total number of time intervals for the rainfall
C   NPRN = Number of time steps to write the output
C   NPLT = Number of time steps to update graphics display
C   JOUT = Row number for the outlet cell
C   KOUT = Column number for the outlet cell
C   SOUT = Bed Slope for the channel at the outlet
C   qmax = Maximum discharge at the outlet (for plotting purposes)
C   WCHOUT = Width of the outlet channel
C   DCHOUT = Depth of the outlet channel
C   RMANOUT = Manning's 'n' for the outlet channel
C   SOVOUT = Slope of the Outlet Cell
C   INDEXINF = Infiltration index (1 for infiltration or 0 for none)
C   NSOIL = Number of soils with different infiltration parameters
C   NCHN = Total number of channels
C   MAXCHN = Maximum number of channel elements plus one
C   IRAIN = Rainfall index (1 for raingages and 0 for uniform rain)
C   CRAIN = Uniform rainfall intensity (IRAIN=0)
C   NRG = Number of rainfall gages (IRAIN=1)
C   NREAD = Ratio between raingage rainfall time step and DT
C   XRG = Column position of each rainfall gage
C   YRG = Row position of each rainfall gage
C
  READ(25,*) M,N,W,NMAN,SDEP
  write(27,9000) m,n,w,nman,sdep
9000 format('INPUT DATA//No. of Rows = ',i5,
  &'No. of Columns = ',i5,'Grid Cell Width = ',
  &f10.3,'No. of Roughness Categories = ',i5,'sdep = ',f10.2)
  READ(25,*) DT,NITER,NITRN,NPRN,NPLT,elconv,chancheck
  write(27,9001) dt,niter,nitrn,nprn,nplt,elconv,chancheck
9001 format('Computational Time Step (seconds) = ',f10.2,
  &'NITER = ',i10,'NITRN = ',i10,'NPRN = ',i10,
  &'NPLT = ',i10,
  &'Elevation Conversion Factor = ',f10.2,
  &'Channel Routing Option = ',f10.2)
  READ(25,*)
JOUT,KOUT,SOUT,qmax,WCHOUT,DCHOUT,RMANOUT,SOVOUT
  write(27,9002) jout,kout,sout,qmax,wchout,dchout,rmanout,
  &sovout
9002 format('Outlet Row = ',i5,'Outlet Column = ',i5,
  &'Outlet Channel Slope = ',f10.4,'QMAX = ',f10.3,

```

```

&/Outlet Channel Width = ',f10.3,'Outlet Channel Depth = ',f10.3,
&/Outlet Channel Roughness Coeff. = ',f10.3,
&/Outlet Overland Slope = ',f10.4)
  READ(25,*) INDEXINF,NSOIL
  write(27,9003) indexinf,nsoil
9003 format('INDEXINF = ',i5,'NSOIL = ',i5)
  READ(25,*) NCHN,MAXCHN
  write(27,9004) nchn,maxchn
9004 format('No. of Channel Links = ',i5,
&/Max. No. of Channel Nodes = ',i5)
  READ(25,*) IRAIN
  write(27,9005) irain
9005 format('IRAIN = ',i5)
C
  IF(IRAIN.EQ.0) READ(25,*) CRAIN
  if (irain .eq. 0) write(27,9006) crain
9006 format('Uniform Rainfall (cm/hr) = ',f10.4)
  IF(IRAIN.EQ.1) READ(25,*) NRG,NREAD
  if (irain .eq. 1) write(27,9007) nrg,nread
9007 format('No. of Raingages = ',i10,'NREAD = ',i10)
  IF(IRAIN.EQ.1) READ(25,*) (XRG(L),YRG(L),L=1,NRG)
  if (irain .eq. 1) then
    write(27,9008)
    write(27,9009) (xrg(l),yrg(l),l=1,nrg)
9008 format('/'   Raingage Locations',
&/   Column   Row'/)
9009 format(f10.2,5x,f10.2)
  endif
C
  READ(25,*) (PMAN(J),cpfactor(1,j),cpfactor(2,j),J=1,NMAN)
  write(27,9010)
  write(27,9011) (pman(j),cpfactor(1,j),cpfactor(2,j),j=1,nman)
9010 format('/' Roughness Coeff.  USLE C-Factor  USLE P-Factor'/)
9011 format(f10.2,10x,f10.2,10x,f10.2)
  IF(INDEXINF.EQ.1) READ(25,*) ((PINF(J,K),K=1,7),J=1,NSOIL)
  if (indexinf .eq. 1) then
    write(27,9012)
    write(27,9013)((pinf(j,k),k=1,7),j=1,nsoil)
9012 format('/'           INFILTRATION PARAMETERS',
&/Hyd. Cond.  Cap. Head  SMD   %Sand   %Silt  ',
&/%Clay  USLE K-Factor  '/')
9013 format(f10.9,f10.5,f10.3,3f10.3,f15.3)
  endif
C
C  This information must be used when one wants to see the

```

C change in Q (dq) between two channel nodes.

C

```

READ(25,*) INDEXDIS,NDIS
write(27,9014) indexdis,ndis
9014 format(/'INDEXDIS = ',i10,/'NDIS = ',i10)
IF(INDEXDIS.EQ.1) READ(25,*) ((IQ(J,K),K=1,2),J=1,NDIS)
if (indexdis .eq. 1) then
write(27,9015)
write(27,9016) ((iq(j,k),k=1,2),j=1,ndis)
9015 format(/' Discharge Gage Locations'      Column  Row',/)
9016 format(2i10)
endif
read(25,*) indexsed,nsed
write(27,9017) indexsed,nsed
9017 format(/'INDEXSED = ',I5,/'NSED = ',I5)
if(indexsed .eq. 1) read(25,*) ((ised(j,k),k=1,3),j=1,nsed)
if (indexsed .eq. 1) then
write(27,9018)
write(27,9019) ((ised(j,k),k=1,3),j=1,nsed)
9018 format(/'      Sediment Gage Locations',
&'      Column  Row  Channel Width'/)
9019 format(3i10)
endif
write(27,9020)
9020 format(/)
write(27,222)
CLOSE(25)

```

C

```

if (chanceck .eq. 1.0) then
IF(NCHN.NE.0) READ(26,*) ((CHP(L,K),K=1,4),L=1,NCHN)
IF(NCHN.NE.0) READ(26,*) (((ICHN(L,J,K),J=1,MAXCHN),
+      K=1,2),L=1,NCHN)
CLOSE(26)
WRITE(29,229) ((IQ(J,K),K=1,2),J=1,NDIS)
endif

```

C

C -----  
C READING SHAP MATIX AND READING ELEVATIONS AND  
INITIALIZATIONS

C

```

C -----
DO 150 J=1,M
DO 150 K=1,N
READ(21,*) ISHP(J,K)
READ(22,*) E(J,K)
E(J,K)=E(J,K)/elconv
IF (NSOIL .NE. 0) THEN

```



```

IF(NSOIL.EQ.1) THEN
ISOIL(J,K)=1
ELSE
READ(24,*) ISOIL(J,K)
ENDIF
ENDIF
IF(NMAN.EQ.1) THEN
IMAN(J,K)=1
ELSE
READ(28,*) IMAN(J,K)
ENDIF
C
H(J,K)=0.
HCH(J,K)=0.
DQOV(J,K)=0.
QOVS(1,J,K)=0.
QOVS(2,J,K)=0.
QOVS(3,J,K)=0.
DQCH(J,K)=0.
VINP(J,K)=0.
RTOT(j,k)=0.
150 CONTINUE
CLOSE(21)
CLOSE(22)
CLOSE(24)
CLOSE(28)
C -----
C Note : IC is the Link number and L is the Node number.
C J is the row location and K is the column location.
C
DO 160 IC=1,NCHN,1
DO 175 L=1,MAXCHN,1
J=ICHN(IC,L,1)
K=ICHN(IC,L,2)
IF(J.LE.0) GO TO 160
C
C When ISHP is equal to 2, then the program knows that this grid
C cell has a channel going through it.
C
if(chancheck .eq. 1.0) then
ISHP(J,K)=2
endif
175 CONTINUE
160 CONTINUE
C -----

```

```

VIN=0.
VOUT=0.
VSUR=0.
VINFTOT=0.
RINDEX=1.
IFCOUNT=1
ICOUNT=1
IPCOUNT=1
AMAXDEPTH=9E-30
AMINDEPTH=9E30
AMAXCDEPTH=9E-30
AMINCDEPTH=9E30
AMAXVINF=9E-30
AMINVINF=9E30
AMAXNETV=9E-30
AMINNETV=9E30
AMAXQSMAX=9E-30
AMINQSMAX=9E30
AMAXRAIN=9E-30
AMINRAIN=9E30
AMAXSUS=9E-30
AMINSUS=9E30
do 950 j=1,m
do 951 k=1,n
VOLS(1,J,K)=0.0
VOLS(2,J,K)=0.0
VOLS(3,J,K)=0.0
SSOIL(1,J,K)=0.0
SSOIL(2,J,K)=0.0
SSOIL(3,J,K)=0.0
QOVS(1,J,K)=0.0
QOVS(2,J,K)=0.0
QOVS(3,J,K)=0.0
QSMAXOUT(J,K)=0.0
951 CONTINUE
950 CONTINUE
C -----
C  TIME LOOP
C -----
DO 10 I=1,NITER
ICALL=0
do 700 j=1,m
do 701 k=1,n
qss(j,k)=0.0
701 continue

```

700 continue

```

IF(I.GT.NITRN) RINDEX=0.
IF(I.LE.NITRN.AND.IRAIN.EQ.1) THEN
IF(((I-1)/NREAD)*NREAD.EQ.(I-1)) THEN
ICALL=1
READ(23,*) (RRG(L),L=1,NRG)
ENDIF
ENDIF

```

C

C Applying the rainfall to each grid cell within the watershed.

C

```

DO 1 J=1,M
DO 1 K=1,N
IF(ISHP(J,K).EQ.0) GO TO 1
IF(IRAIN.EQ.0) THEN

```

C

C Uniform rainfall

C

```

RINT(J,K)=CRAIN
ELSE

```

C

C Spatially distributing the rainfall

C

```

IF(ICALL.EQ.1) CALL RAIN(J,K,NRG,XRG,YRG,RRG,RINT)
ENDIF
IF(I.GT.NITRN) RINT(J,K)=0.

```

C

C Determining the Minimum and Maximum Rainfall Intensity

C

```

IF (RINT(J,K) .LT. AMINRAIN) AMINRAIN=RINT(J,K)
IF (RINT(J,K) .GT. AMAXRAIN) AMAXRAIN=RINT(J,K)
RTOT(J,K)=RTOT(J,K)+RINT(J,K)*DT

```

C

C Computing the portion of the overland depth due to the  
C overland flow.

C

```

HOV=DQOV(J,K)*DT/(W*W)

```

C

C Computing the Total Overland Depth due to the overland flow,  
C previous overland depth, and the addition due to rainfall.

C

```

HOV=HOV+H(J,K)+RINDEX*RINT(J,K)*DT

```

C

C When HOV is less than zero, then a negative depth situation  
C occurs.

```

C
  IF(HOV.LT.0) THEN
    print*,'Negative Depth in the Overland Plane'
    print*,'Grid Cell ',j,k
    stop
  endif
C
C   Calling the Infiltration subroutine. HOV will be modified by
C   subtracting the infiltration losses. NOTE : if the infiltration
C   volume that can be lossed for DT is greater than the amount of
C   surface volume present, then HOV will reduce to zero.
C
  IF(INDEXINF.EQ.1)CALL INFILT(J,K,DT,ISOIL,VINF,PINF,HOV)
  H(J,K)=HOV
C
C   Determining the Minimum and Maximum Overland Depth
C   and the Minimum and Maximum Infiltration Depth
C
  IF (H(J,K) .LT. AMINDEPTH) AMINDEPTH=H(J,K)
  IF (H(J,K) .GT. AMAXDEPTH) AMAXDEPTH=H(J,K)
  IF (VINF(J,K) .LT. AMINVINF) AMINVINF=VINF(J,K)
  IF (VINF(J,K) .GT. AMAXVINF) AMAXVINF=VINF(J,K)
  DQOV(J,K)=0.
C
C   Keeping track of the Total Volume of Rainfall
C   and the Total Volume of Infiltration.
C
  IF(I.EQ.NITER) THEN
    VIN=VIN+RTOT(J,K)*W*W
    vinfot=vinftot+vinf(j,k)*w*w
  endif
  I CONTINUE
C
C   Overland Flow Routing
C
  11 DO 20 J=1,M
    DO 30 K=1,N
      IF(ISHP(J,K).EQ.0) GO TO 30
      DO 40 L=-1,0,1
        JJ=J+L+1
        KK=K-L
        IF(JJ.GT.M.OR.KK.GT.N.OR.ISHP(JJ,KK).EQ.0) GO TO 40
        CALL OVRL(W,IMAN,PMAN,SDEP,J,K,JJ,KK,E,H,DQOV,VOLS,DT,I,
          +QOVS,SSOIL,QSMAXOUT,ISOIL,PINF,IFCOUNT,cpfactor,qss)
      40 CONTINUE

```

```

30 CONTINUE
20 CONTINUE
  if (chanceck .eq. 1.0) then
C
C   Updating the Channel Depths
C
  DO 2 IC=1,NCHN,1
  DO 3 L=1,MAXCHN,1
  J=ICHN(IC,L,1)
  K=ICHN(IC,L,2)
  JJ=ICHN(IC,L+1,1)
  IF(J.LE.0) GO TO 2
  IF(JJ.LT.0) GO TO 2
  WCH=CHP(IC,1)
  DCH=CHP(IC,2)
  SFACTOR=CHP(IC,4)
  DHCH=DQCH(J,K)*DT/(W*SFACTOR*WCH)
  HCH(J,K)=HCH(J,K)+DHCH
  IF(H(J,K).GT.SDEP) THEN
C
C   Adding the volume of water in the overland cell into the channel.
C
  HCH(J,K)=HCH(J,K)+(H(J,K)-SDEP)*W/WCH
  H(J,K)=SDEP
  ENDIF
  HTOP=DCH+H(J,K)
C
C   In the case where the watersurface in the channel is greater
C   than the watersurface in the overland cell, then the volume of
C   water needs to be redistributed.
C
  IF(HCH(J,K).GT.HTOP) THEN
  DH=(HCH(J,K)-HTOP)*WCH/(W*SFACTOR)
  H(J,K)=H(J,K)+DH
  HCH(J,K)=HTOP+DH
  ENDIF
C
C   Determining the Minimum and Maximum Channel Depths
C
  IF (HCH(J,K) .LT. AMINCDEPTH) AMINCDEPTH=HCH(J,K)
  IF (HCH(J,K) .GT. AMAXCDEPTH) AMAXCDEPTH=HCH(J,K)
C
C   Negative depths in the channel
C
  IF(HCH(J,K).LT.0) then

```

```

print*, 'Negative Depth in the Channel'
print*, 'j,k = ',j,k
goto 170
else
endif
DQCH(J,K)=0.
IF(I.EQ.NITER) VSUR=VSUR+HCH(J,K)*W*WCH+H(J,K)*W*W
3 CONTINUE
2 CONTINUE
C
C   Channel Routing
C
DO 50 IC=1,NCHN,1
WCH=CHP(IC,1)
DCH=CHP(IC,2)
RMANCH=CHP(IC,3)
SFACTOR=CHP(IC,4)
DO 60 L=1,MAXCHN-1,1
J=ICHN(IC,L,1)
K=ICHN(IC,L,2)
JJ=ICHN(IC,L+1,1)
KK=ICHN(IC,L+1,2)
C
C   Note : JJJ is a check to see when the end of a channel link
C   has been reached.
C
JJJ=ICHN(IC,L+2,1)
C
C   Note : When JJ is less than zero, then that indicates that
C   the channel routing for the current link is complete.
C
IF(JJ.LE.0) GO TO 50
CALL CHNCHN(NCHN,W,WCH,DCH,RMANCH,SFACTOR,
+J,K,JJ,KK,JJJ,E,HCH,ICHN,CHP,DQCH,NDIS,IQ,Q,
+pman,vols,dt,i,qovs,ssoil,qsmaxout,pinf,ifcount,
+cpfactor,qss)
60 CONTINUE
50 CONTINUE
endif
C
C   Determining the Outflow Discharge
C
HOUT=H(JOUT,KOUT)
ALFA=SQRT(SOVOUT)/PMAN(IMAN(JOUT,KOUT))
QOUTOV=0.

```

```

QOUTCH=0.0
IF(HOUT.GT.SDEP) QOUTOV=W*ALFA*((HOUT-SDEP)**1.667)
H(JOUT,KOUT)=HOUT-QOUTOV*DT/(W*W)
if (chanceck .eq. 1.0) then
HOUT=HCH(JOUT,KOUT)
WPOUT=WCHOUT+2.*HOUT
IF(HOUT.GT.DCHOUT) WPOUT=WCHOUT+2.*DCHOUT
AREAOUT=WCHOUT*HOUT
ALFA=SQRT(SOUT)/RMANOUT
QOUTCH=ALFA*(AREAOUT**1.6667)/(WPOUT**0.6667)
HCH(JOUT,KOUT)=HOUT-QOUTCH*DT/(W*WCHOUT)
endif
QOUT=QOUTOV+QOUTCH
if (qout .gt. qpeak) then
qpeak=qout
tpeak=real(i)*dt/60.
endif

```

C

C Routing Sediment at the OUTLET

C

```

sfout=sout
iinf=isoil(jout,kout)
psand=pinf(iinf,4)
psilt=pinf(iinf,5)
pclay=pinf(iinf,6)
uc=cpfactor(1,iman(jout,kout))
uk=pinf(iinf,7)
up=cpfactor(2,iman(jout,kout))
qtot=qovs(1,jout,kout)+qovs(2,jout,kout)+qovs(3,jout,kout)
vtot=vols(1,jout,kout)+vols(2,jout,kout)+vols(3,jout,kout)
qdtot=qtot+vtot
if (ishp(jout,kout) .eq. 2) then
dumvar=dt
ccc=64150.94
qqq=qout
www=wchout
sss=sfout
else
dumvar=uc*uk*up*dt
qqq=qoutov
sss=sovout
www=w
ccc=64150.94
endif
qs=ccc*www*abs(sss)**1.66*(qqq/www)**2.035*dumvar

```

```

if (qs/dt .gt. qsmaxout(jout,kout)) qsmaxout(jout,kout)=qs/dt
if (qs .gt. qdtot) then
qss(jout,kout)=qdtot
qs=qdtot
else
qss(jout,kout)=qs
endif
if (qsmaxout(jout,kout) .lt. qs/dt) qsmaxout(jout,kout)=qs/dt
if (qs .le. qtot) then
if (qtot .ne. 0.0) then
qpsand=qovs(1,jout,kout)/qtot
qpsilt=qovs(2,jout,kout)/qtot
qpclay=qovs(3,jout,kout)/qtot
qovs(1,jout,kout)=qovs(1,jout,kout)-qs*qpsand
qovs(2,jout,kout)=qovs(2,jout,kout)-qs*qpsilt
qovs(3,jout,kout)=qovs(3,jout,kout)-qs*qpclay
else
endif
endif
if (qs .gt. qtot .and. qs .le. qdtot) then
qs=qs-qtot
qovs(1,jout,kout)=0.0
qovs(2,jout,kout)=0.0
qovs(3,jout,kout)=0.0
if (vtot .ne. 0.0) then
qpsand=vols(1,jout,kout)/vtot
qpsilt=vols(2,jout,kout)/vtot
qpclay=vols(3,jout,kout)/vtot
vols(1,jout,kout)=vols(1,jout,kout)-qs*qpsand
vols(2,jout,kout)=vols(2,jout,kout)-qs*qpsilt
vols(3,jout,kout)=vols(3,jout,kout)-qs*qpclay
else
endif
endif
if (qs .gt. qdtot) then
qs=qs-qdtot
qovs(1,jout,kout)=0.0
qovs(2,jout,kout)=0.0
qovs(3,jout,kout)=0.0
vols(1,jout,kout)=0.0
vols(2,jout,kout)=0.0
vols(3,jout,kout)=0.0
ssoil(1,jout,kout)=ssoil(1,jout,kout)-qs*psand
ssoil(2,jout,kout)=ssoil(2,jout,kout)-qs*psilt
ssoil(3,jout,kout)=ssoil(3,jout,kout)-qs*psilt

```



```

endif
write(6,5000) i,real(i)*dt/60.0,qout*3.28**3.0
5000 format(1x,'Iteration = ',i7,' Time (Min) = ',f15.4,
&' Outflow (CFS) = ',f15.4)
do 5001 ill=1,ndis
if (jout .eq. iq(ill,1) .and. kout .eq. iq(ill,2)) then
q(ill)=qout
endif
5001 continue
C
C Computing the Total Net Erosion or Deposition on each
C grid cell.
C
do 2800 j=1,m
do 2810 k=1,n
totdepv=vols(1,j,k)+vols(2,j,k)+vols(3,j,k)
totscourv=ssoil(1,j,k)+ssoil(2,j,k)+ssoil(3,j,k)
totnetv(j,k)=totdepv+totscourv
totsus(j,k)=qovs(1,j,k)+qovs(2,j,k)+qovs(3,j,k)
if (totnetv(j,k) .lt. aminnetv) aminnetv=totnetv(j,k)
if (totnetv(j,k) .gt. amaxnetv) amaxnetv=totnetv(j,k)
if (qsmaxout(j,k) .lt. aminqsmax) aminqsmax=qsmaxout(j,k)
if (qsmaxout(j,k) .gt. amaxqsmax) amaxqsmax=qsmaxout(j,k)
if (totsus(j,k) .lt. aminsus) aminsus=totsus(j,k)
if (totsus(j,k) .gt. amaxsus) amaxsus=totsus(j,k)
2810 continue
2800 continue
if (icount .eq. nprn .or. i .eq. 1) then
C
C Writing Suspended Sediment Data at Selected Locations
C
do 51 ils=1,nsed
jsed=ised(ils,1)
ksed=ised(ils,2)
wsed=ised(ils,3)
qsedppm(ils)=qss(jsed,ksed)/dt
55 format(1x,12f15.9)
51 continue
write(54,55) i*dt/60.,(qsedppm(ils),ils=1,nsed)
endif
C
C Keeping track of the total outflow volume
C
VOUT=VOUT+QOUT*DT
C

```

```

C----->>>  UNIT CHANGE FROM m3/s TO cfs
C
  IF (ICOUNT .EQ. NPRN .OR. I .EQ. 1) THEN
    WRITE(27,111) I*DT/60.,QOUT*(3.28)**3
    WRITE(29,112) I*DT/60.,
+(Q(ILL)*(3.28)**3,ILL=1,NDIS)
    IF (I .EQ. 1) ICOUNT=ICOUNT+1
    IF (I .NE. 1) ICOUNT=1
    ELSE
    ICOUNT=ICOUNT+1
    ENDIF
C
C  WRITING OUTPUT GRIDS
C
  IF (IFCOUNT .EQ. NPLT .OR. I .EQ. 1) THEN
    print*,'Writing Output Grids, IFCOUNT = ',IFCOUNT
    OPEN(UNIT=38,FILE='JUNK',STATUS='UNKNOWN')
    IF (IFCOUNT .LE. 9) THEN
      WRITE(38,1701) IFCOUNT
      WRITE(38,1702) IFCOUNT
      WRITE(38,1703) IFCOUNT
      WRITE(38,1704) IFCOUNT
      WRITE(38,1706) IFCOUNT
      WRITE(38,1707) IFCOUNT
1701 FORMAT('depth.',i1)
1702 FORMAT('totnetv.',i1)
1703 FORMAT('rain.',i1)
1704 FORMAT('qsmaxout.',i1)
1706 FORMAT('vinf.',i1)
1707 FORMAT('susvol.',i1)
      else
      endif
    IF (IFCOUNT .GT. 9 .AND. IFCOUNT .LE. 99) THEN
      WRITE(38,1001) IFCOUNT
      WRITE(38,1002) IFCOUNT
      WRITE(38,1003) IFCOUNT
      WRITE(38,1004) IFCOUNT
      WRITE(38,1007) IFCOUNT
      WRITE(38,1008) IFCOUNT
1001 FORMAT('depth.',i2)
1002 FORMAT('totnetv.',i2)
1003 FORMAT('rain.',i2)
1004 FORMAT('qsmaxout.',i2)
1007 FORMAT('vinf.',i2)
1008 FORMAT('susvol.',i2)

```

```

else
endif
if (IFCOUNT .gt. 99 .and. IFCOUNT .le. 999) then
WRITE(38,1601) IFCOUNT
WRITE(38,1602) IFCOUNT
WRITE(38,1603) IFCOUNT
WRITE(38,1604) IFCOUNT
WRITE(38,1606) IFCOUNT
WRITE(38,1607) IFCOUNT
1601 FORMAT('depth.',i3)
1602 FORMAT('totnetv.',i3)
1603 FORMAT('rain.',i3)
1604 FORMAT('qsmaxout.',i3)
1606 FORMAT('vinf.',i3)
1607 FORMAT('susvol.',i3)
else
endif
rewind(38)
read(38,1006) dname
read(38,1006) tname
read(38,1006) rname
read(38,1006) qname
read(38,1006) vinfname
read(38,1006) susname
1006 format(a20)
close(38)
C
C   Writing the Output Grids (Depth, Total Net Volume, Rain,
C   QSMAXOUT, and Infiltration )
C
open(unit=39,file=dname,status='unknown')
open(unit=41,file=tname,status='unknown')
open(unit=42,file=rname,status='unknown')
open(unit=43,file=qname,status='unknown')
open(unit=45,file=vinfname,status='unknown')
open(unit=46,file=susname,status='unknown')
do 1010 j1=1,6
write(39,1020) headline(j1)
write(41,1020) headline(j1)
write(42,1020) headline(j1)
write(43,1020) headline(j1)
write(45,1020) headline(j1)
write(46,1020) headline(j1)
1020 format(a80)
1010 continue

```

```

do 1030 j1=1,M
do 1040 k1=1,N
if (ISHP(j1,k1) .eq. 2) then
write(39,*) HCH(j1,k1)*1e3
else
write(39,*) H(j1,k1)*1e3
endif
write(41,*) TOTNETV(j1,k1)*1e6
C
C Note : The rainfall intensity is being written in
C Inches/Hour * 1000
C
write(42,*) RINT(j1,k1)*1000*3600/.0254
write(43,*) QSMAXOUT(j1,k1)*1e6
write(45,*) VINP(j1,k1)*1e6
write(46,*) TOTSUS(j1,k1)*1e6
1040 continue
1030 continue
close(39)
close(41)
close(42)
close(43)
close(45)
close(46)
IFCOUNT=IFCOUNT+1
IF (I .EQ. 1) IPCOUNT=IPCOUNT+1
IF (I .NE. 1) IPCOUNT=1
ELSE
IPCOUNT=IPCOUNT+1
ENDIF
C
C Resetting the variable QSMAXOUT to 0.0
C
DO 2820 J=1,M
DO 2830 K=1,N
QSMAXOUT(J,K)=0.0
2830 CONTINUE
2820 CONTINUE
10 CONTINUE
C
C Writing the Final Output Information
C
WRITE(36,898)
DO 899 J=1,M
DO 899 K=1,N

```

```

IF(ISHP(J,K).EQ.0) GO TO 899
WRITE(36,891) J,K,1000.*H(J,K),1000.*VIN(J,K)
899 CONTINUE
C
C----->>>  UNIT CHANGE FROM m3 TO ft3
C
WRITE(27,113) qpeak*(3.28**3),tpeak,VIN*(3.28**3),
+      VOUT*(3.28**3),100.*VOUT/VIN,VSUR*(3.28**3),
+      100.*VSUR/VIN,VINFTOT*(3.28**3),100.*VINFTOT/VIN
+      ,100.*(VOUT+VSUR+VINFTOT)/VIN
GO TO 172
170 WRITE(27,171) J,K,I*DT,HOV
172 CONTINUE
WRITE(27,(' Stopped at ",I2,".",I2,".",I2)')IHR,IMIN,ISEC
222 FORMAT('/' TIME(MIN) DISCHARGE(CFS)'/)
229 FORMAT('DISCHARGE AT: ',20(2I3,' '))
111 FORMAT(2X,F7.2,F14.3)
112 FORMAT(2X,F7.2,20F10.3)
113 FORMAT('/' PEAK DISCHARGE in CFS=',F15.3' TIME TO PEAK in MIN=',
+ F15.1' VOLUME IN in FT3=',F20.1' VOLUME OUT in FT3=',2F25.3
+ /' SURFACE VOLUME in FT3=',2F25.3' VOLUME INFILTRATED IN FT3=
+ ,2F25.3'/PERCENT MASS BALANCE=',F25.3/)
171 FORMAT('/PROGRAM STOPPED FOR NEGATIVE DEPTH',2I4,2F15.6)
1054 FORMAT(I10)
550 FORMAT(i4)
898 FORMAT(' ROW COLUMN DEPTH(MM) INILTRATION(MM)')
891 FORMAT(2I6,2F10.0)
C
C Writing Min. and Max. values for plotting purposes
C
write(37,*) ''
write(37,*) 'Minimum and Maximum values for the plotting purposes'
write(37,*) ''
write(37,*) 'Min. Overland Depth (m x 1e3)   = ',
&AMINDEPTH*1e3
write(37,*) 'Max. Overland Depth (m x 1e3)   = ',
&AMAXDEPTH*1e3
write(37,*) 'Min. Channel Depth (m x 1e3)    = ',
&AMINCDEPTH*1e3
write(37,*) 'Max. Channel Depth (m x 1e3)    = ',
&AMAXCDEPTH*1e3
write(37,*) 'Min. Tot. Net Vol. (m^3 x 1e6)  = ',
&AMINNETV*1e6
write(37,*) 'Max. Tot. Net Vol. (m^3 x 1e6)  = ',
&AMAXNETV*1e6

```

```

write(37,*) 'Min. VINF (m x 1e6)      = ',
&AMINVINF*1e6
write(37,*) 'Max. VINF (m x 1e6)      = ',
&AMAXVINF*1e6
write(37,*) 'Min. RINT (in/hr x 1000) = ',
&AMINRAIN*1000*3600/.0254
write(37,*) 'Max. RINT (in/hr x 1000) = ',
&AMAXRAIN*1000*3600/.0254
write(37,*) 'Min. QSMAXOUT (m^3/s x 1e6) = ',
&AMINQSMAX*1e6
write(37,*) 'Max. QSMAXOUT (m^3/s x 1e6) = ',
&AMAXQSMAX*1e6
write(37,*) 'Min. Suspended Vol. (m^3 x 1e6) = ',
&AMINSUS*1e6
write(37,*) 'Max. Suspended Vol. (m^3 x 1e6) = ',
&AMAXSUS*1e6
STOP
END
C
C  =====
C  SUBROUTINE RAIN(J,K,NRG,XRG,YRG,RRG,RINT)
C  =====
C
C  DIMENSION XRG(NRG),YRG(NRG),RINT(70,75),RRG(NRG)
C
C  RINT(J,K)=0.
C  TOTDIST=0.
C  TOTRAIN=0.
C
C  if (nrg .eq. 1) then
C    rint(j,k)=rrg(1)
C  else
C    DO 1 L=1,NRG
C      REALJ=J
C      REALK=K
C      DIST=SQRT((REALJ-YRG(L))**2+(REALK-XRG(L))**2)
C
C    When the DIST is less than 1e-5, then the rainfall for that
C    grid cell (J,K) is assumed to be the same as the rainfall at
C    the gage (L).
C
C    IF(DIST.LT.1E-5) THEN
C      RINT(J,K)=RRG(L)
C      GO TO 2
C    ENDIF

```

```

TOTDIST=TOTDIST+1./(DIST**2)
TOTRAIN=TOTRAIN+RRG(L)/(DIST**2)
1 CONTINUE
RINT(J,K)=TOTRAIN/TOTDIST
endif
C
C----->>>  UNIT CHANGE FROM in/hr TO m/s
C
2 RINT(J,K)=RINT(J,K)*0.0254/3600.
RETURN
END
C
C =====
C SUBROUTINE INFILT(J,K,DT,ISOIL,VINF,PINF,HOV)
C =====
C
C INTEGER ISOIL(70,75)
C DIMENSION VINF(70,75),PINF(10,7)
C
C Setting the Infiltration Parameters
C
C IINF=ISOIL(J,K)
C HYDCON=PINF(IINF,1)
C CS=PINF(IINF,2)
C SMD=PINF(IINF,3)
C
C Computing the Rate of Infiltration
C
C P1=HYDCON*DT-2.*VINF(J,K)
C P2=HYDCON*(VINF(J,K)+CS*SMD)
C RINF=(P1+SQRT(P1**2+8.*P2*DT))/(2.*DT)
C
C When the rate of infiltration is greater than HOV/DT,
C then all the water on the overland cell is assumed to be
C infiltrated and the overland depth is reduced to zero.
C
C IF((HOV/DT).LE.RINF) THEN
C RINF=HOV/DT
C HOV=0
C ELSE
C HOV=HOV-RINF*DT
C ENDIF
C
C Accumulated volume of water infiltrated for the grid cell (J,K)
C

```

```
VINF(J,K)=VINF(J,K)+RINF*DT
RETURN
END
```

C  
C

```
=====
SUBROUTINE OVRL(W,IMAN,PMAN,SDEP,J,K,JJ,KK,E,H,DQOV,VOLS,DT,
+I,QOVS,SSOIL,QSMAXOUT,ISOIL,PINF,IFCOUNT,cpfactor,qss,ishp)
```

C  
C

```
=====
DIMENSION E(70,75),H(70,75),DQOV(70,75),PMAN(10),VOLS(3,70,75),
+QOVS(3,70,75),SSOIL(3,70,75),QSMAXOUT(70,75),PINF(10,7),
+cpfactor(2,10),qss(70,75),ishp(70,75)
INTEGER IMAN(70,75),ISOIL(70,75)
DATA A/1./
S0=(E(J,K)-E(JJ,KK))/W
DHDX=(H(JJ,KK)-H(J,K))/W
SF=S0-DHDX+1E-30
HH=H(J,K)
RMAN=PMAN(IMAN(J,K))
IF(SF.LT.0) HH=H(JJ,KK)
IF(SF.LT.0) RMAN=PMAN(IMAN(JJ,KK))
IF(HH.LT.SDEP) RETURN
ALFA=(ABS(SF)**0.5)/RMAN
```

C

C Note : The function SIGN returns the value of A with the sign of SF.

C

C Computing Overland Flow

C

```
DQQ=SIGN(A,SF)*W*ALFA*((HH-SDEP)**1.667)
DQOV(J,K)=DQOV(J,K)-DQQ
DQOV(JJ,KK)=DQOV(JJ,KK)+DQQ
```

C

C Computing the Overland Sediment Flow and Erosion/Deposition

C

```
BB=SIGN(A,SF)
IF (DQQ .EQ. 0.0) GOTO 2870
DQ=ABS(DQQ/W)
```

C

C If BB is greater than 0.0 then the flows goes from (J,K) to  
C (JJ,KK). Therefore, the sediment to satisfy QS needs to be  
C taken from grid cell (J,K). Otherwise, the sediment needs to  
C be taken from grid cell (JJ,KK) to satisfy QS because the flow  
C goes from (JJ,KK) to (J,K).

C

```
IF (BB .GT. 0.0) THEN
```



```

if (ishp(j,k) .eq. 2) goto 2870
IINF=ISOIL(J,K)
PSAND=PINF(IINF,4)
PSILT=PINF(IINF,5)
PCLAY=PINF(IINF,6)
UC=cpfactor(1,iman(j,k))
UK=PINF(IINF,7)
UP=cpfactor(2,iman(j,k))
QTOT=QOVS(1,J,K)+QOVS(2,J,K)+QOVS(3,J,K)
VTOT=VOLS(1,J,K)+VOLS(2,J,K)+VOLS(3,J,K)
QDTOT=QTOT+VTOT
QS=64150.94*W*ABS(SF)**1.66*DQ**2.035*UC*UK*UP*DT
qss(j,k)=qss(j,k)+qs
IF (QSMAXOUT(J,K) .LT. QS/DT) QSMAXOUT(J,K)=QS/DT

```

C

C Taking QS from the suspended sediment on cell (J,K)

C

```

IF (QS .LE. QTOT) THEN
IF (QTOT .NE. 0.0) THEN
QPSAND=QOVS(1,J,K)/QTOT
QPSILT=QOVS(2,J,K)/QTOT
QPCLAY=QOVS(3,J,K)/QTOT
QOVS(1,J,K)=QOVS(1,J,K)-QS*QPSAND
QOVS(2,J,K)=QOVS(2,J,K)-QS*QPSILT
QOVS(3,J,K)=QOVS(3,J,K)-QS*QPCLAY
QOVS(1,JJ,KK)=QOVS(1,JJ,KK)+QS*QPSAND
QOVS(2,JJ,KK)=QOVS(2,JJ,KK)+QS*QPSILT
QOVS(3,JJ,KK)=QOVS(3,JJ,KK)+QS*QPCLAY
ELSE
ENDIF
ENDIF

```

C

C Taking QS from the suspended sediment and sediment deposits  
C on cell (J,K)

C

```

IF (QS .GT. QTOT .AND. QS .LE. QDTOT) THEN
QS=QS-QTOT
QOVS(1,JJ,KK)=QOVS(1,JJ,KK)+QOVS(1,J,K)
QOVS(2,JJ,KK)=QOVS(2,JJ,KK)+QOVS(2,J,K)
QOVS(3,JJ,KK)=QOVS(3,JJ,KK)+QOVS(3,J,K)
QOVS(1,J,K)=0.0
QOVS(2,J,K)=0.0
QOVS(3,J,K)=0.0
IF (VTOT .NE. 0.0) THEN
QPSAND=VOLS(1,J,K)/VTOT

```

```

QPSILT=VOLS(2,J,K)/VTOT
QPCLAY=VOLS(3,J,K)/VTOT
VOLS(1,J,K)=VOLS(1,J,K)-QS*QPSAND
VOLS(2,J,K)=VOLS(2,J,K)-QS*QPSILT
VOLS(3,J,K)=VOLS(3,J,K)-QS*QPCLAY
QOVS(1,JJ,KK)=QOVS(1,JJ,KK)+QS*QPSAND
QOVS(2,JJ,KK)=QOVS(2,JJ,KK)+QS*QPSILT
QOVS(3,JJ,KK)=QOVS(3,JJ,KK)+QS*QPCLAY
ELSE
ENDIF
ENDIF

```

```

C
C   Taking QS from the suspended sediment, deposited sediment, and
C   soil on cell (J,K)
C

```

```

IF (QS .GT. QDTOT) THEN
QS=QS-QDTOT
QOVS(1,JJ,KK)=QOVS(1,JJ,KK)+QOVS(1,J,K)+VOLS(1,J,K)
QOVS(2,JJ,KK)=QOVS(2,JJ,KK)+QOVS(2,J,K)+VOLS(2,J,K)
QOVS(3,JJ,KK)=QOVS(3,JJ,KK)+QOVS(3,J,K)+VOLS(3,J,K)
QOVS(1,J,K)=0.0
QOVS(2,J,K)=0.0
QOVS(3,J,K)=0.0
VOLS(1,J,K)=0.0
VOLS(2,J,K)=0.0
VOLS(3,J,K)=0.0
SSOIL(1,J,K)=SSOIL(1,J,K)-QS*PSAND
SSOIL(2,J,K)=SSOIL(2,J,K)-QS*PSILT
SSOIL(3,J,K)=SSOIL(3,J,K)-QS*PCLAY
QOVS(1,JJ,KK)=QOVS(1,JJ,KK)+QS*PSAND
QOVS(2,JJ,KK)=QOVS(2,JJ,KK)+QS*PSILT
QOVS(3,JJ,KK)=QOVS(3,JJ,KK)+QS*PCLAY
ENDIF

```

```

C
C   Determining how much of the routed sediment dropped out
C   and how much stayed in suspension in cell (JJ,KK)
C
C   NOTE : FALL VELOCITIES (WSAND, WSILT, AND WCLAY ARE FOR
C   MEDIUM GRAIN SIZES AT 20 DEGREES CELSIUS AND ARE IN THE
C   UNITS OF M/S.
C

```

```

WSAND=.036
WSILT=.00022
WCLAY=8.6E-7
VEL=0.0

```

```

IF (HH .NE. 0.0) VEL=ABS(DQQ/(W*HH))
EXP=2.718281828
IF (HH*VEL .NE. 0.0) THEN
TE1=1-EXP**((-1*W*WSAND)/(HH*VEL))
TE2=1-EXP**((-1*W*WSILT)/(HH*VEL))
TE3=1-EXP**((-1*W*WCLAY)/(HH*VEL))
DQSAND=QOVS(1,JJ,KK)*TE1
DQSILT=QOVS(2,JJ,KK)*TE2
DQCLAY=QOVS(3,JJ,KK)*TE3
VOLS(1,JJ,KK)=VOLS(1,JJ,KK)+DQSAND
VOLS(2,JJ,KK)=VOLS(2,JJ,KK)+DQSILT
VOLS(3,JJ,KK)=VOLS(3,JJ,KK)+DQCLAY
QOVS(1,JJ,KK)=QOVS(1,JJ,KK)-DQSAND
QOVS(2,JJ,KK)=QOVS(2,JJ,KK)-DQSILT
QOVS(3,JJ,KK)=QOVS(3,JJ,KK)-DQCLAY
ELSE
ENDIF
ENDIF
IF (BB .LT. 0.0) THEN

```

C

C BB is less than 0.0, so the flow is going from (JJ,KK) to (J,K)

C

```

if (ishp(jj,kk) .eq. 2) goto 2870
IINF=ISOIL(JJ,KK)
PSAND=PINF(IINF,4)
PSILT=PINF(IINF,5)
PCLAY=PINF(IINF,6)
UC=cpfactor(1,iman(jj,kk))
UK=PINF(IINF,7)
UP=cpfactor(2,iman(jj,kk))
QTOT=QOVS(1,JJ,KK)+QOVS(2,JJ,KK)+QOVS(3,JJ,KK)
VTOT=VOLS(1,JJ,KK)+VOLS(2,JJ,KK)+VOLS(3,JJ,KK)
QDTOT=QTOT+VTOT
QS=64150.94*W*ABS(SF)**1.66*DQ**2.035*UC*UK*UP*DT
qss(jj,kk)=qss(jj,kk)+qs
IF (QSMAXOUT(JJ,KK) .LT. QS/DT) QSMAXOUT(JJ,KK)=QS/DT

```

C

C Taking QS from the suspended sediment on cell (JJ,KK)

C

```

IF (QS .LE. QTOT) THEN
IF (QTOT .NE. 0.0) THEN
QPSAND=QOVS(1,JJ,KK)/QTOT
QPSILT=QOVS(2,JJ,KK)/QTOT
QPCLAY=QOVS(3,JJ,KK)/QTOT
QOVS(1,JJ,KK)=QOVS(1,JJ,KK)-QS*QPSAND

```

```

QOVS(2,JJ,KK)=QOVS(2,JJ,KK)-QS*QPSILT
QOVS(3,JJ,KK)=QOVS(3,JJ,KK)-QS*QPCLAY
QOVS(1,J,K)=QOVS(1,J,K)+QS*QPSAND
QOVS(2,J,K)=QOVS(2,J,K)+QS*QPSILT
QOVS(3,J,K)=QOVS(3,J,K)+QS*QPCLAY
ELSE
ENDIF
ENDIF

```

C

C Taking QS from the suspended sediment and sediment deposits  
C on cell (JJ,KK)

C

```

IF (QS .GT. QTOT .AND. QS .LE. QDTOT) THEN
QS=QS-QOVS(1,JJ,KK)-QOVS(2,JJ,KK)-QOVS(3,JJ,KK)
QOVS(1,J,K)=QOVS(1,J,K)+QOVS(1,JJ,KK)
QOVS(2,J,K)=QOVS(2,J,K)+QOVS(2,JJ,KK)
QOVS(3,J,K)=QOVS(3,J,K)+QOVS(3,JJ,KK)
QOVS(1,JJ,KK)=0.0
QOVS(2,JJ,KK)=0.0
QOVS(3,JJ,KK)=0.0
IF (VTOT .NE. 0.0) THEN
QPSAND=VOLS(1,JJ,KK)/VTOT
QPSILT=VOLS(2,JJ,KK)/VTOT
QPCLAY=VOLS(3,JJ,KK)/VTOT
VOLS(1,JJ,KK)=VOLS(1,JJ,KK)-QS*QPSAND
VOLS(2,JJ,KK)=VOLS(2,JJ,KK)-QS*QPSILT
VOLS(3,JJ,KK)=VOLS(3,JJ,KK)-QS*QPCLAY
QOVS(1,J,K)=QOVS(1,J,K)+QS*QPSAND
QOVS(2,J,K)=QOVS(2,J,K)+QS*QPSILT
QOVS(3,J,K)=QOVS(3,J,K)+QS*QPCLAY
ELSE
ENDIF
ENDIF

```

C

C Taking QS from the suspended sediment, deposited sediment, and  
C soil on cell (JJ,KK)

C

```

IF (QS .GT. QDTOT) THEN
QS=QS-QDTOT
QOVS(1,J,K)=QOVS(1,J,K)+QOVS(1,JJ,KK)+VOLS(1,JJ,KK)
QOVS(2,J,K)=QOVS(2,J,K)+QOVS(2,JJ,KK)+VOLS(2,JJ,KK)
QOVS(3,J,K)=QOVS(3,J,K)+QOVS(3,JJ,KK)+VOLS(3,JJ,KK)
QOVS(1,JJ,KK)=0.0
QOVS(2,JJ,KK)=0.0
QOVS(3,JJ,KK)=0.0

```

```

VOLS(1,JJ,KK)=0.0
VOLS(2,JJ,KK)=0.0
VOLS(3,JJ,KK)=0.0
SSOIL(1,JJ,KK)=SSOIL(1,JJ,KK)-QS*PSAND
SSOIL(2,JJ,KK)=SSOIL(2,JJ,KK)-QS*PSILT
SSOIL(3,JJ,KK)=SSOIL(3,JJ,KK)-QS*PCLAY
QOVS(1,J,K)=QOVS(1,J,K)+QS*PSAND
QOVS(2,J,K)=QOVS(2,J,K)+QS*PSILT
QOVS(3,J,K)=QOVS(3,J,K)+QS*PCLAY
ENDIF

```

```

C
C   Determining how much of the routed sediment dropped out
C   and how much stayed in suspension in cell (J,K)
C
C   NOTE : FALL VELOCITIES (WSAND, WSILT, AND WCLAY ARE FOR
C   MEDIUM GRAIN SIZES AT 20 DEGREES CELSIUS AND ARE IN THE
C   UNITS OF M/S.
C

```

```

WSAND=.036
WSILT=.00022
WCLAY=8.6E-7
VEL=0.0
IF (HH .NE. 0.0) VEL=ABS(DQQ/(W*HH))
EXP=2.718281828
IF (HH*VEL .NE. 0.0) THEN
TE1=1-EXP**((-1*W*WSAND)/(HH*VEL))
TE2=1-EXP**((-1*W*WSILT)/(HH*VEL))
TE3=1-EXP**((-1*W*WCLAY)/(HH*VEL))
DQSAND=QOVS(1,J,K)*TE1
DQSILT=QOVS(2,J,K)*TE2
DQCLAY=QOVS(3,J,K)*TE3
VOLS(1,J,K)=VOLS(1,J,K)+DQSAND
VOLS(2,J,K)=VOLS(2,J,K)+DQSILT
VOLS(3,J,K)=VOLS(3,J,K)+DQCLAY
QOVS(1,J,K)=QOVS(1,J,K)-DQSAND
QOVS(2,J,K)=QOVS(2,J,K)-DQSILT
QOVS(3,J,K)=QOVS(3,J,K)-DQCLAY
ELSE
ENDIF
ENDIF

```

```

2870 RETURN
END

```

```

C
C

```

---

```

SUBROUTINE CHNCHN(NCHN,W,WCH,DCH,RMANCH,SFACTOR,

```

+J,K, JJ, KK, JJJ, E, HCH, ICHN, CHP, DQCH, NDIS, IQ, Q,  
 +pman, vols, dt, i, qovs, ssoil, qsmazout, pinf, ifcount,  
 +cpfactor, qss)

C  
 C

---

DIMENSION E(70,75), HCH(70,75), ICHN(50,50,2), CHP(29,3),  
 +DQCH(70,75), IQ(20,2), Q(20), pman(10), vols(3,70,75),  
 +qovs(3,70,75), ssoil(3,70,75), qsmazout(70,75), pinf(10,7),  
 +qss(70,75)

DATA A/1./

C

S0=(E(J,K)-DCH-E(JJ, KK)+DCH)/(W\*SFACTOR)

C

C When JJJ is less than zero, then the end of the channel link  
 C has been reached.

C

IF(JJJ.LT.0) THEN  
 DO 5 IIC=1, NCHN, 1  
 IF(JJ.EQ.ICHN(IIC, 1, 1).AND.KK.EQ.ICHN(IIC, 1, 2)) THEN  
 S0=(E(J,K)-DCH-E(JJ, KK)+CHP(IIC, 2))/(W\*SFACTOR)  
 IJUN=IIC  
 GO TO 7  
 ENDIF  
 5 CONTINUE  
 ENDIF

C

7 DHDX=(HCH(JJ, KK)-HCH(J, K))/(W\*SFACTOR)  
 SF=S0-DHDX+1E-30  
 IF(ABS(SF).LT.1E-20) SF=1E-20  
 HH=HCH(J, K)

C

C IF(SF.LT.0) THEN

C

C It seems that this line should be as follows, otherwise IJUN is  
 C zero and the channel properties will become zero thus causing  
 C a miss calculation in the channel routings.

C

C Billy E. Johnson, May 21, 1996.

C

IF (SF .LT. 0 .AND. JJJ .LT. 0) THEN  
 WCH=CHP(IJUN,1)  
 DCH=CHP(IJUN,2)  
 RMANCH=CHP(IJUN,3)  
 SFACTOR=CHP(IJUN,4)  
 HH=HCH(JJ, KK)

```

ENDIF
WP=WCH+2.*HH
IF(HH.GT.DCH) WP=WCH+2.*DCH
AREA=WCH*HH
DQ=SIGN(A,SF)*(SQRT(ABS(SF))/RMANCH)*(AREA**1.6667)/(WP**0.6667)
DQCH(J,K)=DQCH(J,K)-DQ
DQCH(JJ,KK)=DQCH(JJ,KK)+DQ
DO 367 ILL=1,NDIS
C   IF(SF.GE.0) THEN
C   IF(J.EQ.IQ(ILL,1).AND.K.EQ.IQ(ILL,2)) Q(ILL)=DQ
C   ELSE
C   IF(JJ.EQ.IQ(ILL,1).AND.KK.EQ.IQ(ILL,2)) Q(ILL)=-1.*DQ
C   ENDIF
C
C Routing Upland Sediment within the Channel Network.
C
C This routine does not try to erode the channel banks or the channel bed.
C It simply routes sediment introduced to the channel system from
C Upland Erosion.
C
BB=sign(a,sf)
if (dq .eq. 0.0) goto 2600
if (bb .gt. 0.0) then
qtot=qovs(1,j,k)+qovs(2,j,k)+qovs(3,j,k)
vtot=vols(1,j,k)+vols(2,j,k)+vols(3,j,k)
qdtot=qtot+vtot
qs=8.0*wch*abs(sf)**1.66*(dq/wch)**2.035*dt
if (qs/dt .gt. qsmaxout(j,k)) qsmaxout(j,k)=qs/dt
if (qs .gt. qdtot) then
qss(j,k)=qss(j,k)+qdtot
qs=qdtot
else
qss(j,k)=qss(j,k)+qs
endif
C
C Taking Suspended Sediment from cell (j,k)
C
if (qs .le. qtot) then
if (qtot .ne. 0.0) then
qpsand=qovs(1,j,k)/qtot
qpsilt=qovs(2,j,k)/qtot
qpclay=qovs(3,j,k)/qtot
qovs(1,j,k)=qovs(1,j,k)-qs*qpsand
qovs(2,j,k)=qovs(2,j,k)-qs*qpsilt
qovs(3,j,k)=qovs(3,j,k)-qs*qpclay

```

```

qovs(1,jj,kk)=qovs(1,jj,kk)+qs*qpsand
qovs(2,jj,kk)=qovs(2,jj,kk)+qs*qpsilt
qovs(3,jj,kk)=qovs(3,jj,kk)+qs*qpclay
else
endif
endif
C
C Taking Suspended Sediment and Previous Deposited Sediment from cell (j,k)
C
if (qs .gt. qtot) then
qs=qs-qtot
qovs(1,jj,kk)=qovs(1,jj,kk)+qovs(1,j,k)
qovs(2,jj,kk)=qovs(2,jj,kk)+qovs(2,j,k)
qovs(3,jj,kk)=qovs(3,jj,kk)+qovs(3,j,k)
qovs(1,j,k)=0.0
qovs(2,j,k)=0.0
qovs(3,j,k)=0.0
if (vtot .ne. 0.0) then
qpsand=vols(1,j,k)/vtot
qpsilt=vols(2,j,k)/vtot
qpclay=vols(3,j,k)/vtot
vols(1,j,k)=vols(1,j,k)-qs*qpsand
vols(2,j,k)=vols(2,j,k)-qs*qpsilt
vols(3,j,k)=vols(3,j,k)-qs*qpclay
vols(1,jj,kk)=vols(1,jj,kk)+qs*qpsand
vols(2,jj,kk)=vols(2,jj,kk)+qs*qpsilt
vols(3,jj,kk)=vols(3,jj,kk)+qs*qpclay
else
endif
endif
C
C Determining how much routed sediment dropped out and
C how much stayed in suspension in cell (jj,kk).
C
C Note : Fall Velocities (wsand, wsilt, and wclay are
C for medium grain sizes at 20 degrees celsius and are
C in the units of m/s.
C
wsand=0.036
wsilt=0.00022
wclay=8.6e-7
vel=0.0
if (hh .ne. 0.0) vel=abs(dq/(wch*hh))
exp=2.718281828
if (hh*vel .ne. 0.0) then

```



```

te1=1-exp**((-1*wch*wsand)/(hh*vel))
te2=1-exp**((-1*wch*wsilt)/(hh*vel))
te3=1-exp**((-1*wch*wclay)/(hh*vel))
dqsand=qovs(1,jj,kk)*te1
dqsilt=qovs(2,jj,kk)*te2
dqclay=qovs(3,jj,kk)*te3
vols(1,jj,kk)=vols(1,jj,kk)+dqsand
vols(2,jj,kk)=vols(2,jj,kk)+dqsilt
vols(3,jj,kk)=vols(3,jj,kk)+dqclay
qovs(1,jj,kk)=qovs(1,jj,kk)-dqsand
qovs(2,jj,kk)=qovs(2,jj,kk)-dqsilt
qovs(3,jj,kk)=qovs(3,jj,kk)-dqclay
else
endif
else

```

C

C BB is less than 0.0, so the flow is going from (jj,kk) to (j,k)

C

```

if (dq .eq. 0.0) goto 2600
qtot=qovs(1,jj,kk)+qovs(2,jj,kk)+qovs(3,jj,kk)
vtot=vols(1,jj,kk)+vols(2,jj,kk)+vols(3,jj,kk)
qdtot=qtot+vtot
qs=8.0*wch*abs(sf)**1.66*(dq/wch)**2.035*dt
if (qs/dt .gt. qsmaxout(jj,kk)) qsmaxout(jj,kk)=qs/dt
if (qs .gt. qdtot) then
qss(jj,kk)=qss(jj,kk)+qdtot
qs=qdtot
else
qss(jj,kk)=qss(jj,kk)+qs
endif

```

C

C Taking Suspended Sediment from cell (jj,kk)

C

```

if (qs .le. qtot) then
if (qtot .ne. 0.0) then
qpsand=qovs(1,jj,kk)/qtot
qpsilt=qovs(2,jj,kk)/qtot
qpclay=qovs(3,jj,kk)/qtot
qovs(1,jj,kk)=qovs(1,jj,kk)-qs*qpsand
qovs(2,jj,kk)=qovs(2,jj,kk)-qs*qpsilt
qovs(3,jj,kk)=qovs(3,jj,kk)-qs*qpclay
qovs(1,j,k)=qovs(1,j,k)+qs*qpsand
qovs(2,j,k)=qovs(2,j,k)+qs*qpsilt
qovs(3,j,k)=qovs(3,j,k)+qs*qpclay
else

```

```

endif
endif
C
C Taking Suspended Sediment and Previous Deposited Sediment from cell (jj,kk)
C
if (qs .gt. qtot) then
qs=qs-qtot
qovs(1,j,k)=qovs(1,j,k)+qovs(1,jj,kk)
qovs(2,j,k)=qovs(2,j,k)+qovs(2,jj,kk)
qovs(3,j,k)=qovs(3,j,k)+qovs(3,jj,kk)
qovs(1,jj,kk)=0.0
qovs(2,jj,kk)=0.0
qovs(3,jj,kk)=0.0
if (vtot .ne. 0.0) then
qpsand=vols(1,jj,kk)/vtot
qpsilt=vols(2,jj,kk)/vtot
qpclay=vols(3,jj,kk)/vtot
vols(1,jj,kk)=vols(1,jj,kk)-qs*qpsand
vols(2,jj,kk)=vols(2,jj,kk)-qs*qpsilt
vols(3,jj,kk)=vols(3,jj,kk)-qs*qpclay
vols(1,j,k)=vols(1,j,k)+qs*qpsand
vols(2,j,k)=vols(2,j,k)+qs*qpsilt
vols(3,j,k)=vols(3,j,k)+qs*qpclay
else
endif
endif
C
C Determining how much routed sediment dropped out and
C how much stayed in suspension in cell (j,k).
C
wsand=0.036
wsilt=0.00022
wclay=8.6e-7
if (hh .ne. 0.0) vel=abs(dq/(wch*hh))
exp=2.718281828
if (hh*vel .ne. 0.0) then
te1=1-exp**((-1*wch*wsand)/(hh*vel))
te2=1-exp**((-1*wch*wsilt)/(hh*vel))
te3=1-exp**((-1*wch*wclay)/(hh*vel))
dqsand=qovs(1,j,k)*te1
dqsilt=qovs(2,j,k)*te2
dqclay=qovs(3,j,k)*te3
vols(1,j,k)=vols(1,j,k)+dqsand
vols(2,j,k)=vols(2,j,k)+dqsilt
vols(3,j,k)=vols(3,j,k)+dqclay

```

```
qovs(1,j,k)=qovs(1,j,k)-dqsand
qovs(2,j,k)=qovs(2,j,k)-dqsilt
qovs(3,j,k)=qovs(3,j,k)-dqclay
else
endif
endif
367 CONTINUE
2600 RETURN
END
```

**Example ASCII Input Data for CASC2D**

















**CHN.DAT - Goodwin Creek Channel Data.**

28.99 4.0 0.047 1.0  
 23.71 4.2 0.047 1.0  
 7.48 4.11 0.047 1.0  
 23.45 4.34 0.047 1.0  
 22.42 3.98 0.047 1.0  
 23.35 4.34 0.047 1.0  
 15.70 3.4 0.047 1.0  
 13.65 3.83 0.047 1.0  
 15.24 4.5 0.047 1.0  
 7.42 4.5 0.047 1.0  
 17.70 4.7 0.047 1.0  
 6.00 3.0 0.047 1.0  
 37.97 4.97 0.047 1.0  
 7.42 4.5 0.047 1.0  
 28.24 5.32 0.047 1.0  
 23.63 6.05 0.047 1.0

14 14 13 13 13 13 12 12 12 11 11 11 11 11 11 -1 0 0 0 0 0 0  
 68 67 67 66 65 64 64 63 62 62 61 60 59 58 57 -1 0 0 0 0 0 0

11 11 11 11 11 12 12 13 13 14 14 15 15 16 16 17 -1 0 0 0 0 0  
 57 56 55 54 53 53 52 52 51 51 50 50 49 49 48 48 -1 0 0 0 0 0

18 18 18 19 19 19 18 17 17 -1 0 0 0 0 0 0 0 0 0 0 0  
 53 52 51 51 50 49 49 49 48 -1 0 0 0 0 0 0 0 0 0 0 0

17 17 17 17 16 16 16 15 15 14 14 14 14 -1 0 0 0 0 0 0 0  
 48 47 46 45 45 44 43 43 42 42 41 40 39 -1 0 0 0 0 0 0 0

8 9 9 9 9 9 9 9 9 10 10 10 11 12 13 14 -1 0 0 0 0 0  
 48 48 47 46 45 44 43 42 41 41 40 39 39 39 39 39 -1 0 0 0 0 0

14 14 14 14 15 15 16 16 17 18 18 19 19 20 20 21 22 -1 0 0 0 0  
 39 38 37 36 36 35 35 34 34 34 33 33 32 32 31 31 31 -1 0 0 0 0

27 27 28 28 28 28 27 27 26 25 25 24 24 -1 0 0 0 0 0 0 0  
 49 48 48 47 46 45 44 44 43 43 43 42 42 41 -1 0 0 0 0 0 0

24 23 23 23 23 22 22 22 22 22 22 22 -1 0 0 0 0 0 0 0  
 41 41 40 39 38 37 37 36 35 34 33 32 31 -1 0 0 0 0 0 0 0

22 22 22 23 24 24 24 24 25 -1 0 0 0 0 0 0 0 0 0 0 0  
 31 30 29 29 29 28 27 26 26 -1 0 0 0 0 0 0 0 0 0 0 0

33 32 31 31 30 29 29 28 28 27 27 26 26 25 -1 0 0 0 0 0 0 0  
31 31 31 30 30 30 29 29 28 28 27 27 26 26 -1 0 0 0 0 0 0 0

25 25 25 25 25 25 25 25 26 -1 0 0 0 0 0 0 0 0 0 0 0  
26 25 24 23 22 21 20 19 18 18 -1 0 0 0 0 0 0 0 0 0 0

38 37 36 36 35 35 34 34 33 33 32 31 31 30 30 29 29 28 28 27 26 -1  
26 26 26 25 25 24 24 23 23 22 22 22 21 21 20 20 19 19 18 18 18 -1

26 26 26 26 26 27 27 28 28 29 29 30 31 -1 0 0 0 0 0 0 0 0  
18 17 16 15 14 14 13 13 12 12 11 11 11 -1 0 0 0 0 0 0 0 0

36 35 35 34 34 33 33 33 33 32 32 31 31 -1 0 0 0 0 0 0 0 0  
18 18 17 17 16 16 15 14 13 13 12 12 11 -1 0 0 0 0 0 0 0 0

31 31 32 32 33 33 34 35 35 36 37 38 38 -1 0 0 0 0 0 0 0 0  
11 10 10 9 9 8 8 8 7 7 7 7 6 -1 0 0 0 0 0 0 0 0

38 39 40 40 41 42 42 42 43 43 0 0 0 0 0 0 0 0 0 0 0 0  
6 6 6 5 5 5 4 3 3 2 0 0 0 0 0 0 0 0 0 0 0 0

**DATA1 - Goodwin Creek Job Control Data for  
October 17-18, 1981**

44 75 121.951 3 0.  
5. 5760 2532 12 120 100.0 1.0  
43 2 0.01 1500. 23.63 6.05 0.037 0.01  
1 4  
16 22  
1  
17 12  
3.5 41.5  
14.5 24.5  
32.5 18.5  
45.5 13.5  
41.5 6.5  
44.0 23.0  
59.0 8.0  
58.0 14.0  
63.0 12.0  
18.0 25.0  
28.0 24.0  
33.0 21.0  
22.0 32.0  
30.0 31.0  
37.0 28.0  
39.0 16.0  
53.0 17.0  
0.07 0.07 1.0  
0.110 0.008 1.0  
0.05 0.65 1.0  
3.2722E-5 0.0495 0.42 1.0 0.00 0.00 0.12  
2.6E-6 0.1101 0.42 0.62 0.26 0.12 0.27  
1.4E-6 0.1668 0.42 0.10 0.75 0.15 0.40  
2.78E-7 0.2730 0.42 0.08 0.42 0.50 0.38  
1 6  
43 2  
26 14  
21 31  
22 32  
17 45  
11 60  
1 11  
42 4 0  
26 14 0

21	31	0
22	32	0
17	45	0
11	60	0
10	56	0
20	56	0
17	62	0
14	68	0
28	28	0